fpp

flicker pupil perimetry

In search of an objective visual field test for young or neurologically impaired patients

UMC Utrecht Brain Center

Brendan L. Portengen

flicker pupil perimetry

In search of an objective visual field test
for young or neurologically impaired patients

Flikker pupil perimetrie
Op zoek naar een objectieve gezichtsveldtest voor
jonge of neurologisch aangedane patiënten
(met een samenvatting in het Nederlands)

Colofon

The research in this thesis was financially supported by the ODAS Stichting, Rotterdamse Stichting Blindenbelangen, Janivo Stichting, Dr. F.P. Fischer Stichting and Stichting Vrienden UMC Utrecht.

Publication of this thesis was kindly supported by Rotterdamse Stichting Blindenbelangen, Stichting Blindenhulp, Landelijk Stichting voor Blinden en Slechtzienden, Neurofibromatose Vereniging Nederland, Thea Pharma, Rockmed BV, ChipSoft and Low Vision Totaal

Cover design, illustration & design lay-out:
Brendan Portengen & Koen Portengen
Cover photo: Jos Aalbers
Printed by: Ridderprint
ISBN: 978-94-6483-730-8

Proefschrift

ter verkrijging van de graad van doctor aan
de Universiteit Utrecht op gezag van de
rector magnificus, prof. dr. H.R.B.M. Kummeling,
ingevolge het besluit van het college voor
promoties in het openbaar te verdedigen op

dinsdag 27 februari 2024 des middags te 12.15 uur

door

Brendan Lucas Portengen
Geboren op 21 mei 1992 te Leiden

Promotor:
Prof. dr. S.M. Imhof

Co-promotoren:
Dr. G.L. Porro
Dr. M. Naber

Beoordelingscommissie:
Prof. dr. K.P.J. Braun (voorzitter)
Prof. dr. F.W. Cornelissen
Prof. dr. M.M. van Genderen
Prof. dr. E.W. Hoving
Prof. dr. S. van der Stigchel

Table of contents

Introduction

1.1 General introduction

It is easy to take healthy vision for granted. In contrast, at least 2.2 billion people worldwide suffer from vision impairment (Bourne et al., 2021). Impaired vision can have a huge impact on a personal and economic level. In young children it can cause delays in motor, language, emotional, social and cognitive development, while adults experience a lower quality of life through higher rates of depression and difficulty completing various daily tasks such as personal hygiene, reading, navigating and driving (Reding & Potes, 1988; Warren, 2009). The visual field (VF) is an important factor in perceived quality of life (Ivers et al., 1998; Ramrattan et al., 2001; Sherwood et al., 1998; Valbuena et al., 1999). The VF refers to the total area in which objects can be seen during steady fixation of the gaze in one direction (Traquair, 1928) and typically extends 50 visual degrees nasal and superior, 70 degrees inferior, and 90 degrees temporal (Heijl et al., 2012). Although its prevalence is often underestimated, studies estimate that 3-17% of people aged over 40 years suffer from VF loss (Ramrattan et al., 2001; Taylor et al., 1997). Additionally, one of the most common causes of low vision in children is neurological impairment

Figure 1. Transversal cross-section of the visual pathway and overview of possible visual field defects caused by lesions (red lines) in the brain (black = visual field loss).

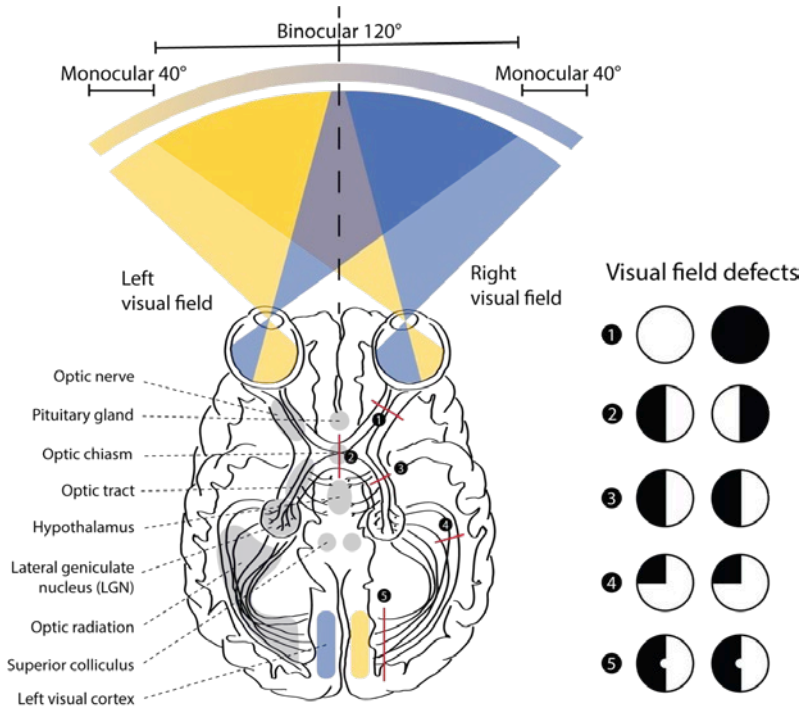

(Boonstra et al., 2012; Kong et al., 2012), of which VF loss may be one of the first symptomatic signs (Van Genderen et al., 2012). This thesis focuses on the diagnosis of visual field defects (VFD) in young and/or neurologically impaired patients.

VF loss can be caused by many diseases of the eye, optic nerve or brain ***(see Figure 1)***. In neurologically impaired patients, lesions posterior to the optic chiasm typically result in bilateral vision loss affecting the contralateral VF while respecting the vertical midline (i.e. homonymous hemianopia). The causes of such VFDs are dependent on age: most common causes of homonymous hemianopia in adults are stroke and trauma (Goodwin, 2014), while tumors most commonly impact the VF in children (G. T. Liu & Galetta, 1997). Early and proper diagnosis of a VFD in young and/or neurologically impaired individuals is crucial since it plays an important role in the diagnosis, follow-up and rehabilitation of these patients (Bova et al., 2008; Hart et al., 2013; Jacobson et al., 2010; Molineus et al., 2013; Pike et al., 1994; Reding & Potes, 1988; Van Genderen et al., 2012) and thus increasing their quality of life. The perfect VF test should possess certain characteristics: high accuracy, efficient, robust measurements, repeatable, able to reproduce comparable data for follow-up, and provide comfort to both patient and examiner. While the perfect test unfortunately does not exist yet, especially the latter is of paramount importance for young and/or neurologically impaired patients. In this thesis we explore a novel form of VF assessment for this patient population. Before we extend on this, it is important to understand the tests that are currently used in clinical practice. The next section discusses the VF tests that are currently performed in clinical practice.

1.2 Visual field tests for neurologically impaired patients and young children

The assessment of the visual field (VF) is an instrumental component of ophthalmological and neurological examination in the clinical practice. VF tests generally are relatively cheap and non-invasive. With it, clinicians can pinpoint the suspected location of damage along the visual pathway (Anderson et al., 2009; Breu et al., 2008; Classé, 1989; Gutteridge, 1985; Phu et al., 2017; Turpin et al., 2003). For example, the clinician will suspect a lesion of the optic chiasm if the patient portrays a bitemporal VFD ***(see Figure 1)***. Most tests that are currently used in practice consist of subjective methods, meaning that they harness

the patient's psychophysical response to a certain stimulus to get a measure of their VF sensitivity. This section discusses some tests used in young and neurologically impaired patients.

1.2.1 Subjective perimetry

Standard automated perimetry (SAP)

Automated perimetry (SAP) has become the standard for assessment and monitoring of the VF (Heijl, 2012; Johnson et al., 2011; Landers et al., 2010; Rowe, 2008). The core principles of SAP have not changed since 1945 and still hold true in current methods. The subjective visual threshold (i.e. the smallest level of light a patient can detect) to a small bright white stimulus against a dim white background is measured across several locations within the visual field. This stimulus can either have a fixed location (i.e. static perimetry) or it can move from the periphery to the center of the VF until it is seen by the subject (i.e. kinetic perimetry). SAP, a static perimetry method, typically presents light stimuli at predetermined locations but at varying intensities to determine the visual threshold. All SAP methods restrict head movement with a head-chinrest and require the patient to fix their gaze at a fixation target in the center while concentrating on detecting the appearance of a light stimulus somewhere across the VF for an extended amount of time. Nowadays, the automated Humphrey Field Analyzer (HFA; see ***Figure 1*** for an example of a test result) is widely used in clinical practice, often combined with the Swedish Interactive Threshold Algorithm (SITA) strategy (i.e. a certain testing algorithm which reduces testing time and increases reliability). Although the HFA SITA is considered the gold standard perimetry test, certain technical characteristics complicate reliable visual field assessment in young and/or neurologically impaired patients. A learning curve in patients without perimetric experience (Pierre-Filho et al., 2006) means at least two tests must be performed for a reliable assessment. Additionally, some studies showed that test results were not comparable (i.e. large test-retest variability) when repeated within a subject (Artes et al., 2002; Piltz & Starita, 1990; Wall et al., 2009) but also when comparing results between different perimeters (Fredette et al., 2015; Wall et al., 2010). As a result of this, the ability to track VF loss progression is negatively impacted. It is also important to note that certain traits of young and/or neurologically impaired patients, such as a lack of concentration, short attention span, psycho-motor impairment and intolerance to head restrictions, further impede reliable VF assessment (Morales & Brown, 2001; Murray et al., 2009; Tschopp et al., 1998).

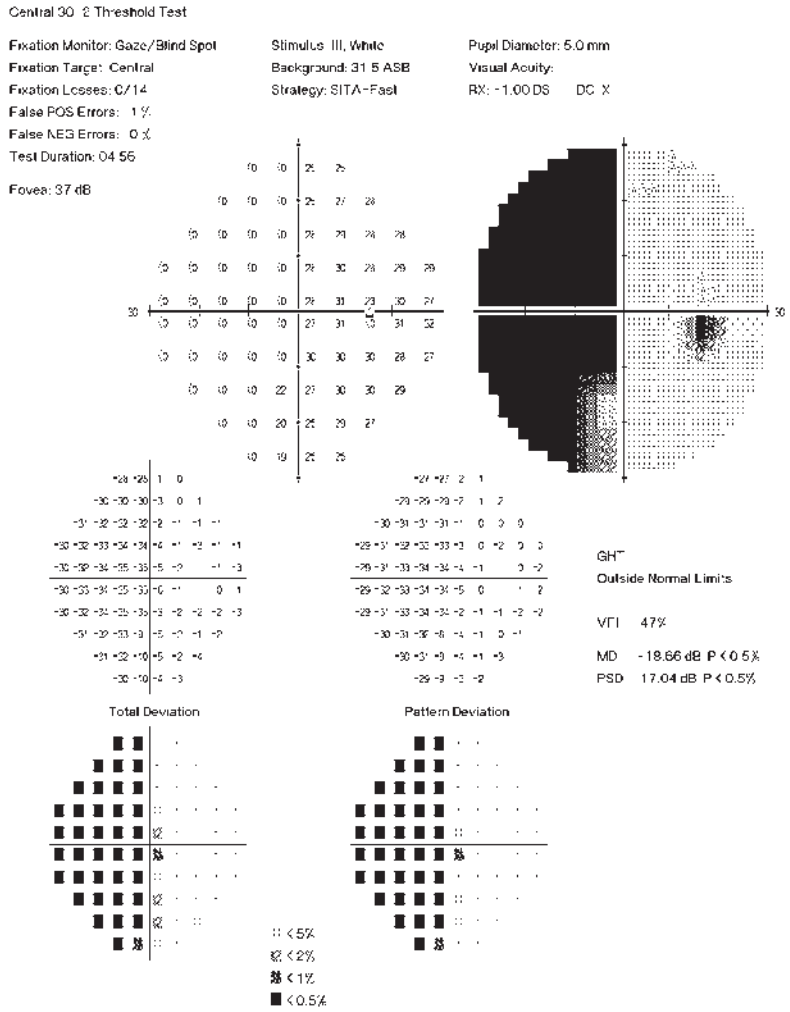

Figure 2. Example of a Humphrey Field Analyzer (HFA) test result of a right eye. Shown here is a left sided homonymous hemianopia (black = visual field loss).

Confrontational and behavioral methods

Finding a VFD is of special importance in the clinical pediatric neuro-oncological and ophthalmological practice. It may facilitate an early diagnosis of a neurological impairment or even a brain tumor. A progression in VF loss may represent a decisive finding in changing therapeutic and rehabilitation strategies, avoiding childhood blindness in some cases (Bova et al., 2008; Hart et al., 2013; Jacobson et al., 2010; Molineus et al., 2013; Pike et al., 1994; Reding & Potes, 1988; Van Genderen et al., 2012). However, VF examination in children remains a challenge (Good et al., 1994; Mohn & Van Hof-Van Duin, 1983; Porro, Hofmann, Wittebol-Post, Van Nieuwenhuizen, Van Der Schouw, et al., 1998; Wilson et al., 1991) and often leads to unreliable results (Bjerre et al., 2014; Jariyakosol & Peragallo, 2015; Morales & Brown, 2001;

Patel et al., 2015; Tschopp et al., 1998). This may partly explain why the amount of undiagnosed VFDs in children with brain tumors is high (Harbert et al., 2012; Y. Liu et al., 2019; Nuijts et al., 2022).Because modern SAP methods are often unsuccessful in children younger than 6 years, clinicians currently still resort to behavioral methods, such as confrontational methods (Koenraads et al., 2015; Mohn & Van Hof-Van Duin, 1983; Porro et al., 1998; Sheridan, 1973), binocular directional preference (Hermans et al., 1994) or kinetic double-arc perimetry (Dobson et al., 1998; Good et al., 1994) to assess these young or neurologically impaired patients. All these methods employ a stimulus which is moved from periphery to the central visual field until it elicits a response from the child. The behavioral visual field (BEFIE) screening test especially is a valuable tool in the detection of visual fields when SAP fails (Koenraads et al., 2015). This kinetic behavioral visual field test uses a white fixation target on a rod and a graded semi-circular black metal arc with a white stimulus on top which is introduced from behind the child's visual field and moved from periphery to center until the stimulus is seen (Porro et al., 1998). Despite its merit, the test requires time and a trained examiner and observer to gain the cooperation of the child and obtain reliable mono- or binocular (i.e. testing either one or two eyes simultaneously) results.

1.2.2 Objective perimetry

To circumvent some problems associated with subjective perimetry, such as the inability of the patient to communicate whether a stimulus was seen, some tests incorporate objective methods. Objective perimetry eliminates the need for a patient's psychophysical response and may thus be more suited to young and/or neurologically impaired patients. Here we will discuss three objective tests used for VF assessment in neurologically impaired patients.

Visual evoked potential (VEP)

The brain receives information from the eye to build a percept of the world. When light enters the eye, it is converted to an electrical signal by the photoreceptors in the retina, subsequently travelling through the entire visual pathway (i.e. from the eye through the optic nerve, optic chiasm, optic tract and optic radiation; see ***Figure 2*** to eventually reach the primary visual cortex (V1). The integrity of this visual pathway can be objectively and functionally measured using visual evoked potential (VEP) technology (Arruga et al., 1980; Barrett et al., 1976; Blumenhardt & Halliday, 1979; Blumhardt et al., 1977; Shagass et al., 1976). Similar to an electroencephalogram, electrodes overlaying the scalp above the primary visual cortex record the electrical potentials evoked by visual light stimuli, often consisting of flashing light-emitting diodes (LEDs), transient and steady state pattern reversal (i.e. a changing checkerboard pattern) and pattern on-/offset (Odom et al., 2016; Pail et al., 2017). Since any abnormality along the visual pathway affects the VEP's reading, it can be difficult to pinpoint small or localized lesions. These noisy measurements may thus be unable to fully dissociate patients from controls (Bengtsson & Choong, 2002). Also, before measurements can be made, the patient must cooperate for an extended time while the electrodes are applied to the scalp.

Optical coherence tomography (OCT)

Another method that could potentially serve as an objective and non-invasive alternative to subjective perimetry is optical coherence tomography (OCT), which yields high-resolution cross-sectional images of the retina and optic nerve (Fercher, 2010; Fujimoto et al., 2000). Recent studies evaluated the role of OCT in visual field assessment of neurologically impaired patients by measuring thickness of two retinal layers: retinal nerve fiber layer (RNFL) and the inner plexiform layer of the retinal ganglion cell layer (RGC-IPL) (Danesh-Meyer et al., 2008; Donaldson & Margolin, 2021; Tieger et al., 2017). Lesions in the posterior visual pathway (i.e. in the brain) can cause function loss and thinning of connected retinal layers through a process called trans-synaptic retrograde degeneration. The OCT even seemed capable in predicting VFDs of children aged 3-6 years (Bowl et al., 2018). However, traditional table-mounted OCT still requires the child's cooperation and ability to fixate their gaze and showed only moderate diagnostic accuracy (Nuijts et al., 2023).

Pupil perimetry (PP)

Another objective method uses the pupillomotor response to light stimuli as a measure of the degree of visual attention and consciousness (Naber et al., 2011, 2013; Strauch et al., 2022) or visual sensitivity. Conventional pupil perimetry (PP) methods either use an HFA perimeter or computer monitor to present the light stimuli while the pupillary response to it is measured with an infra-red eye tracker. In short, a strong pupil response is measured when a light stimulus is presented in the intact visual field, while only weak responses are evoked by stimuli in the damaged VF. Scientific evidence for its feasibility in young and/or neurologically impaired patients is limited but promising due to its simple, noninvasive and objective nature (Cibis et al., 1975; Kardon et al., 1991; Maeda et al., 2017; Naber et al., 2018;

Rajan et al., 2002; Schmid et al., 2005; Skorkovská, Wilhelm, et al., 2009; Takizawa et al., 2018). Furthermore, test duration is shorter than with SAP and, depending on the eye tracker applied, head fixation may not be necessary. Due to theoretical and technological improvements, diagnostic performance has improved since its first description in 1975. Especially its latest iteration, the PP method by Naber et al (2018), coined gaze-contingent flicker pupil perimetry, showed high diagnostic accuracy in adult hemianopic patients. Because of the above-mentioned promising characteristics, pupil perimetry will be the focus of this thesis. The next section will elaborate on how the pupillary response serves as an estimate of visual function.

1.3 The pupil as an objective measure of visual sensitivity

1.3.1 Anatomy of the visual pathway

The pupil, essentially just a hole created by the iris muscles to let through light, constricts and dilates in response to increasing and decreasing light levels. As simple as that may seem, many structures are involved in the regulation of pupil size (see Figures 2 and 3; Irene E. Loewenfeld, 1999; McDougal & Gamlin, 2015; Strauch et al., 2022). When light enters the eye through the pupil and subsequently shines upon the retina, it activates photoreceptors (i.e. rods and cones) which are situated in the outer plexiform layer. In turn, the photoreceptors activate bipolar and retinal ganglion cells, whose axons bundle to eventually form the optic nerve and enter the brain. Here the axons of the nasal hemiretina cross with axons of the other eye in the optic chiasm so that the left hemisphere receives information of the right visual field and vice versa ***(see Figure 1)***. Once the signal reaches the midbrain, multiple processes are simultaneously set in motion.
To facilitate visual processing, the majority (~90%) of the ganglion cell axons form the lateral root of the optic tract to reach the lateral geniculate nucleus (LGN) in the thalamus. The signal is then spread out through the optic radiation and eventually terminates onto the primary visual cortex (striate cortex or V1) in the occipital lobe where it and other extrastriate areas of the brain will begin to process distinct aspects of the visual information (e.g., from luminance and color to shapes and objects).

The other 10% of the ganglion cell axons make up the medial root of the optic tract which terminates in the superior colliculus (SC) and

the pretectal nuclei to eventually play a role in pupil size modulation. Pupil size is regulated by two muscles: the musculus sphincter pupillae (constriction) and the musculus dilator pupillae (dilation) of the iris. They are controlled by the antagonistic parasympathetic and sympathetic pathways of the autonomic nervous system. On the one hand, the parasympathetic pathway constricts the pupil through projection of the pretectal olivary nucleus (PON) onto the Edinger-Westphal (EW) nucleus and subsequently the ciliary ganglion of the m. sphincter pupillae. On the other, the sympathetic nervous system facilitates pupil dilation through direct retinal input to the hypothalamus which in turn projects to the intermediolateral cell column (IML) of the spinal cord. The IML then projects to the superior cervical ganglia (SCG) and the long and short ciliary nerves of the m. dilator pupillae. However, pupil size modulation is not limited to this balanced (para)sympathetic activity in response to light.

1.3.2 Cognitive effects on pupil responses

In addition to pupillary responses to luminance (i.e. the pupil light response), the pupil exhibits so-called orienting responses to several contrast modalities, such as spatial frequency (Barbur et al., 1992) and color contrast (Barbur et al., 1992; Gamlin et al., 1998; Kelbsch et al., 2019; Tsujimura et al., 2006; Walkey et al., 2005). Interestingly, both pupillary light and orienting responses are also modulated by higher-level cognitive processing (i.e. attention; Binda & Gamlin, 2017; Binda & Murray, 2015; Mathôt & Van der Stigchel, 2015; Naber et al., 2013). The pupil orienting responses are mediated by the superior colliculus (SC), which serves as a central hub for the integration of multisensory, arousal and cognitive signals (Strauch et al., 2022; Wang & Munoz, 2015), receiving sensory signals from (among others) the retina and cognitive signals from the frontal eye fields (FEF) and basal ganglia. It then projects this signal onto the EW nucleus to subsequently evoke a pupillary response. The influence of the frontoparietal attention network on the pupil presumably explains why the pupil constricts if an illusory bright stimulus, such as the sun, is shown (Binda & Murray, 2015; Laeng & Endestad, 2012; Naber & Nakayama, 2013) and pupil responses are weakened when stimuli are introduced in the blind visual fields of patients with occipital damage (Cibis et al., 1975; Kardon, 1992; Maeda et al., 2017; Naber et al., 2018; Schmid et al., 2005; Skorkovská, Wilhelm, et al., 2009). In sum, we have now learned that the pupil serves not as a simple light reflex, but rather manifests as a complex psychophysical signal that can thus be used as an objective measure of visual sensitivity.

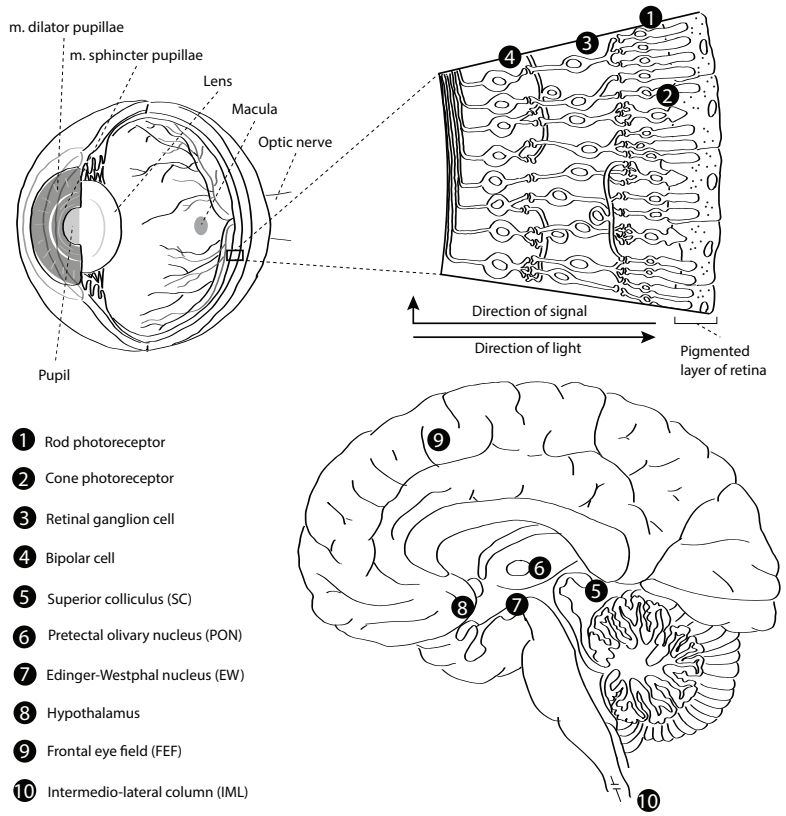

Figure 3. Schematic overview of the pupillary visual pathway: the eye, a cross-section of the retina and a sagittal view of the brain showing the structures involved in modulating pupil size.

1.4 History and evolution of pupil perimetry

1.4.1 The origins of pupil perimetry

To understand where current techniques within pupil perimetry come from and what problems remain unsolved, we first go through some important milestones ***(see Figure 4)*** in the development of pupil perimetry. Although the implementation of pupil perimetry has only recently surged, its origins go back more than 70 years. As early as 1949, German Professor Heinrich Harms first measured pupillary responses at different regions in the VF with his "Pupillenperimetrie" method (Harms, 1949). In his studies, he found reduced pupillary responses to light presented in the visual fields of patients with post-chiasmal lesions and amblyopia. His work inspired many scientists to further study the pupil as an objective measure of visual field assessment.

Another such milestone in the development of pupil perimetry was the invention of the infra-red pupillograph by Lowenstein & Loewenfeld (1958), two pioneers in the study of pupillary function. They combined

a static perimetry test with an electronic pupillograph (i.e. a device which could record pupil size). This pupillograph allowed Bresky & Charles (Bresky & Charles, 1969) to investigate the visual and pupillary thresholds in healthy subjects and patients with pre- and post-chiasmal lesions. Their research showed that visual and pupillary thresholds correlated in post-chiasmal lesions, but implementation in clinical practice at that time was hindered by time-consuming analyses of pupil traces.

After these initial discoveries, Cibis and colleagues (1975) set out to confirm Heddaeus' theory (1880) of pupillary hemiakinesia (Wernicke hemianopic phenomenon, i.e. absence of pupillary light response when the blind part of the retina is stimulated) by combining a static perimeter with a pupillograph. Their apparatus proved capable in detecting decreased – or sometimes even absent – pupillary responses to stimuli presented in the damaged VF of hemianopic patients.

This correlation between visual field loss and reduced pupillary responses sparked the interest of Thompson and colleagues (1980, 1981). They not only studied the relationship between visual field loss, pupillary defects, but also confirmed that measurements of the pupil can be objectively used as a parameter for visual field loss on a continuous scale (instead of binary; seen or not seen) by comparing pupil reactions to stimuli with results of a Goldmann perimeter.

Simultaneously, Charlier & Hache (1982) were the first to consider pupil perimetry as a clinical tool to overcome the inherent disadvantages of the existing visual field tests (i.e. discomfort, subject training and subjectivity) in practice, whereas previously the interest mainly lay

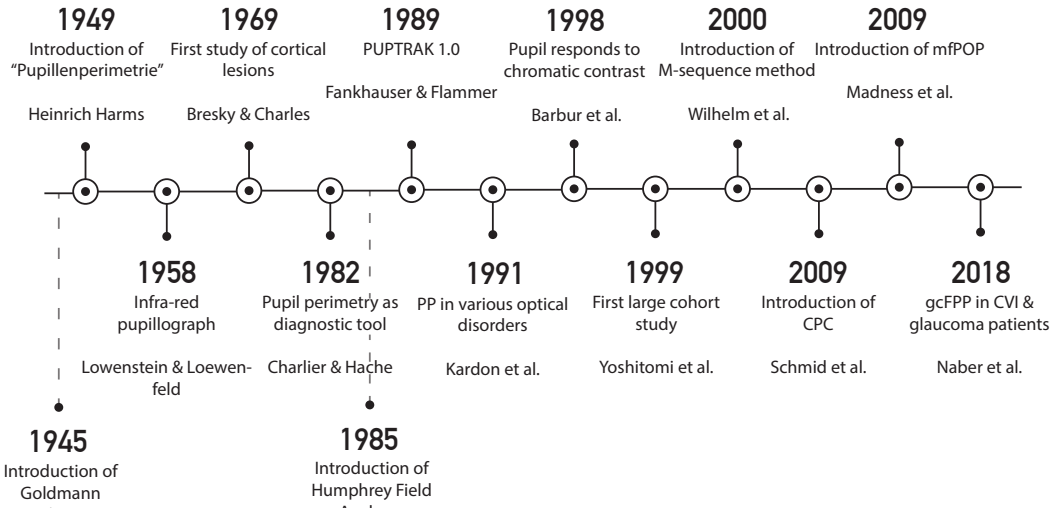

Figure 4. Timeline depicting important milestones in the development of pupil perimetry.

in the theoretical domain. Inspired by the studies conducted by Thompson and colleagues, Fankhauser & Flammer (1989) developed the PUPTRAK 1.0 which could assess the pupils monocularly. The device consisted of an Octopus 201 perimetrer, infra-red LEDs and an infra-red sensitive camera which recorded the pupil diameter. However, they still experienced difficulties in not only quantifying the miniscule pupil constrictions and dilations, but also in analyzing the large quantities of pupil data generated by the apparatus. Then, in 1991, Dr. Randy H. Kardon arose as a new pioneer in the field of pupil perimetry (Kardon et al., 1991). His team linked a computerized infra-red pupillometer which could record the eye 60 times per second (i.e. 6 to 7 times faster than the PUPTRAK 1.0) to an HFA perimeter. In doing so, measurements of all regions of the VF, even beyond the central 30 degrees, were now possible. This technological improvement marks the start of a surge in studies within the field of pupil perimetry.

1.4.2 Pupillometry in practice

In the late 90's, researchers began applying the objective pupil perimetry method to map visual field defects caused by distinct ophthalmologic diseases, such as amblyopia (Donahue et al., 1997), Leber's hereditary optic neuropathy (LHON) (Bremner et al., 1999) and autosomal dominant optic atrophy (Bremner et al., 2001). Importantly, Yoshitomi and colleagues published the first large cohort study (Yoshitomi et al., 1999) in which both SAP and Kardon's pupil perimetry method were used to assess the visual fields in patients suffering from glaucoma, postgeniculate lesions, retinitis pigmentosa, LHON, pituitary tumors, anterior ischemic optic neuropathy or functional field loss. They found overall good correlation between the two methods. However, the perceptual threshold values and pupil responses were misaligned in LHON and optic neuritis, indicating that some conditions damage pupillary input differently than they damage visual input. Nevertheless, this study signified pupil perimetry's potential clinical use in other diseases.

While the abovementioned researchers studied aberrant pupillary thresholds in patients, others impacted the field of pupillary research by conducting more basic research in rhesus monkeys and humans. These studies taught us that the pupil responds not only to luminance contrast (Ukai, 1985), but also to a multitude of contrast modalities, such as changes in spatial frequency (Barbur et al., 1992) and chromatic contrast (Barbur et al., 1998; Gamlin et al., 1998; Walkey et al., 2005). Interestingly, by mapping the normal pupillary sensitivity across the visual field in healthy subjects, Schmid, Wilhelm & Wilhelm (2000) found that the pupil responds differently to the same stimulus introduced at different visual field locations. In studying these pupillary visual field anisotropies, they systematically showed that pupil responses are strongest when introduced in the center of the visual field and decrease as retinal eccentricity increases. Additionally, stronger pupillary responses were found when stimuli are introduced in the upper and temporal hemifields. Wilhelm & colleagues not only contributed to basic knowledge of the pupil, but also introduced the m-sequence technique (Wilhelm et al., 2000) in an attempt to reduce the effect of straylight on pupil responses. The authors noticed that single stimulus presentations also scattered rays of light to neighboring retinal regions, resulting in visual sensitivity maps with low spatial resolution. This technique harnesses a complex (semi-random) mathematical pattern to simultaneously present multiple stimuli which changes at a set frequency, leading to a net luminance change of close to zero over time (and thus no detectable changes in global luminance over time). All above-mentioned findings eventually led to the development of three distinctly different pupil perimetry methods, which will be introduced in the following section.

1.4.3 Current pupil perimetry methods

Mutifocal pupillographic objective perimetry (mfPOP)

In 2009, an Australian group first introduced their multifocal pupillographic objective perimetry (mfPOP) method (Maddess et al., 2009). Their method improved on Wilhelm & colleagues' m-sequence technique (Wilhelm et al., 2000) by presenting spatially sparse multifocal stimuli in a binocular manner. Dichoptic stimulation enabled them to assess independent efferent pupil functions through measurement of both direct and consensual pupillary responses. Over the years, this group conducted many studies to improve the method's accuracy (Carle et al., 2013; James et al., 2012; Maddess et al., 2013; Rosli et al., 2018; Sabeti, James, et al., 2011) and to assess its diagnostic performance in various clinical subgroups, such as glaucoma (Carle et al., 2011, 2014, 2015; Maddess et al., 2009, 2013), age-related macular degeneration (Rai et al., 2022; Sabeti et al., 2013, 2014; Sabeti, Maddess, et al., 2011), diabetes (Bell et al., 2010; Coombes et al., 2012; Sabeti et al., 2022) and multiple sclerosis (Ali et al., 2014).

Chromatic pupil campimetry

Whereas mfPOP uses a multifocal stimulus presentation, a German group developed the unifocal chromatic pupil campimetry (CPC)

method, an adoption of the pupil campimetry method (Schmid et al., 2005). It combines focal with chromatic stimulation through the use of single (instead of the multiple stimuli used in mfPOP) chromatic light stimuli of adjustable size, intensity and wavelength to assess photoreceptor-specific retinal function (Kelbsch et al., 2020). They showed the method could distinguish patients with retinitis pigmentosa from participants with feigned VF loss (Skorkovská, Lüdtke, et al., 2009), but also found that pupil campimetry was capable of assessing changes in pupillary sensitivity in patients with pre- and retrogeniculate lesions (Maeda et al., 2017; Skorkovská, Wilhelm, et al., 2009), glaucoma (Kelbsch et al., 2016) and exudative age-related macular degeneration (Kelbsch et al., 2020).

Gaze-contingent flicker pupil perimetry (gcFPP)

The most recent method was introduced in 2018 by Naber & colleagues (Naber et al., 2018). Similar to the CPC method it uses a unifocal stimulus presentation, but instead of a single stimulus presentation, the stimulus flickers black-and-white at a 2 Hz frequency. The evoked phasic pupillary responses served not only to increase reliability, but also to measure multiple pupil latencies and response amplitudes in a shorter amount of time ***(see Figure 5)***. Additionally, fixation problems were prevented by using a gaze-contingent stimulus presentation. Accurate retinotopic stimulation

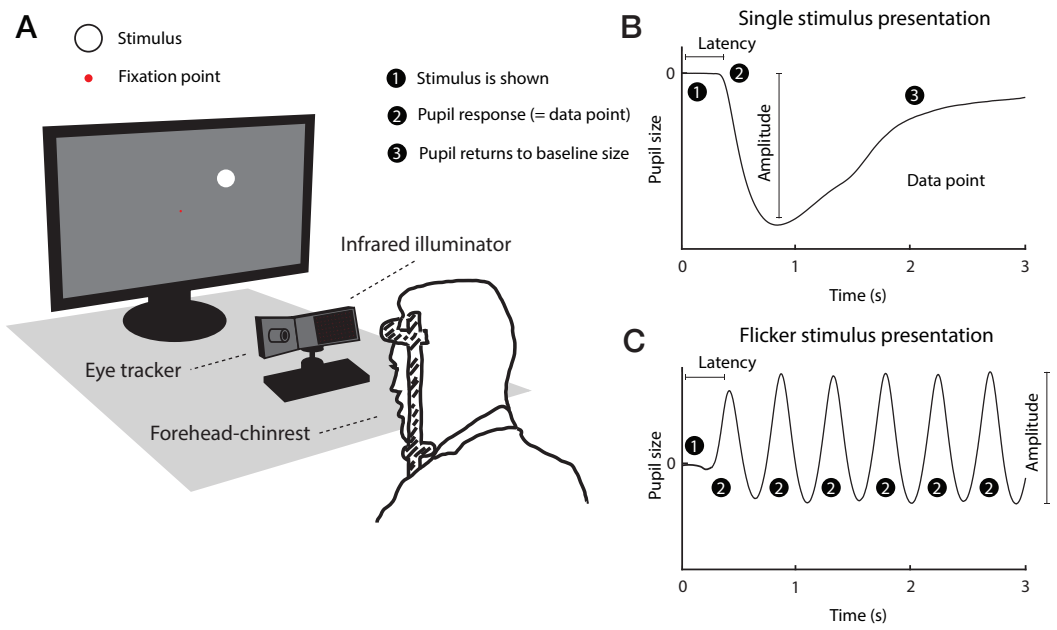

Figure 5. Schematic (A) showing a pupil perimetry set-up with a patient situated in a forehead-chinrest with a mounted eye tracker and before a monitor which depicts a red fixation point and a white light stimulus. The plot in (B) shows the pupillary response to a single stimulus where pupil size decreases from its baseline pupil size (i.e. amplitude) following stimulation after a certain latency period, while (C) shows the oscillatory pupil response to a flickering stimulus. Notice it creates multiple datapoints as opposed to a single stimulus presentation.

could then be ensured by correcting for saccades online. Finally, a covert attention task was implemented to evoke stronger pupillary responses (Binda et al., 2013; Mathôt et al., 2013; Naber et al., 2013). The gaze-contingent flicker pupil perimetry (gcFPP) method found high accuracy and showed particular promise for the objective visual field assessment in neurologically impaired patients.

1.5 Aims and outline of this thesis

This thesis aimed to develop an objective and reliable tool for the early diagnosis of visual field defects in young and/or neurologically impaired patients as addition to the current diagnostic work-up since this is a patient population in which the current gold standard for visual field assessment (standard automated perimetry or SAP) is not always suited and feasible alternatives are sparse.

In **chapter 2** we retrospectively assess the reliability of current VF tests in neurologically impaired children and stress the need for an alternative testing method. Then, in **chapter 3**, we introduce an objective alternative, called pupil perimetry (PP), and conduct an in-depth comparison of three distinct PP methods. Subsequently, **chapter 4** benchmarks the method which performed best in chapter 3, i.e. gaze-contingent flicker pupil perimetry (gcFPP), in healthy individuals by detecting the blind spot and visual field anisotropies. **Chapter 5** further improves on the design of gcFPP through the introduction of a chromatic component to the stimulus design and seeks to find the optimal trade-off between luminance and color contrast to elicit strong and robust pupillary responses in healthy adults. Then, **chapter 6** further tries to improve pupillary responses and diagnostic performance of gcFPP through alterations in global and local color contrast and luminance in neurologically impaired adults. After introducing the various improvements made in the previous chapters, **chapter 7** investigates the diagnostic performance of the gcFPP method and a newly developed virtual reality version of the gcFPP method, VRgcFPP, in neurologically impaired adults by assessing diagnostic accuracy and test-retest reliability. After establishing its performance in adults, **chapter 8** evaluates the feasibility of the novel VRgcFPP method in healthy young children and investigates which fixation task best captures the child's attention while also evoking robust pupillary responses. Finally, in **chapter 9** we discuss the critical findings of the studies included in this thesis, elaborate on some possible future directions and end with a summary for your convenience.

1.6 References

Ali, E. N., Maddess, T., James, A. C., Voicu, C., & Lueck, C. J. (2014). Pupillary response to sparse multfocal stimuli in multiple sclerosis patients. *Multiple Sclerosis Journal, 20*(7), 854–861. https://doi.org/10.1177/1352458513512708

Anderson, A. J., Shuey, N. H., & Wall, M. (2009). Rapid confrontation screening for peripheral visual field defects and extinction. *Clinical and Experimental Optometry, 92*(1). https://doi.org/10.1111/j.1444-0938.2008.00280.x

Arruga, J., Feldon, S. E., Hoyt, W. F., & Aminoff, M. J. (1980). Monocularly and binocularly evoked visual responses to patterned half-field stimulation. *Journal of the Neurological Sciences, 46*(3). https://doi.org/10.1016/0022-510X(80)90052-0

Artes, P. H., Iwase, A., Ohno, Y., Kitazawa, Y., & Chauhan, B. C. (2002). Properties of perimetric threshold estimates from full threshold, SITA standard, and SITA fast strategies. *Investigative Ophthalmology and Visual Science, 43*(8), 2654–2659. https://iovs.arvojournals.org/article.aspx?articleid=2124008

Barbur, Harlow, & Sahraie. (1992). Pupillary responses to stimulus structure, colour and movement. *Ophthalmic and Physiological Optics, 12*(2), 137–141. https://doi.org/10.1111/j.1475-1313.1992.tb00276.x

Barbur, Wolf, & Lennie. (1998). Visual processing levels revealed by response latencies to changes in different visual attributes. *Proceedings of the Royal Society B: Biological Sciences, 265*(1412), 2321–2325. https://doi.org/10.1098/rspb.1998.0578

Barrett, G., Blumhardt, L., Halliday, A. M., Halliday, E., & Kriss, A. (1976). A paradox in the lateralisation of the visual evoked response. *Nature, 261*(5557). https://doi.org/10.1038/261253a0

Bell, A., James, A. C., Kolic, M., Essex, R. W., & Maddess, T. (2010). Dichoptic Multifocal Pupillography Reveals Afferent Visual Field Defects in Early Type 2 Diabetes. *Investigative Ophthalmology & Visual Science, 51*(1), 602–608. https://doi.org/10.1167/iovs.09-3659

Bengtsson, B., & Choong, Y. F. (2002). Evaluation of VEP perimetry in normal subjects and glaucoma patients. *Acta Ophthalmologica Scandinavica, 80*(6). https://doi.org/10.1034/j.1600-0420.2002.800612.x

Binda, P., & Gamlin, P. D. (2017). Renewed Attention on the Pupil Light Reflex. In *Trends in Neurosciences* (Vol. 40, Issue 8, pp. 455–457). NIH Public Access. https://doi.org/10.1016/j.tins.2017.06.007

Binda, P., & Murray, S. O. (2015). Keeping a large-pupilled eye on high-level visual processing. In *Trends in Cognitive Sciences* (Vol. 19, Issue 1, pp.1–3). Trends Cogn Sci. https://doi.org/10.1016/j.tics.2014.11.002

Binda, P., Pereverzeva, M., & Murray, S. O. (2013). Attention to bright surfaces enhances the pupillary light reflex. *Journal of Neuroscience, 33*(5), 2199–2204. https://doi.org/10.1523/JNEUROSCI.3440-12.2013

Bjerre, A., Codina, C., & Griffiths, H. (2014). Peripheral Visual Fields in Children and Young Adults Using Semi-automated Kinetic Perimetry: Feasibility of Testing, Normative Data, and Repeatability. *Neuro-Ophthalmology, 38*(4), 189–198. https://doi.org/10.3109/01658107.2014.902971

Blumenhardt, L. D., & Halliday, A. M. (1979). Hemisphere contributions to the composition of the pattern-evoked potential waveform. *Experimental Brain Research, 36*(1). https://doi.org/10.1007/BF00238467

Blumhardt, L. D., Barrett, G., & Halliday, A. M. (1977). The asymmetrical visual evoked potential to pattern reversal in one half field and its significance for the analysis of visual field defects. *British Journal of Ophthalmology, 61*(7). https://doi.org/10.1136/bjo.61.7.454

Boonstra, N., Limburg, H., Tijmes, N., Van Genderen, M., Schuil, J., & Van Nispen, R. (2012). Changes in causes of low vision between 1988 and 2009 in a Dutch population of children. *Acta Ophthalmologica, 90*(3). https://doi.org/10.1111/j.1755-3768.2011.02205.x

Bourne, R. R. A., Steinmetz, J. D., Saylan, M., Mersha, A. M., Weldemariam, A. H., Wondmeneh, T. G., Sreeramareddy, C. T., Pinheiro, M., Yaseri, M., Yu, C., Zastrozhin, M. S., Zastrozhina, A., Zhang, Z. J., Zimsen, S. R. M., Yonemoto, N., Tsegaye, G. W., Vu, G. T., Vongpradith, A., Renzaho, A. M. N., … Vos, T. (2021). Causes of blindness and vision impairment in 2020 and trends over 30 years, and prevalence of avoidable blindness in relation to VISION 2020: The Right to Sight: An analysis for the Global Burden of Disease Study. *The Lancet Global Health, 9*(2). https://doi.org/10.1016/S2214-109X(20)30489-7

Bova, S. M., Giovenzana, A., Signorini, S., La Piana, R., Uggetti, C., Bianchi, P. E., & Fazzi, E. (2008). Recovery of visual functions after early acquired occipital damage. *Developmental Medicine & Child Neurology, 50*(4), 311–315. https://doi.org/10.1111/j.1469-8749.2008.02044.x

Bowl, W., Knobloch, R., Schweinfurth, S., Holve, K., Stieger, K., & Lorenz, B. (2018). Structure-Function Correlation in Hemianopic Vision Loss in Children Aged 3-6 Years Using OCT and SVOP, and Comparison with Adult Eyes. *Ophthalmic Research, 60*(4), 221–230. https://doi.org/10.1159/000480296

Bremner, F. D., Shallo-Hoffmann, J., Riordan-Eva, P., & Smith, S. E. (1999). Comparing pupil function with visual function in patients with Leber's hereditary optic neuropathy. *Investigative Ophthalmology and Visual Science, 40*(11).

Bremner, F. D., Tomlin, E. A., Shallo-Hoffmann, J., Votruba, M., & Smith, S. E. (2001). The pupil in dominant optic atrophy. *Investigative Ophthalmology and Visual Science, 42*(3).

Bresky, R. H., & Charles, S. (1969). Pupil motor perimetry. *American Journal of Ophthalmology, 68*(1). https://doi.org/10.1016/0002-9394(69)94941-1

Breu, F., Guggenbichler, S., & Wollmann, J. (2008). NHMRC Guidelines for the Screening, Prognosis, Diagnosis, Management and Prevention of Glaucoma. *Vasa, 7*.

Carle, C. F., James, A. C., Kolic, M., Essex, R. W., & Maddess, T. (2014). Luminance and colour variant pupil perimetry in glaucoma. *Clinical & Experimental Ophthalmology, 42*(9), 815–824. https://doi.org/10.1111/ceo.12346

Carle, C. F., James, A. C., Kolic, M., Essex, R. W., & Maddess, T. (2015). Blue multifocal pupillographic objective perimetry in glaucoma. *Investigative Ophthalmology and Visual Science, 56*(11), 6394–6403. https://doi.org/10.1167/iovs.14-16029

Carle, C. F., James, A. C., Kolic, M., Loh, Y.-W. W., & Maddess, T. (2011). High-Resolution Multifocal Pupillographic Objective Perimetry in Glaucoma. *Investigative Ophthalmology & Visual Science, 52*(1), 604–610. https://doi.org/10.1167/iovs.10-5737

Carle, C. F., James, A. C., & Maddess, T. (2013). The pupillary response to color and luminance variant multifocal stimuli. *Investigative Ophthalmology and Visual Science, 54*(1), 467–475. https://doi.org/10.1167/iovs.12-10829

Charlier, J. R., & Hache, J. C. (1982). New instrument for monitoring eye fixation and pupil size during the visual field examination. *Medical & Biological Engineering & Computing, 20*(1). https://doi.org/10.1007/BF02441846

Cibis, G. W., Campos, E. C., & Aulhorn, E. (1975). Pupillary Hemiakinesia in Suprageniculate Lesions. *Archives of Ophthalmology, 93*(12). https://doi.org/10.1001/archopht.1975.01010020954004

Classé, J. G. (1989). Legal aspects of visual field assessment. *Journal of the American Optometric Association, 60*(12).

Coombes, C., Sabeti, F., Baker, L., Cheung, V., Chiou, M., Kolic, M., James, A., Nolan, C., & Maddess, T. (2012). Clinical utility of multifocal pupillographic objective perimetry in type 1 diabetes. *Clinical and Experimental Ophthalmology, 40*(15), 108. https://iovs.arvojournals.org/article.aspx?articleid=2146849

Danesh-Meyer, H. V., Papchenko, T., Savino, P. J., Law, A., Evans, J., & Gamble, G. D. (2008). In vivo retinal nerve fiber layer thickness measured by optical coherence tomography predicts visual recovery after surgery for parachiasmal tumors. *Investigative Ophthalmology and Visual Science, 49*(5). https://doi.org/10.1167/iovs.07-1127

Dobson, V., Brown, A. M., Harvey, E. M., & Narter, D. B. (1998). Visual field extent in children 3.5-30 months of age tested with a double-arc LED perimeter. *Vision Research, 38*(18). https://doi.org/10.1016/S0042-6989(97)00437-9

Donahue, S. P., Moore, P., & Kardon, R. H. (1997). Automated pupil perimetry in amblyopia: Generalized depression in the involved eye. *Ophthalmology, 104*(12), 2161–2167. https://doi.org/10.1016/S0161-6420(97)30046-3

Donaldson, L., & Margolin, E. (2021). Visual fields and optical coherence tomography (OCT) in neuro-ophthalmology: Structure-function correlation. In *Journal of the Neurological Sciences* (Vol. 429). https://doi.org/10.1016/j.jns.2021.118064

Fankhauser, F., & Flammer, J. (1989). Puptrak 1.0 - a new semiautomated system for pupillometry with the Octopus perimeter: A preliminary report. *Documenta Ophthalmologica, 73*(3). https://doi.org/10.1007/BF00155093

Fercher, A. F. (2010). Optical coherence tomography – development, principles, applications. *Zeitschrift Für Medizinische Physik, 20*(4). https://doi.org/10.1016/j.zemedi.2009.11.002

Fredette, M. J., Giguère, A., Anderson, D. R., Budenz, D. L., & McSoley, J. (2015). Comparison of matrix with humphrey field analyzer II with SITA. *Optometry and Vision Science, 92*(5). https://doi.org/10.1097/OPX.0000000000000583

Fujimoto, J. G., Pitris, C., Boppart, S. A., & Brezinski, M. E. (2000). Optical coherence tomography: An emerging technology for biomedical imaging and optical biopsy. In *Neoplasia* (Vol. 2, Issues 1–2). https://doi.org/10.1038/sj.neo.7900071

Gamlin, P. D. R., Zhang, H., Harlow, A., & Barbur, J. L. (1998). Pupil responses to stimulus color, structure and light flux increments in the rhesus monkey. *Vision Research, 38*(21), 3353–3358. https://doi.org/10.1016/S0042-6989(98)00096-0

Good, W. V, Jan, J. E., DeSa, L., Barkovich, A. J., Groenveld, M., & Hoyt, C. S. (1994). Cortical visual impairment in children. *Survey of Ophthalmology, 38*(4), 351–364. https://doi.org/10.1016/0039-6257(94)90073-6

Goodwin, D. (2014). Homonymous hemianopia: Challenges and solutions. In *Clinical Ophthalmology* (Vol. 8). https://doi.org/10.2147/OPTH.S59452

Gutteridge, I. F. (1985). Should visual field examination be a routine part of ophthalmic practice? *Documenta Ophthalmologica, 59*(4). https://doi.org/10.1007/BF00159167

Harbert, M. J., Yeh-Nayre, L. A., O'Halloran, H. S., Levy, M. L., & Crawford, J. R. (2012). Unrecognized visual field deficits in children with primary central nervous system brain tumors. *Journal of Neuro-Oncology, 107*(3), 545–549. https://doi.org/10.1007/s11060-011-0774-3

Harms, H. (1949). Grundlagen, Methodik und Bedeutung der Pupillenperimetrie für die Physiologie und Pathologie des Sehorgans. *Albrecht von Graefes Archiv Für Ophthalmologie Vereinigt Mit Archiv Für Augenheilkunde, 149*(1–3). https://doi.org/10.1007/BF00684506

Hart, M. G., Sarkies, N. J., Santarius, T., & Kirollos, R. W. (2013). Ophthalmological outcome after resection of tumors based on the pineal gland. *Journal of Neurosurgery, 119*(2), 420–426. https://doi.org/10.3171/2013.3.JNS122137

Heijl, A. (2012). The Field Analyzer Primer: Effective Perimetry. In *Carl Zeiss Meditec, Inc.*

Heijl, A., Patella, V. M., & Bengtsson, B. (2012). The Field Analyzer Primer. In *Effective Perimetry*.

Hermans, A. J. M., Van Hof-Van Duin, J., & Oudesluys-Murphy, A. M. (1994). Visual outcome of low-birth-weight infants (1500-2500 g) at one year of corrected age. *Acta Paediatrica, International Journal of Paediatrics, 83*(4). https://doi.org/10.1111/j.1651-2227.1994.tb18128.x

Irene E. Loewenfeld. (1999). *The pupil: Anatomy, physiology and clinical applications.* (2nd edition). Butterworth-Heinemann.

Ivers, R. Q., Cumming, R. G., Mitchell, P., & Attebo, K. (1998). Visual impairment and falls in older adults: The blue mountains eye study. *Journal of the American Geriatrics Society, 46*(1). https://doi.org/10.1111/j.1532-5415.1998.tb01014.x

Jacobson, L., Rydberg, A., Eliasson, A.-C., Kits, A., & Flodmark, O. (2010). Visual field function in school-aged children with spastic unilateral cerebral palsy related to different patterns of brain damage. *Developmental Medicine & Child Neurology, 52*(8), e184–e187. https://doi.org/10.1111/j.1469-8749.2010.03650.x

James, A. C., Kolic, M., Bedford, S. M., & Maddess, T. (2012). Stimulus parameters for multifocal pupillographic objective perimetry. *Journal of Glaucoma, 21*(9), 571–578. https://doi.org/10.1097/IJG.0b013e31821e8413

Jariyakosol, S., & Peragallo, J. H. (2015). The Effects of Primary Brain Tumors on Vision and Quality of Life in Pediatric Patients. *Seminars in Neurology, 35*(5). https://doi.org/10.1055/s-0035-1563571

Johnson, C. A., Wall, M., & Thompson, H. S. (2011). A history of perimetry and visual field testing. In *Optometry and Vision Science* (Vol. 88, Issue 1). https://doi.org/10.1097/OPX.0b013e3182004c3b

Kardon, R. H. (1992). Pupil perimetry. In *Current Opinion in Ophthalmology* (Vol. 3, Issue 5, pp. 565–570). https://doi.org/10.1097/00055735-199210000-00002

Kardon, R. H., Kirkali, P. A., & Thompson, H. S. (1991). Automated Pupil Perimetry Pupil Field Mapping in Patients and Normal Subjects. *Ophthalmology, 98*(4), 485–496. https://doi.org/10.1016/S0161-6420(91)32267-X

Kelbsch, C., Lange, J., Wilhelm, H., Wilhelm, B., Peters, T., Kempf, M., Kuehlewein, L., & Stingl, K. (2020). Chromatic pupil campimetry reveals functional defects in exudative age-related macular degeneration with differences related to disease activity. *Translational Vision Science and Technology, 9*(6), 5–5. https://doi.org/10.1167/tvst.9.6.5

Kelbsch, C., Maeda, F., Strasser, T., Blumenstock, G., Wilhelm, B., Wilhelm, H., & Peters, T. (2016). Pupillary responses driven by ipRGCs and classical photoreceptors are impaired in glaucoma. *Graefe's Archive for Clinical and Experimental Ophthalmology, 254*(7), 1361–1370. https://doi.org/10.1007/s00417-016-3351-9

Kelbsch, C., Stingl, K., Kempf, M., Strasser, T., Jung, R., Kuehlewein, L., Wilhelm, H., Peters, T., Wilhelm, B., & Stingl, K. (2019). Objective measurement of local rod and cone function using gaze-controlled chromatic pupil campimetry in healthy subjects. *Translational Vision Science and Technology, 8*(6). https://doi.org/10.1167/tvst.8.6.19

Koenraads, Y., Braun, K. P. J., van der Linden, D. C. P., Imhof, S. M., & Porro, G. L. (2015). Perimetry in young and neurologically impaired children: the Behavioral Visual Field (BEFIE) Screening Test revisited *JAMA Ophthalmology, 133*(3), 319–325. https://doi.org/10.1001/jamaophthalmol.2014.5257

Kong, L., Fry, M., Al-Samarraie, M., Gilbert, C., & Steinkuller, P. G. (2012). An update on progress and the changing epidemiology of causes of childhood blindness worldwide. *Journal of AAPOS, 16*(6). https://doi.org/10.1016/j.jaapos.2012.09.004

Laeng, B., & Endestad, T. (2012). Bright illusions reduce the eye's pupil. *Proceedings of the National Academy of Sciences of the United States of America, 109*(6), 2162–2167. https://doi.org/10.1073 pnas.1118298109

Landers, J., Sharma, A., Goldberg, I., & Graham, S. L. (2010). Comparison of visual field sensitivities between the Medmont automated perimeter and the Humphrey field analyser. *Clinical and Experimental Ophthalmology, 38*(3). https://doi.org/10.1111/j.1442-9071.2010.02246.x

Liu, G. T., & Galetta, S. L. (1997). Homonymous hemifield loss in childhood. *Neurology, 49*(6). https://doi.org/10.1212/WNL.49.6.1748

Liu, Y., Abongwa, C., Ashwal, S., Deming, D. D., & Winter, T. W. (2019). Referral for Ophthalmology Evaluation and Visual Sequelae in Children with Primary Brain Tumors. *JAMA Network Open, 2*(8). https://doi.org/10.1001/jamanetworkopen.2019.8273

Maddess, T., Bedford, S. M., Goh, X. L., & James, A. C. (2009). Multifocal pupillographic visual field testing in glaucoma. *Clinical & Experimental Ophthalmology, 37*(7), 678–686. https://doi.org/10.1111/j.1442-9071.2009.02107.x

Maddess, T., Essex, R. . W., Kolic, M., Carle, C. F. ., & James, A. C. (2013). High- versus low-density multifocal pupillographic objective perimetry in glaucoma. *Clinical & Experimental Ophthalmology, 41*(2), 140–147. https://doi.org/10.1111/ceo.12016

Maeda, F., Kelbsch, C., Straßer, T., Skorkovská, K., Peters, T., Wilhelm, B., & Wilhelm, H. (2017). Chromatic pupillography in hemianopia patients with homonymous visual field defects. *Graefe's Archive for Clinical and Experimental Ophthalmology, 255*(9), 1837–1842. https://doi.org/10.1007/s00417-017-3721-y

Mathôt, S., van der Linden, L., Grainger, J., & Vitu, F. (2013). The pupillary light response reveals the focus of covert visual attention. *PloS One, 8*(10). https://doi.org/10.1371/journal.pone.0078168

Mathôt, S., & Van der Stigchel, S. (2015). New Light on the Mind's Eye: The Pupillary Light Response as Active Vision. *Current Directions in Psychological Science, 24*(5), 374–378. https://doi.org/10.1177/0963721415593725

McDougal, D. H., & Gamlin, P. D. (2015). Autonomic control of the eye. *Comprehensive Physiology, 5*(1). https://doi.org/10.1002/cphy.c140014

Mohn, G., & Van Hof-Van Duin, J. (1983). Behavioural and electrophysiological measures of visual functions in children with neurological disorders. *Behavioural Brain Research, 10*(1). https://doi.org/10.1016/0166-4328(83)90163-8

Molineus, A., Boxberger, N., Redlich, A., & Vorwerk, P. (2013). Time to diagnosis of brain tumors in children: A single-centre experience. *Pediatrics International, 55*(3), 305–309. https://doi.org/10.1111/ped.12095

Morales, J., & Brown, S. M. (2001). The feasibility of short automated static perimetry in children. *Ophthalmology, 108*(1), 157–162. https://doi.org/10.1016/S0161-6420(00)00415-2

Murray, I. C., Fleck, B. W., Brash, H. M., Macrae, M. E., Tan, L. L., & Minns, R. A. (2009). Feasibility of saccadic vector optokinetic perimetry: a method of automated static perimetry for children using eye tracking. *Ophthalmology, 116*(10), 2017–2026. https://doi.org/10.1016/j.ophtha.2009.03.015

Naber, M., Alvarez, G. A., & Nakayama, K. (2013). Tracking the allocation of attention using human pupillary oscillations. *Frontiers in Psychology, 4*, 919. https://doi.org/10.3389/fpsyg.2013.00919

Naber, M., Frässle, S., & Einhäuser, W. (2011). Perceptual rivalry: Reflexes reveal the gradual nature of visual awareness. *PLoS ONE, 6*(6), e20910. https://doi.org/10.1371/journal.pone.0020910

Naber, M., & Nakayama, K. (2013). Pupil responses to high-level image content. *Journal of Vision, 13*(6), 7–7. https://doi.org/10.1167/13.6.7

Naber, M., Roelofzen, C., Fracasso, A., Bergsma, D. P., van Genderen, M., Porro, G. L., Dumoulin, S. O., & van der Schouw, Y. T. (2018). Gaze-Contingent Flicker Pupil Perimetry Detects Scotomas in Patients With Cerebral Visual Impairments or Glaucoma. *Frontiers in Neurology, 9*(July), 558. https://doi.org/10.3389/fneur.2018.00558

Nuijts, M. A., Stegeman, I., Porro, G. L., Bennebroek, C. A. M., van Seeters, T., Proudlock, F. A., Schouten – van Meeteren, A. Y. N., & Imhof, S. M. (2023). Diagnostic accuracy of retinal optical coherence tomography in children with a newly diagnosed brain tumour. *Acta Ophthalmologica, n/a*(n/a). https://doi.org/https://doi.org/10.1111/aos.15650

Nuijts, M. A., Stegeman, I., Van Seeters, T., Borst, M. D., Bennebroek, C. A. M., Buis, D. R., Naus, N. C., Porro, G. L., Van Egmond-Ebbeling, M. B., Voskuil-Kerkhof, E. S. M., Pott, J. R., Franke, N. E., De Vos-Kerkhof, E., Hoving, E. W., Schouten-Van Meeteren, A. Y. N., & Imhof, S. M. (2022). Ophthalmological Findings in Youths With a Newly Diagnosed Brain Tumor. *JAMA Ophthalmology, 140*(10), 982–993. https://doi.org/10.1001/JAMAOPHTHALMOL.2022.3628

Odom, J. V., Bach, M., Brigell, M., Holder, G. E., McCulloch, D. L., Mizota, A., & Tormene, A. P. (2016). ISCEV standard for clinical visual evoked potentials: (2016 update). *Documenta Ophthalmologica, 133*(1). https://doi.org/10.1007/s10633-016-9553-y

Pail, M., Goldemundová, S., Skorkovská, K., & Brázdil, M. (2017). Neurological and neuropsychological investigation in patients with homonymous visual field defects. In *Homonymous Visual Field Defects.* https://doi.org/10.1007/978-3-319-52284-5_10

Patel, D. E., Cumberland, P. M., Walters, B. C., Russell-Eggitt, I., Rahi, J. S., & OPTIC study group, O. study. (2015). Study of Optimal Perimetric Testing in Children (OPTIC): Feasibility, Reliability and Repeatability of Perimetry in Children. *PloS One, 10*(6), e0130895. https://doi.org/10.1371/journal.pone.0130895

Phu, J., Khuu, S. K., Yapp, M., Assaad, N., Hennessy, M. P., & Kalloniatis, M. (2017). The value of visual field testing in the era of advanced imaging: clinical and psychophysical perspectives. In *Clinical and Experimental Optometry* (Vol. 100, Issue 4). https://doi.org/10.1111/cxo.12551

Pierre-Filho, P. de T. P., Schimiti, R. B., Cabral de Vasconcellos, J. P., & Costa, V. P. (2006). Sensitivity and specificity of frequency-doubling technology, tendency-oriented perimetry, SITA Standard and SITA Fast perimetry in perimetrically inexperienced individuals. *Acta Ophthalmologica Scandinavica, 84*(3), 345–350. https://doi.org/10.1111/j.1600-0420.2006.00639.x

Pike, M. G., Holmstrom, G., Vries, L. S., Pennock, J. M., Drew, K. J., Sonksen, P. M., & Dubowitz, L. M. S. (1994). Patterns Of Visual Impairment Associated With Lesions Of The Preterm Infant Brain. *Developmental Medicine & Child Neurology, 36*(10), 849–862. https://doi.org/10.1111/j.1469-8749.1994.tb11776.x

Piltz, J. R., & Starita, R. J. (1990). Test-retest variability in glaucomatous visual fields. In *American Journal of Ophthalmology* (Vol. 109, Issue 1, pp. 109–110). https://doi.org/10.1016/s0002-9394(14)75602-8

Porro, G., Hofmann, J., Wittebol-Post, D., Van Nieuwenhuizen, O., Schouw, Y. T. Van Der, Schilder, M. B. H. H., Dekker, M. E. M. M., & Treffers, W. F. (1998). A new behavioral visual field test for clinical use in pediatric neuro-ophthalmology. *Neuro-Ophthalmology, 19*(4), 205–214. https://doi.org/10.1076noph.19.4.205.3939

Rai, B. B., Sabeti, F., Carle, C. F., Rohan, E. M., van Kleef, J. P., Essex, R. W., Barry, R. C., & Maddess, T. (2022). Rapid Objective Testing of Visual Function Matched to the ETDRS Grid and Its Diagnostic Power in Age-Related Macular Degeneration. *Ophthalmology Science, 2*(2). https://doi.org/10.1016/j.xops.2022.100143

Rajan, M. S., Bremner, F. D., & Riordan-Eva, P. (2002). Pupil perimetry in the diagnosis of functional visual field loss. *Journal of the Royal Society of Medicine, 95*(10), 498–500. https://doi.org/10.1258/jrsm.95.10.498

Ramrattan, R. S., Wolfs, R. C. W., Panda-Jonas, S., Jonas, J. B., Bakker, D., Pols, H. A., Hofman, A., & De Jong, P. T. V. M. (2001). Prevalence and causes of visual field loss in the elderly and associations with impairment in daily functioning: The Rotterdam Study. *Archives of Ophthalmology, 119*(12). https://doi.org/10.1001/archopht.119.12.1788

Reding, M. J., & Potes, E. (1988). Rehabilitation outcome following initial unilateral hemispheric stroke: Life Table Analysis Approach. *Stroke, 19*(11). https://doi.org/10.1161/01.STR.19.11.1354

Rosli, Y., Carle, C. F., Ho, Y., James, A. C., Kolic, M., Rohan, E. M. F., & Maddess, T. (2018). Retinotopic effects of visual attention revealed by dichoptic multifocal pupillography. *Scientific Reports 2018 8:1, 8*(1), 1–13. https://doi.org/10.1038/s41598-018-21196-1

Rowe, F. (2008). Visual Fields via the Visual Pathway. In *Visual Fields via the Visual Pathway.* https://doi.org/10.1002/9780470759271

Sabeti, F., Carle, C. F., Nolan, C. J., Jenkins, A. J., James, A. C., Baker, L., Coombes, C. E., Cheung, V., Chiou, M., & Maddess, T. (2022). Multifocal pupillographic objective perimetry for assessment of early diabetic retinopathy and generalised diabetes-related tissue injury in persons with type 1 diabetes. *BMC Ophthalmology 2022 22:1, 22*(1), 1–13. https://doi.org/10.1186/S12886-022-02382-2

Sabeti, F., James, A. C., Essex, R. W., & Maddess, T. (2013). Multifocal pupillography identifies retinal dysfunction in early age-related macular degeneration. *Graefe's Archive for Clinical and Experimental Ophthalmology, 251*(7), 1707–1716. https://doi.org/10.1007/s00417-013-2273-z

Sabeti, F., James, A. C., & Maddess, T. (2011). Spatial and temporal stimulus variants for multifocal pupillography of the central visual field. *Vision Research 51*(2), 303–310. https://doi.org/10.1016/J.VISRES.2010.10.015

Sabeti, F., Maddess, T., Essex, R. W., & James, A. C. (2011). Multifocal pupillographic assessment of age-related macular degeneration. *Optometry and Vision Science, 88*(12), 1477–1485. https://doi.org/10.1097/OPX.0b013e318235af61

Sabeti, F., Maddess, T., Essex, R. W., Saikal, A., James, A. C., & Carle, C. F. (2014). Multifocal pupillography in early age-related macular degeneration. *Optometry and Vision Science, 91*(8), 904–915. https://doi.org/10.1097/OPX.0000000000000319

Schmid, R., Luedtke, H., Wilhelm, B. J., & Wilhelm, H. (2005). Pupil campimetry in patients with visual field loss. *European Journal of Neurology, 12*(8), 602–608. https://doi.org/10.1111/j.1468-1331.2005.01048.x

Shagass, C., Amadeo, M., & Roemer, R. A. (1976). Spatial distribution of potentials evoked by half-field pattern-reversal and pattern-onset stimuli. *Electroencephalography and Clinical Neurophysiology, 41*(6). https://doi.org/10.1016/0013-4694(76)90006-7

Sheridan, M. D. (1973). The STYCAR Graded-balls Vision Test. *Developmental Medicine & Child Neurology,15*(4). https://doi.org/10.1111/j.1469-8749.1973.tb05062.x

Sherwood, M. B., Garcia-Siekavizza, A., Meltzer, M. I., Hebert, A., Burns, A. F., & McGorray, S. (1998). Glaucoma's impact on quality of life and its relation to clinical indicators: A pilot study. *Ophthalmology, 105*(3). https://doi.org/10.1016/S0161-6420(98)93043-3

Skorkovská, K., Lüdtke, H., Wilhelm, H., & Wilhelm, B. (2009). Pupil campimetry in patients with retinitis pigmentosa and functional visual field loss. *Graefe's Archive for Clinical and Experimental Ophthalmology, 247*(6), 847–853. https://doi.org/10.1007/s00417-008-1015-0

Skorkovská, K., Wilhelm, H., Lüdtke, H., & Wilhelm, B. (2009). How sensitive is pupil campimetry in hemifield loss? *Graefe's Archive for Clinical and Experimental Ophthalmology, 247*(7), 947–953. https://doi.org/10.1007/s00417-009-1040-7

Strauch, C., Wang, C.-A., Einhäuser, W., Van der Stigchel, S., & Naber, M. (2022). Pupillometry as an integrated readout of distinct attentional networks. *Trends in Neurosciences, 0*(0). https://doi.org/10.1016/j.tins.2022.05.003

Takizawa, G., Miki, A., Maeda, F., Goto, K., Araki, S., Yamashita, T., Ieki, Y., Kiryu, J., & Yaoeda, K. (2018). Relative Afferent Pupillary Defects in Homonymous Visual Field Defects Caused by Stroke of the Occipital Lobe Using Pupillometer. *Neuro-Ophthalmology, 42*(3). https://doi.org/10.1080/01658107.2017.1367012

Taylor, H. R., Livingston, P. M., Stanislavsky, Y. L., & McCarty, C. A. (1997). Visual impairment in Australia: Distance visual acuity, near vision, and visual field findings of the Melbourne visual impairment project. *American Journal of Ophthalmology, 123*(3). https://doi.org/10.1016/S0002-9394(14)70128-X

Thompson, H. S., Corbett, J. J., & Cox, T. A. (1981). How to measure the relative afferent pupillary defect. *Survey of Ophthalmology, 26*(1). https://doi.org/10.1016/0039-6257(81)90124-7

Thompson, H. S., Watzke, R. C., & Weinstein, J. M. (1980). Pupillary dysfunction in macular disease. *Transactions of the American Ophthalmological Society, Vol. 78.*

Tieger, M. G., Hedges, T. R., Ho, J., Erlich-Malona, N. K., Vuong, L. N., Athappilly, G. K., & Mendoza-Santiesteban, C. E. (2017). Ganglion cell complex loss in chiasmal compression by brain tumors. *Journal of Neuro-Ophthalmology, 37*(1). https://doi.org/10.1097/WNO.0000000000000424

Traquair, H. M. (1928). An Introduction to Clinical Perimetry. *Southern Medical Journal, 21*(3). https://doi.org/10.1097/00007611-192803000-00031

Tschopp, C., Safran, A. B., Viviani, P., Bullinger, A., Reicherts, M., & Mermoud, C. (1998). Automated visual field examination in children aged 5–8 years: Part I: Experimental validation of a testing procedure. *Vision Research, 38*(14), 2203–2210. https://doi.org/10.1016/S0042-6989(97)00368-4

Tsujimura, S. I., Wolffsohn, J. S., & Gilmartin, B. (2006). Pupil response to color signals in cone-contrast space. *Current Eye Research, 31*(5), 401–408. https://doi.org/10.1080/02713680600681327

Turpin, A., McKendrick, A. M., Johnson, C. A., & Vingrys, A. J. (2003). Properties of Perimetric Threshold Estimates from Full Threshold, ZEST, and SITA-like Strategies, as Determined by Computer Simulation. *Investigative Ophthalmology and Visual Science, 44*(11). https://doi.org/10.1167/iovs.03-0023

Ukai, K. (1985). Spatial pattern as a stimulus to the pupillary system. *Journal of the Optical Society of America A, 2*(7), 1094–1100. https://doi.org/10.1364/josaa.2.001094

Valbuena, M., Bandeen-Roche, K., Rubin, G. S., Munoz, B., & West, S. K. (1999). Self-reported assessment of visual function in a population-based study: The SEE project. *Investigative Ophthalmology and Visual Science, 40*(2).

Van Genderen, M., Dekker, M., Pilon, F., & Bals, I. (2012). Diagnosing cerebral visual impairment in children with good visual acuity. *Strabismus, 20*(2), 78–83. https://doi.org/10.3109/09273972.2012.680232

Walkey, H. C., Hurden, A., Moorhead, I. R., Taylor, J. A. F., Barbur, J. L., & Harlow, J. A. (2005). Effective contrast of colored stimuli in the mesopic range: a metric for perceived contrast based on achromatic luminance contrast. *Journal of the Optical Society of America A, 22*(1), 17–28. https://doi.org/10.1364/josaa.22.000017

Wall, M., Woodward, K. R., Doyle, C. K., & Artes, P. H. (2009). Repeatability of automated perimetry: A comparison between standard automated perimetry with stimulus size III and V, matrix, and motion perimetry. *Investigative Ophthalmology and Visual Science, 50*(2), 974–979. https://doi.org/10.1167/iovs.08-1789

Wall, M., Woodward, K. R., Doyle, C. K., & Zamba, G. (2010). The effective dynamic ranges of standard automated perimetry sizes III and V and motion and matrix perimetry. *Archives of Ophthalmology, 128*(5). https://doi.org/10.1001/archophthalmol.2010.71

Wang, C. A., & Munoz, D. P. (2015). A circuit for pupil orienting responses: Implications for cognitive modulation of pupil size. In *Current Opinion in Neurobiology* (Vol. 33). https://doi.org/10.1016/j.conb.2015.03.018

Warren, M. (2009). Pilot study on activities of daily living limitations in adults with hemianopsia. *American Journal of Occupational Therapy, 63*(5). https://doi.org/10.5014/ajot.63.5.626

Wilhelm, H. (2000). *Original paper Pupillomotor campimetry in normals Rüdiger Schmid Barbara Wilhelm. 49*(0), 7–14.

Wilhelm, H., Neitzel, J., Wilhelm, B., Beuel, S., Lüdtke, H., Kretschmann, U., & Zrenner, E. (2000). Pupil Perimetry using M-Sequence Stimulation Technique. *Investigative Ophthalmology & Visual Science, 41*(5), 1229–1238. https://dx.doi.org/

Wilson, M., Quinn, G., Dobson, V., & Breton, M. (1991). Normative values for visual fields in 4- to 12-year-old children using kinetic perimetry. *Journal of Pediatric Ophthalmology and Strabismus, 28*(3).

Yoshitomi, T., Matsui, T., Tanakadate, A., & Ishikawa, S. (1999). Comparison of Threshold Visual Perimetry and Objective Pupil Perimetry in Clinical Patients. *Journal of Neuro-Ophthalmology, 19*(2), 89–99. https://doi.org/10.1097/00041327-199906000-00003

Lessons learned from 23 years of experience in testing visual fields of neurologically impaired children

Portengen BL
Koenraads Y
Imhof SM
Porro GL

2.1 Abstract

We sought to investigate the reliability of standard conventional perimetry (SCP) in neurologically impaired (NI) children using the examiner-based assessment of reliability scoring system and to determine the difference in time to diagnosis of a visual field defect between SCP and a behavioural visual field (BVF) test. Patient records of 115 NI children were retrospectively analysed. The full field Peritest (FFP) had best reliability with 44% 'good' scores versus 22% for Goldmann perimetry ($p < .001$). The mean age of NI children able to perform SCP was 8.3 years versus 4.6 years for the BVF test ($p < .001$). Use of BVF test may significantly reduce time to diagnosis.

2.2 Introduction

Children suffering from neurological impairment (NI) may show various visual impairments, such as a decreased visual acuity, visual field defects (VFD), disorders of eye movements and disorders of higher visual processing, which may be diagnosed as cerebral visual impairment (CVI; Bosch et al., 2014; Dutton & Jacobson, 2001; Philip & Dutton, 2014). CVI, defined by Sakki et al. (2018) as *"a verifiable visual dysfunction which cannot be attributed to disorders of the anterior visual pathways or any potentially co-occurring ocular impairment"*, is the main cause of childhood visual disability in developed countries. It may have a pre-, peri- or postnatal origin with a prevalence between 10 and 22 cases per 10,000 births (Gilbert et al., 1999; Philip & Dutton, 2014).

Although the need for the development and refinement of approaches which allow early detection of gross VFDs has recently been stressed by Patel et al. (2019) retrospective studies of the visual field (VF) in a large cohort of NI children with or without CVI are lacking in the current literature. Several techniques can be used to examine the VF in children, such as standard conventional perimetry (SCP), confrontational behavioural visual field (BVF) methods (such as the Behavioural Visual Field [BEFIE] screening test, the use of Stycar balls or double-arc perimetry (Porro, Hofmann, Wittebol-post, et al., 1998; Quinn et al., 1991) or eye-tracker and multifocal visual evoked potential techniques. However, despite these various options, it can still be difficult to measure VF in NI children (Bjerre et al., 2014; Good et al., 1994; Murray et al., 2009; Patel, Cumberland, Walters, Russell-Eggitt, Cortina-Borja, et al., 2015) due to a lack of concentration, short attention span, psycho-motor impairment or retardation and intolerance to the restrictions of head movement required to perform most of these tests (Morales & Brown, 2001; Murray et al., 2009; Tschopp et al., 1998).

Detection of a VFD in NI children is important because it may represent one of the first symptomatic signs (van Genderen et al., 2012) or contribute to finding the right diagnosis in pathologies such as paediatric stroke, cerebral palsy and periventricular leukomalacia (Bova et al., 2008; Eken et al., 1995; Jacobson et al., 2002, 2010; Pike et al., 1994). It could also aid parents and caregivers to understand the child's visual behaviour, resulting in better acceptance, improved quality of life and more adequate rehabilitation strategies (Hart et al., 2013; Molineus et al., 2013).

To the best of our knowledge a comparison of SCP with a confrontational BVF method for testing VF in NI children searching for a potential gain in time to diagnosis of a VFD has never been performed. The aim of this study is to describe the results of SCP in a cohort of NI children. Additionally, we sought to confirm a potential gain in time to diagnose a VFD by using a BVF test.

2.3 Methods

2.3.1 Patient selection

This study retrospectively followed all NI children that underwent a confrontational BVF test before the age of 12 and who also underwent SCP at the Utrecht University Hospital from January 1995 until June 2018. The study was approved by the institutional ethical committee of the University Medical Center Utrecht which also deemed that the collection of written informed consent to this study was not necessary. Publication of the child pictured in the photograph in ***Figure 1*** was authorized by obtaining written informed consent.

2.3.2 Data collection

The patient files were retrospectively analysed. The collected demographic and clinical characteristics included sex, age at examination and type of pathology. Data of the earliest SCP tests with best representation of VF were gathered. If multiple SCP tests were used in an individual child, our preference went initially to Goldmann perimetry. When this was lacking, data of the first performed full field Peritest (FFP) or the first performed Humphrey Field Analyzer (HFA) including peripheral stimuli were recorded. As last resort, data on the first performed central Peritest (CP) were gathered. If scores differed

per eye, the score of the best eye was included. If the scores were the same, those of the right eye were included.

2.3.3 Standard conventional perimetry (SCP)

The SCP tests used in our center were manual kinetic testing on the Goldmann perimeter, semiautomatic-static testing on the Peritest (Rodenstock, Germany; Greve et al., 1982) and automatic-static testing on the HFA. The Peritest used a measure point in the fovea to determine the sensitivity threshold. Stimuli could be presented 2, 4, or 6 decibel supra-liminal. Light intensity was adjusted for the sensitivity decrease in the periphery. The CP protocol consisted of either 75 or 150 points within the inner 25 degrees of the VF. The FFP protocol consisted of the central Peritest with an additional 55 points above 25 degrees of the VF.

All children that were tested with the Goldmann perimeter and the HFA, were tested with the V4 isopter and the 120-point protocol respectively. Due to the retrospective nature of this study, exact protocol times were not listed. All SCP tests took approximately 30-40 minutes with breaks included. As soon as SCP was possible for a child, they were tested with the CP or an SCP test with periphery, if it were possible. The treating ophthalmologist chose between Goldmann, FFP and HFA.

2.3.4 Confrontational behavioral measurement

The confrontational BVF method used in our center is the BEFIE screening test ***(see Figure 1)***, a simple kinetic BVF test, designed in our institution with the aim of testing children of preverbal ages or NI children (Porro, Hofmann, Wittebol-Post, et al., 1998). The BEFIE test, which requires an examiner and an observer, is easy to apply in clinical practice and creates a high intrinsic motivation for the child to co-operate due to the game-like interaction between examiner, observer and patient. With this test, peripheral VFDs such as hemianopic, quadrantanopic or concentric VFDs can be detected in children as young as four months of age (Koenraads et al., 2015).

2.3.5 SCP test reliability in neurologically impaired (NI) children

To gain insight into the reliability of SCP tests in children with NI, the examiner-based assessment of reliability (EBAR) scoring system was used (Patel, Cumberland, Walters, Russell-Eggitt, Rahi, et al., 2015). To score tests more objectively, cooperation and fixation were dichotomised using the test results with comments made by the examiner. The scores were made by matching the descriptions of the EBAR scoring system with our retrospectively gathered results and comments. SCP tests were rated "good" when cooperation and fixation both had a score of "+". "Poor" ratings were given if cooperation and/or fixation were rated as "-" and an SCP test was scored as "fair" when cooperation and fixation were intermediate. Patients were excluded when no comment was given on the test result. Additionally, follow-up data of all children that underwent a second SCP test at this institution were gathered to compare whether the first and second SCP test were similar or different. If there were any apparent reasons for deterioration of disease and/or VFD, patients were excluded for this sub-analysis.

2.3.6 Average age

The children's age during the earliest SCP test with best representation was compared with their age during the earliest reliable monocular BEFIE test. This analysis was performed in order to find the average age at which NI children are able to perform perimetry tests and to examine the potential gain in time to diagnose a VFD should the BEFIE test be routinely incorporated into ophthalmological practice. After their first full ophthalmological

Figure 1. The behavioural visual field screening test. Equipment includes a rod with a level attached to it used for positioning (1), a graded semicircular black metal arc with a white stimulus at the end (2), and a white fixation target on a rod (3).

and orthoptic investigation including the first BEFIE test, the NI children obtained a regular follow-up using the BEFIE test until SCP was possible. All BEFIE tests were performed by the same examiner (GP). Reasons for exclusion for this analysis were: no monocular, but only binocular BEFIE tests, BEFIE and SCP tests performed on same day (for example before epilepsy surgery in accordance with local protocol) or age above 12 during the first BEFIE test.

2.3.7 Statistical analysis

Reliability was calculated using the chi-square test. Due to the large sample size and the normality of data in the BEFIE test age group, the analysis for average age difference between SCP and BEFIE was calculated using the paired sample t-test. All statistical tests were performed using IBM SPSS Statistics for Macintosh, version 25 (IBM Corp., Armonk, NY, USA).

2.4 Results

In total 138 children were eligible for this study of which 115 NI children (69 boys) were included after implementation of the exclusion criteria. The mean age in which the NI children could perform an SCP test was 8.3 (range 4.5-17.4 standard deviation [SD] 2.5) years. The majority of the children suffered from neoplasms or stroke/haemorrhage. Most children had normal VFs or suffered from (partial) hemianopias or quadrantanopias. Of the types of SCP tests used, 43% were FFP, 23% were Goldmann perimetry, 30% were CP and 4% were HFA tests. For more details on pathologies present see *Table 1*.

Table 1. Baseline table showing the different pathologies present in the neurologically impaired children.

PATHOLOGIES	n (%)
Neoplasm	36 (31)
Stroke/haemorrhage	34 (30)
High intracranial pressure	13 (11)
Cyst	8 (7)
Asphyxia/periventricular leukomalacia	8 (7)
Lesion/dysplasia	6 (5)
Epilepsy	5 (4)
Unknown	3 (3)
Trauma	2 (2)
Total	**115 (100)**

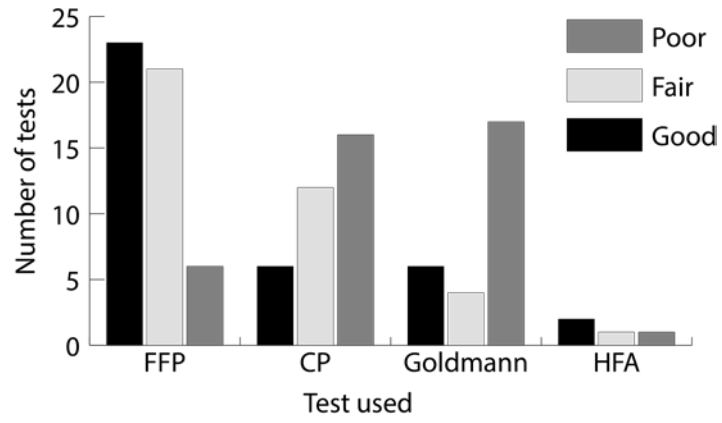

Figure 2. Results of the EBAR scoring system per SCP test: fullfield Peritest (FFP); central Peritest (CP); Goldmann perimetry; and Humphrey Field Analyzer (HFA).

2.4.1 Reliability of SCP tests in NI children

All 115 children were included to measure the reliability of SCP tests, but due to the small number of children tested with central and full field HFA tests (1 and 3 respectively), results obtained using these two methods were excluded for the statistical analysis. In total, 37 were rated "good", 38 as "fair", 40 as "poor". The ratings for the different SCP tests are shown in ***Figure 2*** and ***Table 2***. Among the FFP tests, 46% (23) had "good" reliability, 42% (21) were rated as "fair" and 12% (6) as "poor". For Goldmann perimetry, 22% (6) had a "good" reliability, 15% (4) were rated as "fair" and 63% (17) as "poor". Among the CP tests, 18% (6) had a "good" reliability, 35% (12) were rated as "fair" and 47% (16) as "poor". The difference between SCP tests was significant with a $p < .001$.

Table 2. Number of Standard Conventional Perimetry (SCP) tests used for the cohort of neurologically impaired children. Examiner Based Assessment of Reliability (EBAR) scores (i.e. Good, Fair or Poor) per SCP type is shown. Gender percentages calculated horizontally of total in subgroup. Percentages of Total calculated vertically.

STANDARD CONVENTIONAL PERIMETRY	Male (%)	Female (%)	Total (%)
Full Field Peritest	**28 (56)**	**22 (44)**	**50 (43)**
Good	*11*	*12*	*23*
Fair	*14*	*7*	*21*
Poor	*3*	*3*	*6*
Central Peritest	**25 (74)**	**9 (26)**	**34 (30)**
Good	*4*	*2*	*6*
Fair	*10*	*2*	*12*
Poor	*11*	*5*	*16*
Goldmann	**13 (48)**	**14 (52)**	**27 (23)**
Good	*2*	*4*	*6*
Fair	*4*	*0*	*4*
Poor	*7*	*10*	*17*
Humphrey Field Analyzer	**3 (75)**	**1 (25)**	**4 (4)**
Good	*1*	*1*	*2*
Fair	*1*	*0*	*1*
Poor	*1*	*0*	*1*
Total	**69 (60)**	**46 (40)**	**115 (100)**

Out of 115 children, 45 children (84 eyes) underwent more than one SCP test. The mean age at which these children were able to perform the first SCP test per method was: 7.2 (range 5.3-9.8, SD 1.2) years for the CP, 7.5 (range 4.5-10.7, SD 1.5) years for the FP and 8.6 (range 5.6-14.6, SD 2.6) years for Goldmann perimetry. The average age at which they performed their second test was 9.0 (range 5.0-16.5, SD 2.5) years. 86.9% of all second SCP results were congruent with those of the first test. For CP, FFP and Goldmann percentage of congruence was 89.7%, 81.3% and 91.3% respectively. Nine eyes showed deterioration of VF and two showed improvement ***(Figure 3)***.

2.4.2 Average age

For the comparison between the average age during the first BEFIE test and during the first SCP test, 104 out of the total 115 children were included. For this subgroup, the mean age in which the first monocular BEFIE test was possible for children with NI was 4.5 (range 0.7-11.8, SD 2.4) years. The mean age at which SCP was possible for children with NI was 8.2 (range 4.5-17.4, SD 2.5) years. The mean total difference between the first BEFIE test and the first SCP test was 3.7 years (95% confidence intervals 3.15-4.21, $p < .001$).

2.4.3 Comparison between BEFIE and SCP results

58.8% of the children had the same results on BEFIE and SCP tests. 17.1% had similar results without clinical difference. In 24,2% the results were different, either due to one test showing a VFD whereas the other did not (20.7%), or due to both showing different VFDs (3.5%), see ***Table 3***.

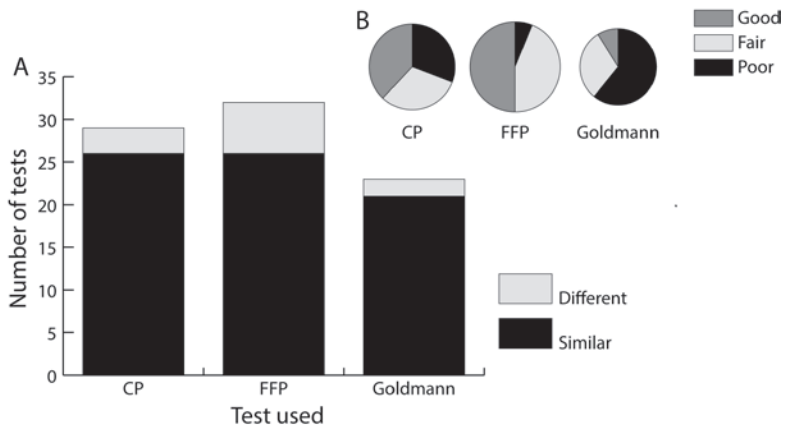

Figure 3. Comparison between the first and second SCP tests for the central Peritest (CP), the full field Peritest (FFP) and the Goldmann perimetry for all eyes of children that underwent a second SCP test. A shows the number of tests that had clinically similar or different results per SCP test. B shows the distribution of the EBAR scoring system results per SCP test for this subcohort.

VISUAL FIELD DEFECT	BEFIE n (%)	SCP n (%)
NO DEFECT	134 (65)	92 (42)
HEMIANOPIA	26 (13)	33 (15)
PARTIAL HEMIANOPIA	20 (10)	10 (5)
QUADRANTANOPIA	1 (1)	8 (4)
PARTIAL QUADRANTANOPIA	12 (6)	22 (10)
SPREAD SCOTOMAS	0 (0)	23 (10)
PERIPHERAL DEFECT	0 (0)	13 (6)
CONCENTRIC DEFECT	12 (6)	12 (5)
CENTROCECAL SCOTOMA	0 (0)	8 (4)
TOTAL	**205 (100)**	**221 (100)**

Table 3. Comparison of visual field defects detected by the behavioural visual field (BEFIE) screening test and standard conventional perimetry (SCP) per eye. Results scored per eye. Note that percentages do not always exactly add up to 100% due to rounding of numbers.

2.5 Discussion

With data gathered over a period of 23 years, this is the longest and, as far as we know, only retrospective study of the testing of VFs in such a large cohort of NI children with or without CVI. This is probably due to the commonly underestimated importance of examining VF in this group and the well-known methodological difficulties (Bjerre et al., 2014; Good et al., 1994; Murray et al., 2009; Patel, Cumberland, Walters, Russell-Eggitt, Cortina-Borja, et al., 2015), such as a lack of concentration, short attention span, psycho-motor impairment or retardation and the intolerance to the restrictions of head movement required to perform most SCP tests (Morales & Brown, 2001; Murray et al., 2009; Tschopp et al., 1998). Furthermore, there is little evidence regarding the reliability of SCP in children with NI, a group of children that is at higher risk of developing a VFD (Patel et al., 2019). Also, there is little consensus on how to approach these measurements, both in healthy as in NI children. In a recent study, Goldmann and Humphrey field tests, the two most common perimetric tests used in children, have shown to be reliable in healthy children using the EBAR scoring system (Patel, Cumberland, Walters, Russell-Eggitt, Rahi, et al., 2015). Patel et al measured the reliability of the discontinued Goldmann and the Octopus perimeters in children with NI, while other authors limited their measurements to confrontation methods or the Amsler test (Guzzetta et al., 2009; Kozeis et al., 2007; Patel et al., 2019).

2.5.1 Pathologies

Out of all NI children who were able to perform both a BEFIE test and a SCP test, the majority suffered from neoplasm (30.9%) or

stroke/haemorrhage (26.6%). This could suggest that when these are the causes of NI, children may have a higher chance to be able to perform an SCP test, due to plasticity of the brain (Kozeis, 2010). On the contrary, these data could be biased by a high prevalence of these pathologies in our centre. Therefore, more research is needed to support these data and hypotheses.
Although this study did focus on the various brain pathologies, it did not include their localisations. Therefore, no assumptions can be made about which SCP test is more reliable for each localization. An assumption on which SCP test tends to be more reliable for each pathology group cannot be made, due to the small number of children in each group.

2.5.2 Perimetry tests used

Only 24.6% of NI children managed to complete a Goldmann perimetry and only 26.6% completed a CP, whereas the majority of all participants (44.9%) managed to complete an FFP. Therefore, a Peritest could be suggested when the commonly used Goldmann perimetry is likely to fail (Patel, Cumberland, Walters, Russell-Eggitt, Cortina-Borja, et al., 2015). Unfortunately, internationally the Peritest is nowadays not routinely used, even though it was reported to perform well in the few studies that described it (Greve et al., 1982; Hotchkiss et al., 1985; Langerhorst et al., 1992) and the same will probably happen to the discontinued Goldmann perimeter. Currently, the most commonly used perimetry test in children is the HFA, although recent studies have opted for the Octopus perimetry as a replacement for the Goldmann perimeter (Patel, Cumberland, Walters, Russell-Eggitt, Rahi, et al., 2015; Patel et al., 2018, 2019). In a recent study comparing both Goldmann with Octopus perimetry, broad agreement was found and these tests were recommended for children over eight-years-old with neuro-ophthalmologic disease (Patel et al., 2019).
We believe that eye tracking applications might prove useful when testing VFs in children in the future (Aslam et al., 2018; Murray et al., 2016, 2018). Furthermore, predicting VFDs using OCT seems to be possible in children with a developmental age of 3-6 years (Bowl et al., 2018).
In our centre the Octopus perimeter is not available and the HFA is sparsely used in children due to the extensive and positive experience of staff in testing children with or without NI using the Peritest (Greve et al., 1976; Hardus et al., 2000). Hence, a comparison of Octopus perimeter and HFA was not possible in our retrospective study.

Therefore, we suggest prospective studies using the two above-mentioned, more widely used, VF tests for a conclusive comparison.

2.5.3 Reliability of SCP tests in NI children

Due to the retrospective nature of this study, the results of the EBAR analysis might not be perfectly representative. Although a prospective study could incorporate the score definitions more accurately, in our opinion the data obtained give a fairly accurate representation of SCP reliability in children with NI. Although both kinetic and static perimetry should be considered in the NI child, the FFP, a static VF test, has a significantly higher reliability score for the first measurement of VF in NI children. On the opposite, the Goldmann perimeter, a kinetic VF test and one of the more commonly used SCP tests in clinical practice for testing children (Morales & Brown, 2001; Patel, Cumberland, Walters, Russell-Eggitt, Cortina-Borja, et al., 2015; Patel et al., 2019), has been shown to be highly reliable in healthy ones (Patel, Cumberland, Walters, Russell-Eggitt, Rahi, et al., 2015). It showed only a 22% “good” reliability in NI children in our cohort, probably due to a prolonged learning curve in comparison with the Peritest.
Pathology, localisation and severity can predict which SCP method could be more suited or might have a higher chance of a successful measurement of VF. For instance, in damage to the periventricular matter or to the parieto-occipital region, the sensitivity of movement perception might be reduced, consequently rendering the kinetic perimetry less applicable (Guzzetta et al., 2009).
The CP had high numbers of “poor” ratings. This is probably due to more severe pathology, as this sample of NI children were only able to perform this shorter test of the central field and not more difficult tests.
When looking at the results of the comparison between the first and second SCP tests, there are a few limitations. Although the numbers give a fair perspective as to what age a clinically significant VFD can be detected, a prospective study with a correct set-up would be needed to accurately determine specificity and sensitivity of these tests. Furthermore, only a small portion of the cohort performed more than one SCP test. The reasons for the paucity of visual field testing during follow-up remain unknown in our retrospective analysis. Also, even though the most apparent reasons for deterioration, e.g. surgery, were excluded, differing results between the first and the second test could still originate from progression of disease or neuronal plasticity (Guzzetta et al., 2010). Lastly, all

SCP tests used are subjective tests, complicating efforts to perfectly replicate a previous test.
Interestingly, even though the majority of Goldmann tests were made with a 'poor' EBAR reliability score, 91,3% of the children showed similar VFDs at follow-up. Though the EBAR scoring system has proved to be a useful tool to determine whether a visual field test is executed reliably (Guzzetta et al., 2009; Patel et al., 2019), in our cohort a lower EBAR score did not seem to correlate with a lower chance of finding a clinically significant VFD. The reason for this disparity in results is unknown to the authors, but it could be due to the use of stricter EBAR protocols, resulting in a bias towards more 'poor' scores. Another explanation may be that reliability indices for the EBAR scoring system contribute little to test-retest reliability, much like traditional perimetry indices (Bengtsson, 2000).

2.5.4 Average age

An important finding in this study is that the mean age at which a NI child can perform an SCP test is 8.3 years. Furthermore, this study has shown that a monocular BEFIE test for testing the peripheral VF can be successfully performed on average 3.7 years earlier than an SCP test. This is due to the adaptations at the psycho-motor impairment of the NI child and the game-like interaction between the child and the examiner and observer (Koenraads et al., 2015). These characteristics make it very suitable for healthy children of preverbal ages as well. This finding highlights the importance of a wider clinical application of this behavioural test, especially when considering that Koenraads et al. already showed a specificity of 98% and sensitivity of 60%, which increased to 80% when only absolute PVF defects at SCP are taken into account (Koenraads et al., 2015). From these results and the congruence found in our study, we can conclude that using a behavioural visual field test, like the BEFIE screening test, leads to a high probability of diagnosing a clinically significant VFD in children affected by cortical damage. Please note that the BEFIE test is unable to diagnose central and relative VFDs, whereas a percentage of the NI children in this study were proven to have these defects. If those were to be excluded, the congruence could potentially be higher.
Considering that VFDs may represent as one of the first symptomatic signs of CVI in children (van Genderen et al., 2012), such a considerable time gain of 3.7 years in the diagnosis of a VFD using the BEFIE test could help to drastically lower the doctor delay in diagnosing CVI in children. Furthermore, it could help parents and caregivers to understand the child's behaviour, resulting in better acceptance, improved quality of life and more adequate treatment or rehabilitation strategies (Hart et al., 2013; Molineus et al., 2013).
In addition, as 29% of all NI children tested were able to have only their central visual field tested with SCP, while in all of them it was possible to test the peripheral VF using the BEFIE test, the BEFIE test could be a useful complementary test in addition to SCP.

2.5.5 Limitations

This study has several limitations; first of all those associated with a retrospective study. In addition, this study reports the experience of a single center cohort, in which only one examiner (the ophthalmologist GP) performed all of the BEFIE tests, helped by different observers, who were all orthoptists. No inter-user data of the BEFIE test was hence gathered, while the SCP tests were performed by different technicians.
The BEFIE test requires a trained observer and examiner and it has the limitation of only testing the peripheral VF. Therefore, we strongly suggest the development of a reliability scoring system for the BEFIE test prior to widespread implementation in specialized ophthalmology departments. Alternatively, we recommend the development of a better BVF test or ultimately an objective measurement of VF in children, less influenced by a lack of co-operation, attention or psychomotor impairment. Our centre has extensive experience using the Peritest for testing children, resulting in a larger cohort of NI children that performed the Peritest than HFA, which is nowadays considered the state-of-the-art when testing VF in children.(Walters et al., 2012) A prospective study, without the above-mentioned limitations, could further clarify which SCP test is best suited for NI children.

2.6 Conclusion

In conclusion, this retrospective study from 23 years of experience in testing VFs of NI children showed that the FFP was the most reliable VF screening test. A BVF test, such as the BEFIE test led to a significant gain in time to diagnose a peripheral VFD of 3.7 years. We emphasise the importance of an early diagnosis of a peripheral VFD by means of any available BVF test in clinical practice as it can lead to better care for NI children.

2.7 References

Aslam, T. M., Ali, Z. C., Wang, Y., Fenerty, C., Biswas, S., Tsamis, E., & Henson, D. B. (2018). Diagnostic Performance and Repeatability of a Novel Game-Based Visual Field Test for Children. *Investigative Opthalmology & Visual Science, 59*(3), 1532. https://doi.org/10.1167/iovs.17-23546

Bengtsson, B. (2000). Reliability of computerized perimetric threshold tests as assessed by reliability indices and threshold reproducibility in patients with suspect and manifest glaucoma. *Acta Ophthalmologica Scandinavica, 78*(5), 519–522. https://doi.org/10.1034/j.1600-0420.2000.078005519.x

Bjerre, A., Codina, C., & Griffiths, H. (2014). Peripheral Visual Fields in Children and Young Adults Using Semi-automated Kinetic Perimetry: Feasibility of Testing, Normative Data, and Repeatability. *Neuro-Ophthalmology, 38*(4), 189–198. https://doi.org/10.3109/01658107.2014.902971

Bosch, D. G., Boonstra, F. N., Willemsen, M. A., Cremers, F. P., & de Vries, B. B. (2014). Low vision due to cerebral visual impairment: differentiating between acquired and genetic causes. *BMC Ophthalmology, 14*(1), 59. https://doi.org/10.1186/1471-2415-14-59

Bova, S. M., Giovenzana, A., Signorini, S., La Piana, R., Uggetti, C., Bianchi, P. E., & Fazzi, E. (2008). Recovery of visual functions after early acquired occipital damage. *Developmental Medicine & Child Neurology, 50*(4), 311–315. https://doi.org/10.1111/j.1469-8749.2008.02044.x

Bowl, W., Knobloch, R., Schweinfurth, S., Holve, K., Stieger, K., & Lorenz, B. (2018). Structure-Function Correlation in Hemianopic Vision Loss in Children Aged 3-6 Years Using OCT and SVOP, and Comparis on with Adult Eyes. *Ophthalmic Research, 60*(4), 221–230. https://doi.org/10.1159/000480296

Dutton, G. N., & Jacobson, L. K. (2001). Cerebral visual impairment in children. *Seminars in Neonatology, 6*(6), 477–485. https://doi.org/10.1053/SINY.2001.0078

Eken, P., de Vries, L. S., van der Graaf, Y., Meiners, L. C., & van Nieuwenhuizen, O. (1995). Haemorrhagic-ischaemic lesions of the neonatal brain: correlation between cerebral visual impairment, neurodevelopmental outcome and MRI in infancy. *Developmental Medicine and Child Neurology, 37*(1), 41–55. http://www.ncbi.nlm.nih.gov/pubmed/7530219

Gilbert, C. E., Anderton, L., Dandona, L., & Foster, A. (1999). Prevalence of visual impairment in children: A review of available data. *Ophthalmic Epidemiology, 6*(1), 73–82. https://doi.org/10.1076/opep.6.1.73.1571

Good, W. V, Jan, J. E., DeSa, L., Barkovich, A. J., Groenveld, M., & Hoyt, C. S. (1994). Cortical visual impairment in children. *Survey of Ophthalmology, 38*(4), 351–364. https://doi.org/10.1016/0039-6257(94)90073-6

Greve, E. L., Dannheim, F., & Bakker, D. (1982). The Peritest, a new automatic and semi-automatic perimeter. *International Ophthalmology, 5*(3), 201–214.

Greve, E. L., Groothuyse, M. T., & Verduin, W. M. (1976). Automation of perimetry. Documenta Ophthalmologica. *Advances in Ophthalmology, 40*(2), 243–254.

Guzzetta, A., D'acunto, G., Rose, S., Tinelli, F., Boyd, R., & Cioni, G. (2010). Plasticity of the visual system after early brain damage. In *Developmental Medicine and Child Neurology* (Vol. 52, Issue 10, pp. 891–900). John Wiley & Sons, Ltd. https://doi.org/10.1111/j.1469-8749.2010.03710.x

Guzzetta, A., Tinelli, F., Del Viva, M. M., Bancale, A., Arrighi, R., Pascale, R. R., & Cioni, G. (2009). Motion perception in preterm children: role of prematurity and brain damage. *NeuroReport, 20*(15), 1339–1343. https://doi.org/10.1097/WNR.0b013e328330b6f3

Hardus, P., Verduin, W. M., Postma, G., Stilma, J. S., Berendschot, T. T. J. M., & Veelen, C. W. M. (2000). Concentric Contraction of the Visual Field in Patients with Temporal Lobe Epilepsy and Its Association with the Use of Vigabatrin Medication. *Epilepsia, 41*(5), 581–587. https://doi.org/10.1111/j.1528-1157.2000.tb00212.x

Hart, M. G., Sarkies, N. J., Santarius, T., & Kirollos, R. W. (2013). Ophthalmological outcome after resection of tumors based on the pineal gland. *Journal of Neurosurgery, 119*(2), 420–426. https://doi.org/10.3171/2013.3.JNS122137

Hotchkiss, M. L., Robin, A. L., Quigley, H. A., & Pollack, I. P. (1985). A Comparison of Peritest Automated Perimetry and Goldmann Perimetry. *Archives of Ophthalmology, 103*(3), 397–403. https://doi.org/10.1001/archopht.1985.01050030093030

Jacobson, L., Rydberg, A., Eliasson, A.-C., Kits, A., & Flodmark, O. (2010). Visual field function in school--aged children with spastic unilateral cerebral palsy related to different patterns of brain damage. *Developmental Medicine & Child Neurology, 52*(8), e184–e187. https://doi.org/10.1111/j.1469-8749.2010.03650.x

Jacobson, L., Ygge, J., Flodmark, O., & Ek, U. (2002). Visual and perceptual characteristics, ocular motility and strabismus in children with periventricular leukomalacia. *Strabismus, 10*(2), 179–183. https://doi.org/10.1076/stra.10.2.179.8132

Koenraads, Y., Braun, K. P. J., van der Linden, D. C. P., Imhof, S. M., & Porro, G. L. (2015). Perimetry in young and neurologically impaired children: the Behavioral Visual Field (BEFIE) Screening Test revisited. *JAMA Ophthalmology, 133*(3), 319–325. https://doi.org/10.1001/jamaophthalmol.2014.5257

Kozeis, N. (2010). Brain visual impairment in childhood: mini review. *Hippokratia, 14*(4), 249–251.

Kozeis, N., Anogeianaki, A., Mitova, D. T., Anogianakis, G., Mitov, T., & Klisarova, A. (2007). Visual function and visual perception in cerebral palsied children. *Ophthalmic and Physiological Optics, 27*(1), 44–53. https://doi.org/10.1111/j.1475-1313.2006.00413.x

Langerhorst, C. T., Bakker, D., Felius, J., & van den Berg, T. J. (1992). Discrepancies between single stimulus and multiple stimulus visual field examinations with the Peritest semi-automated perimeter in glaucoma patients. Documenta Ophthalmologica. *Advances in Ophthalmology, 82*(1–2), 135–140.

Molineus, A., Boxberger, N., Redlich, A., & Vorwerk, P. (2013). Time to diagnosis of brain tumors in children: A single-centre experience. *Pediatrics International, 55*(3), 305–309. https://doi.org/10.1111/ped.12095 Morales, J., & Brown, S. M. (2001). The feasibility of short automated static perimetry in children. Ophthalmology, 108(1), 157–162. https://doi.org/10.1016/S0161-6420(00)00415-2

Murray, I. C., Cameron, L. A., McTrusty, A. D., Perperidis, A., Brash, H. M., Fleck, B. W., & Minns, R. A. (2016). Feasibility, Accuracy, and Repeatability of Suprathreshold Saccadic Vector Optokinetic Perimetry. *Translational Vision Science & Technology, 5*(4), 15. https://doi.org/10.1167/tvst.5.4.15

Murray, I. C., Fleck, B. W., Brash, H. M., Macrae, M. E., Tan, L. L., & Minns, R. A. (2009). Feasibility of saccadic vector optokinetic perimetry: a method of automated static perimetry for children using eye tracking. *Ophthalmology, 116*(10), 2017–2026. https://doi.org/10.1016/j.ophtha.2009.03.015

Murray, I. C., Schmoll, C., Perperidis, A., Brash, H. M., McTrusty, A. D., Cameron, L. A., Wilkinson, A. G., Mulvihill, A. O., Fleck, B. W., & Minns, R. A. (2018). Detection and characterisation of visual field defects using Saccadic Vector Optokinetic Perimetry in children with brain tumours. *Eye*, 1. https://doi.org/10.1038/s41433-018-0135-y

Patel, Cumberland, P. M., Walters, B. C., Russell-Eggitt, I., Cortina-Borja, M., Rahi, J. S., & OPTIC Study Group. (2015). Study of Optimal Perimetric Testing In Children (OPTIC): Normative Visual Field Values in Children. *Ophthalmology, 122*(8), 1711–1717. https://doi.org/10.1016/j.ophtha.2015.04.038

Patel, D. E., Cumberland, P. M., Walters, B. C., Cortina-Borja, M., & Rahi, J. S. (2019). Study of Optimal Perimetric Testing in Children (OPTIC): Evaluation of kinetic approaches in childhood neuro-ophthalmic disease. *British Journal of Ophthalmology, 103*(8), 1085–1091. https://doi.org/10.1136/bjophthalmol-2018-312591

Patel, D. E., Cumberland, P. M., Walters, B. C., Russell-Eggitt, I., Brookes, J., Papadopoulos, M., Khaw, P. T., Viswanathan, A. C., Garway-Heath, D., Cortina-Borja, M., & Rahi, J. S. (2018). Comparison of Quality and Output of Different Optimal Perimetric Testing Approaches in Children With Glaucoma. *JAMA Ophthalmology, 136*(2), 155. https://doi.org/10.1001/jamaophthalmol.2017.5898

Patel, D. E., Cumberland, P. M., Walters, B. C., Russell-Eggitt, I., Rahi, J. S., & OPTIC study group, O. study. (2015). Study of Optimal Perimetric Testing in Children (OPTIC): Feasibility, Reliability and Repeatability of Perimetry in Children. *PloS One, 10*(6), e0130895. https://doi.org/10.1371/journal.pone.0130895

Philip, S. S., & Dutton, G. N. (2014). Identifying and characterising cerebral visual impairment in children: a review. *Clinical and Experimental Optometry, 97*(3), 196–208. https://doi.org/10.1111/cxo.12155

Pike, M. G., Holmstrom, G., Vries, L. S., Pennock, J. M., Drew, K. J., Sonksen, P. M., & Dubowitz, L. M. S. (1994). Patterns Of Visual Impairment Associated With Lesions Of The Preterm Infant Brain. *Developmental Medicine & Child Neurology, 36*(10), 849–862. https://doi.org/10.1111/j.1469-8749.1994.tb11776.x

Porro, G., Hofmann, J., Wittebol-Post, D., van Nieuwenhuizen, O., van der Schouw, Y. T., Schilder, M. B. H., Dekker, M. E. M., & Treffers, W. F. (1998). A new behavioral visual field test for clinical use in pediatric neuro-ophthalmology. *Neuro-Ophthalmology, 19*(4), 205–214. https://doi.org/10.1076/noph.19.4.205.3939

Porro, G., Hofmann, J., Wittebol-post, D., Van, O., Schouw, Y. T. Van Der, Schilder, M. B. H., Dekker, M. E. M., Treffers, W. F., & Hofmann, J. (1998). *A new behavioral visual field test for clinical use in pediatric neuro-ophthalmology. 19*(4), 205–214. https://doi.org/10.1076/noph.19.4.205.3939

Quinn, G. E., Fea, A. M., & Minguini, N. (1991). Visual fields in 4- to 10-year-old children using Goldmann and double-arc perimeters. *Journal of Pediatric Ophthalmology and Strabismus, 28*(6), 314–319. http://www.ncbi.nlm.nih.gov/pubmed/1757855

Sakki, H. E. A., Dale, N. J., Sargent, J., Perez-Roche, T., & Bowman, R. (2018). Is there consensus in defining childhood cerebral visual impairment? A systematic review of terminology and definitions. *The British Journal of Ophthalmology, 102*(4), 424–432. https://doi.org/10.1136/bjophthalmol-2017-310694

Tschopp, C., Safran, A. B., Viviani, P., Bullinger, A., Reicherts, M., & Mermoud, C. (1998). Automated visual field examination in children aged 5–8 years: Part I: Experimental validation of a testing procedure. *Vision Research, 38*(14), 2203–2210. https://doi.org/10.1016/S0042-6989(97)00368-4

van Genderen, M., Dekker, M., Pilon, F., & Bals, I. (2012). Diagnosing Cerebral Visual Impairment in Children with Good Visual Acuity. *Strabismus, 20*(2), 78–83. https://doi.org/10.3109/09273972.2012.680232

Walters, B. C., Rahi, J. S., & Cumberland, P. M. (2012). Perimetry in Children: Survey of Current Practices in the United Kingdom and Ireland. *Ophthalmic Epidemiology, 19*(6), 358–363. https://doi.org/10.3109/09286586.2012.718027

Comparison of unifocal, flicker and multifocal pupil perimetry methods in healthy adults

Journal of Vision (2022) doi: 10.1167/jov.22.9.7

Portengen BL
Porro GL
Imhof SM
Naber M

3.1. Abstract

To this day the most popular method of choice for testing visual field defects (VFD) is subjective standard automated perimetry. However, a need has arisen for an objective, and less time-consuming method. Pupil perimetry (PP), which employs pupil responses to onsets of bright stimuli as indications of visual sensitivity, fulfills these requirements. It is currently unclear which PP method most accurately detects VFD. Hence, the purpose of this study is to compare three PP methods for measuring pupil responsiveness. Unifocal (UPP), flicker (FPP), and multifocal PP (MPP) were compared by monocularly testing the inner 60 degrees of vision at 44 wedge-shaped locations. The VF sensitivity of 18 healthy adult participants (mean age and SD 23.7 ± 3.0 years) was assessed, each under three different artificially simulated scotomas for ~4.5 min each (i.e., stimulus was not or only partially present) conditions: quadrantanopia, a 20-, and 10-degrees diameter scotoma.
Stimuli that were fully present on screen evoked strongest, partially present stimuli evoked weaker, and absent stimuli evoked the weakest pupil responses in all methods. However, the pupil responses in FPP showed stronger discriminative power for present versus absent trials (median d-prime = 6.26 ± 2.49, AUC = 1.0 ± 0) and MPP performed better for fully present versus partially present trials (median d-prime = 1.19 ± 0.62, AUC = 0.80 ± 0.11).
We conducted the first in-depth comparison of three PP methods. Gaze-contingent FPP had best discriminative power for large (absolute) scotomas, while MPP performed slightly better with small (relative) scotomas.

3.2 Introduction

To this day the method of choice for clinically testing the visual field (VF) is standard automated perimetry (SAP). Current SAP devices (e.g., Humphrey Field Analyzer [HFA], Octopus perimeter) systematically measure VF loss by (1) restricting head movement with a forehead-chinrest, (2) asking patients to fixate a central target, and (3) give a motor response when a visual change (usually a temporary increase in luminance or change in color) is shown at one of n (typically ~54-76) locations across the VF. This procedure of SAP brings along several shortcomings; testing is subjective as it relies on introspective reports due to its psychophysical nature, strict fixation is required, observers need to exert prolonged attention, and learning effects and incorrect motor responses distort measurements. Also, poor reproducibility has been described for SAP (test-retest variability of single threshold estimates approximating the dynamic range of the instrument; Artes et al., 2002; Piltz & Starita, 1990). The test-retest variability likely stems from the small stimuli used in SAP and their displacement due to fixational jitter or microsaccades, and learning and fatigue effects (Maddess, 2014; Numata et al., 2017; Wall et al., 2009).
Alternative perimetry methods utilize measurements like visual evoked potentials (i.e., measurement of electrophysiological responses with electrodes positioned on the scalp near the occipital bone), saccadic vector optokinetic perimetry (i.e., saccade measurement in response to visual cues with eye tracking technology), preferential looking responses, saccadic response times, behavioral visual field tests and pupillometry (Allen et al., 2012; Gestefeld et al., 2020; Harding et al., 2002; Koenraads et al., 2015; Pel et al., 2013). Here we specifically focus on pupil perimetry (PP), which emerges as a relatively young and unpursued, but also promising method. While scientists claim to have improved this form of perimetry, few methodological approaches currently exist and have not yet been compared. Therefore, it is currently unknown how the pupil can best be used as a measure of visual sensitivity.
Optimization strategies so far limited their explorative scope to changing the number of stimuli shown simultaneously across the VF (spatial sparseness) and the frequency of presentations within a certain time window (sparseness of events). In general, three distinct methods that vary across these two factors can be discerned: (1) unifocal PP (UPP), which consists of a single stimulus presentation (i.e., high spatial sparseness) shown for a relatively long period of time (i.e., high sparseness of events; e.g., Kardon et al. (1991)); (2) flicker PP (FPP), recently developed by our lab, consisting of a single flickering stimulus presentation (i.e., high spatial sparseness) at gaze-contingent locations, which allows for repeated and precise retinotopic stimulation (i.e., low sparseness of events with regard to the number of luminance changes), circumventing noise and fixation problems that typically occur in slow presentation paradigms (Naber et al., 2018; Portengen et al., 2021); and (3) multifocal PP (MPP), showing multiple stimuli in parallel for relatively long durations (i.e., low spatial sparseness and high sparseness of events; e.g., Maddess et al. (2009), Tan et al. (2001), Wilhelm et al. (2000)); ***see Figure 1***.
FPP shows very promising results for application in neurologically

impaired subjects affected by cerebral visual impairment on account of its gaze-contingent stimulus presentation with multiple measurements in a short time period (Naber et al., 2018), but a comparison between different PP methods has not yet been performed.
The aim of this study consists of the comparison of sensitivities and specificities across three PP methods.

3.3 Methods

3.3.1 Participants

All participants (12 females and 6 males, mean age and SD 23.7 ± 3.0 years) comprised of students and staff of the Psychology department of Utrecht University with Dutch nationality and Caucasian ethnicity (as observed by the experimenters). All reported having normal uncorrected or corrected visual acuity and no visual or neurological disorders. The experiment conformed to the ethical principles of the Declaration of Helsinki and was preregistered and approved by the local ethical committee of the University Utrecht (approval number: FETC19-006). Participants received (financial) reimbursement for participation and travel and gave informed written consent before the experiment. They were unaware of the purpose of the experiment and were only told that the eye-tracker measured their eye movements. Participants were debriefed about the purpose of the experiment afterwards.

3.3.2 Apparatus & stimuli

Stimuli were generated on a Dell desktop computer with Windows 7 operating system (Microsoft, Redmond, Washington), using MATLAB (MathWorks, Natick, MA, USA) with the Psychtoolbox 3 and Eyelink toolbox extensions (Brainard, 1997; Cornelissen et al., 2002; Kleiner et al., 2007; Pelli, 1997). A linearized (gamma-correction factor 2.2) OLED65B8PLA LG (LG Electronics, Seoul, South Korea) presentation monitor displayed the stimuli at a resolution of 1920 by 1080 pixels with a refresh rate of 60 Hz. The screen measured 143 cm in width and 63 cm in height. The participant's viewing distance was held stable at 65 cm with a chin- and forehead rest. Pupil size and gaze was recorded monocularly with an Eyelink 1000 eye-tracker (SR Research, Ontario, Canada; 0.5-degree accuracy of gaze location) placed 40 cm in front of the observer below the monitor. Eye-tracker calibration sessions consisted of the presentation of a five-point calibration grid and lasted ~1 min. Note that the Eyelink tracker software outputs pupil size in arbitrary units rather than absolute pupil diameter in millimeters. The experiment was conducted in a darkened room without ambient light.

Stimulus paradigms

The three tested methods included unifocal PP (UPP), flicker PP (FPP) and multifocal PP (MPP), which were tested consecutively in all participants (with short breaks in between the methods and stimulus paradigms; see below) in random order using random permutation. UPP consisted of single, one-by-one stimulus presentations, in the form of white wedges, presented at random order across all 44 stimulus locations, each for a duration of 1 second followed by a 5 second blank screen interval ***(Figure 1a and Supplementary Video S1 - UPP)***. FPP (Naber et al., 2018) consisted of a 2 Hz flickering wedge with a change in luminance between black and white for a duration of 6 seconds sequentially presented at each individual location ***(Figure 1b and Supplementary Video S2 - FPP)***. For MPP, approximately half of the stimulus locations were stimulated in parallel, and the stimulation pattern changed at a rate of 2 Hz for 256 seconds. The interval between stimuli was thus 0.25 seconds, resulting in a total of 1056 stimulus change events per location ***(see Figure 1c and Supplementary Video S3 - MPP)***. Note that we chose to change temporal and spatial factors of current MPP methods to enable better comparisons with the FPP method. To ensure that the temporal pattern of luminance changes for each wedge location correlated the least as possible to the patterns of the other wedge locations (anticorrelation across wedges improves sensitivity), an m-sequence algorithm was used (Buračas & Boynton, 2002).
To compare the three methods, we assessed scotoma detection accuracy. As such, observers observed stimuli presented within, at the border, and outside of areas in which the wedge stimuli were not visible (i.e., not shown). We created three scotoma versions with these artificial VFDs (aVFD): a stimulus wedge could either be fully present, partially present, or absent ***(Figure 2)***. The aVFDs were randomly placed in the upper right or left quadrant of the stimulus map per participant. Simulating VFDs in healthy participants is a known strategy (e.g., Gestefeld et al., 2020) with the following advantages: (i) it allows the exact controlling of which part of the visual field is masked and (ii) bypasses the need to burden patients with having to participate in a study that compares stimulus protocols rather than a newly developed diagnostic method.

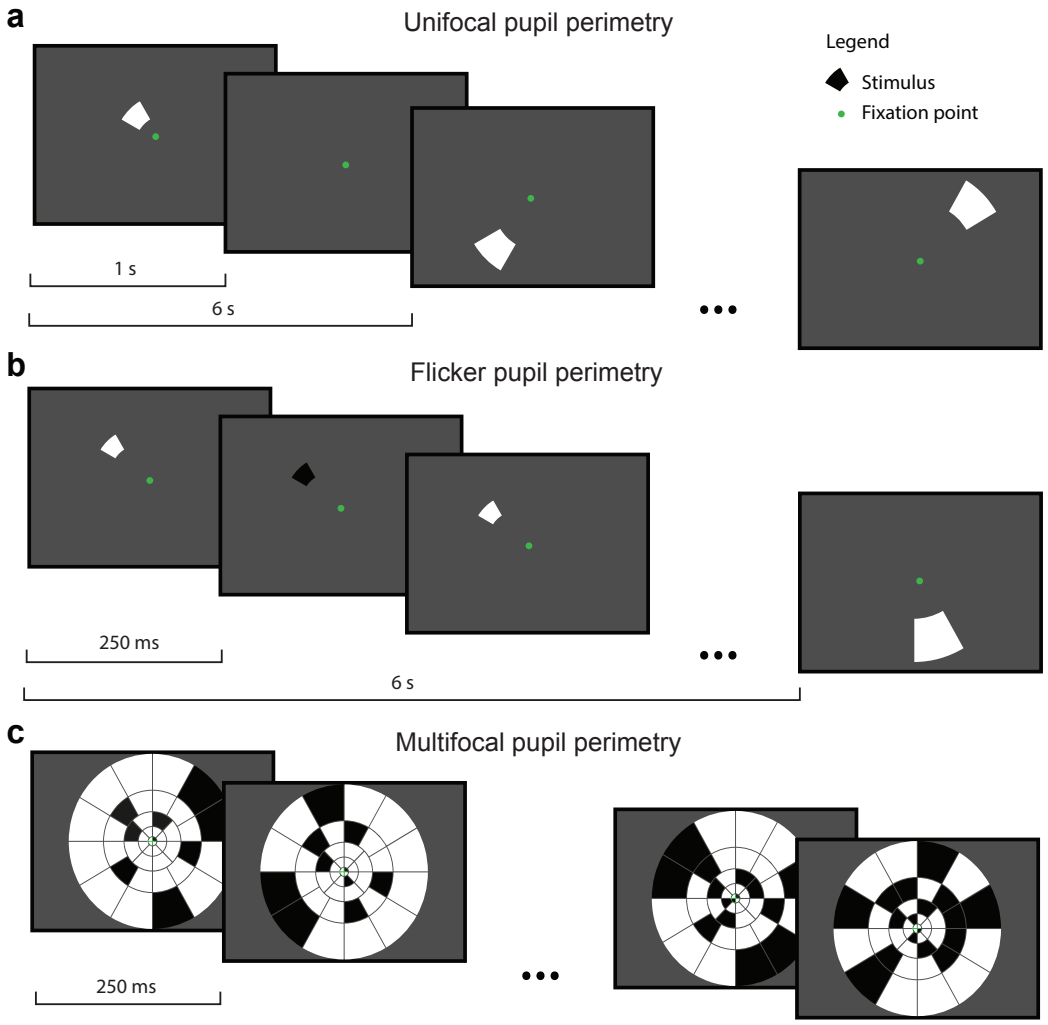

Figure 1. The three pupil perimetry (PP) methods. (a) Unifocal PP consisted of a single 1s duration stimulus presentation followed by a 5s interval after which another stimulus location was presented. See panel c for all stimulus locations used in all methods. (b) Flicker PP consisted of black-and-white 2 Hz flickering stimulus presentations for 6s per stimulus location. (c) Multifocal PP consisted of the stimulation of several stimulus locations in parallel at any given time point. The temporal stimulation pattern followed an M-sequence calculated with the algorithm of Buračas & Boynton (2002) with 2 Hz refresh rate of stimulus patterns. This ensured best statistical independence across wedges, resulting in the most precise weighting of contributions per wedge to the pupil responses during the analysis. The stimuli for all three methods consisted of 44 wedges of the same size per stimulus location across methods. See Supplementary Video S1-3 for an example of the three methods.

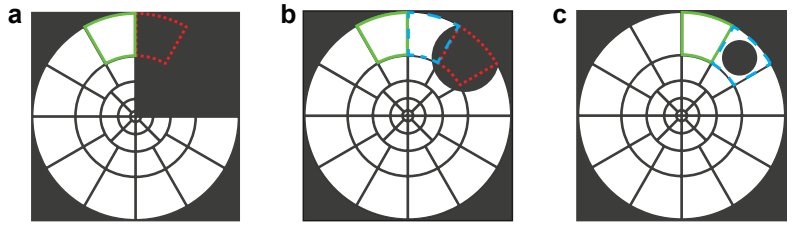

Figure 2. Stimulus location maps per artificial scotoma condition, each consisting of 44 wedges. To compare how well each pupil perimetry method could detect different scotoma types, three artificially simulated visual field defects (aVFDs) were created: quadrantanopia (a), relatively large scotoma (b), and a relatively small scotoma (c). Scotomas were placed either at the upper right or left corner of the visual field. These aVFDs resulted in three distinct wedge visibility conditions: fully present (solid green line), partially present (dashed blue), and absent (dotted red).

Stimulus map

Stimulus locations consisted of 44 wedges distributed across 5 eccentricity rings in the central 60-degree field of vision, both temporally and nasally ***(see Figures 1c and 2)***. The stimulus layout closely resembled other multifocal pupil perimetry protocols (Sabeti et al., 2017; Wilhelm et al., 2000). The wedges differed in size per eccentricity ring (radial width = eccentricity1.12; in degrees) to adjust for the cortical magnification factor (i.e., stimuli in the fovea are processed by more cortical tissue) and the distribution of photosensitive retinal cells. The stimulus wedges were white (212 cd/m2) and the background was dark-gray (25 cd/m2 for UPP and FPP, 13 cd/m2 for MPP to counteract the slightly stronger local contrasts due to the presence of multiple stimuli) rather than black to reduce straylight effects (i.e., to elevate response thresholds of non-stimulated locations; Portengen et al., 2021). A green bull's eye (0.1-degree radius; not shown in the figures) in the center served as a fixation point.

3.3.3 Procedure

Participants were instructed to fixate the center of the screen but covertly pay attention to the wedges. To ensure that participants paid attention to the stimuli, participants had to press spacebar in response to the appearance of cues (Naber et al., 2013). Cues consisted of a wedge with thin red edges that appeared in ~40 percent of the trials for 0.25 seconds. Participants were tested on varying times of the day. Only the right eye was tested and recorded, leaving the left eye patched. Test duration for each method was 792 seconds (6s stimulus presentation, 44 stimulus regions, 3 aVFDs). Total duration of the experiment, including instructions, eye-tracker calibration and breaks, was between 40 and 60 min per participant. All stimuli were presented in a gaze-contingent manner, meaning that the eye tracking software follows the subject's direction of fixation and updates the position of the stimuli on the monitor real-time to reflect changes in direction of gaze.

3.3.4 Analysis

Pupil size data were restructured from the continuous recording with an event-related approach using a series of steps. First, blink periods were deleted from continuous data. Blink on- and offsets were detected by setting a speed threshold of 3 standard deviations (SD) above the mean. The removed blink periods were interpolated with a cubic method using the interp1 MATLAB function. In the case of UPP, we used the trial start events to window pupil responses to each trial (and thus to each wedge; every 6s) in 3s epochs. For FPP, we chose a 5s epoch between 1-6 seconds after stimulus onset, therewith ignoring the initial constriction in the first second that tends to have a divergent and variable amplitude which complicates accurate FFT power estimations. In the case of MPP, we applied an event-related approach, creating 3000ms epochs per luminance change (every 250ms). The pupil data was then filtered per trial. Pupil traces from trial start to trial end were saved in a matrix with each row representing a trial and each column representing a timepoint. Pupil sizes were then baseline corrected by subtracting pupil size at stimulus onset. Except for MPP, pupil size was filtered for low frequency noise by subtracting a low-pass Butterworth fit (3rd order, 0.2 Hz cutoff). This correction allowed comparisons across participants and for FPP it ensured that the 2 Hz signal fluctuated around zero for proper frequency analyses. Also, pupil size data were filtered to remove high-frequency noise by applying a low-pass Butterworth filter (5th order, 30 Hz cutoff). UPP and FPP trials were removed if the pupil size variance within a trial crossed a threshold of 4 SD above the mean. The latter removal procedure was iterated in 3 loops. Note that for UPP and MPP, pupil size moves back to baseline before the end of the 3s epoch duration.

Subsequently, pupil size as a function of time from trial or epoch onset was first normalized across eccentricities. The average pupil traces for trials with stimulations of the largest eccentricity (fifth outer ring) without scotomas served as a baseline and any deviations from its average pupil trace for the other eccentricities were corrected. The pupil sensitivity was determined from the filtered pupil traces in a different manner per perimetry method: For UPP, the pupil constriction amplitude was used as a measure of pupil sensitivity. It was extracted per trial by subtracting minimum pupil size within a 200-1200ms time window after trial onset (i.e., the period a pupil constriction has ended) from the maximum pupil size within a 0-500ms time window after trial onset (i.e., the period a pupil constriction starts). For FPP, pupil oscillation power from a periodogram at 2 Hz served as a measure of pupil sensitivity. Full trial periods of pupil size were each converted to the frequency domain using a Lomb-Scargle algorithm. The convergence and calculation of pupil oscillation power was independent of and thus not affected by individual variability in phase (Naber et al., 2018; Portengen et al., 2021). For MPP, pupil sensitivity was operationalized as the absolute area under the event-related pupil response (ERPR) averaged across all luminance changes per wedge within a time window of 250-1500ms (i.e., the period an ERPR was present and not yet moved back to baseline). For consistency we reference to all three different manners of pupil measurement calculation as *pupil responsiveness* from now on.

To determine whether pupil responsiveness differed across scotoma types, we performed a repeated measures ANOVA. Two-dimensional pupil sensitivity maps were created with a harmonic spline interpolation to fill the gaps between the centers of the 44 stimulus wedge locations. The performance of each perimetry method was based on how well the method distinguished between present and absent stimuli across trials. The comparison across methods was made with the index d prime (i.e., an index of the discriminability of a signal, given by the separation between the peaks of the probability distributions, defined in z scores), the area under the curve (AUC) of the receiver operating characteristics (ROC), and the adjusted effect size for small sample sizes (Hedge's g). The d prime, and AUC values per participant were compared across the three methods with paired double-sided t tests. Stimulus protocol scripts, data, and analysis files are available on https://osf.io/bqwk8.

3.4 Results

We were interested in how the three different pupil perimetry methods differed with respect to how well they detected an aVFD. First, we inspected whether the pupil responded according to our expectations: a relatively fast constriction after stimulus onset and a slower return to baseline for UPP, pupil size oscillations at a rate of approximately 2 Hz for FPP, and significant response to luminance changes per wedge for MPP. These expectations were confirmed (***Figure 3a;*** See Supplementary ***Figure S1*** for responses per scotoma condition).

Next, we checked whether trials with absent and partially absent

stimuli evoked weaker pupil responses than trials with present stimuli. Indeed, the pupil responsiveness differed significantly across visibility conditions for all three methods (***Figure 3b;*** See Supplementary ***Table S1*** and ***S2***, for ANOVA results and post-hoc comparisons).

To inspect differences in pupil responsiveness across stimulus locations, we plotted visual field sensitivity heatmaps ***(Figure 4)***. These maps showed that pupil responses significantly decreased in the scotoma regions, especially for the scotoma types quadrantanopia and large scotoma. The maps of the small scotoma condition contained somewhat increased variability in response (i.e., noise) across the visual field. Also, both the pupil responsiveness in scotoma regions and the amount of noise across all regions appeared to be lowest for the FPP method.

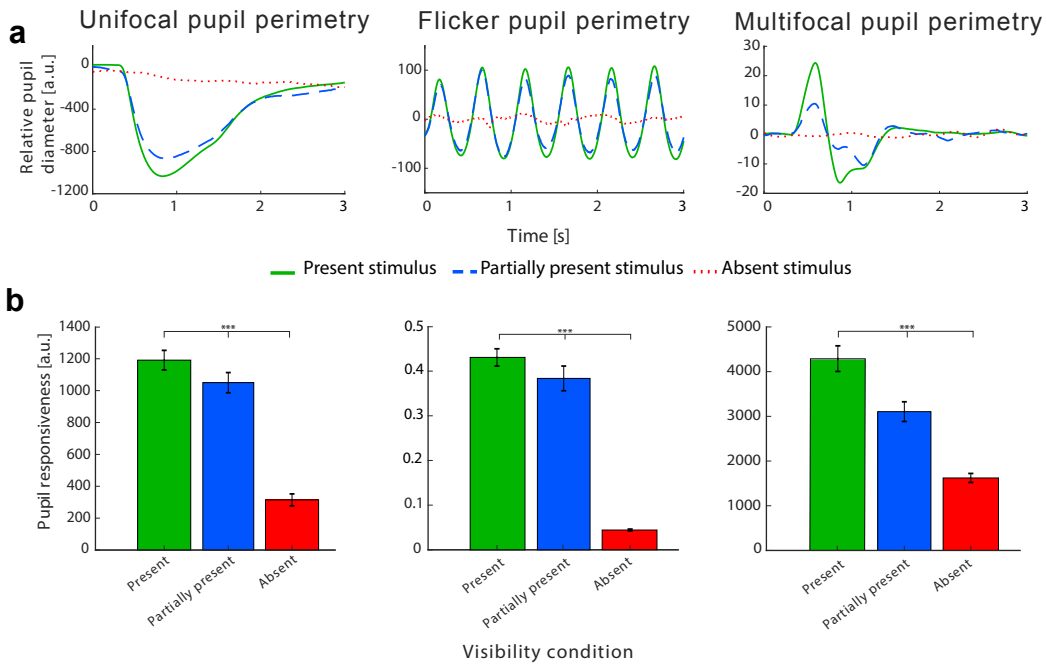

Figure 3. Pattern of pupil responsiveness as a function of time averaged across locations per participant for unifocal pupil perimetry (UPP), flicker pupil perimetry (FPP) and multifocal pupil perimetry (MPP). (a) Pupil traces per visibility condition; present (solid green), partially present (dashed blue) and absent (dotted red) stimuli. Note that only the first three seconds of the FPP stimulus duration were depicted to improve comparability across methods. (b) Pupil responsiveness per visibility condition (same colors as Figure 3a) per method (panels) averaged across participants with standard errors from the mean. See Figure S1 in supplementary materials for results per scotoma condition. Note that the scale of the y-axis differs across methods and between panel a and b because of the distinct ways the pupil responsiveness is calculated per method (see Methods section; this does not harm the within-subject comparisons).

To inspect how well the PP methods dissociated between unstimulated (artificial scotomas) and stimulated (intact) VF, we created histograms of trial probability as a function of pupil responsiveness for present, partially present, and absent stimulus conditions per PP method ***(Figure 5a)***. To quantify the dissociation performance of the PP methods, we calculated d-prime, AUC, and Hedge's g values per participants, which showed highest sensitivity for the FPP method for present versus absent trials (***Figure 5b;*** median d-prime values: UPP = 4.65 ± 1.54, FPP = 6.26 ± 2.49, MPP = 3.07 ± 1.17; ***See Table 1***) and partially present versus absent trials (Figure 5b; median d-prime values: UPP = 3.73 ± 2.29, FPP = 13.84 ± 6.46, MPP = 3.14 ± 1.74). Differences were smaller for present versus partially present trials (***Figure 5b;*** median d-prime values: UPP = 0.87 ± 0.94, FPP = 0.78 ± 1.07, MPP = 1.19 ± 0.62). Statistically comparing the d-prime and AUC values per participant across methods (***Figure 5b;*** See Supplementary ***Figure S2*** for violin plots, and ***Table S3*** and ***Table S4***, for statistics) revealed that FPP produced the least overlapping and most separated pupil sensitivities between absent and present, and partially present versus absent stimulus conditions. MPP performed best for distinguishing present versus partially present trials.

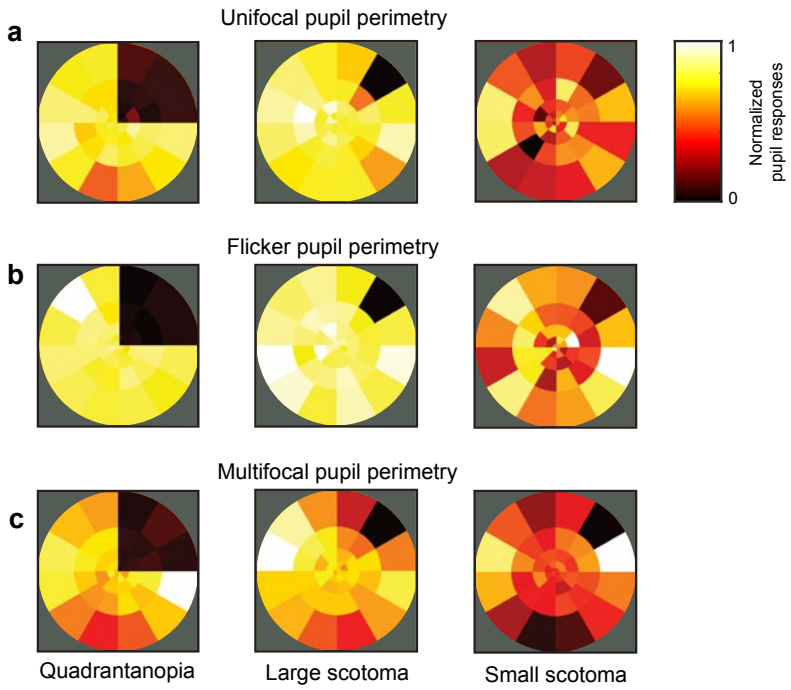

Figure 4. Normalized high-resolution pupil responsiveness visual field heatmaps averaged across all participants per pupil perimetry method (i.e., unifocal [a], flicker [b], and multifocal [c] pupil perimetry) and artificial scotoma condition (left: quadrantanopia, center: large scotoma, right: small scotoma). Maps of pupil responses from conditions in which artificial scotomas were presented on the left hemifield were horizontally flipped to create this figure. For the quadrantanopia and large scotoma conditions, pupil responses significantly decreased across all methods. The small scotoma condition produced more variance in pupil responsiveness across locations in all methods. Flicker pupil perimetry produced few spurious results in scotoma locations and the least variance across all locations.

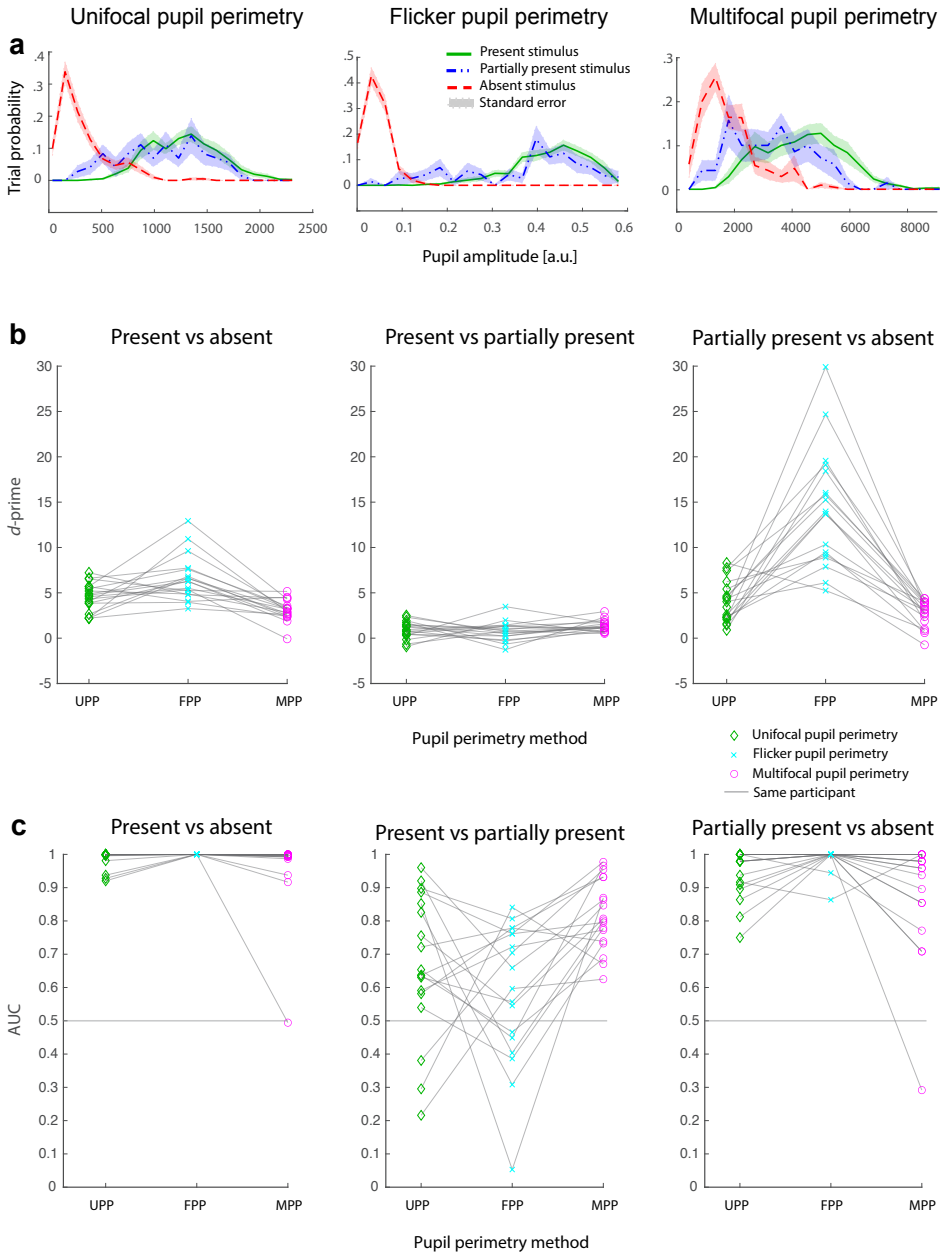

Figure 5. Sensitivity comparison of three pupil perimetry (PP) methods; unifocal (UPP), flicker (FPP) and multifocal pupil perimetry (MPP). (a) Shows the number of trials per pupil sensitivity for present (blue continuous line), partially present (green dash and dotted line) and absent (red dashed line) stimuli per PP method (panels). (b) Depicts d-prime plots per PP method (marker colors) per participant (transparent gray lines connecting markers) for present versus absent (left panel), present versus partially present (middle panel), and partially present versus absent (right panel) stimuli; higher d-prime values correspond to greater distinctive properties. (c) Shows AUC plots per PP method (marker colors) per participant (dotted black lines) for present versus absent (left panel), present versus partially present (middle panel), and partially present versus absent (right panel) stimuli.

			Partially present	Absent
Unifocal PP	*Present*	*AUC ± SD*	0.65 ± 0.21	0.99 ± 0.03
		d-prime ± SD	0.87 ± 0.94	4.65 ± 1.54
		Hedge's g (CI)	0.60 (0.33; 0.88)	3.01 (2.82; 3.22)
	Partially present	*AUC ± SD*		0.98 ± 0.07
		d-prime		3.73 ± 2.29
		Hedge's g (CI)		2.57 (2.15; 3.08)
Flicker PP	*Present*	*AUC ± SD*	0.63 ± 0.21	1.0 ± 0.00
		d-prime ± SD	0.78 ± 1.07	6.26 ± 2.49
		Hedge's g (CI)	0.57 (0.22; 0.93)	5.05 (4.77; 5.38)
	Partially present	*AUC ± SD*		1.0 ± 0.03
		d-prime ± SD		13.84 ± 6.46
		Hedge's g (CI)		4.54 (3.78; 5.65)
Multifocal PP	*Present*	*AUC ± SD*	0.80 ± 0.11	0.99 ± 0.12
		d-prime ± SD	1.19 ± 0.62	3.07 ± 1.17
		Hedge's g (CI)	0.79 (0.54; 1.02)	1.94 (1.79; 2.10)
	Partially present	*AUC ± SD*		0.96 ± 0.18
		d-prime ± SD		3.14 ± 1.74
		Hedge's g (CI)		1.35 (1.02; 1.72)

Table 1. Comparison of visibility conditions per pupil perimetry method (area under the receiver operating characteristics curve, d-prime, and corrected effect size measures through Hedge's g). Median values are reported for AUC and d-prime. SD = standard deviation, CI = confidence interval

3.5 Discussion

This is the first study comparing three different PP methods. From our results we can conclude that all three PP methods show high discriminative power for differentiating between present and absent stimuli, and between partially present and absent stimuli in healthy adults.

Especially FPP turned out to be qualified to distinguish between present and absent (and partially present) stimuli. One explanation for FPPs high diagnostic accuracy might be that the combination of the single stimulus presentation with an increased number of pupillary measurements in a short time period resulted in multiple, reliable phasic pupil responses (i.e., decreasing the chance of incidental pupil fluctuations). These responses could in turn be particularly well suited to distinguish between within-field anisotropies as opposed to looking at average sensitivity across the visual field and between damaged and intact visual fields in a clinical

setting (Naber et al., 2018). Others used flickering stimuli at higher frequencies (i.e., 15 and 30 Hz; James et al., 2012; Sabeti et al., 2014). However, frequencies above 3-4 Hz do not evoke the oscillating pupil responses inherent to the flickering method of this study (Naber et al., 2013). The results suggest that a stimulus paradigm with high spatial sparseness and low sparseness of events leads to overall best power in dissociating present, partially present and absent stimuli. The high pupil sensitivity to detect hemianopic and quadrantanopic scotomas due to cortical damage, and glaucoma-caused scotomas, displayed in the first FPP study of Naber et al. (2018), endorse the results found in this study.

Our results showed small between-subject differences for sensitivity measures across visibility conditions and PP methods. Conversely, large individual variation was seen in present versus partially present trials; distinguishing between these conditions remains a challenge when using PP methods (MPP performed only slightly better). This imprecision can partly be explained by the use of large stimulus sizes, which sacrifices spatial precision in the peripheral visual field. The presentation of large stimuli is a prerequisite for evoking more reliable pupil responses, but results in coarse sensitivity maps.

It is also not yet possible to dissociate exact VFD locations within a stimulus wedge. To resolve this, a similar stimulus map used by Maddess et al. (2013), which employs overlapping stimuli shown at different time intervals, or smaller stimuli at more locations like Naber et al. (2018) could be used (with weaker pupil responses as a result). Thus, PP methods are currently more suited for screening purposes than for regular follow-up and monitoring small changes in the visual field across time. Conversely, because of the flexible set-up of pupil perimetry, protocols can easily be interchanged and adjusted. Varying PP protocols could be incorporated for different goals; larger and less stimuli to quickly screen for clinically significant VFDs, and smaller stimuli at more locations to accurately detect small changes during follow-up. Further development could entail automation of a direct diagnostic report and a scotoma edge detection algorithm.

Note, however, that improvements can still be made to the current PP paradigms. Most developments have been reported for MPP (Carle et al., 2015, 2022; Sabeti et al., 2011, 2013; Tan et al., 2001; Wilhelm et al., 2000). Our MPP variant was performed with a relatively high framerate (a possible change in luminance every 250ms) and long stimulus-on durations and thus differed from state-of-the-art MPP methods in some respects. For example, the method of Wilhelm et al. (2000) involved a scaled honeycomb array and covered 50 degrees of visual field, their stimuli were presented with a 50% probability in each test-region, similar to the original ERG multifocal method proposed by Sutter (1991; 1992); Tan et al. (2001) created temporally more sparse stimuli by inserting blank frames between frames containing stimuli; Sabeti et al. (2011), and Ho et al. (2010) used colored stimuli and a higher presentation frequency, resulting in high temporal sparseness due to short stimulus durations and long inter-stimulus intervals. The most recent MPP method of Carle et al. (2022) features a clustered volley technique, which brings the stimuli closer to each other, and longer interstimulus times than previous iterations, actually making it resemble FPP more with respect to spatiotemporal properties. However, Carle et al.'s MPP method also implements color, luminance balancing (i.e., variance in luminance across stimulus locations) and no black stim-off region. Nonetheless, these improvements can also be implemented in FPP (and UPP), meaning that the here reported differences across PP methods remain valid despite the use of rather basic stimulus paradigms.

It is possible that pupil responses become more sensitive when evoked with fewer stimulus changes per second (e.g., 1 Hz instead of 2 Hz) and a spatial sparseness somewhere in between the range of 1 and approximately half of the 44 locations, as pupil responses seem to be stronger when more stimuli are shown, even at a constant luminance (Castaldi et al., 2021). Although out of scope of the current study, an optimal spatial and temporal sparseness remains to be found. Nonetheless, the main advantage of endorsing a lower temporal sparseness lies within more data points per trial and consequently shorter testing times.

While unifocal and flicker PP methods benefit from an attentional cueing paradigm (Binda & Murray, 2015; Einhäuser, 2017; Mathôt & Van der Stigchel, 2015; Naber et al., 2013; Portengen et al., 2021), evidence has been provided that a centrally directed attentional task and covertly directed attention reduces signal quality on multifocal methods (Rosli et al., 2018). This likely stems from a divided attention across multiple simultaneously shown stimuli.

The current study used a dark gray background to suppress the influence of stray light (seen with black backgrounds) and to increase pupil responsiveness (as compared to a lighter gray background; Portengen et al., 2021). This testing method may be improved even more by implementing chromatic properties, such as hue, brightness and saturation, to strengthen pupil response amplitudes driven by contrasts between those properties and to isolate the retinal opsin, rhodopsin or melanopsin pathways (Carle et al., 2015; Chibel et al.,

2016; Maeda et al., 2017). The use of narrow band yellow (around 580 nm) rather than full visible spectrum white (the latter includes blue light) stimuli may reduce blue-color-sensitive melanopsin retinal ganglion cell activity and its effect on pupil responses and therewith could contribute to a more accurate diagnosis of VFDs specifically caused by cortical damage (Rosli et al., 2018).

A limitation of the current study is that no normative data from a "no scotoma condition" was used in the analysis, and left versus right visual fields per participant may have contained small biases due to temporal versus nasal anisotropies. Although these biases did not hamper the comparison between methods, overall discriminative power could be weaker than when normative data were used.

Another limitation pertains to the use of hard edges for the artificially simulated VFDs, which do not accurately represent real world situations with actual visual field defects. Although simulating VFDs in healthy participants is an established strategy (e.g., Gestefeld et al., 2020), it does not mimic VFDs entirely. Real scotomas tend to have smooth edges with a gradual gradient from visible to invisible. Due to limitations of the used computer, computing soft edged wedges leads to technical problems such as slower frame rates. The wedges were created in real-time to ensure a different order of appearance for each participant. In future studies, this could be resolved by creating multiple videos with random presentation orders in advance rather than on-line stimulus buffering. Regardless, several studies showed promising results with PP in more realistic situations, such as detecting the blind spot (Portengen et al., 2021) and testing patients suffering from VFDs (e.g., Carle et al., 2015; Chibel et al., 2016; Kardon, 1992; Maeda et al., 2017; Naber et al., 2018; Rajan et al., 2002; Schmid et al., 2005; Skorkovská, Lüdtke, et al., 2009; Skorkovská, Wilhelm, et al., 2009; Tan et al., 2001; Yoshitomi et al., 1999). Future studies testing subjects with visual field defects due to neurological impairment will further clarify the role of PP in testing visual fields.

As a last point, it is important to stress PPs advantages over SAP. In addition to its high accuracy in detecting artificial scotomas, PP is an objective method for testing VF in a short amount of time (~4 minutes per eye and method). This is comparable to subjective fast SAP methods, such as Swedish Interactive Testing Algorithm (SITA) 24-2 FAST and Tendency-Oriented Perimetry (TOP). Combined with the minimal cooperation required, this method might have merit for application in young children or neurologically impaired subjects affected by cerebral visual impairment who generally show difficulties in completing an SAP test reliably (Patel et al., 2015; Wong & Sharpe, 2000). Current alternatives for young or neurologically impaired children are behavioral perimetry tests, such as the behavioural visual field (BEFIE) screening test. The BEFIE test shows high specificity and sensitivity for absolute peripheral VFDs in neurologically impaired children (Koenraads et al., 2015). Additionally, the BEFIE test detects VFDs 4 years earlier than SAP (Portengen et al., 2020). However, limitations of the BEFIE test are the need of two assessors along with the inability to test the central VF and detect relative scotomas. PP circumvents these limitations and might be a suitable alternative to objectively test this patient group. Future studies may determine whether PP can map the visual fields of children in an accurate, quick and engaging way.

3.6 Conclusion

To conclude, we conducted the first in-depth comparison of three PP methods. All methods performed reasonably well in discerning simulated scotomas in healthy adults but gaze-contingent flicker pupil perimetry was superior in differentiating between (partially) present and absent stimuli whereas multifocal pupil perimetry slightly better discerned present from partially present stimuli.

3.7 References

Allen, L. E., Slater, M. E., Proffitt, R. V., Quarton, E., & Pelah, A. (2012). A new perimeter using the preferential looking response to assess peripheral visual fields in young and developmentally delayed children. *Journal of AAPOS, 16*(3), 261–265. https://doi.org/10.1016/j.jaapos.2012.01.006

Artes, P. H., Iwase, A., Ohno, Y., Kitazawa, Y., & Chauhan, B. C. (2002). Properties of perimetric threshold estimates from full threshold, SITA standard, and SITA fast strategies. *Investigative Ophthalmology and Visual Science, 43*(8), 2654–2659. https://iovs.arvojournals.org/article.aspx?articleid=2124008

Binda, P., & Murray, S. O. (2015). Spatial attention increases the pupillary response to light changes. *Journal of Vision, 15*(2), 1–1. https://doi.org/10.1167/15.2.1

Brainard, D. H. (1997). The Psychophysics Toolbox. *Spatial Vision, 10*(4), 433–436. https://doi.org/10.1163/156856897X00357

Buračas, G. T., & Boynton, G. M. (2002). Efficient design of event-related fMRI experiments using m-sequences. *NeuroImage, 16*(3 I), 801–813. https://doi.org/10.1006/nimg.2002.1116

Carle, C. F., James, A. C., Kolic, M., Essex, R. W., & Maddess, T. (2015). Blue multifocal pupillographic objective perimetry in glaucoma. *Investigative Ophthalmology and Visual Science, 56*(11), 6394–6403. https://doi.org/10.1167/iovs.14-16029

Carle, C. F., James, A. C., Sabeti, F., Kolic, M., Essex, R. W., Shean, C., Jeans, R., Saikal, A., Licinio, A., & Maddess, T. (2022). Clustered Volleys Stimulus Presentation for Multifocal Objective Perimetry. *Translational Vision Science and Technology, 11*(2), 5–5. https://doi.org/10.1167/tvst.11.2.5

Castaldi, E., Pomè, A., Cicchini, G. M., Burr, D., & Binda, P. (2021). Pupil size automatically encodes numerosity. *Journal of Vision, 21*(9), 2302. https://doi.org/10.1167/jov.21.9.2302
Chibel, R., Sher, I., Ben Ner, D., Mhajna, M. O., Achiron, A., Hajyahia, S., Skaat, A., Berchenko, Y., Oberman, B., Kalter-Leibovici, O., Freedman, L., & Rotenstreich, Y. (2016). Chromatic Multifocal Pupillometer for Objective Perimetry and Diagnosis of Patients with Retinitis Pigmentosa. *Ophthalmology, 123*(9), 1898–1911. https://doi.org/10.1016/j.ophtha.2016.05.038
Cornelissen, F. W., Peters, E. M., & Palmer, J. (2002). The Eyelink Toolbox: Eye tracking with MATLAB and the Psychophysics Toolbox. *Behavior Research Methods, Instruments, and Computers, 34*(4), 613–617. https://doi.org/10.3758/BF03195489
Einhäuser, W. (2017). The pupil as marker of cognitive processes. In *Cognitive Science and Technology* (pp. 141–169). Springer, Singapore. https://doi.org/10.1007/978-981-10-0213-7_7
Gestefeld, B., Grillini, A., Marsman, J. B. C., & Cornelissen, F. W. (2020). Using natural viewing behavior to screen for and reconstruct visual field defects. *Journal of Vision, 20*(9), 1–16. https://doi.org/10.1167/JOV.20.9.11
Harding, G. F. A., Spencer, E. L., Wild, J. M., Conway, M., & Bohn, R. L. (2002). Field-specific visual-evoked potentials: Identifying field defects in vigabatrin-treated children. *Neurology, 58*(8), 1261–1265. https://doi.org/10.1212/WNL.58.8.1261
Ho, Y.-L., Wong, S. S. Y., Carle, C. F., James, A. C., Kolic, M., Maddess, T., & Goh, X.-L. (2010). Multifocal Pupillographic Perimetry With White and Colored Stimuli. *Journal of Glaucoma, 20*(6), 336–343. https://doi.org/10.1097/ijg.0b013e3181efb097
James, A. C., Kolic, M., Bedford, S. M., & Maddess, T. (2012). Stimulus parameters for multifocal pupillographic objective perimetry. *Journal of Glaucoma, 21*(9), 571–578. https://doi.org/10.1097/IJG.0b013e31821e8413
Kardon, R. H. (1992). Pupil perimetry. In *Current Opinion in Ophthalmology* (Vol. 3, Issue 5, pp. 565–570). https://doi.org/10.1097/00055735-199210000-00002
Kardon, Randy H., Kirkali, P. A., & Thompson, H. S. (1991). Automated Pupil Perimetry Pupil Field Mapping in Patients and Normal Subjects. *Ophthalmology, 98*(4), 485–496. https://doi.org/10.1016/S0161-6420(91)32267-X
Kleiner, M., Brainard, D. H., Pelli, D. G., Broussard, C., Wolf, T., & Niehorster, D. (2007). What's new in Psychtoolbox-3? A free cross-platform toolkit for psychophysiscs with Matlab and GNU/Octave. In *Cognitive and Computational Psychophysics* (Vol. 36). http://www.psychtoolbox.org
Koenraads, Y., Braun, K. P. J., van der Linden, D. C. P., Imhof, S. M., & Porro, G. L. (2015). Perimetry in young and neurologically impaired children: the Behavioral Visual Field (BEFIE) Screening Test revisited. *JAMA Ophthalmology, 133*(3), 319–325. https://doi.org/10.1001/jamaophthalmol.2014.5257
Maddess, T. (2014). Modeling the relative influence of fixation and sampling errors on retest variability in perimetry. *Graefe's Archive for Clinical and Experimental Ophthalmology, 252*(10), 1611–1619. https://doi.org/10.1007/s00417-014-2751-y
Maddess, T., Bedford, S. M., Goh, X. L., & James, A. C. (2009). Multifocal pupillographic visual field testing in glaucoma. *Clinical & Experimental Ophthal mology, 37*(7), 678–686. https://doi.org/10.1111/j.1442-9071.2009.02107.x
Maddess, T., Essex, R. . W., Kolic, M., Carle, C. F. ., & James, A. C. (2013). High- versus low-density multifocal pupillographic objective perimetry in glaucoma. *Clinical & Experimental Ophthalmology, 41*(2), 140–147. https://doi.org/10.1111/ceo.12016
Maeda, F., Kelbsch, C., Straßer, T., Skorkovská, K., Peters, T., Wilhelm, B., & Wilhelm, H. (2017). Chromatic pupillography in hemianopia patients with homonymous visual field defects. *Graefe's Archive for Clinical and Experimental Ophthalmology, 255*(9), 1837–1842. https://doi.org/10.1007/s00417-017-3721-y
Mathôt, S., & Van der Stigchel, S. (2015). New Light on the Mind's Eye: The Pupillary Light Response as Active Vision. *Current Directions in Psychological Science, 24*(5), 374–378. https://doi.org/10.1177/0963721415593725
Naber, M., Alvarez, G. A., & Nakayama, K. (2013). Tracking the allocation of attention using human pupillary oscillations. *Frontiers in Psychology, 4*, 919. https://doi.org/10.3389/fpsyg.2013.00919
Naber, M., Roelofzen, C., Fracasso, A., Bergsma, D. P., van Genderen, M., Porro, G. L., Dumoulin, S. O., & van der Schouw, Y. T. (2018). Gaze-Contingent Flicker Pupil Perimetry Detects Scotomas in Patients With Cerebral Visual Impairments or Glaucoma. *Frontiers in Neurology, 9*(July), 558. https://doi.org/10.3389/fneur.2018.00558
Numata, T., Maddess, T., Matsumoto, C., Okuyama, S., Hashimoto, S., Nomoto, H., & Shimomura, Y. (2017). Exploring test-retest variability using high-resolution perimetry. *Translational Vision Science and Technology 6*(5), 8–8. https://doi.org/10.1167/tvst.6.5.8
Patel, D. E., Cumberland, P. M., Walters, B. C., Russell-Eggitt, I., Rahi, J. S., & OPTIC study group, O. study. (2015). Study of Optimal Perimetric Testing in Children (OPTIC): Feasibility, Reliability and Repeatability of Perimetry in Children. *PloS One, 10*(6), e0130895. https://doi.org/10.1371/journal.pone.0130895
Pel, J. J. M., van Beijsterveld, M. C. M., Thepass, G., & van der Steen, J. (2013). Validity and Repeatability of Saccadic Response Times Across the Visual Field in Eye Movement Perimetry. *Translational Vision Science & Technology, 2*(7), 3. https://doi.org/10.1167/tvst.2.7.3
Pelli, D. G. (1997). The VideoToolbox software for visual psychophysics: Transforming numbers into movies. *Spatial Vision, 10*(4), 437–442. https://doi.org/10.1163/156856897X00366
Piltz, J. R., & Starita, R. J. (1990). Test-retest variability in glaucomatous visual fields. In *American Journal of Ophthalmology* (Vol. 109, Issue 1, pp. 109–110). https://doi.org/10.1016/s0002-9394(14)75602-8
Portengen, B. L., Koenraads, Y., Imhof, S. M., & Porro, G. L. (2020). Lessons Learned from 23 Years of Experience in Testing Visual Fields of Neurologically Impaired Children. *Neuro-Ophthalmology, 44*(6), 361–370. https://doi.org/10.1080/01658107.2020.1762097
Portengen, B. L., Roelofzen, C., Porro, G. L., Imhof, S. M., Fracasso, A., & Naber, M. (2021). Blind spot and visual field anisotropy detection with flicker pupil perimetry across brightness and task variations. *Vision Research, 178*(October 2020), 79–85. https://doi.org/10.1016/j.visres.2020.10.005
Rajan, M. S., Bremner, F. D., & Riordan-Eva, P. (2002). Pupil perimetry in the diagnosis of functional visual field loss. *Journal of the Royal Society of Medicine, 95*(10), 498–500. https://doi.org/10.1258/jrsm.95.10.498
Rosli, Y., Carle, C. F., Ho, Y., James, A. C., Kolic, M., Rohan, E. M. F., & Maddess, T. (2018). Retinotopic effects of visual attention revealed by dichoptic multifocal pupillography. *Scientific Reports, 8*(1), 1–13. https://doi.org/10.1038/s41598-018-21196-1
Sabeti, F., James, A. C., Carle, C. F., Essex, R. W., Bell, A., & Maddess, T. (2017). Comparing multifocal pupillographic objective perimetry (mfPOP) and multifocal visual evoked potentials (mfVEP) in retinal diseases. *Scientific Reports, 7*, 45847. https://doi.org/10.1038/srep45847
Sabeti, F., James, A. C., Essex, R. W., & Maddess, T. (2013). Multifocal pupillography identifies retinal dysfunction in early age-related macular degeneration. *Graefe's Archive for Clinical and Experimental Ophthalmology, 251*(7), 1707–1716. https://doi.org/10.1007/s00417-013-2273-z
Sabeti, F., James, A. C., & Maddess, T. (2011). Spatial and temporal stimulus variants for multifocal pupillography of the central visual field. *Vision Research, 51*(2), 303–310. https://doi.org/10.1016/J.VISRES.2010.10.015
Sabeti, F., Maddess, T., Essex, R. W., Saikal, A., James, A. C., & Carle, C. F. (2014). Multifocal pupillography in early age-related macular degeneration. *Optometry and Vision Science, 91*(8), 904–915. https://doi.org/10.1097/OPX.0000000000000319
Schmid, R., Luedtke, H., Wilhelm, B. J., & Wilhelm, H. (2005). Pupil campimetry in patients with visual field loss. *European Journal of Neurology, 12*(8), 602–608. https://doi.org/10.1111/j.1468-1331.2005.01048.x
Skorkovská, K., Lüdtke, H., Wilhelm, H., & Wilhelm, B. (2009). Pupil campimetry in patients with retinitis pigmentosa and functional visual field loss. *Graefe's Archive for Clinical and Experimental Ophthalmology, 247*(6), 847–853. https://doi.org/10.1007/s00417-008-1015-0
Skorkovská, K., Wilhelm, H., Lüdtke, H., & Wilhelm, B. (2009). How sensitive is pupil campimetry in hemifield loss? *Graefe's Archive for Clinical and Experimental Ophthalmology, 247*(7), 947–953. https://doi.org/10.1007/s00417-009-1040-7
Sutter, E. E. (1991). Fast m-transform. A fast computation of cross-correlations with binary m-sequences. *SIAM Journal on Computing, 20*(4), 686–694. https://doi.org/10.1137/0220043
Sutter, E. E., & Tran, D. (1992). The field topography of ERG components in man-I. The photopic luminance response. *Vision Research, 32*(3), 433–446. https://doi.org/10.1016/0042-6989(92)90235-B
Tan, L., Kondo, M., Sato, M., Kondo, N., & Miyake, Y. (2001). Multifocal pupillary light response fields in normal subjects and patients with visual field defects. *Vision Research, 41*(8), 1073–1084. https://doi.org/10.1016/S0042-6989(01)00030-X
Wall, M., Woodward, K. R., Doyle, C. K., & Artes, P. H. (2009). Repeatability of automated perimetry: A comparison between standard automated perimetry with stimulus size III and V, matrix, and motion perimetry. *Investigative Ophthalmology and Visual Science, 50*(2), 974–979. https://doi.org/10.1167/iovs.08-1789
Wilhelm, H., Neitzel, J., Wilhelm, B., Beuel, S., Lüdtke, H., Kretschmann, U., & Zrenner, E. (2000). Pupil Perimetry using M-Sequence Stimulation Technique. *Investigative Ophthalmology & Visual Science, 41*(5), 1229–1238. https://dx.doi.org/
Wong, A. M. F., & Sharpe, J. A. (2000). A comparison of tangent screen, goldmann, and humphrey perimetry in the detection and localization of occipital lesions. *Ophthalmology, 107*(3), 527–544. https://doi.org/10.1016/S0161-6420(99)00092-5
Yoshitomi, T., Matsui, T., Tanakadate, A., & Ishikawa, S. (1999). Comparison of Threshold Visual Perimetry and Objective Pupil Perimetry in Clinical Patients. *Journal of Neuro-Ophthalmology, 19*(2), 89–99. https://doi.org/10.1097/00041327-199906000-00003

3.8 Supplementary material

Figure S1. Pupil responsiveness averaged across all trials (i.e., including absent trials) per scotoma condition. Plots show pupil response amplitudes per pupil perimetry method (panels) per scotoma condition (colors) averaged across participants with standard errors from the mean. Note that pupil responses differ across methods due to different calculation methods and note the arbitrary unit (a.u.) due to the lacking distance measurements by the EyeLink eye tracker.

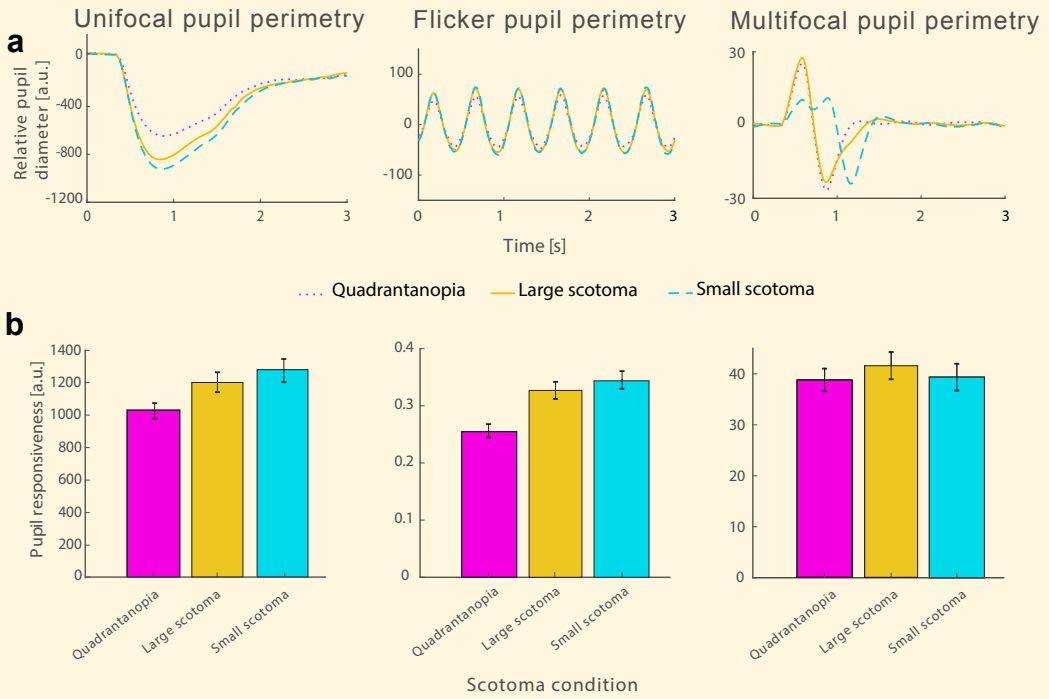

Figure S2. Sensitivity comparison of three pupil perimetry (PP) methods; unifocal (UPP), flicker (FPP) and multifocal pupil perimetry (MPP). (a) Depicts d-prime violin plots (mean and median represented by black and red line) per PP method (marker colors) per participant (markers) for present versus absent (left panel), present versus partially present (middle panel), and partially present versus absent (right panel) stimuli; higher d-prime values correspond to greater distinctive properties. (b) Shows AUC violin plots (mean and median represented by black and red line) per PP method (marker colors) per participant (markers) for present versus absent (left panel), present versus partially present (middle panel), and partially present versus absent (right panel) stimuli.

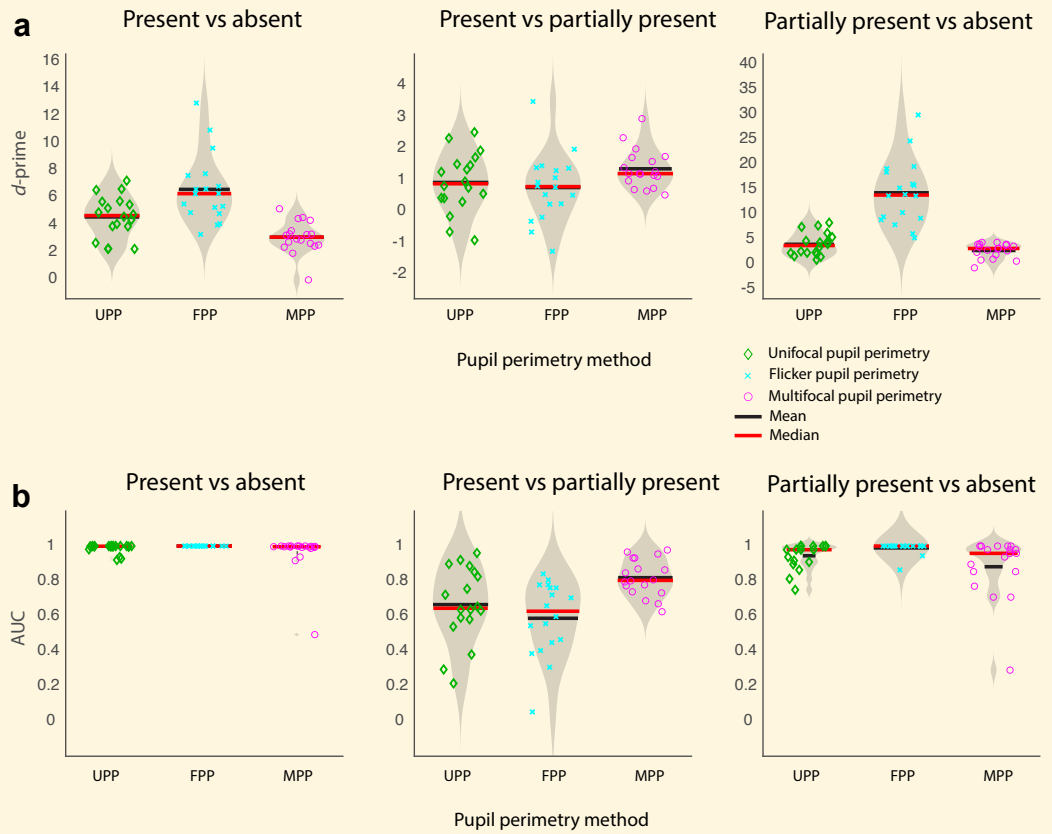

	Unifocal PP	Flicker PP	Multifocal PP
ANOVA visibility conditions	$F(2,17) = 103.29$, $P < .001$	$F(2,17) = 218.13$, $P < .001$	$F(2,17) = 99.30$, $P < .001$
ANOVA scotoma conditions	$F(2,17) = 18.41$, $P < .001$	$F(2,17) = 60.14$, $P < .001$	$F(2,17) = 1.90$, $P = 0.17$

Table S1. Differences in pupil responsiveness per visibility and scotoma condition per method.

		Partially present	Absent
Unifocal PP	*Present*	$t(17) = 3.56$, P = .002	$t(17) = 15.83$, P < .001
	Partially present		$t(17) = 11.38$, P < .001
Flicker PP	*Present*	$t(17) = 1.33$, P = .20	$t(17) = 8.00$, P < .001
	Partially present		$t(17) = 5.56$, P < .001
Multifocal PP	*Present*	$t(17) = 0.09$, P = .93	$t(17) = 5.28$, P < .001
	Partially present		$t(17) = 3.14$, P = .006

Table S2. Paired two-sided student's t-test statistically comparing pupil responsiveness across all visibility conditions (i.e., present, partially present, and absent) within each three pupil perimetry (PP) method.

		Flicker PP	Multifocal PP
Unifocal PP	*Present vs absent*	$t(17) = -2.87$, P = .01	$t(17) = 4.72$, P < .001
	Present vs partially present	$t(17) = 0.40$, P = .69	$t(17) = -1.86$, P = .08
	Partially present vs absent	$t(17) = -5.92$, P < .001	$t(17) = 2.11$, P = .049
Flicker PP	*Present vs absent*		$t(17) = 5.77$, P < .001
	Present vs partially present		$t(17) = -2.07$, P = 0.05
	Partially present vs absent		$t(17) = 8.38$, P < .001

Table S3. Statistical d-prime comparisons across the three pupil perimetry (PP) methods and across the three visibility conditions (present, partially present and absent) using paired two-sided student's t-tests

		Flicker PP	Multifocal PP
Unifocal PP	*Present vs absent*	$t(17) = -2.13$, P = .048	$t(17) = 0.87$, P = .40
	Present vs partially present	$t(17) = 0.98$, P = .34	$t(17) = -3.14$, P = .006
	Partially present vs absent	$t(17) = -2.35$, P = .03	$t(17) = 1.41$, P = .18
Flicker PP	*Present vs absent*		$t(17) = 1.40$, P = .18
	Present vs partially present		$t(17) = -4.31$, P < .001
	Partially present vs absent		$t(17) = 2.48$, P = .024

Table S4. Statistical AUC comparisons across the three pupil perimetry (PP) methods and across the three visibility conditions (present, partially present and absent) using paired two-sided student's t-tests

Blind spot and visual field anisotropy detection with flicker pupil perimetry across brightness and task variations

Vision Research (2021) doi: 10.1016/j.visres.2020.10.005

Portengen BL
Roelofzen C
Porro GL
Imhof SM
Fracasso A
Naber M

4.1. Abstract

The pupil can be used as an objective measure for testing sensitivities across the visual field (Pupil perimetry; PP). The recently developed gaze-contingent flicker PP (gcFPP) is a promising novel form of PP, with improved sensitivity due to retinotopically stable and repeated flickering stimulations, in a short time span. As a diagnostic tool gcFPP has not yet been benchmarked in healthy individuals. The main aims of the current study were to investigate whether gcFPP has the sensitivity to detect the blind spot, and upper versus lower visual field differences that were found before in previous studies. An additional aim was to test for the effects of attentional requirements and background luminance. A total of thirty individuals were tested with gcFPP across two separate experiments. The results showed that pupil oscillation amplitudes were smaller for stimuli presented inside as compared to outside the blind spot. Amplitudes also decreased as a function of eccentricity (i.e., distance to fixation) and were larger for upper as compared to lower visual fields. We measured the strongest and most sensitive pupil responses to stimuli presented on dark- and mid-gray backgrounds, and when observers covertly focused their attention to the flickering stimulus. GcFPP thus evokes pupil responses that are sensitive enough to detect local, and global differences in pupil sensitivity. The findings further encourage (1) the use of a gray background to prevent straylight without affecting gcFPPs sensitivity and (2) the use of an attention task to enhance pupil sensitivity.

4.2. Introduction

The diagnostic applicability of the dynamics of the eye's pupil has been a topic of research for various disciplines (Lussier, Olson, & Aiyagari, 2019; Naber, Alvarez, & Nakayama, 2013; Reuten, van Dam, & Naber, 2018; Wilhelm et al., 2000). In experimental ophthalmological studies, the pupil is used for testing the visual field (VF) sensitivity using pupil perimetry (PP) (Carle, James, Kolic, Loh, & Maddess, 2011; Kardon, Kirkali, & Thompson, 1991; Schmid, Luedtke, Wilhelm, & Wilhelm, 2005). This application was developed to meet a demand for objective perimetry in ophthalmology, to examine patients who have difficulty cooperating with standard automated perimetry (SAP) (Wilhelm et al., 2000) and circumvent malingering. Our research group developed a novel form of PP, termed gaze-contingent flicker PP (gcFPP), which evokes multiple pupil responses by showing 2 Hz flickering stimuli across the VF. A gaze-contingent stimulus presentation ensures that the retinal location is fixed by use of an eye-tracker. A gaze-contingent stimulus presentation can correct for saccades online. We have demonstrated its potential in detecting large VF defects caused by cerebral visual impairment and glaucoma (Naber et al., 2018). Its high diagnostic sensitivity compared to other PP paradigms stems from more measurements in shorter time spans and accurate retinotopic stimulation with gaze-contingent stimulus presentations. Flicker perimetry has been applied before (Luu et al., 2013; Phipps, Dang, Vingrys, & Guymer, 2004). However, these studies chose a high flicker frequency (12-18 Hz) rather than a slow frequency (2 Hz) as in the current study. Using a low frequency evokes a sequence of pupil oscillations, while a high frequency evokes a single pupil constriction, a stimulus paradigm equivalent to static perimetry.

Our first aim is to test whether the gcFPP protocol is capable of detecting subtle differences in VF testing to further confirm its usefulness in testing VF sensitivities beyond patients with large scotomas. One way to ascertain gcFPP's sensitivity is by detecting the reduced pupil sensitivities in the blind spot (i.e., the punctum caecum; a retinal location without photoreceptor cells where the optic nerve passes through the optics disc towards the brain). Another manner to assess the sensitivity of gcFPP is to measure how well pupil oscillation amplitudes can be used to detect VF anisotropies, such as identifying higher sensitivities to light changes in upper as compared to bottom VFs (Hong, Narkiewicz, & Kardon, 2001; Naber et al., 2018; Sabeti, James, & Maddess, 2011; Skorkovská, Wilhelm, Lüdtke, Wilhelm, & Kurtenbach, 2014; Tan, Kondo, Sato, Kondo, & Miyake, 2001; Wilhelm et al., 2000). The detection performance of the blind spot and anisotropies can best be examined in healthy participants rather than patients for practical reasons. Healthy participants are easier to recruit and can withstand higher testing demands such as relatively long examinations. The subjective visibility ratings by the healthy observers will then serve as ground truth for comparison to pupil response amplitudes in and around the blind spot.

Our second aim is to test for the effects of design and contextual factors that may interfere or enhance its sensitivity. For example, PP stimuli are typically presented on a black background (Skorkovská, Lüdtke, Wilhelm, & Wilhelm, 2009) in order to maximize visual contrast and therewith pupil oscillation amplitudes. However, dark backgrounds tend to reduce the threshold for photo-sensitive retinal cells to respond, leading to unwanted activation due to stray

light (e.g., a stimulus presented in the blind spot may still stimulate sensitive regions surrounding the blind spot due to light scatter). To circumvent this, our gcFPP protocol uses a (mid) gray background. However, it is currently unknown to what degree the increase of background luminance has detrimental effects on pupil sensitivity. A brighter background prevents straylight but also lowers Michelson contrast between the flickering stimulus and background and thus the pupil's responsiveness. We set to examine the ideal background illumination to minimize stray light effects and maximize pupil oscillation amplitudes in gcFPP.

Our third aim is to investigate the effects of the focus of attention of the observer. The pupillary light reflex does not only respond to retinal illumination. Instead, changes of pupil size are also modulated by top-down factors, such as the attentional state of the participant, with empirical evidence indicating that covert spatial attention can augment the pupillary responses (Binda & Murray, 2015; Binda, Pereverzeva, & Murray, 2013; Mathôt, van der Linden, Grainger, & Vitu, 2013; Naber et al., 2013; Naber & Nakayama, 2013). In our previous study (Naber et al., 2018), a covert attention detection task was used to evoke reliable pupil responses. A direct comparison between different attentional states in gcFPP has not yet been tested.

4.3 Methods

4.3.1 Participants

A total of thirty subjects participated in this study. One participant was excluded due to technical issues, resulting in twelve participants (11 females, age: *M* = 22.3, SD = 2.3) for Experiment 1 (blind spot detection), and eighteen tested observers (11 females, age: *M* = 21.9, SD = 1.5) for Experiment 2 (attention, luminance and visual field anisotropies). All participants were Dutch and reported having normal or corrected-to-normal visual acuity and having no visual disorders or neurological disorders. Participants were unaware of the purpose of the experiment and were only told that the eye-tracker measured their eye movements. Participants received financial reimbursement or study credit for participation, gave informed written consent on paper before the experiment, and were debriefed afterwards about the purpose of the experiment. This study conformed to the ethical principles of the Declaration of Helsinki, and was approved by the local ethical committee of the University Medical Center Utrecht (Approval number: 09/350).

4.3.2 Apparatus and stimuli

We used the same setup and stimuli for both experiments which were equivalent to those described by Naber and colleagues (2018). We generated stimuli on a Dell desktop computer with Windows 7 operating system (Microsoft, Redmond, Washington), MATLAB (Mathworks, Natick, MA, USA), and the Psychophysics toolbox extension (Brainard, 1997; Pelli, 1997). Stimuli were presented on an LED Asus ROG swift monitor (AsusTek Computer Inc., Taipei, Taiwan) that displayed 1920 by 1080 pixels at a 100 Hz refresh rate. The screen was 60 cm in width and 35 cm in height (320 cd/m2 maximum luminance), and the participant's viewing distance to the screen was fixed at 55 cm with a chin and forehead rest. We recorded pupil size and gaze angle using an Eyelink 1000 eye-tracker camera (SR Research, Ontario, Canada; 0.5-degree accuracy of gaze location) that was placed 40 cm in front of the participant below the screen. For the eye-tracker calibration we used a thirteen-point calibration grid which took ~3 min per eye. Both experiments were conducted in a darkened room without ambient light.

Experiment 1 – Blind spot detection

The stimuli (see ***Figure 1a*** and ***1b***) consisted of (i) a black and white bull's eye that was used to ensure fixation (0.4 degree radius), (ii) a flickering disk that was presented on a dark gray background (80 cd/m2) at separate locations per trial (randomized) centered around the estimated location of the blind spot (14 degrees from the vertical meridian; 2 degrees below the horizontal meridian; Wang et al., 2017), and (iii) a 2 Hz stream of characters superimposed on the disk for a letter detection task to ensure participants remained engaged with each stimulus (see Figure 1; also see Naber, Alvarez, & Nakayama, 2013 for details). When testing the left eye, the fixation point was placed on the right side (7.5 deg from the screen's center) of the screen and vice versa for the right eye. We used a gaze-contingent paradigm, meaning that the disk locations were corrected online with the same angle and amplitude read-out from the eye-tracker to ensure a stable flicker stimulation in retinal coordinates (also see Naber et al., 2018). Flicker rate was set at 2 Hz with a square wave step, and the change in stimulus luminance was between black at 0.01 cd/m2 and white at 320 cd/m2 luminance. The flickering disk had a width of 3.5 degrees in visual angle. The physiological blind spot typically has a width of 8- and height of 10 degrees in visual angle (Armaly, 1969; Safran, Mermillod, Mermoud, Weisse, & Desangles, 1993). Experiment 1 consisted of 130 trials (65 stimulus

location; one block for pupil measurements, another block for visibility ratings). Trials were randomized and each trial consisted of one stimulus presentation for 6 seconds.

Experiment 2 – Attention, luminance and visual field anisotropies

For experiment 2, we used the same stimuli but the locations of the stimuli were centered at a 9-degree maximum eccentricity around fixation that consisted of a black and white bull's eye (see ***Figure 1a*** and ***1c)***. Furthermore, the flickering disk that was presented on a light gray background (240 cd/m^2), mid gray background (160 cd/m^2) or dark gray background (80 cd/m^2). The stream of characters was either not shown, shown at fixation, or shown on top of the flickering disk (see Procedure for details) For this experiment, the flickering disk was increased to a width of 4 degrees in visual angle to increase pupil sensitivity. Experiment 2 consisted of 432 trials (3 attention conditions x 3 luminance conditions x 48 stimulus locations). Trials were randomized and each trial consisted of one stimulus presentation for 2 seconds.

Figure 1. (a) Procedure: observers fixated the bull's eye, while the flickering disk was presented in the periphery. A gaze-contingent stimulus presentation was used to ensure that the retinal location of the stimulus was fixed. (b) Stimulus locations experiment 1: the flickering disk was located at 5 radial distances from the blind spot's center (0-, 1-, 2-, 7-, and 10-degree eccentricity, 16 angles). The bull's eye was placed on the left side of the screen when testing the right eye and vice versa. (c) Stimulus locations experiment 2: the flickering disk was located at 3 radial distances (4.5-, 6.75-, and 9-degree eccentricity, 16 angles).

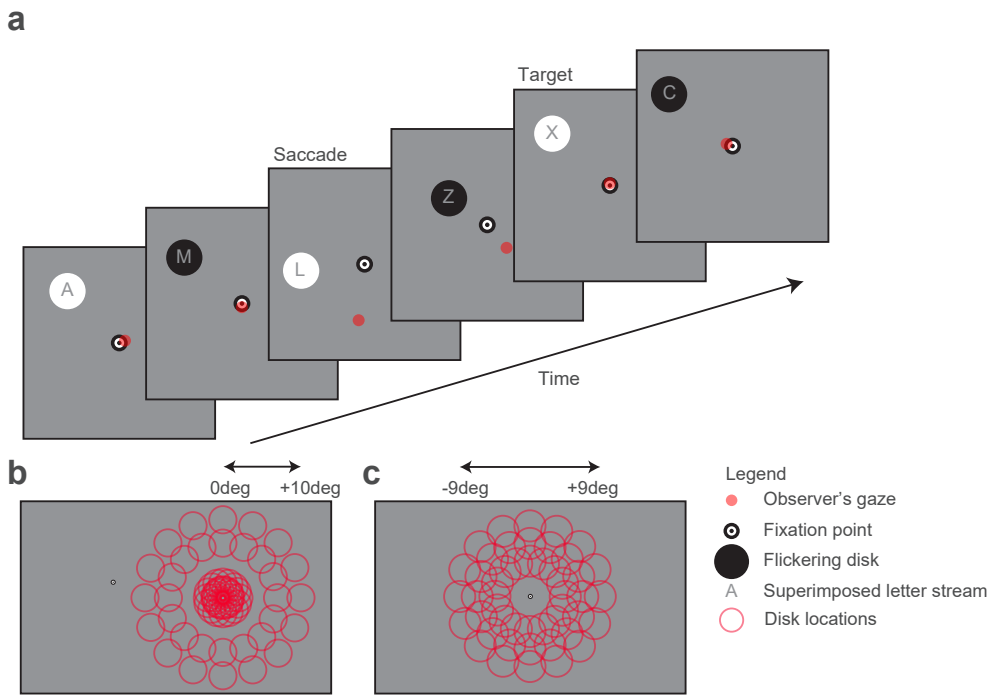

4.3.3 Procedure

Participants were tested on varying times of the day. Eye dominance was tested by using the "hole-in-the card test" (Ding et al., 2018). Five out of eleven in exp. 1 and four out of seventeen in exp 2 had left eye dominance. Depending on left and right eye dominance, stimuli were either presented in and around the blind spot that was located right or left from fixation in experiment 1, respectively. Due to the lacking information on how the Eyelink software calculates pupil size, we could only roughly estimate participants' average pupil sizes (M = 4.9mm, SD = 1.1mm) and standard deviation across trial time (M = 0.03mm, SD = 0.01mm) in millimeters (As a reference pupil, we held a black dot with a fixed radius drawn on a piece of paper in front of the camera at the same distance as the eyes of our participants).

Experiment 1 – Blind spot detection

The non-dominant eye of the participant (counterbalanced) was patched with a black eye patch to ensure monocular viewing with the dominant eye. In the subjective part of the experiment we asked the participants to rate the visibility of each flickering disk on a 11-point Likert scale (0 = fully invisible, 10 = fully visible), whereas in the objective part of the experiment we asked the participants to fixate the bull's eye. No letters were shown during the subjective part of experiment 1 to prevent participants from reporting letter visibility instead of disk visibility.

Experiment 2 – Attention, luminance and visual field anisotropies

Participants viewed the stimuli binocularly. To better understand how instructions and task requirements affect the accuracy of gcFPP, we also investigated the effect of attention on the sensitivity of pupil responses. Three attention tasks were tested in different blocks. In the passive attention task, participants only fixated the bull's eye. For the distracted attention task, participants were instructed to silently count the number of appearances of a letter 'X' among the stream of letters, changing at a rate of 2 Hz, presented at the center of the bull's eye. Participants indicated how many X's they had seen after all trials. For the covert attention task, those letters were instead superimposed on the stimulus disk and participants had to covertly attend the X's while maintaining fixation at the bull's eye.

4.3.4 Analysis

First, we detected and removed blink episodes from the pupil data by setting a speed threshold of >4SD above the mean. Blink episodes

were interpolated with a cubic method. Each recorded pupil trace was transformed per observer from pupil size as a function of time during the experiment to 3000ms epochs of pupil size measurements with respect to each stimulus onset. The resulting multiple pupil size traces were then band-pass filtered to remove low- (subtraction of a 2nd order fit with 1 Hz cut-off frequency) and high-frequency (replacing with a 5th order fit with 15 Hz cut-off frequency) noise, baseline corrected (through lowpass fit subtraction) and z-normalized to enable comparisons across participants, checked for trial outliers (>3 SD above the mean) in variance across locations (average of 1.4% ±0.7% of stimulus trials excluded per observer), and assigned to a condition matrix. Note that the Eyelink tracker software outputs pupil size in arbitrary units rather than absolute pupil diameter in millimeters.

The resulting pupil data matrices per condition were transformed to the frequency spectrum domain with a fast Fourier transform (FFT) per 3000ms stimulus trial. The resulting spectrum contained power values around the target frequency of 2 Hz for 21 different frequencies between 0 and 4 Hz. The pupil oscillation power at 2 Hz, computed by taking the maximum power within a range of 1.6 to 2.4 Hz to capture small deviations from the target frequency, served as the reference measurement of pupil response amplitude to each 2 Hz flickering stimulus per VF location. This measure was shown to have highest sensitivity in detecting differences in pupil sensitivity (Naber et al., 2018).

Two-dimensional high-resolution pupil sensitivity maps (e.g., ***see Figure 2c***) were created with MatLab's biharmonic spline interpolation across visual field locations. Comparisons in pupil sensitivities between inside versus outside the physiological blind spot were made by calculating the area under the curve (AUC; range: 0.5-1.0; for more info, see (Macmillan & Creelman, 2004)) on pupil oscillation amplitudes. An AUC of 0.5 means that the amplitude value distributions of the blind spot and the rest of the tested visual field fully overlap (i.e., not dissociable; no sensitivity) while an AUC of 1.0 means that the compared distributions are fully dissociable (i.e., a high sensitivity). Paired double-sided t-tests were conducted to statistically assess whether amplitudes and AUC's differed significantly across VF locations. Reported correlations are of type Pearson's rho. To determine statistical significance of differences in amplitudes and AUC's across eccentricities, attention tasks, and background brightness's, repeated measures ANOVA and paired double-sided t-tests were conducted. Figure 2a and 2c were calculated with the following analysis steps: First, we created a sensitivity map per participant. Second, we horizontally flipped the heatmaps of participants whoms left eye was tested (because of left eye dominance). Third, we averaged all maps across participants to a single average heat map. Fourth, the map was normalized such that black represents the minimum (Subjective visibility score: 0.4; pupil power exp 1: 0.1; exp 2: 2.0) and white the maximum (Subjective visibility score: 9.8; pupil power exp 1: 6.5; exp 2: 4.8).

4.4 Results

4.4.1 Results and discussion experiment 1 – Blind spot detection

In experiment 1 we set to test whether we could locate the physiological blind spot by means of detecting a decrease in pupil power. First, we located the blind spot by examining the subjective visibility ratings by observers across the VF (***Figure 2a***). A significant decrease in visibility ratings was observed for the expected locations inside the blind spot as compared to outside the blind spot (***Figure 2b***; $t(11) = 13.32$, $p < .001$). On average the actual blind spot location was slightly shifted to the right as compared to our expectations and thus from the probed locations, meaning that we underestimated the eccentricity of the blind spot. Note, however, that the blind spot locations are more in line with studies mapping it 16 degrees rather than 14 degrees from the vertical axis (Armaly, 1969; Safran et al., 1993). The objective pupil powers plotted across the VF showed a similar pattern as the subjective visibility ratings (***Figure 2c***). Pupil powers also correlated significantly with visibility ratings (M = .28, SD = .19; $t(11) = 4.59$, $p < .001$). To test for differences in pupil powers between inside and outside blind spot regions, we divided the VF based on the visibility ratings by using a 50% percentile threshold per observer. Pupil power was significantly lower for stimuli presented inside as compared to outside the rating-based blind spot regions (***Figure 2d***; $t(11) = 4.06$, $p = .001$) and the area under the curve also scored significantly above chance (***Figure 2e***; $t(11) = 8.75$, $p < .001$). To summarize the results, we found that gcFPP has a sensitivity that is sufficient to detect the blind spots in healthy observers, suggesting that it can potentially be used to detect relatively small scotomas in patients with VF defects.

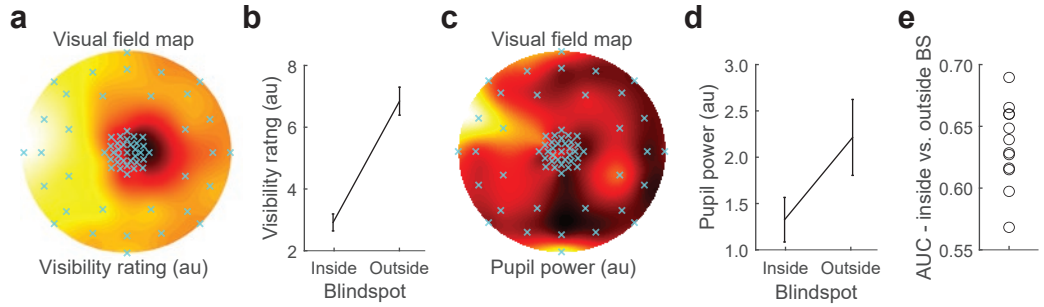

Figure 2. (a) Heatmap of visibility ratings around blind spot averaged across observers. Brighter (or hotter) colors indicate stronger pupil oscillation amplitudes. Note that the colors represent arbitrary values. Black and white values reflect the normalized lower (black) and upper (bright) limits of visibility ratings per observer, respectively. Also note that fixation was either on the left or right, outside the plot and is not displayed here. (b) Visibility ratings for inside versus outside blind spot location averaged across observers. Error bars indicate the standard error of the mean. (c) Heatmap of pupil powers around blind spot averaged across observers. (d) Pupil power for inside versus outside blind spot locations. (e) Area under the curve (AUC) of signal detection's receiver operator characteristic that compared pupil power distributions of inside versus outside blind spot locations (BS) across observers.

4.4.2 Results and discussion experiment 2 – Attention, luminance and visual field anisotropies

We first inspected whether the 2 Hz flickering stimuli evoked the expected oscillatory pattern in the pupil traces. As shown in ***Figure 3a*** this expectation was confirmed. Pupil size oscillated at a rate of approximately 2 Hz. Next we investigated whether the amplitudes of these oscillations, measured as the signal power at 2 Hz frequency in the Fourier domain, varied across the background brightness and attention task conditions. The pupil power varied substantially across conditions (***Figure 3b***), with the largest observed for a dark gray background with attention directed to the flickering disk. A two-way repeated measures ANOVA indicated that pupil power significantly varied as a function of background brightness (BB) attention task (AT), no interaction was observed (BB: $F(2,32) = 31.09$, $p < .001$; AT: $F(2,32) = 5.46$, $p = .009$; BB*AT: $F(4,64) = 1.99$, $p = .106$. Next, we examined whether the above-mentioned conditions performed best at detecting VF anisotropies. Typical VF anisotropies in pupil perimetry consist of a decrease in pupil responsiveness for peripheral as compared to foveal and superior (i.e., upper) as compared to inferior (i.e., lower) VFs (Hong et al., 2001; Naber et al., 2018; Skorkovská et al., 2014; Tan et al., 2001)[1]. We first plotted pupil power across stimulus locations as a heat map (***Figure 3c***). As further confirmed in repeated measures ANOVAs, pupil power varied significantly across eccentricities (***Figure 3d***; $F(2,32) = 46.76$, $p < .001$) and post-hoc comparisons indicated a decrease in pupil amplitudes as eccentricity (i.e., distance to fixation) increases (***Table S1***). Pupil amplitudes were also significantly stronger in upper as compared to low VFs (***Figure 3e***; $F(2,16) = 16.41$, $p < .001$; for post-hoc statistics, see ***Table S2***). Using signal detection theory, we calculated the sensitivity of pupil power as a measure to dissociate between lower and upper VFs (***Figure 3f***), which is a comparison most representative to VF defects of patients in clinical practice. Anisotropy detection sensitivity, operationalized as the area under the curve of a receiver-operator characteristic (AUC; see Methods – Analysis for details) varied significantly across background brightness conditions with largest sensitivity for the dark gray and mid gray backgrounds ($F(2,16) = 3.56$, $p = .040$; for post-hoc comparisons, see ***Table S3***). Sensitivities did not vary significantly across attention tasks ($F(2,16) = 2.24$, $p = .123$). To conclude, gcFPP achieved highest sensitivity as a measure to detect VF anisotropies when stimuli were presented on a relatively dark gray background.

[1] We could not assess the visual field anisotropy of temporal (i.e., towards the temples) versus nasal (i.e., towards the nose) locations because in Experiment 2 observers watched the stimuli binocularly.

Figure 3. (a) Pupil oscillations averaged across observers. The dotted lines indicate the standard error from the mean. (b) Pupil oscillation power per background brightness (x-axis) and covert attention condition (colors; legend). (c) Heatmap of relative pupil power across the visual field (VF) averaged across all conditions and averaged across observers. Brighter (or hotter) colors indicate stronger pupil oscillation amplitudes. The minimum (black) and maximum (white) pupil amplitudes varied across observers. This plot represents the average of amplitudes, which values were normalized to a fixed range per observer. Note that observers fixated the center of the plot and the cyan crosses indicate the locations of the stimuli. (d) Pupil power per stimulus eccentricity in visual degrees. (e) Pupil power lower to upper visual regions. (f) Area under the curve (AUC) of signal detection's receiver operator characteristic that compared pupil power distributions of upper and lower VFs averaged across observers per background luminance (black) and (g) attention condition (gray).

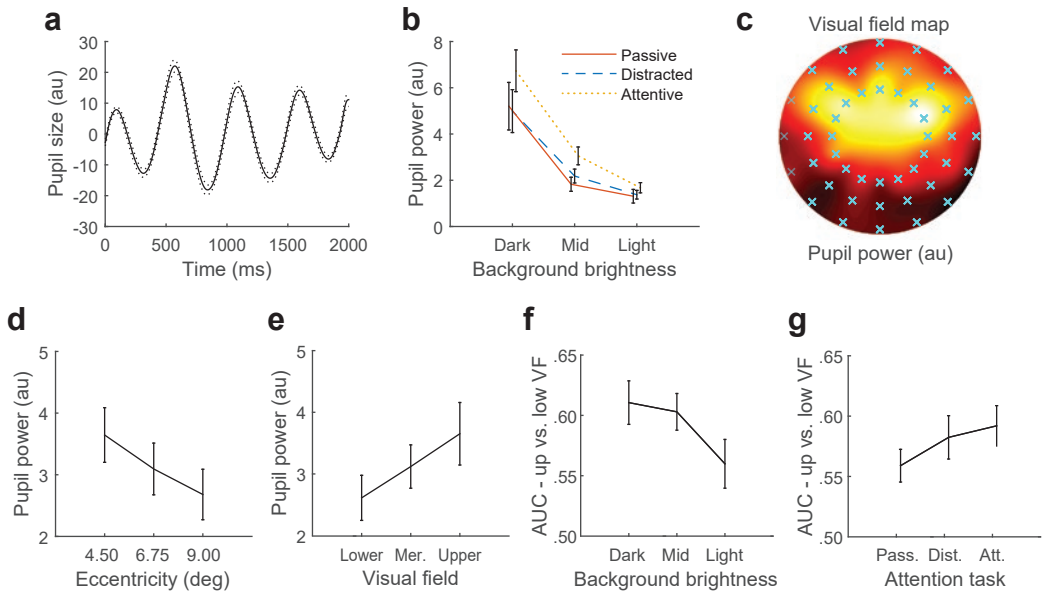

4.5 General discussion

The main objectives of this study were (i) to estimate how successful gcFPP is in detecting the blind spot and VF anisotropies in healthy individuals and (ii) to examine maximum pupil sensitivity across background illuminations and (iii) task designs.

To our knowledge this is the first study that benchmarked PP's capability to detect the blind spot. Previous research, however, already used the physiological blind spot as a proxy of a small scotoma to assess other non-pupillometric perimetry techniques (Asman et al., 1999; Bek & Lund-Andersen, 1989; Mutlukan & Damato, 1993). Measuring the blind spot in healthy participants allowed us to test participants for longer time periods than possible with patients that have pathological scotomas. Our current and previous findings (Naber et al., 2018) show gcFPP can detect small scotomas like the physiological blind spot and larger defects such as hemianopia in patients suffering from cerebral visual impairment or glaucoma, suggesting gcFPP could be a viable objective alternative to SAP. It should, however, be noted that there was a decrease in sensitivity below the blind spot in Figure 2c. This could possibly result from variabilities in photoreceptor cell densities, the cortical magnification factor, or variations in luminance across the LCD screen.

Regarding VF anisotropies, previous studies found strongest pupil responses in the center of the VF, weaker responses in the periphery, and stronger pupil responses in the upper and temporal than lower and nasal VFs, respectively (Hong et al., 2001; Naber et al., 2013, 2018; Sabeti et al., 2011; Skorkovská et al., 2014; Tan et al., 2001; Wilhelm et al., 2000). Our results are consistent with these previous observations.

We have also found that flickering stimuli presented over a dark-gray background evoked the strongest pupil responses as opposed to mid- and light-gray backgrounds. Furthermore, attended rather than unattended stimuli evoked strongest pupil responses to flickering on- and offsets. Surprisingly, different attentional conditions and background levels had comparable sensitivities in detecting VF anisotropies. This suggests that the selection of background luminance below 160 cd/m^2 and the type of attention task does not greatly impact gcFPP sensitivity.

PP has the potential to meet the demand for an objective alternative to SAP, which is the current gold standard for testing the VF. However, multiple variants of PP currently exist; the gcFPP (Naber et al., 2018) of the current study, unifocal PP (e.g., Schmid et al., 2005), in which a single stimulus appears at a given retinotopic location once, and multifocal PP (e.g., Wilhelm et al., 2000), which stimulates multiple retinotopic locations simultaneously. Future studies are needed to compare the sensitivities across methods using a common paradigm. Additionally, test-retest variability needs to be tested to examine PP's diagnostic accuracy.

This study focused on optimizing pupil responses to visual stimuli by ways of changing background luminance and manipulating the degree of attention for these stimuli. Other interesting stimulus design factors that could be considered to improve gcFPP are spatial and temporal sparseness; i.e. optimizing the pupillary response by changing the number of stimuli shown simultaneously across the VF (spatial sparseness) and the frequency of presentations within a certain time window (temporal sparseness). The current gcFPP protocol only shows a single stimulus repeatedly (high spatial sparseness, low temporal sparseness), while Sabeti and colleagues (2011) showed that high spatial and temporal sparseness resulted in better performance with multifocal PP. One of the characteristics of the 2 Hz flicker used in this study is its low temporal sparseness (i.e., relatively many stimulus changes). This frequency was chosen to increase the amount of pupillary measurements within a relatively short time window (Naber et al., 2018), but a higher temporal sparseness (i.e., lower frequency) could possibly result in stronger pupil responses. More investigations into these stimulus factors will be needed to find the optimum diagnostic sensitivity.

Our results show that when observers conduct a detection task with letters superimposed on the flickering target stimulus, larger pupil responses are evoked than when observers perform a distraction task at fixation or passively view a fixation dot. This is in line with literature showing that increased focused attention on the target stimulus results in enhanced pupillary responses (Binda & Murray, 2015; Binda et al., 2013; Binda, Pereverzeva, & Murray, 2014; Carrasco, Ling, & Read, 2004; Laeng & Endestad, 2012; Mathôt et al., 2013; Naber et al., 2013; Naber & Nakayama, 2013). Based on these results it is tempting to suggest that drawing covert attention to the stimuli improves gcFPP's diagnostic sensitivity. However, the results also showed that the sensitivity in detecting upper vs lower visual field anisotropies does not differ along several attentional conditions. The question remains whether this inconsistency generalizes to the detection of – much less subtle – scotomas. Nonetheless, adding an additional task in the same position of the stimulus is not detrimental for gcFPP's sensitivity and makes the task more engaging for observers.

Note that the perimetry method was benchmarked based on its sensitivity in dissociating pupil amplitude values of upper versus lower VFs in healthy individuals. Stimuli were however always visible to the observer, a situation which is not comparable to clinical practice. GcFPP can also be used to map the regions in the VFs where stimuli are not detected by the observer in patients with an absolute scotoma (Naber et al., 2018).

This study had some limitations. The first one concerns our gcFPP protocol, because only stimuli with the same size at all eccentricities were used. For clinical and/or diagnostic purposes the stimuli should be corrected for the cortical magnification factor and the density distributions of the photoreceptor cell types to take into account eccentricity effects and therewith to more accurately assess the VF in patients.

Another limitation concerned the background. This study investigated the optimal background luminance for gcFPP. Three backgrounds were tested; a light-, mid-, and dark gray background. Although the objective of the study was to assess differences across different shades of gray, which all prevent stray light to some degree, a black background condition could have served as a useful control condition. However, there are three reasons we did not add it to the current study. First, an extra condition would prolong test duration. Second, we were mainly interested in exploring lighter backgrounds and whether these would lead to more specific results. Third, and most importantly, LCD screens have a very long persistence with a white-on-black stimulus (Lagroix, Yanko, & Spalek, 2012).

In our current and previous pupil perimetry protocols, stimulus size was always around 4 visual degrees. It is important to note that standard perimetry uses much smaller ~0.5 degree stimulus sizes, allowing VF testing at a much higher spatial resolution. An increase in stimulus size at the expense of spatial resolution must be made to ensure strong enough responses in pupil perimetry. Consequently, PP is probably not accurate at detecting small scotomas (<3 degrees). Additionally, PP cannot detect full field deficits present in both eyes because then within field comparisons will not show large differences in pupil sensitivity.

Although the objective pupil powers plotted across the VF did not show an identical pattern, analysis showed that it was possible to predict the blind spot. The darker regions outside the blind spot can be attested to the VF anisotropies generally found in pupil perimetry. Furthermore, Figures 2b and 2d show standard error bars; standard deviations, which measures variability from the individual data values to the mean, would raise applicability for clinical use.

As described in a paper by Ghodrati and colleagues (Ghodrati, Morris, & Price, 2015), LCD screens are not really homogenous in luminance across the screen. Note, however, that the stimuli surrounding the blind spot were closer to the center of the screen than the edge and potentially changes position erratically due to the gaze contingent nature of the design. Following from this, the results can hardly be explained by potential inhomogeneities of the LCD.

Last, the current results could be biased by the overrepresentation of women and young adults in our sample. While no gender differences in pupil responses to these types of stimuli have so far been reported in the literature, age norms should be developed prior to clinical use of PP.

4.6 Conclusion

To conclude, we have demonstrated gcFPP's usefulness in detecting local and global differences in pupil sensitivity and we recommend to use dark to mid gray backgrounds and to ensure observer's attention to stimuli with task-relevant targets.

4.7 References

Armaly, M. F. (1969). The Size and Location of the Normal Blind Spot. *Archives of Ophthalmology, 81*(2), 192–201. https://doi.org/10.1001/archopht.1969.00990010194009

Asman, P., Fingeret, M., Robin, A., Wild, J., Pacey, I., Greenfield, D., … Ritch, R. (1999). Kinetic and static fixation methods in automated threshold perimetry. *Journal of Glaucoma, 8*(5), 290–296. Retrieved from http://www.ncbi.nlm.nih.gov/pubmed/10529927

Bek, T., & Lund-Andersen, H. (1989). The influence of stimulus size on perimetric detection of small scotomata. *Graefe's Archive for Clinical and Experimental Ophthalmology, 227*(6), 531–534. https://doi.org/10.1007/BF02169446

Binda, P., & Murray, S. O. (2015). Spatial attention increases the pupillary response to light changes. *Journal of Vision, 15*(2), 1–1. https://doi.org/10.1167/15.2.1

Binda, P., Pereverzeva, M., & Murray, S. O. (2013). Attention to bright surfaces enhances the pupillary light reflex. *Journal of Neuroscience, 33*(5), 2199–2204. https://doi.org/10.1523/JNEUROSCI.3440-12.2013

Binda, P., Pereverzeva, M., & Murray, S. O. (2014). Pupil size reflects the focus of feature-based attention. *Journal of Neurophysiology, 112*(12), 3046–3052. https://doi.org/10.1152/jn.00502.2014

Brainard, D. H. (1997). The Psychophysics Toolbox. *Spatial Vision, 10*(4), 433–436. https://doi.org/10.1163/156856897X00357

Carle, C. F., James, A. C., Kolic, M., Loh, Y.-W. W., & Maddess, T. (2011). High-Resolution Multifocal Pupillographic Objective Perimetry in Glaucoma. *Investigative Ophthalmology & Visual Science, 52*(1), 604–610. https://doi.org/10.1167/iovs.10-5737

Carrasco, M., Ling, S., & Read, S. (2004). Attention alters appearance. *Nature Neuroscience, 7*(3), 308–313. https://doi.org/10.1038/nn1194

Hong, S., Narkiewicz, J., & Kardon, R. H. (2001).

Comparison of Pupil Perimetry and Visual Perimetry in Normal Eyes: Decibel Sensitivity and Variability. *Investigative Ophthalmology & Visual Science, 42*(5), 957–965. Retrieved from https://dx.doi.org/

Kardon, R. H., Kirkali, P. A., & Thompson, H. S. (1991). Automated Pupil Perimetry Pupil Field Mapping in Patients and Normal Subjects. *Ophthalmology, 98*(4), 485–496. https://doi.org/10.1016/S0161-6420(91)32267-X

Laeng, B., & Endestad, T. (2012). Bright illusions reduce the eye's pupil. *Proceedings of the National Academy of Sciences of the United States of America, 109*(6), 2162–2167. https://doi.org/10.1073/pnas.1118298109

Lagroix, H. E. P., Yanko, M. R., & Spalek, T. M. (2012). LCDs are better: Psychophysical and photometric estimates of the temporal characteristics of CRT and LCD monitors. *Attention, Perception, and Psychophysics, 74*(5), 1033–1041. https://doi.org/10.3758/s13414-012-0281-4

Lussier, B. L., Olson, D. W. M., & Aiyagari, V. (2019, October 1). Automated Pupillometry in Neurocritical Care: Research and Practice. *Current Neurology and Neuroscience Reports*. Current Medicine Group LLC 1. https://doi.org/10.1007/s11910-019-0994-z

Luu, C. D., Dimitrov, P. N., Wu, Z., Ayton, L. N., Makeyeva, G., Aung, K. Z., … Guymer, R. H. (2013). Static and flicker perimetry in age-related macular degeneration. *Investigative Ophthalmology & Visual Science, 54*(5), 3560–3568. https://doi.org/10.1167/iovs.12-10465

Macmillan, N. A., & Creelman, C. D. (2004). *Detection Theory: A User's Guide: 2nd edition. Detection Theory: A User's Guide: 2nd edition.* Psychology Press. https://doi.org/10.4324/9781410611147

Mathôt, S., van der Linden, L., Grainger, J., & Vitu, F. (2013). The pupillary light response reveals the focus of covert visual attention. *PloS One, 8*(10). https://doi.org/10.1371/journal.pone.0078168

Mutlukan, E., & Damato, B. E. (1993). Computerised perimetry with moving and steady fixation in children. *Eye (Basingstoke), 7*(4), 554–561. https://doi.org/10.1038/eye.1993.121

Naber, M., Alvarez, G. A., & Nakayama, K. (2013). Tracking the allocation of attention using human pupillary oscillations. *Frontiers in Psychology, 4*, 919. https://doi.org/10.3389/fpsyg.2013.00919

Naber, M., & Nakayama, K. (2013). Pupil responses to high-level image content. *Journal of Vision, 13*(6), 7–7. https://doi.org/10.1167/13.6.7

Naber, M., Roelofzen, C., Fracasso, A., Bergsma, D. P., van Genderen, M., Porro, G. L., … van der Schouw, Y. T. (2018). Gaze-Contingent Flicker Pupil Perimetry Detects Scotomas in Patients With Cerebral Visual Impairments or Glaucoma. *Frontiers in Neurology, 9*(July), 558. https://doi.org/10.3389/fneur.2018.00558

Pelli, D. G. (1997). The VideoToolbox software for visual psychophysics: Transforming numbers into movies. *Spatial Vision, 10*(4), 437–442. https://doi.org/10.1163/156856897X00366

Phipps, J. A., Dang, T. M., Vingrys, A. J., & Guymer, R. H. (2004). Flicker perimetry losses in age-related macular degeneration. *Investigative Ophthalmology and Visual Science, 45*(9), 3355–3360. https://doi.org/10.1167/iovs.04-0253

Reuten, A., van Dam, M., & Naber, M. (2018). Pupillary responses to robotic and human emotions: The uncanny valley and media equation confirmed. *Frontiers in Psychology, 9*(MAY). https://doi.org/10.3389/fpsyg.2018.00774

Sabeti, F., James, A. C., & Maddess, T. (2011). Spatial and temporal stimulus variants for multifocal pupillography of the central visual field. *Vision Research, 51*(2), 303–310. https://doi.org/10.1016/J.VISRES.2010.10.015

Safran, A. B., Mermillod, B., Mermoud, C., Weisse, C. De, & Desangles, D. (1993). Characteristic features of blind spot size and location, when evaluated with automated perimetry: Values obtained in normal subjects. *Neuro-Ophthalmology, 13*(6), 309–315. https://doi.org/10.3109/01658109309044579

Schmid, R., Luedtke, H., Wilhelm, B. J., & Wilhelm, H. (2005). Pupil campimetry in patients with visual field loss. *European Journal of Neurology, 12*(8), 602–608. https://doi.org/10.1111/j.1468-1331.2005.01048.x

Skorkovská, K., Lüdtke, H., Wilhelm, H., & Wilhelm, B. (2009). Pupil campimetry in patients with retinitis pigmentosa and functional visual field loss. *Graefe's Archive for Clinical and Experimental Ophthalmology, 247*(6), 847–853. https://doi.org/10.1007/s00417-008-1015-0

Skorkovská, K., Wilhelm, H., Lüdtke, H., Wilhelm, B., & Kurtenbach, A. (2014). Investigation of summation mechanisms in the pupillomotor system. *Graefe's Archive for Clinical and Experimental Ophthalmology, 252*(7), 1155–1160. https://doi.org/10.1007/s00417-014-2677-4

Tan, L., Kondo, M., Sato, M., Kondo, N., & Miyake, Y. (2001). Multifocal pupillary light response fields in normal subjects and patients with visual field defects. *Vision Research, 41*(8), 1073–1084. https://doi.org/10.1016/S0042-6989(01)00030-X

Wang, M., Shen, L. Q., Boland, M. V., Wellik, S. R., De Moraes, C. G., Myers, J. S., … Elze, T. (2017). Impact of Natural Blind Spot Location on Perimetry. *Scientific Reports, 7*(1). https://doi.org/10.1038/s41598-017-06580-7

Wilhelm, H., Neitzel, J., Wilhelm, B., Beuel, S., Lüdtke, H., Kretschmann, U., & Zrenner, E. (2000). Pupil Perimetry using M-Sequence Stimulation Technique. *Investigative Ophthalmology & Visual Science, 41*(5), 1229–1238. Retrieved from https://dx.doi.org

4.8 Supplementary material

	4.50 visual degree	6.75 visual degree
6.75 visual degree	$t(16) = 7.69$, $p < .001$	
9.00 visual degree	$t(16) = 8.59$, $p < .001$	$t(16) = 3.73$, $p = .001$

Table S1. Post-hoc comparisons of pupil power across eccentricities

	Lower	Meridian
Meridian	$t(16) = 2.46$, $p < .026$	
Upper	$t(16) = 3.91$, $p = .001$	$t(16) = 5.54$, $p < .001$

Table S2. Post-hoc comparisons of pupil power across vertical meridian

	Dark gray	Mid gray
Mid gray	$t(16) = 0.34$, $p = .074$	
Light gray	$t(16) = 2.72$, $p = .015$	$t(16) = 2.15$, $p = .047$

Table S3. Post-hoc comparisons of AUC across background conditions

The trade-off between luminance and color contrast assessed with pupil responses

Translational Vision Science & Technology (2023) doi: 10.1167/tvst.12.1.15

Portengen BL
Porro GL
Imhof SM
Naber M

5.1 Abstract

PURPOSE A scene consisting of a white stimulus on a black background incorporates strong luminance contrast. When both stimulus and background receive different colors, luminance contrast decreases but color contrast increases. Here we seek to characterize the pattern of stimulus salience across varying trade-offs of color and luminance contrasts by using the pupil light response.

METHODS Three experiments were conducted with 17, 16, and 17 healthy adults. For all experiments, a flickering stimulus (2 Hz; alternating color to black) was presented superimposed on a background with a complementary color to the stimulus (i.e., opponency colors in human color perception; blue and yellow for Experiment 1; red and green for Experiment 2; equiluminant red and green for Experiment 3). Background luminance varied between 0-45% to trade off luminance and color contrast with the stimulus. By comparing the locus of the optimal trade-off between color and luminance across different color axes, we explore the generality of the trade-off.

RESULTS The strongest pupil responses were found when a substantial amount of color contrast was present (at the expense of luminance contrast). Pupil response amplitudes increased by 15-30% after addition of color contrast. An optimal pupillary responsiveness was reached at a background luminance setting of 20-35% color contrast across several color axes.

CONCLUSION These findings imply that a substantial component of pupil light responses incorporate color processing. More sensitive pupil responses and more salient stimulus designs can be achieved by adding subtle levels of color contrast between stimulus and background.

TRANSLATIONAL RELEVANCE More robust pupil responses will enhance tests of the visual field with pupil perimetry.

5.2 Introduction

The pupil light response (PLR) is often considered to be a simple subcortical reflex arc. Its neural pathway presumably consists of photoreceptors, bipolar and retinal ganglion cells with their axons forming the optic nerve, intercalated neurons in the midbrain, the oculomotor nerve, and short ciliary nerves innervating the pupillary sphincter muscle. The activation of this pathway through a bright stimulus onset results in a pupil constriction in response to an increase in retinal illumination (Binda & Gamlin, 2017; Maeda et al., 2017; Mathôt et al., 2016; Mathôt & Van der Stigchel, 2015; Strauch et al., 2022). However, recent developments suggest that in addition to objective, physical retinal illumination, such pupil responses depend on multiple factors beyond light levels, including the degree a stimulus is salient and draws attention (Strauch et al., 2022). These pupil orienting responses seem to not be dependent on sensory modality (Knapen et al., 2016; van Hooijdonk et al., 2019; Wetzel et al., 2016) and are enhanced by multisensory presentation (Strauch et al., 2020; Van der Stoep et al., 2021; Wang et al., 2017). Moreover, the speed and amplitude of pupil responses scale with stimulus salience (Bertheaux et al., 2020; van Hooijdonk et al., 2019; Wang et al., 2014). This novel view explains why subjectively perceived brightness and the degree of awareness for the presented stimulus rather than its physical properties determine pupil response amplitudes (Laeng & Endestad, 2012; Mathôt & Van der Stigchel, 2015; Naber et al., 2011; Sperandio et al., 2018; Suzuki et al., 2019). Furthermore, experience with stimulus content (Naber & Nakayama, 2013), the degree and locus of attention (Acquafredda et al., 2022; Binda et al., 2013; Binda & Murray, 2015b; Mathôt et al., 2013; Naber et al., 2013; B. L. Portengen et al., 2021; Rosli et al., 2018a), and visual sensitivity (Binda & Murray, 2015a; Mathôt & Van der Stigchel, 2015; Naber et al., 2018; B. Portengen et al., 2022; B. L. Portengen et al., 2021, 2022) all shape pupil responses. In summary, a pupillary response amplitude reflects how well a stimulus draws attention and is processed. In line with this, the pupil not only responds to brightness but also to other stimulus properties such as luminance contrast (Ukai, 1985), spatial frequency (Barbur et al., 1992), numerosity (Castaldi et al., 2021), and color hue (Gamlin et al., 1998; Kelbsch et al., 2019; Tsujimura et al., 2006; Walkey et al., 2005). Two distinct pathways process stimulus color and luminance. Through retinal ganglion cells (RGCs), short (S-), medium (M-), and long (L-) wavelength sensitive photoreceptors provide input to the parvocellular (P) pathway, which is most sensitive to chromatic features, and the more luminance driven magnocellular (M) pathway (Kremers et al., 1993; Lee et al., 1990, 2007; Martin et al., 2001; Smith et al., 1992). Nonetheless, these features must interact somewhere in the hierarchy of visual processing to create a coherent

percept. While these features have been studied in isolation, it remains unclear how they may interact and affect pupil responses together. A pupil response thus likely incorporates a multitude of distinct though additive pupil responses (Knapen et al., 2016; Naber & Murphy, 2020; Strauch et al., 2020; Van der Stoep et al., 2021; Wierda et al., 2012). Here we focus on investigating to what degree pupil size changes incorporate responses to both luminance and color contrast between stimulus and background. How these two stimulus features interact with respect to saliency is not trivial as each form of contrast may increase separately, though only at the expense of the other. Effects of the presentation of chromatic stimuli on pupil size have been tested in the context of visual field sensitivity assessment (i.e. pupil perimetry; Carle et al., 2014, 2015; Kelbsch et al., 2020; Maeda et al., 2017; Rosli et al., 2018; Tatham et al., 2014). As blue and yellow, and red and green, are complementary, opponency colors for the human visual system (i.e., as modelled by the CIELAB color space, a three-dimensional color space defined by the International Commission on Illumination (CIE) which covers the entire gamut of human color perception; see ***Figure 1A***), they perfectly lend themselves to investigate the effect of color contrast on the pupil response.
The main aim of this study is to investigate whether the addition of color contrast to luminance contrast between a stimulus and the background evokes a stronger pupil response. However, adding color contrast to a scene always comes at the expense of luminance contrast. To explain this more clearly, imagine a white stimulus on a black background. In this case the stimulus has 100% luminance contrast with its background. By adding color to the stimulus, some degree of color contrast with the background is added but luminance contrast decreases (e.g., a yellow stimulus is not as bright as a white stimulus). Color contrast can be enhanced even more by adding a complementary, opponency color to the background, again at the expense of luminance contrast (a blue background is not as dark as a black background; for a visualization of the interaction between color and luminance contrasts, see ***Figures 1B*** and ***1C***). The question posed here is where the optimal balance between luminance and color contrast may be found across the color space. This may depend firstly on the shape and curvature of color space representations and secondly to which degree luminance contrast is preferred over color contrast by the visual and pupillary system. In this study we aim to improve pupillary measures of visual field sensitivity by manipulating luminance and color contrast between stimulus and background to find the most optimal pupil response.

In summary, this study aims to explore to what degree the pupil responds to color contrast with respect to luminance contrast and to investigate whether this response generalizes across directions in color space.

Figure 1. Spherical CIELAB color space (A) modelling color distances to reflect how well colors (and accompanying luminance levels) can be discerned from each other (i.e., color contrasts) in human color perception. Horizontal distance from center (gray) corresponds to color contrast, vertical distance from black to white corresponds to luminance. White outline connecting colors blue with complementary yellow (Experiment 1) and white dashed outline connecting red with complementary red (Experiment 2 & 3) highlight the color spaces targeted in this study. An intersection plane of the sphere (B) shows equal distances (white lines) between stimulus (yellow) and background (black to blue) per color contrast level (0-45%). Depending on the yet unknown dimensions of color space and the pupil's sensitivity to luminance contrast (vertical axis) with respect to color contrast (horizontal axis), the most salient appearance, and thus strongest pupil response (i.e., where the overshoot of white lines (dotted gray) is longest) may be evoked by using one of several possible background color contrast levels ranging from high luminance contrast to high color contrast. This is illustrated in (C), where a fully luminant yellow stimulus is offset to variations of the background with the complementary color blue, varying from high luminance contrast when the background has low brightness to high color contrast when the background displays high brightness.

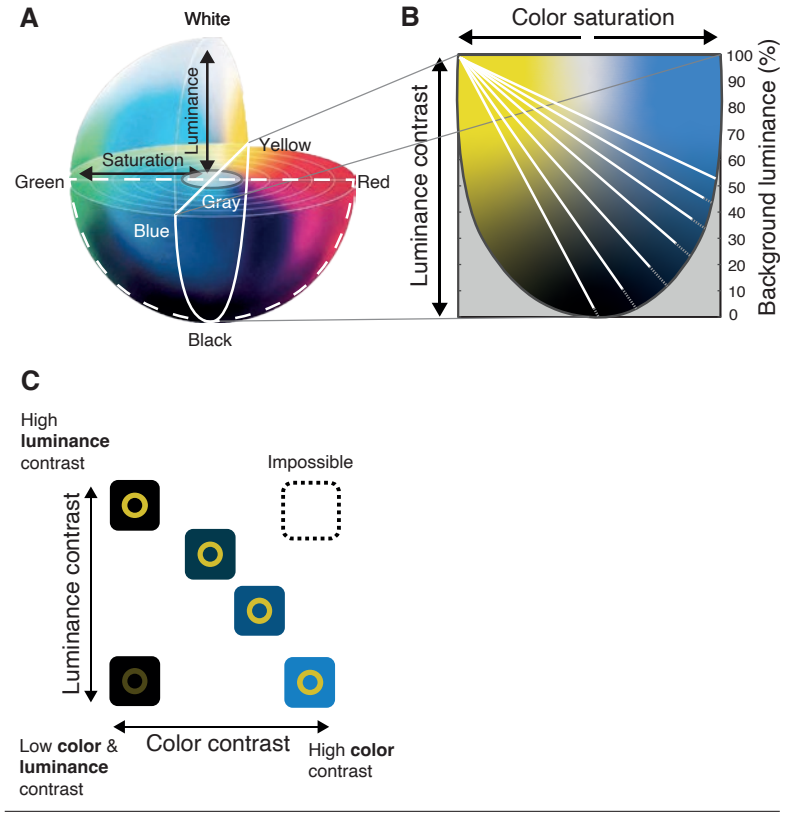

5.3 Methods

5.3.1 Participants

The participants of the three experiments consisted of 17 (11 females), 16 (10 females), and 17 (11 females) healthy Dutch students and staff with Caucasian ethnicity (mean age (SD) 22.8 (3.5), 22.9 (2.6), and 23.2 (4.2), respectively). Subjects were screened for color blindness using the Ishihara test (Clark, 1924) and had normal or corrected-to-normal visual acuity. Furthermore, we verbally inquired about the presence of visual or neurological disorders; none of the subjects reported to have any. All experiments were approved by the local ethical committee of Utrecht University (approval number FETC19-006) and conformed to the ethical considerations of the Declaration of Helsinki. Participants gave written informed consent prior to participation. Furthermore, they received (financial) reimbursement for participation (€8 per hour).

5.3.2 Apparatus and stimuli

All experiments were conducted in a darkened room without ambient light. Stimuli were generated on a Dell desktop computer with Windows 7 operating system (Microsoft, Redmond, Washington), using MatLab (Mathworks, Natick, MA, USA) and the Psychtoolbox 3 and Eyelink toolbox extensions (Brainard, 1997; Cornelissen et al., 2002; Kleiner et al., 2007; Pelli, 1997). We used a 143 by 63 cm OLED65B8PLA LG (LG Electronics, Seoul, South Korea) monitor with a resolution of 1920 by 1080 and a refresh rate of 60 Hz to display stimuli. Pupil size and gaze angle of the right eye were tracked with an Eyelink 1000 eye-tracker (SR Research, Ontario, Canada; 0.5-degree accuracy of gaze angle) connected to a separate Dell desktop computer with Windows 7 operating system, which recorded the right eye from above through a hot (infra-red reflecting) mirror (tower mount). We used the Eyelink toolbox extension for the Psychtoolbox (Cornelissen et al., 2002) on the presentation computer to communicate and synchronize stimulus presentations with the pupil size recordings on the eye tracking computer. Start and stop triggers, and stimulus presentation messages were sent from the presentation computer to the eye tracking computer by means of an ethernet cable with negligible latency (for more details, see the SR-Research manual). A participant's head and viewing distance were fixed using a forehead- and chinrest at 75 cm distance from the monitor. A schematic of the used apparatus is shown in ***Figure 2D***. Eye tracker calibration procedure consisted of a five-point grid and took ~1 min. The Eyelink tracker software outputs pupil size in arbitrary units rather than absolute pupil diameter in millimeters, and we refrained from converting the units as the current study only concerns within-subject comparisons.

Experiment 1 – Background color contrast yellow/blue

The stimuli consisted of yellow or blue colored annuli with 100% luminance (at 141 and 143 cd/m2 respectively; see Supplementary ***Table S1***), each presented at one of five possible eccentricities (see ***Figure 2A***). The width of each annulus was increased as a function

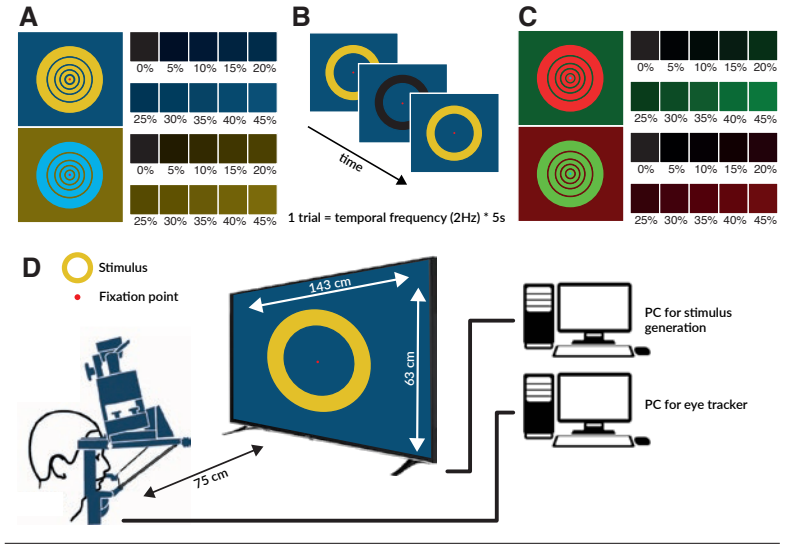

Figure 2. Stimulus color and background color conditions for Experiment 1 are shown in panel (A). The upper-left panel shows 5 yellow stimulus locations across different eccentricities (4, 8, 12, 17 and 23 degrees from fixation point) superimposed on a blue background. Note that the pictures are cropped for aesthetical reasons; the background actually extended further to the left and right to fill the entire monitor screen with 16:9 aspect ratio. The smaller panels adjacent to the left panel pertain the different background color contrast conditions (0-45%) upon which the stimuli were superimposed. The lower panels show the blue colored stimuli and their complementary yellow background color contrasts. The experiment consisted of 100 trials (5 stimulus rings * 2 stimulus colors * 10 background color contrasts). An example of a trial procedure can be seen in panel (B). One of the five annuli flickered from color to black for 5 seconds at a 2 Hz frequency around a red fixation point. This was repeated for all background color contrast conditions, locations, and stimulus colors in random order. Procedure and stimulus dimensions of Experiment 2 and 3 (C) were equal to Experiment 1, but used red stimuli superimposed on a green background (upper panel) and vice versa (lower panel). (D) shows a schematic arrangement used for the pupil measurements in a darkened room. Participant's heads were fixed in a forehead-chinrest under the tower-mounted eye tracker which was positioned in front of the presentation monitor. The presentation monitor and eye tracker were connected to separate computers.

of eccentricity using a cortical magnification factor (radial width = eccentricity1.12 in degrees) to activate approximately equal numbers of neurons by both central and peripheral stimuli (e.g., see Rosenholtz (2016)). Stimuli flickered between colored (i.e., blue or yellow) and black annuli at 2 Hz for five seconds per trial, and a red fixation point was placed at the center of the presentation monitor. A flicker paradigm was used as it is known to produce oscillatory pupillary light responses (PLRs) with amplitudes reflecting the degree a stimulus onset is visually processed (i.e., stimulus salience; Naber et al. (2018) and Portengen et al. (2021, 2022)). The stimuli were superimposed on a complementary colored background (i.e., opposite colors in CIELAB color space, see ***Figure 2***), which varied in background color contrast depending on the trial's condition (0-45% with intervals of 5% in random order to minimize effects of time; see Supplementary ***Table S1***). Each unique combination of eccentricities (5x), colors (2x), color contrast (10x) condition was tested once (100 trials).

Experiment 2 and 3 – Background color contrast red/green

Experiments 2 and 3 were identical to Experiment 1 aside from the different complementary color pairs used: green and red colored annuli flickered between colored and black (***Figure 2c***). Since the 100% luminant red and green colored annuli used in Experiment 2 differed significantly in brightness (52 cd/m^2 and 171 cd/m^2 respectively; see Supplementary ***Table S1***) because of the OLED screen properties and the infrared hot mirror, Experiment 3 used green annuli with 55% luminance to achieve physical equiluminance with the 100% luminant red stimuli. Each unique combination of eccentricities (5x), colors (2x), color contrast (10x) condition was tested once (100 trials) for each experiment.

5.3.3 Modelled weights of color contrast in relation to luminance contrast

We modelled the relative degree of luminance and color contrast between stimulus and background per variation of the background color contrasts conditions (see ***Figure 3***). The weight of color contrast in relation to luminance contrast was varied across models, basically simulating size changes in the horizontal dimension of color contrast in ***Figure 1B***. By varying this weight, the distance in color space between stimulus and background (white lines in ***Figure 1B***) changed, with an optimal distance at varying background color contrasts. In doing so, the relative contribution (i.e., weight) of color contrast to pupillary responses (relative to luminance contrast) could be determined after the experimental search for the optimum.

Figure 3. Modelled distance in color space (i.e., white lines in Fig. 1B) per background color contrast (0-45 %). Each colored line represents a different weight (range: 0.5 to 1) assigned to the color contrast space relative to luminance contrast space between background and stimulus. A weight of 0.5 means that the horizontal width of the color space as displayed in Figure 1B, representing visual sensitivities to color contrasts, is equal to the height of the color space, representing visual sensitivities to luminance contrasts. A weight of 1.0 means that the width of the color space in Figure 1b scales by a factor two, modelling color contrast as sensitive as luminance contrast. This weight determines at what color brightness the background contrasts optimally with the stimulus color (i.e., the largest distance in the modelled color space; see white/gray lines in Fig. 1B). Circles on the colored traces highlight the optimal background color (and luminance) contrast with the stimulus (i.e., where dotted gray line is longest in Fig. 1B).

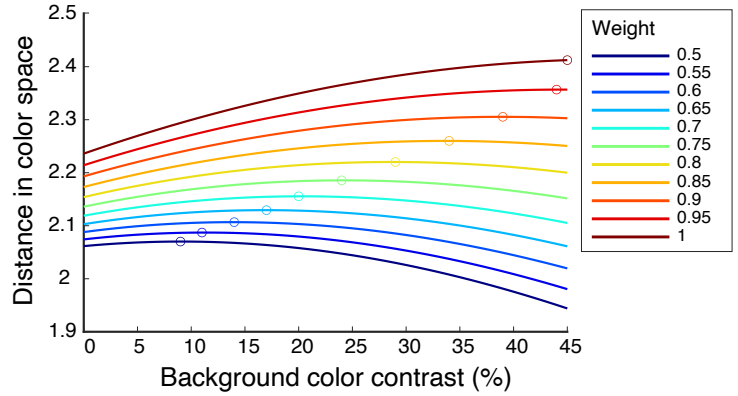

Procedure

*Participants were instructed to continuously gaze at the red fixation point in the middle of the screen. We additionally instructed participants to covertly attend the flickering stimuli, each presented in a gaze-contingent manner, to evoke strong pupil responses (Binda & Murray, 2015b; B. L. Portengen et al., 2021) Participants were tested at varying times of the day. Only the right eye was recorded, the left eye was patched with an (adhesive) eye patch. Eye tracker recalibrations were performed whenever participants indicated to want a break. Each experiment lasted 500 seconds (5 stimulus locations * 5 seconds per location * 10 background color contrast conditions * 2 stimulus colors), excluding (re)calibration and breaks.*

5.3.4 Analysis

The continuous pupil recordings were analyzed in an event-related manner with the first stimulus onset per new location as start events. Blinks were detected and filtered using a speed threshold of 4 standard deviations (SD) above the mean. The detected blink periods shorter than 600ms were interpolated with a cubic method (interp1 MATLAB function). Trials with less than 80% pupil data were removed from the analysis. To filter out low frequency noise, we subtracted pupil traces filtered with a 2nd order Butterworth filter with a 1 Hz cut-off frequency (i.e., we applied a high-pass filter) which produced baseline corrected traces showing pupillary oscillation patterns around zero. This is a necessity for proper frequency analyses. After this baseline correction, we removed high frequency noise by filtering the high-pass filtered pupil traces with a 5th order Butterworth filter with a 15 Hz cut-off frequency. Pupil traces were filtered per event (i.e., per stimulus location) and saved in a matrix with each row presenting a trial and each column representing a timepoint. Pupil traces were converted to power spectral density estimates in the frequency domain by computing a Lomb-Scargle periodogram using a fast Fourier transform per trial. This power measurement reflects the amplitude in the pupillary oscillation patterns evoked by a stimulus. For simplification, we refer to this measurement as the pupil response amplitude from now on. These pupil response amplitudes served as the main dependent variable (Naber et al., 2018; B. Portengen et al., 2022; B. L. Portengen et al., 2021, 2022). To determine statistical significance of differences in pupil amplitudes across background color contrast conditions and stimulus color conditions, we performed a two-way repeated measures ANOVA. Paired double-sided t-tests were performed to test for differences in pupil amplitudes across conditions as a post-hoc test. Experiment data, and analysis files are available on https://osf.io/yzavk.

5.4 Results

5.4.1 Results and discussion Experiment 1 – yellow/blue

In Experiment 1, we set out to explore which background color contrast condition produced the strongest pupil responses. First, we inspected whether the pupil properly responded to the 2 Hz flickering. As shown in ***Figure 4A*** this prerequisite was met. The average pupil traces consisted of a 2 Hz oscillatory pattern reflecting the responses to stimulus on- and off-sets. Next, we investigated whether pupil response amplitudes differed across background color contrast conditions within each chromatic stimulus color variant. The lines in ***Figure 4B*** depict the participants group average of pupil response amplitudes across background color contrast conditions per stimulus variant. A two-way repeated measures ANOVA revealed a significant main effect of color contrast ($F_{9,19}$ = 6.15, p < .001, *partial* η^2 = 0.28), but not for stimulus color ($F_{1,19}$ = 3.84, p = 0.07, *partial* η^2 = 0.19). There was no interaction between the two main effects. This means that the pupil responses did not differ significantly between yellow and blue backgrounds but did differ across background color contrast. The strongest pupil responses were found within the range of 25-35% background color contrast (see Supplementary ***Table S2*** and ***S3*** for post-hoc comparisons). Pupil responses were 15-20% lower for 0% background color contrast. To conclude, a background color contrast of approximately 30% evokes the strongest pupil responses for both color background variants. ***Figure 3*** represents the modelled distance in color space between stimulus and background as a function of background color contrast per color contrast weight in relation to luminance contrast. A weight of 0.8 (i.e., 80%) corresponded to an optimal distance (and pupil response amplitude) at 30% background color contrast.

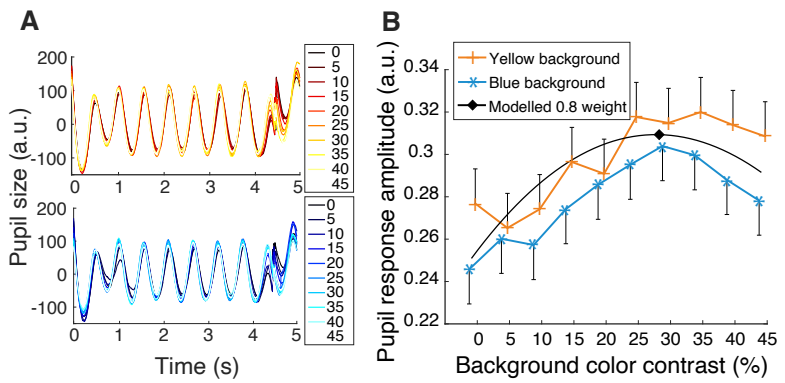

Figure 4. Average pupil traces (A) for yellow (upper panel) and blue (lower panel) background colors across participants. Each trace represents a different background color contrast trace represents a different background color contrast (0-45%). Pupil responses follow roughly the same oscillatory pattern of 2 Hz across experiment conditions. Average pupil response amplitudes per background color contrast are shown in (B) with standard errors around the mean. An optimal pupil response for both colors is found between 25-35% background color contrast. This optimum corresponded with an 80% relative contribution (i.e., weight) of color contrast to pupillary responses relative to luminance contrast (black trace with optimum ~30% background color contrast). Note that all pupil sizes are outputted in arbitrary units (a.u.) rather than absolute millimeters due to the Eyelink tracker software.

5.4.2 Results and discussion Experiment 2 – red/green

The goal in Experiments 2 and 3 was to investigate whether the results found in Experiment 1 generalize across different directions within the color space. Firstly, similar to the previous experiment, the pupil showed appropriate responses to the 2 Hz flickering stimulus on- and offsets (see ***Figures 5A*** and ***5B***). Next, differences between pupil response amplitudes across all background color contrasts

within the different chromatic stimulus variants were explored. ***Figure 5A and 5B*** show the pupil response amplitudes per background color contrast and stimulus color condition averaged across trials and participants. As in Experiment 1, a two-way repeated measures ANOVA revealed a significant main effect of background color contrast ($F_{9,19}$ = 6.02, p < .001, *partial* η^2 = 0.29). Not surprisingly, Experiment 2 also resulted in a significant main effect for stimulus color ($F_{1,19}$ = 28.59, p = < .001, *partial* η^2 = 0.31) because brightness differed substantially between the red and green flickering stimulus (see Supplementary ***Table S1*** also for the CIE color coordinates). There were no interactions between the two main effects. This means that the pupil responses significantly differed across background color contrasts. Similar to Experiment 1, pupil responses were weakest (15-30% lower compared to optimum) when no color contrast was present (i.e., background was black; see Supplementary ***Table S4*** and ***S5*** for post-hoc comparisons) but got stronger as color contrast increased. For the green background with red stimulus condition pupil responses significantly weakened when color contrast was

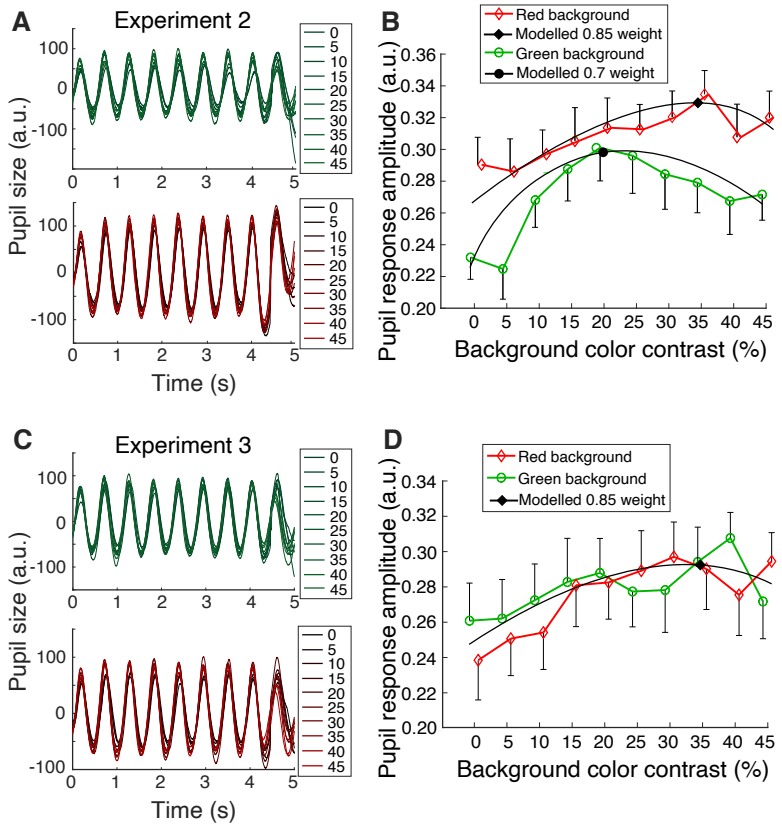

Figure 5. Same as Figure 4 but now for experiment 2 and 3 in which red versus green background and stimulus colors were displayed. Note that the modelled weights of Experiment 2 are different due to a significant main effect of stimulus color (see paragraph 3.2 in the Results section).

increased beyond an optimum of approximately 20%, whereas pupil responses weakened significantly for the red background with green stimulus condition beyond the optimum of 40% (see Supplementary ***Table S4*** and ***S5***).

5.4.3 Results and discussion Experiment 3 – equiluminant red/green

Like the two previous experiments, the two-way repeated measures ANOVA in Experiment 3 showed a significant main effect of background color contrast ($F_{9,19}$ = 4.50, p < .001, *partial* η^2 = 0.11). In contrast to experiment 2, in experiment 3 we succeeded in controlling for previous brightness differences between the red and green stimulus conditions (no significant main effect for stimulus color; $F_{1,19}$ = 0.28, p = .61, *partial* η^2 = 0.003). Again, weakest pupil responses were recorded in the absence of color contrast (see Supplementary ***Table S6*** and ***S7***) and gradually increased ~20% to find an optimum around 30-40% background color contrast. The model portrayed in ***Figure 3*** revealed a relative weight of approximately 0.85 (background color contrast in relation to luminance contrast) to find the optimal distance and pupil response amplitude at 35% background color contrast. Contrary to Experiment 2, no significantly weaker pupil responses were found beyond the optima for both conditions. To conclude, an additive color contrast component to luminance contrast results in stronger pupil responses with an occasional optimal response pattern at an intermediate color contrast level for a selective set of background and stimulus colors.

5.5 General discussion

The main objective of this study was to investigate the contribution of color contrast (relative to luminance contrast) to pupillary responses that reflect stimulus salience. We specifically aimed to explore whether adding color contrast between a stimulus and its background (at the expense of luminance contrast) enhanced pupil responses amplitudes to stimulus onsets.
Our findings support the notion that, in the context of enhancing pupil responses to stimuli, an optimal balance exists between luminance and color contrast (between background and stimulus); for all investigated color directions (i.e., yellow, blue, green, and red colors), pupil size changed strongest when a substantial amount of color contrast was present (e.g., a ~30% background color contrast

for blue and yellow). The improvement in such pupil orienting responses acquired through the addition of color contrast could originate from a combined effect of physiological, psychological and neurological factors (Brown et al., 2012; Donofrio, 2011; Drew et al., 2001; Odgaard et al., 2003; Strauch et al., 2022; Zele, Adhikari, et al., 2018). The pupil responses to chromatic stimuli presumably consist of multiple components. One such component consists of parvo- (P) and magnocellular (M) pathways projecting to the lateral geniculate nucleus, whereas the tonic, wavelength-opponent RGCs that project to the P pathway are most sensitive to chromatic modulation and the phasic non-opponent RGCs projecting to the M pathway which supports luminance flicker detection (Kremers et al., 1993; Lee et al., 1990, 2007; Martin et al., 2001; Smith et al., 1992). Others stem from an interaction between cortical (frontal-parietal attention network) and subcortical (superior colliculus) processes involved in orienting responses that feedback to the more reflexive pupillary pathway (Strauch et al., 2022). As such, the degree the pupil constricts in response to a stimulus onset reflects how well the visual system processes features like color. That the pupil showed utilization in assessing human sensitivity to varying features demonstrates this more clearly (Barbur et al., 1992; Sahraie & Barbur, 1997). An example includes reproducing the contrast sensitivity function. The pupil showed peak responsiveness for gratings with 3 cycles per visual degree contrast variations (Barbur & Thomson, 1987; Cocker et al., 1994). This optimal response to spatial frequencies matches the contrast-sensitivity function, indicating that the pupil could be an objective measure of visual sensitivity (and visual acuity). Similar conclusions can be drawn from numerous pupil perimetry studies showing that pupil response amplitudes weaken when stimuli are presented in a scotoma or blind spot (e.g. Carle et al., 2022; R. H. Kardon et al., 1991; Kelbsch et al., 2021; Maeda et al., 2017; Naber et al., 2018; B. L. Portengen et al., 2021, 2022; Skorkovská, Wilhelm, et al., 2009; L. Tan et al., 2001). Our results suggest that the dynamics of human color perception and dimensions of color space representations may also be assessed accurately, objectively, and quickly by inspecting pupil responses to changes in color. The novel findings of this study could also positively impact several ophthalmological practices, such as (i) enhancing pupil perimetry's accuracy, (ii) objectively mapping degrees of color blindness, but also (iii) improving saliency of traffic lights or presentation slides.

The created models in which we systematically varied the weight of feature dimensions of luminance and color revealed that approximately a 0.7-0.85 weight ratio of color contrast with respect to luminance contrast best explains the variations in observed pupil response amplitudes across background color contrasts. This ratio is relatively high and means that, in the context of pupillary color representation of the visual system, the horizontal color dimension in ***Figure 1B*** has an approximately 70-85% length of the vertical luminance dimension. Similarly, weaker though substantial contributions of chromatic contrast to the pupillary response were found in humans and the rhesus monkey (Barbur et al., 1998; Gamlin et al., 1998). They compared pupillary reactions to contrasting chromatic stimuli with spatially equivalent achromatic stimuli and found a ratio of ~0.5 between pupil response amplitudes of chromatic versus nonchromatic stimuli.

An additive color contrast component to luminance contrast resulted in stronger pupil responses rather than simply luminance contrast (i.e., when background was black) in all experiments and thus across axes of the color space. Previous studies teach us that the pupil responds to a multitude of contrast modalities, such as changes in luminance (Ukai, 1985), spatial frequency (Barbur et al., 1992), and color contrast (Barbur et al., 1992; Gamlin et al., 1998; Kelbsch et al., 2019; Tsujimura et al., 2006; Walkey et al., 2005). Salient changes within these modalities evoke an orienting response consisting of a pupil constriction (Strauch et al., 2022). Our findings confirm that these pupil responses are enhanced by multisensory presentation in an additive manner (in this case color and luminance). For a selective set of color combinations, these responses even showed an optimal response pattern (i.e., the red stimulus with a 20% green background color contrast and green stimulus with 40% red background color contrast of Experiment 2) with significantly weaker responses at both extremes of the background color contrast range. These results confirm that some parts of the color space represented in the human visual system portrays a curvature as displayed in ***Figure 1A*** and ***1B***. Although similar, an optimal response pattern was not found for the blue-yellow and equiluminant red-green axes. This could mean that color space is not represented by a sphere (***Figure 1A***) with the same curvature for every color axis or that a larger range of background color contrasts (e.g., 0-60%) is needed to find the optimum response pattern for other color combinations. Future studies may adapt the current pupillometry paradigm to explore a full range of contrasts and colors to test these possibilities.

The here reported novel findings will be of value to visual field testing through pupil perimetry, because the optimal balance between

luminance and color contrast lead to stronger and thus likely more robust pupil responses. Another advantage lies in the use of colors to dissociate contributions of distinct pathways to pupil responses (Gooley et al., 2012; Spitschan & Woelders, 2018), such as isolating melanopsin-directed responses (Spitschan & Woelders, 2018; Uprety et al., 2021). Intrinsically photosensitive retinal ganglion cells (ipRGCs) receive input via bipolar cells through short-wavelength (S-) cone OFF, medium-wavelength (M-) and long-wavelength (L-) sensitive cone and rod ON inputs (Dacey et al., 2005a; Gamlin et al., 2007; Young & Kimura, 2008; Zele, Feigl, et al., 2018). Additionally, ipRGCs express the photopigment melanopsin (which action spectrum peaks at 482 nm and overlaps all three cone types), which renders them directly photosensitive (Berson et al., 2002; Dacey et al., 2005b; Hattar et al., 2002). Melanopsin cells mediate the PLR by projecting to the suprachiasmatic nucleus, intergeniculate leaflet and pretectal olivary nuclei (Chen et al., 2011; Gooley et al., 2003; Hattar et al., 2002). As rod/cone photoreceptors and melanopsin differ substantially in their response properties, light stimuli can be designed to preferentially assess their function in patients with retinal diseases (Carle et al., 2013; R. Kardon et al., 2011; Kelbsch et al., 2019; Najjar et al., 2021; Rukmini et al., 2019; T. E. Tan et al., 2022). Unfortunately, the approach used in this study was not feasible to specifically target distinct photoreceptor pathways, but it will be interesting for future research to explore how luminance and color processes in the retina interact and contribute to the here found optimal pupil sensitivities.

Subsequently, the repeated gaze-contingent flickering stimulus presentation reported in this study conveniently lends itself to make optimal use of the newfound optimal color contrast between stimulus and background. In future studies the addition of not only temporal but also spatial color contrast (e.g., a red, green and yellow checker pattern within the stimulus) to the stimulus-on region might be of value.

This study incorporates some limitations. Firstly, as our study contains only results from healthy adults that did not undergo an ophthalmic examination, our findings cannot be extrapolated to patient populations with complete certainty. Moreover, although out of scope of the current study, we did not compare a 100% luminance contrast (i.e., white versus black) to the combined color and luminance contrast (i.e., the upper part of the color space in ***Figure 1A*** is not yet probed). It thus remains unclear whether adding color contrast to stimuli results in greater diagnostic accuracies in detecting visual field defects with the pupil. Future clinical studies might provide more clarity regarding the sensitivity of this.

5.6 Conclusion

To conclude, a pupil response to a stimulus contains multiple overlapping components: one component responding to changes in luminance and another additive component responding to changes in color. Stronger pupil responses can be achieved by combining color and luminance contrast between stimulus and background.

5.7 References

Acquafredda, M., Binda, P., & Lunghi, C. (2022). Attention Cueing in Rivalry: Insights from Pupillometry. *Eneuro, 9*(3), ENEURO.0497-21.2022. https://doi.org/10.1523/eneuro.0497-21.2022

Barbur, Harlow, & Sahraie. (1992). Pupillary responses to stimulus structure, colour and movement. *Ophthalmic and Physiological Optics, 12*(2), 137–141. https://doi.org/10.1111/j.1475-1313.1992.tb00276.x

Barbur, J. L., & Thomson, W. D. (1987). Pupil response as an objective measure of visual acuity. *Ophthalmic and Physiological Optics, 7*(4), 425–429. https://doi.org/10.1111/j.1475-1313.1987.tb00773.x

Barbur, Wolf, & Lennie. (1998). Visual processing levels revealed by response latencies to changes in different visual attributes. *Proceedings of the Royal Society B: Biological Sciences, 265*(1412), 2321–2325. https://doi.org/10.1098/rspb.1998.0578

Berson, D. M., Dunn, F. A., & Takao, M. (2002). Phototransduction by retinal ganglion cells that set the circadian clock. *Science, 295*(5557), 1070–1073. https://doi.org/10.1126/science.1067262

Bertheaux, C., Toscano, R., Fortunier, R., Roux, J. C., Charier, D., & Borg, C. (2020). Emotion Measurements Through the Touch of Materials Surfaces. *Frontiers in Human Neuroscience, 13*, 455. https://doi.org/10.3389/FNHUM.2019.00455/BIBTEX

Binda, P., & Gamlin, P. D. (2017). Renewed Attention on the Pupil Light Reflex. In *Trends in Neurosciences* (Vol. 40, Issue 8, pp. 455–457). NIH Public Access. https://doi.org/10.1016/j.tins.2017.06.007

Binda, P., & Murray, S. O. (2015a). Keeping a large--pupilled eye on high-level visual processing. In *Trends in Cognitive Sciences* (Vol. 19, Issue 1, pp. 1–3). Trends Cogn Sci. https://doi.org/10.1016/j.tics.2014.11.002

Binda, P., & Murray, S. O. (2015b). Spatial attention increases the pupillary response to light changes. *Journal of Vision, 15*(2), 1–1. https://doi.org/10.1167/15.2.1

Binda, P., Pereverzeva, M., & Murray, S. O. (2013). Attention to bright surfaces enhances the pupillary light reflex. *Journal of Neuroscience, 33*(5), 2199–2204. https://doi.org/10.1523/JNEUROSCI.3440-12.2013

Brainard, D. H. (1997). The Psychophysics Toolbox. *Spatial Vision, 10*(4), 433–436. https://doi.org/10.1163/156856897X00357

Brown, T. M., Tsujimura, S. I., Allen, A. E., Wynne, J., Bedford, R., Vickery, G., Vugler, A., & Lucas, R. J. (2012). Melanopsin-based brightness discrimination in mice and humans. *Current Biology, 22*(12), 1134–1141. https://doi.org/10.1016/j.cub.2012.04.039

Carle, C. F., James, A. C., Kolic, M., Essex, R. W., & Maddess, T. (2014). Luminance and colour variant pupil perimetry in glaucoma. *Clinical & Experimental Ophthalmology, 42*(9), 815–824. https://doi.org/10.1111/ceo.12346

Carle, C. F., James, A. C., Kolic, M., Essex, R. W., & Maddess, T. (2015). Blue multifocal pupillographic objective perimetry in glaucoma. *Investigative Ophthalmology and Visual Science, 56*(11), 6394–6403. https://doi.org/10.1167/iovs.14-16029

Carle, C. F., James, A. C., & Maddess, T. (2013). The pupillary response to color and luminance variant multifocal stimuli. *Investigative Ophthalmology and Visual Science, 54*(1), 467–475. https://doi.org/10.1167/iovs.12-10829

Carle, C. F., James, A. C., Sabeti, F., Kolic, M., Essex, R. W., Shean, C., Jeans, R., Saikal, A., Licinio, A., & Maddess, T. (2022). Clustered Volleys Stimulus Presentation for Multifocal Objective Perimetry. *Translational Vision Science and Technology, 11*(2), 5–5. https://doi.org/10.1167/tvst.11.2.5

Castaldi, E., Pomè, A., Cicchini, G. M., Burr, D., & Binda, P. (2021). Pupil size automatically encodes numerosity. *Journal of Vision, 21*(9), 2302. https://doi.org/10.1167/jov.21.9.2302

Chen, S. K., Badea, T. C., & Hattar, S. (2011). Photoentrainment and pupillary light reflex are mediated by distinct populations of ipRGCs. *Nature 2011 476:7358, 476*(7358), 92–95. https://doi.org/10.1038/nature10206

Chibel, R., Sher, I., ben Ner, D., Mhajna, M. O., Achiron, A., Hajyahia, S., Skaat, A., Berchenko, Y., Oberman,

B., Kalter-Leibovici, O., Freedman, L., & Rotenstreich, Y. (2016). Chromatic Multifocal Pupillometer for Objective Perimetry and Diagnosis of Patients with Retinitis Pigmentosa. *Ophthalmology, 123*(9), 1898–1911. https://doi.org/10.1016/j.ophtha.2016.05.038

Clark, J. H. (1924). The Ishihara Test for Color Blindness. *American Journal of Physiological Optics, 5*.

Cocker, K. D., Moseley, M. J., Bissenden, J. G., & Fielder, A. R. (1994). Visual acuity and pupillary responses to spatial structure in infants. *Investigative Ophthalmology and Visual Science, 35*(5), 2620–2625. https://iovs.arvojournals.org/article.aspx?articleid=2161200

Cornelissen, F. W., Peters, E. M., & Palmer, J. (2002). The Eyelink Toolbox: Eye tracking with MATLAB and the Psychophysics Toolbox. *Behavior Research Methods, Instruments, and Computers, 34*(4), 613–617. https://doi.org/10.3758/BF03195489

Dacey, D. M., Liao, H. W., Peterson, B. B., Robinson, F. R., Smith, V. C., Pokomy, J., Yau, K. W., & Gamlin, P. D. (2005a). Melanopsin-expressing ganglion cells in primate retina signal colour and irradiance and project to the LGN. *Nature 2005 433:7027, 433*(7027), 749–754. https://doi.org/10.1038/nature03387

Dacey, D. M., Liao, H. W., Peterson, B. B., Robinson, F. R., Smith, V. C., Pokomy, J., Yau, K. W., & Gamlin, P. D. (2005b). Melanopsin-expressing ganglion cells in primate retina signal colour and irradiance and project to the LGN. *Nature 2005 433:7027, 433*(7027), 749–754. https://doi.org/10.1038/nature03387

Donofrio, R. L. (2011). Review Paper: The Helmholtz-Kohlrausch effect. *Journal of the Society for Information Display, 19*(10), 658. https://doi.org/10.1889/jsid19.10.658

Drew, P., Sayres, R., Watanabe, K., & Shimojo, S. (2001). Pupillary response to chromatic flicker. *Experimental Brain Research, 136*(2), 256–262. https://doi.org/10.1007/s002210000605

Einhäuser, W. (2017). The pupil as marker of cognitive processes. In *Cognitive Science and Technology* (pp. 141–169). Springer, Singapore. https://doi.org/10.1007/978-981-10-0213-7_7

Gamlin, P. D. R., McDougal, D. H., Pokorny, J., Smith, V. C., Yau, K. W., & Dacey, D. M. (2007). Human and macaque pupil responses driven by melanopsin-containing retinal ganglion cells. *Vision Research, 47*(7), 946–954. https://doi.org/10.1016/J.VISRES.2006.12.015

Gamlin, P. D. R., Zhang, H., Harlow, A., & Barbur, J. L. (1998). Pupil responses to stimulus color, structure and light flux increments in the rhesus monkey. *Vision Research, 38*(21), 3353–3358. https://doi.org/10.1016/S0042-6989(98)00096-0

Gestefeld, B., Grillini, A., Marsman, J. B. C., & Cornelissen, F. W. (2020). Using natural viewing behavior to screen for and reconstruct visual field defects. *Journal of Vision, 20*(9), 1–16. https://doi.org/10.1167/JOV.20.9.11

Gooley, J. J., Lu, J., Fischer, D., & Saper, C. B. (2003). A Broad Role for Melanopsin in Nonvisual Photoreception. *Journal of Neuroscience, 23*(18), 7093–7106. https://doi.org/10.1523/JNEUROSCI.23-18-07093.2003

Gooley, J. J., Mien, I. H., st. Hilaire, M. A., Yeo, S. C., Chua, E. C. P., van Reen, E., Hanley, C. J., Hull, J. T., Czeisler, C. A., & Lockley, S. W. (2012). Melanopsin and Rod-Cone Photoreceptors Play Different Roles in Mediating Pupillary Light Responses during Exposure to Continuous Light in Humans. *The Journal of Neuroscience, 32*(41), 14242. https://doi.org/10.1523/JNEUROSCI.1321-12.2012

Hattar, S., Liao, H. W., Takao, M., Berson, D. M., & Yau, K. W. (2002). Melanopsin-containing retinal ganglion cells: Architecture, projections, and intrinsic photosensitivity. *Science, 295*(5557), 1065–1070. https://doi.org/10.1126/science.1069609

Ho, Y.-L., Wong, S. S. Y., Carle, C. F., James, A. C., Kolic, M., Maddess, T., & Goh, X.-L. (2010). Multifocal Pupillographic Perimetry With White and Colored Stimuli. *Journal of Glaucoma, 20*(6), 336–343. https://doi.org/10.1097/ijg.0b013e3181efb097

James, A. C., Kolic, M., Bedford, S. M., & Maddess, T. (2012). Stimulus parameters for multifocal pupillographic objective perimetry. *Journal of Glaucoma, 21*(9), 571–578. https://doi.org/10.1097/IJG.0b013e31821e8413

Kardon, R., Anderson, S. C., Damarjian, T. G., Grace, E. M., Stone, E., & Kawasaki, A. (2011). Chromatic Pupillometry in Patients with Retinitis Pigmentosa. *Ophthalmology, 118*(2), 376–381. https://doi.org/10.1016/J.OPHTHA.2010.06.033

Kardon, R. H. (1992). Pupil perimetry. In Current Opinion in *Ophthalmology* (Vol. 3, Issue 5, pp. 565–570). https://doi.org/10.1097/00055735-199210000-00002

Kardon, R. H., Kirkali, P. A., & Thompson, H. S. (1991). Automated Pupil Perimetry Pupil Field Mapping in Patients and Normal Subjects. *Ophthalmology, 98*(4), 485–496. https://doi.org/10.1016/S0161-6420(91)32267-X

Kelbsch, C., Lange, J., Wilhelm, H., Wilhelm, B., Peters, T., Kempf, M., Kuehlewein, L., & Stingl, K. (2020). Chromatic pupil campimetry reveals functional defects in exudative age-related macular degeneration with differences related to disease activity. *Translational Vision Science and Technology, 9*(6), 5–5. https://doi.org/10.1167/tvst.9.6.5

Kelbsch, C., Stingl, K., Jung, R., Kempf, M., Richter, P., Strasser, T., Peters, T., Wilhelm, B., Wilhelm, H., & Tonagel, F. (2021). How lesions at different locations along the visual pathway influence pupillary reactions to chromatic stimuli. *Graefe's Archive for Clinical and Experimental Ophthalmology, 1*, 1–11. https://doi.org/10.1007/s00417-021-05513-5

Kelbsch, C., Stingl, K., Kempf, M., Strasser, T., Jung, R., Kuehlewein, L., Wilhelm, H., Peters, T., Wilhelm, B., & Stingl, K. (2019). Objective measurement of local rod and cone function using gaze-controlled chromatic pupil campimetry in healthy subjects. *Translational Vision Science and Technology, 8*(6). https://doi.org/10.1167/tvst.8.6.19

Kleiner, M., Brainard, D. H., Pelli, D. G., Broussard, C., Wolf, T., & Niehorster, D. (2007). What's new in Psychtoolbox-3? A free cross-platform toolkit for psychophysiscs with Matlab and GNU/Octave. In *Cognitive and Computational Psychophysics* (Vol. 36). http://www.psychtoolbox.org

Knapen, T., De Gee, J. W., Brascamp, J., Nuiten, S., Hoppenbrouwers, S., & Theeuwes, J. (2016). Cognitive and ocular factors jointly determine pupil responses under equiluminance. *PLoS ONE, 11*(5), e0155574. https://doi.org/10.1371/journal.pone.0155574

Koenraads, Y., Braun, K. P. J., van der Linden, D. C. P., Imhof, S. M., & Porro, G. L. (2015). Perimetry in young and neurologically impaired children: the Behavioral Visual Field (BEFIE) Screening Test revisited. *JAMA Ophthalmology, 133*(3), 319–325. https://doi.org/10.1001/jamaophthalmol.2014.5257

Kremers, J., Martin, P. R., Valberg, A., & Lee, B. B. (1993). Physiological mechanisms underlying psychophysical sensitivity to combined luminance and chromatic modulation. *JOSA A, Vol. 10, Issue 6, Pp. 1403-1412, 10*(6), 1403–1412. https://doi.org/10.1364/JOSAA.10.001403

Laeng, B., & Endestad, T. (2012). Bright illusions reduce the eye's pupil. *Proceedings of the National Academy of Sciences of the United States of America, 109*(6), 2162–2167. https://doi.org/10.1073/pnas.1118298109

Lee, B. B., Sun, H., & Zucchini, W. (2007). The temporal properties of the response of macaque ganglion cells and central mechanisms of flicker detection. *Journal of Vision, 7*(14), 1.1. https://doi.org/10.116/7.14.1

Lee, B. B., Valbergt, A., Martin, P. R., Smith, V. C., & Pokorny, J. (1990). Luminance and chromatic modulation sensitivity of macaque ganglion cells and human observers. *JOSA A, Vol. 7, Issue 12, Pp. 2223-2236, 7*(12), 2223–2236. https://doi.org/10.1364/JOSAA.7.002223

Maddess, T., Essex, R. . W., Kolic, M., Carle, C. F. ., & James, A. C. (2013). High- versus low-density multifocal pupillographic objective perimetry in glaucoma. *Clinical & Experimental Ophthalmology, 41*(2), 140–147. https://doi.org/10.1111/ceo.12016

Maeda, F., Kelbsch, C., Straßer, T., Skorkovská, K., Peters, T., Wilhelm, B., & Wilhelm, H. (2017). Chromatic pupillography in hemianopia patients with homonymous visual field defects. *Graefe's Archive for Clinical and Experimental Ophthalmology, 255*(9), 1837–1842. https://doi.org/10.1007/s00417-017-3721-y

Martin, P. R., Lee, B. B., White, A. J. R., Solomon, S. G., & Rüttiger, L. (2001). Chromatic sensitivity of ganglion cells in the peripheral primate retina. *Nature 2001 410*:6831, 410(6831), 933–936. https://doi.org/10.1038/35073587

Mathôt, S., Melmi, J. B., Van Der Linden, L., & Van Der Stigchel, S. (2016). The mind-writing pupil: A human-computer interface based on decoding of covert attention through pupillometry. *PLoS ONE, 11*(2), e0148805. https://doi.org/10.1371/journal.pone.0148805

Mathôt, S., van der Linden, L., Grainger, J., & Vitu, F. (2013). The pupillary light response reveals the focus of covert visual attention. *PloS One, 8*(10). https://doi.org/10.1371/journal.pone.0078168

Mathôt, S., & Van der Stigchel, S. (2015). New Light on the Mind's Eye: The Pupillary Light Response as Active Vision. *Current Directions in Psychological Science, 24*(5), 374–378. https://doi.org/10.1177/0963721415593725

Naber, M., Alvarez, G. A., & Nakayama, K. (2013). Tracking the allocation of attention using human pupillary oscillations. *Frontiers in Psychology, 4*, 919. https://doi.org/10.3389/fpsyg.2013.00919

Naber, M., Frässle, S., & Einhäuser, W. (2011). Perceptual rivalry: Reflexes reveal the gradual nature of visual awareness. *PLoS ONE, 6*(6), e20910. https://doi.org/10.1371/journal.pone.0020910

Naber, M., & Murphy, P. (2020). Pupillometric investigation into the speed-accuracy trade-off in a visuo--motor aiming task. *Psychophysiology, 57*(3), e13499. https://doi.org/10.1111/psyp.13499

Naber, M., & Nakayama, K. (2013). Pupil responses to high-level image content. *Journal of Vision, 13*(6), 7–7. https://doi.org/10.1167/13.6.7

Naber, M., Roelofzen, C., Fracasso, A., Bergsma, D. P., van Genderen, M., Porro, G. L., Dumoulin, S. O., & van der Schouw, Y. T. (2018). Gaze-Contingent Flicker Pupil Perimetry Detects Scotomas in Patients With Cerebral Visual Impairments or Glaucoma. *Frontiers in Neurology, 9*(July), 558. https://doi.org/10.3389/fneur.2018.00558

Najjar, R. P., Rukmini, A. v, Finkelstein, M. T., Nusinovici, S., Mani, B., Nongpiur, M. E., Perera, S., Husain, R., Aung, T., & Milea, D. (2021). Handheld chromatic pupillometry can accurately and rapidly reveal functional loss in glaucoma. *British Journal of Ophthalmology, 0*, bjophthalmol-2021-319938. https://doi.org/10.1136/BJOPHTHALMOL-2021-319938

Odgaard, E. C., Arieh, Y., & Marks, L. E. (2003). Cross--modal enhancement of perceived brightness: Sensory interaction versus response bias. *Perception and Psychophysics, 65*(1), 123–132. https://doi.org/10.3758/BF03194789

Patel, D. E., Cumberland, P. M., Walters, B. C., Russell-Eggitt, I., Rahi, J. S., & OPTIC study group, O. study. (2015). Study of Optimal Perimetric Testing in Children (OPTIC): Feasibility, Reliability and Repeatability of Perimetry in Children. *PloS One, 10*(6), e0130895. https://doi.org/10.1371/journal.pone.0130895

Pelli, D. G. (1997). The VideoToolbox software for visual psychophysics: Transforming numbers into movies. *Spatial Vision, 10*(4), 437–442. https://doi.org/10.1163/156856897X00366
Portengen, B. L., Koenraads, Y., Imhof, S. M., & Porro, G. L. (2020). Lessons Learned from 23 Years of Experience in Testing Visual Fields of Neurologically Impaired Children. *Neuro-Ophthalmology, 44*(6), 361–370. https://doi.org/10.1080/01658107.2020.1762097
Portengen, B. L., Porro, G. L., Imhof, S. M., & Naber, M. (2022). Comparison of unifocal, flicker, and multifocal pupil perimetry methods in healthy adults. *Journal of Vision, 22*(9), 7. https://doi.org/10.1167/jov.22.9.7
Portengen, B. L., Roelofzen, C., Porro, G. L., Imhof, S. M., Fracasso, A., & Naber, M. (2021). Blind spot and visual field anisotropy detection with flicker pupil perimetry across brightness and task variations. *Vision Research, 178*(October 2020), 79–85. https://doi.org/10.1016/j.visres.2020.10.005
Portengen, B., Naber, M., Jansen, D., Boomen, C. van den, Imhof, S., & Porro, G. (2022). Maintaining fixation by children in a virtual reality version of pupil perimetry. *Journal of Eye Movement Research, 15*(3). https://doi.org/10.16910/JEMR.15.3.2
Rajan, M. S., Bremner, F. D., & Riordan-Eva, P. (2002). Pupil perimetry in the diagnosis of functional visual field loss. *Journal of the Royal Society of Medicine, 95*(10), 498–500. https://doi.org/10.1258/jrsm.95.10.498
Rosenholtz, R. (2016). Capabilities and Limitations of Peripheral Vision. In *Annual review of vision science* (Vol. 2, pp. 437–457). Annual Reviews. https://doi.org/10.1146/annurev-vision-082114-035733
Rosli, Y., Carle, C. F., Ho, Y., James, A. C., Kolic, M., Rohan, E. M. F., & Maddess, T. (2018a). Retinotopic effects of visual attention revealed by dichoptic multifocal pupillography. *Scientific Reports 2018 8:1, 8*(1), 1–13. https://doi.org/10.1038/s41598-018-21196-1
Rosli, Y., Carle, C. F., Ho, Y., James, A. C., Kolic, M., Rohan, E. M. F., & Maddess, T. (2018b). Retinotopic effects of visual attention revealed by dichoptic multifocal pupillography. *Scientific Reports, 8*(1), 1–13. https://doi.org/10.1038/s41598-018-21196-1
Rukmini, A. v., Milea, D., & Gooley, J. J. (2019). Chromatic Pupillometry Methods for Assessing Photoreceptor Health in Retinal and Optic Nerve Diseases. Frontiers in Neurology, 10(FEB), 76. https://doi.org/10.3389/FNEUR.2019.00076
Sabeti, F., James, A. C., Essex, R. W., & Maddess, T. (2013). Multifocal pupillography identifies retinal dysfunction in early age-related macular degeneration. *Graefe's Archive for Clinical and Experimental Ophthalmology, 251*(7), 1707–1716. https://doi.org/10.1007/s00417-013-2273-z
Sabeti, F., James, A. C., & Maddess, T. (2011). Spatial and temporal stimulus variants for multifocal pupillography of the central visual field. *Vision Research, 51*(2), 303–310. https://doi.org/10.1016/J.VISRES.2010.10.015
Sabeti, F., Maddess, T., Essex, R. W., Saikal, A., James, A. C., & Carle, C. F. (2014). Multifocal pupillography in early age-related macular degeneration. *Optometry and Vision Science, 91*(8), 904–915. https://doi.org/10.1097/OPX.0000000000000319
Sahraie, A., & Barbur, J. L. (1997). Pupil response triggered by the onset of coherent motion. *Graefe's Archive for Clinical and Experimental Ophthalmology, 235*(8), 494–500. https://doi.org/10.1007/BF00947006
Schmid, R., Luedtke, H., Wilhelm, B. J., & Wilhelm, H. (2005). Pupil campimetry in patients with visual field loss. *European Journal of Neurology, 12*(8), 602–608. https://doi.org/10.1111/j.1468-1331.2005.01048.x
Skorkovská, K., Lüdtke, H., Wilhelm, H., & Wilhelm, B. (2009). Pupil campimetry in patients with retinitis pigmentosa and functional visual field loss. *Graefe's Archive for Clinical and Experimental Ophthalmology, 247*(6), 847–853. https://doi.org/10.1007/s00417-008-1015-0
Skorkovská, K., Wilhelm, H., Lüdtke, H., & Wilhelm, B. (2009). How sensitive is pupil campimetry in hemifield loss? *Graefe's Archive for Clinical and Experimental Ophthalmology, 247*(7), 947–953. https://doi.org/10.1007/s00417-009-1040-7
Smith, V. C., Lee, B. B., Pokorny, J., Martin, P. R., & Valberg, A. (1992). Responses of macaque ganglion cells to the relative phase of heterochromatically modulated lights. *The Journal of Physiology, 458*(1),191. https://doi.org/10.1113/JPHYSIOL.1992.SP019413
Sperandio, I., Bond, N., & Binda, P. (2018). Pupil Size as a Gateway Into Conscious Interpretation of Brightness. *Frontiers in Neurology, 9*, 1070. https://doi.org/10.3389/fneur.2018.01070
Spitschan, M., & Woelders, T. (2018). The method of silent substitution for examining melanopsin contributions to pupil control. *Frontiers in Neurology, 9*(NOV), 941. https://doi.org/10.3389/FNEUR.2018.00941/BIBTEX
Strauch, C., Koniakowsky, I., & Huckauf, A. (2020). Decision making and oddball effects on pupil size: Evidence for a sequential process. *Journal of Cognition, 3*(1), 1–17. https://doi.org/10.5334/joc.96
Strauch, C., Wang, C.-A., Einhäuser, W., Van der Stigchel, S., & Naber, M. (2022). Pupillometry as an integrated readout of distinct attentional networks. *Trends in Neurosciences, 0*(0). https://doi.org/10.1016/j.tins.2022.05.003
Sutter, E. E. (1991). Fast m-transform. A fast computation of cross-correlations with binary m-sequences. *SIAM Journal on Computing, 20*(4), 686–694. https://doi.org/10.1137/0220043
Sutter, E. E., & Tran, D. (1992). The field topography of ERG components in man-I. The photopic luminance response. *Vision Research, 32*(3), 433–446. https://doi.org/10.1016/0042-6989(92)90235-B

Suzuki, Y., Minami, T., Laeng, B., & Nakauchi, S. (2019). Colorful glares: Effects of colors on brightness illusions measured with pupillometry. *Acta Psychologica, 198*, 102882. https://doi.org/10.1016/j.actpsy.2019.102882
Tan, L., Kondo, M., Sato, M., Kondo, N., & Miyake, Y. (2001). Multifocal pupillary light response fields in normal subjects and patients with visual field defects. *Vision Research, 41*(8), 1073–1084. https://doi.org/10.1016/S0042-6989(01)00030-X
Tan, T. E., Finkelstein, M. T., Tan, G. S. W., Tan, A. C. S., Chan, C. M., Mathur, R., Wong, E. Y. M., Cheung, C. M. G., Wong, T. Y., Milea, D., & Najjar, R. P. (2022). Retina neural dysfunction in diabetes revealed with handheld chromatic pupillometry. *Clinical & Experimental Ophthalmology, 50*(7), 745–756. https://doi.org/10.1111/CEO.14116
Tatham, A. J., Meira-Freitas, D., Weinreb, R. N., Zangwill, L. M., & Medeiros, F. A. (2014). Detecting glaucoma using automated pupillography. *Ophthalmology, 121*(6), 1185–1193. https://doi.org/10.1016/j.ophtha.2013.12.015
Tsujimura, S. I., Wolffsohn, J. S., & Gilmartin, B. (2006). Pupil response to color signals in cone-contrast space. *Current Eye Research, 31*(5), 401–408. https://doi.org/10.1080/02713680600681327
Ukai, K. (1985). Spatial pattern as a stimulus to the pupillary system. *Journal of the Optical Society of America A, 2*(7), 1094–1100. https://doi.org/10.1364/josaa.2.001094
Uprety, S., Uprety, S., Zele, A. J., Zele, A. J., Feigl, B., Feigl, B., Feigl, B., Cao, D., Adhikari, P., & Adhikari, P. (2021). Optimizing methods to isolate melanopsin-directed responses. *JOSA A, Vol. 38, Issue 7, Pp. 1051-1064, 38*(7), 1051–1064. https://doi.org/10.1364/JOSAA.423343
Van der Stoep, N., Van der Smagt, M. J., Notaro, C., Spock, Z., & Naber, M. (2021). The additive nature of the human multisensory evoked pupil response. *Scientific Reports, 11*(1), 1–12. https://doi.org/10.1038/s41598-020-80286-1
van Hooijdonk, R., Mathot, S., Schat, E., Spencer, H., van der Stigchel, S., & Dijkerman, H. C. (2019). Touch-induced pupil size reflects stimulus intensity, not subjective pleasantness. *Experimental Brain Research, 237*(1), 201–210. https://doi.org/10.1007/S00221-018-5404-2/FIGURES/6
Walkey, H. C., Hurden, A., Moorhead, I. R., Taylor, J. A. F., Barbur, J. L., & Harlow, J. A. (2005). Effective contrast of colored stimuli in the mesopic range: a metric for perceived contrast based on achromatic luminance contrast. *Journal of the Optical Society of America A, 22*(1), 17–28. https://doi.org/10.1364/josaa.22.000017
Wang, C. A., Blohm, G., Huang, J., Boehnke, S. E., & Munoz, D. P. (2017). Multisensory integration in orienting behavior: Pupil size, microsaccades, and saccades. *Biological Psychology, 129*, 36–44. https://doi.org/10.1016/J.BIOPSYCHO.2017.07.024
Wang, C. A., Boehnke, S. E., Itti, L., & Munoz, D. P. (2014). Transient Pupil Response Is Modulated by Contrast-Based Saliency. *Journal of Neuroscience, 34*(2), 408–417. https://doi.org/10.1523/JNEUROSCI.3550-13.2014
Wetzel, N., Buttelmann, D., Schieler, A., & Widmann, A. (2016). Infant and adult pupil dilation in response to unexpected sounds. *Developmental Psychobiology, 58*(3), 382–392. https://doi.org/10.1002/DEV.21377
Wierda, S. M., Van Rijn, H., Taatgen, N. A., & Martens, S. (2012). Pupil dilation deconvolution reveals the dynamics of attention at high temporal resolution. *Proceedings of the National Academy of Sciences of the United States of America, 109*(22), 8456–8460. https://doi.org/10.1073/pnas.1201858109
Wilhelm, H., Neitzel, J., Wilhelm, B., Beuel, S., Lüdtke, H., Kretschmann, U., & Zrenner, E. (2000). Pupil Perimetry using M-Sequence Stimulation Technique. *Investigative Ophthalmology & Visual Science, 41*(5), 1229–1238. https://dx.doi.org/
Wong, A. M. F., & Sharpe, J. A. (2000). A comparison of tangent screen, goldmann, and humphrey perimetry in the detection and localization of occipital lesions. *Ophthalmology, 107*(3), 527–544. https://doi.org/10.1016/S0161-6420(99)00092-5
Yoshitomi, T., Matsui, T., Tanakadate, A., & Ishikawa, S. (1999). Comparison of Threshold Visual Perimetry and Objective Pupil Perimetry in Clinical Patients. *Journal of Neuro-Ophthalmology, 19*(2), 89–99. https://doi.org/10.1097/00041327-199906000-00003
Young, R. S. L., & Kimura, E. (2008). Pupillary correlates of light-evoked melanopsin activity in humans. *Vision Research, 48*(7), 862–871. https://doi.org/10.1016/J.VISRES.2007.12.016
Zele, A. J., Adhikari, P., Feigl, B., & Cao, D. (2018). Cone and melanopsin contributions to human brightness estimation. *Journal of the Optical Society of America A, 35*(4), B19–B25. https://doi.org/10.1364/josaa.35.000b19
Zele, A. J., Feigl, B., Adhikari, P., Maynard, M. L., & Cao, D. (2018). Melanopsin photoreception contributes to human visual detection, temporal and colour processing. *Scientific Reports 2018 8:1, 8*(1), 1–10. https://doi.org/10.1038/s41598-018-22197-w

5.8 Supplementary material

		Yellow		Blue		Red		Green	
		Luminance (cd/m²)	CIE (x,y)	Luminance (cd/m²)	CIE (x,y)	Luminance (cd/m²)	CIE (x,y)	Luminance (cd/m²)	CIE (x,y)
Stimulus color contrast conditions	*100*	141	458,508	143	189,265	52.4	593,306	171	254,628
	45	18.4	463,501	19.5	175,211	10.4	666,324	30.6	268,674
	40	13.9	458,505	14.9	176,218	7.6	665,325	22.6	270,673
	35	9.7	461,494	10.8	178,223	5.1	665,327	15.4	273,672
	30	6.3	459,499	7.6	180,224	3.6	662,330	10.7	273,672
	25	3.7	461,480	4.9	182,235	2.2	661,333	6.4	279,668
	20	1.9	447,445	2.6	182,228	1.3	645,345	3.4	286,662
	15	ND	ND	1	189,224	0.6	614,369	1.2	310,639
	10	ND	ND	ND	ND	ND	ND	ND	ND
	5	ND	ND	ND	ND	ND	ND	ND	ND
	0	ND	ND	ND	ND	ND	ND	ND	ND

Table S1 Luminance (in cd/m2) and CIE coordinates (x,y) across color contrast conditions and colors measured with a PR-650 SpectraScan Colorimeter (Photo Research Inc., Chatsworth, CA, USA) as displayed on the presentation monitor used in this study. The annular stimuli comprised of 100% luminant colors (top row) and the luminance and corresponding CIE coordinates of the various background colors (0-45% color contrast) can be found in the rows below it. ND = not detected due to luminance levels below the photometer's detection threshold.

	0	5	10	15	20	25	30	35	40
5	*t* = 1.11, *p* = .28								
10	*t* = 0.78, *p* = .44	*t* = 0.29, *p* = .78							
15	***t* = 2.58, *p* = .02**	*t* = 0.94, *p* = .36	*t* = 1.09, *p* = .29						
20	***t* = 2.82, *p* = .01**	*t* = 1.58, *p* = .13	*t* = 1.67, *p* = .11	*t* = 0.63, *p* = .54					
25	***t* = 3.27, *p* < .01**	***t* = 2.99, *p* < .01**	***t* = 3.06, *p* < .01**	*t* = 1.88, *p* = .08	*t* = 0.51, *p* = .62				
30	***t* = 3.99, *p* = .001**	***t* = 3.29, *p* < .01**	***t* = 3.61, *p* < .01**	*t* = 2.11, *p* = .05	*t* = 1.36, *p* = .19	*t* = 0.71, *p* = .49			
35	***t* = 3.90, *p* = .001**	*t* = 2.10, *p* = .05	*t* = 1.99, *p* = .06	*t* = 1.68, *p* = .11	*t* = 0.76, *p* = .46	*t* = 0.23, *p* = .82	*t* = 0.26, *p* = .80		
40	*t* = 2.04, *p* = .06	*t* = 1.22, *p* = .24	*t* = 1.33, *p* = .20	*t* = 0.67, *p* = 0.51	*t* = 0.10, *p* = .92	*t* = 0.35, *p* = .73	*t* = 0.69, *p* = .50	*t* = 0.55, *p* = .59	
45	***t* = 2.59, *p* = .02**	*t* = 1.30, *p* = .21	*t* = 1.37, *p* = .19	*t* = 0.36, *p* = .72	*t* = 0.43, *p* = .67	*t* = 1.21, *p* = .24	*t* = 1.58, *p* = .13	*t* = 1.08, *p* = .30	*t* = 0.47, *p* = .64

Table S2 Paired double-sided student's t-test across blue background color contrasts with yellow stimulus. Rows and columns represent the background color contrasts in (%) as used in this study and compare pupil responses to yellow annuli with different background color contrasts. Significant results are indicated with bold font.

	0	5	10	15	20	25	30	35	40
5	*t* = 1.08, *p* = .30								
10	*t* = -0.21, *p* = .84	*t* = 0.73, *p* = .47							
15	*t* = 1.31, *p* = .21	*t* = 2.03, *p* = .06	*t* = 1.41, *p* = .12						
20	*t* = 0.92, *p* = .37	*t* = 1.52, *p* = .15	*t* = 1.24, *p* = .23	*t* = -0.39, *p* = .70					
25	***t* = 2.51, *p* = .02**	***t* = 3.44, *p* < .01**	***t* = 2.86, *p* = .01**	*t* = 1.56, *p* = .14	*t* = 2.0, *p* = .06				
30	*t* = 1.80, *p* = .09	***t* = 2.73, *p* = .01**	***t* = 2.18, *p* = .04**	*t* = 1.25, *p* = .23	*t* = 1.66, *p* = .12	*t* = 0.24, *p* = .82			
35	***t* = 3.27, *p* < .01**	***t* = 4.24, *p* < .001**	***t* = 4.46, *p* < .001**	*t* = 1.69, *p* = .11	***t* = 2.63, *p* = .02**	*t* = 0.23, *p* = .82	*t* = 0.40, *p* = .70		
40	***t* = 2.25, *p* = .04**	***t* = 2.69, *p* = .02**	***t* = 2.82, *p* = .01**	*t* = 0.91, *p* = .37	*t* = 2.11, *p* = .05	*t* = 0.25, *p* = .80	*t* = 0.06, *p* = .95	*t* = 0.62, *p* = .54	
45	***t* = 2.42, *p* = .03**	***t* = 3.20, *p* = .01**	***t* = 3.24, *p* = .01**	*t* = 0.76, *p* = .46	*t* = 1.58, *p* = .13	*t* = 0.77, *p* = .45	*t* = 0.43, *p* = .67	*t* = 1.22, *p* = .24	*t* = 0.48, *p* = .64

Table S3 Paired double-sided student's t-test across yellow background color contrasts with blue stimulus. Rows and columns represent the background color contrasts in (%) as used in this study and compare pupil responses to blue annuli with different background color contrasts. Significant results are indicated with bold font.

	0	5	10	15	20	25	30	35	40
5	*t* = -0.52, *p* = .61								
10	***t* = 3.04**, ***p* = .008**	***t* = 3.62**, ***p* = .003**							
15	***t* = 4.52**, ***p* < .001**	***t* = 4.13**, ***p* < .001**	*t* = 1.22, *p* = .24						
20	***t* = 4.45**, ***p* < .001**	***t* = 4.26**, ***p* < .001**	***t* = 2.17**, ***p* = .05**	*t* = 1.21, *p* = .24					
25	***t* = 3.45**, ***p* = .004**	***t* = 3.96**, ***p* = .001**	*t* = 1.80, *p* = .09	*t* = 0.48, *p* = .64	*t* = -0.36, *p* = .73				
30	***t* = 2.99**, ***p* = .009**	***t* = 2.77**, ***p* = .01**	*t* = 0.95, *p* = .36	*t* = -0.21, *p* = .84	*t* = -1.16, *p* = .26	*t* = -0.78, *p* = .45			
35	***t* = 2.62**, ***p* = .02**	***t* = 2.44**, ***p* = .03**	*t* = 0.72, *p* = .48	*t* = -0.43, *p* = .67	*t* = -1.35, *p* = .20	*t* = -1.26, *p* = .23	*t* = -0.32, *p* = .75		
40	***t* = 2.31**, ***p* = .04**	***t* = 2.14**, ***p* = .05**	*t* = -0.04, *p* = .97	*t* = -1.41, *p* = .18	***t* = -4.24**, ***p* < .001**	***t* = -2.21**, ***p* = .04**	*t* = -1.54, *p* = .15	*t* = -0.87, *p* = .40	
45	***t* = 2.56**, ***p* = .02**	***t* = 2.31**, ***p* = .04**	*t* = 0.23, *p* = .82	*t* = -1.02, *p* = .32	***t* = -2.18**, ***p* = .05**	*t* = -1.63, *p* = .12	*t* = -1.02, *p* = .33	*t* = -0.64, *p* = .53	*t* = 0.34, *p* = .74

Table S4 Paired double-sided student's t-test across green background color contrasts with red stimulus for experiment 2 (non-equiluminant complementary colors). Rows and columns represent the background color contrasts in (%) as used in this study and compare pupil responses to red annuli with different background color contrasts. Significant results are indicated with bold font

	0	5	10	15	20	25	30	35	40
5	*t* = -0.35, *p* = .73								
10	*t* = 0.55, *p* = .59	*t* = 0.81, *p* = .43							
15	*t* = 0.94, *p* = .36	*t* = 1.21, *p* = .25	*t* = 0.74, *p* = .47						
20	***t* = 2.16**, ***p* = .05**	*t* = 1.69, *p* = .11	*t* = 1.47, *p* = .16	*t* = 0.67, *p* = .51					
25	*t* = 2.11, *p* = .05	***t* = 2.17**, ***p* = .05**	***t* = 3.80**, ***p* = .002**	*t* = 0.65, *p* = .52	*t* = -0.09, *p* = .93				
30	***t* = 2.47**, ***p* = .03**	***t* = 3.01**, ***p* = .008**	*t* = 1.80, *p* = .09	*t* = 0.82, *p* = .43	*t* = 0.42, *p* = .68	*t* = 0.57, *p* = .58			
35	***t* = 3.16**, ***p* = .007**	***t* = 3.63**, ***p* = .002**	***t* = 6.45**, ***p* < .001**	***t* = 2.36**, ***p* = .03**	*t* = 1.54, *p* = .14	***t* = 2.75**, ***p* = .01**	*t* = 1.08, *p* = .30		
40	*t* = 1.05, *p* = .31	*t* = 1.17, *p* = .26	*t* = 0.82, *p* = .43	*t* = 0.17, *p* = .87	*t* = -0.40, *p* = .69	*t* = -0.37, *p* = .72	*t* = -0.68, *p* = .51	***t* = -2.13**, ***p* = .05**	
45	***t* = 2.26**, ***p* = .04**	***t* = 3.39**, ***p* = .004**	*t* = 1.72, *p* = .11	*t = 0.82,* *p* = .42	*t* = -.40, *p* = .70	*t* = 0.55, *p* = .59	*t* = -0.05, *p* = .96	*t* = -1.30, *p* = .21	*t* = 0.81, *p* = .43

Table S5 Paired double-sided student's t-test across red background color contrasts with green stimulus for experiment 2 (non-equiluminant complementary colors). Rows and columns represent the background color contrasts in (%) as used in this study and compare pupil responses to green annuli with different background color contrasts. Significant results are indicated with bold font.

	0	5	10	15	20	25	30	35	40
5	*t* = 0.14, *p* = .89								
10	*t* = 1.11, *p* = .28	*t* = 1.15, *p* = .27							
15	*t* = 1.89, *p* = .08	*t* = 1.96, *p* = .07	*t* = 0.81, *p* = .43						
20	***t* = 2.52**, ***p* = .02**	*t* = 1.98, *p* = .06	*t* = 1.20, *p* = .25	*t* = 0.38, *p* = .71					
25	*t* = 1.08, *p* = .30	*t* = 1.01, *p* = .33	*t* = 0.31, *p* = .76	*t* = -0.33, *p* = .74	*t* = -0.81, *p* = .43				
30	*t* = 1,02, *p* = .32	*t* = 0.99, *p* = .33	*t* = 0.31, *p* = .76	*t* = -0.30, *p* = .77	*t* = -0.52, *p* = .61	*t* = 0.06, *p* = .95			
35	***t* = 2.16**, ***p* = .05**	***t* = 3.13**, ***p* = .006**	*t* = 1.77, *p* = .10	*t* = 0.76, *p* = .46	*t* = 0.40, *p* = .70	*t* = 0.98, *p* = .34	*t* = 0.87, *p* = .40		
40	***t* = 2.77**, ***p* = .01**	***t* = 2.91**, ***p* = .01**	***t* = 2.37**, ***p* = .03**	*t* = 1.21, *p* = .25	*t* = 1.13, *p* = .27	*t* = 1.78, *p* = .09	*t* = 1.54, *p* = .14	*t* = 0.87, *p* = .40	
45	*t* = 0.66, *p* = .52	*t* = 0.74, *p* = .47	*t* = 0.05, *p* = .96	*t* = -0.72, p = .48	*t* = -0.87, *p* = .40	*t* = -0.32, *p* = .75	*t* = -0.40, *p* = .69	*t* = -1.54, *p* = .14	*t* = -1.88, *p* = .08

Table S6 Paired double-sided student's t-test across green background color contrasts with red stimulus for experiment 3 (equiluminant complementary colors). Rows and columns represent the background color contrasts in (%) as used in this study and compare pupil responses to red annuli with different background color contrasts. Significant results are indicated with bold font

	0	5	10	15	20	25	30	35	40
5	*t* = 0.89, *p* = .39								
10	*t* = 1.67, *p* = .11	*t* = 0.30, *p* = .77							
15	***t* = 3.35**, ***p* = .004**	***t* = 2.15**, ***p* = .05**	*t* = 2.06, *p* = .06						
20	***t* = 2.82**, ***p* = .01**	***t* = 2.79**, ***p* = .01**	***t* = 2.31**, ***p* = .03**	*t* = 0.13, *p* = .90					
25	***t* = 3.26**, ***p* = .005**	***t* = 2.82**, ***p* = .01**	***t* = 2.51**, ***p* = .02**	*t* = 0.58, *p* = .57	*t* = 0.42, *p* = .68				
30	***t* = 7.18**, ***p* < .001**	***t* = 4.11**, ***p* < .001**	***t* = 6.06**, ***p* < .001**	*t* = 1.60, *p* = .13	*t* = 1.19, *p* = .25	*t* = 0.64, *p* = .53			
35	***t* = 3.47**, ***p* = .003**	***t* = 2.72**, ***p* = .02**	***t* = 2.73**, ***p* = .01**	*t* = 0.69, *p* = .50	*t* = 0.50, *p* = .63	*t* = 0.07, *p* = .94	*t* = -0.51, *p* = .62		
40	***t* = 2.36**, ***p* = .03**	*t* = 1.60, *p* = .13	*t* = 1.38, *p* = .19	*t* = -0.38, *p* = .71	*t* = -0.41, *p* = .68	*t* = -0.72, *p* = .48	*t* = -1.49, *p* = .16	*t* = -1.02, *p* = .32	
45	***t* = 4.30**, ***p* < .001**	***t* = 3.45**, ***p* = .003**	***t* = 3.68**, ***p* = .002**	*t* = 1.21, *p* = .24	*t* = 0.97, *p* = .35	*t* = 0.48, *p* = .64	*t* = -0.27, *p* = .79	*t* = 0.29, *p* = .76	*t* = 1.41, *p* = .18

Table S7 Paired double-sided student's t-test across red background color contrasts with green stimulus for experiment 3 (equiluminant complementary colors). Rows and columns represent the background color contrasts in (%) as used in this study and compare pupil responses to green annuli with different background color contrasts. Significant results are indicated with bold font.

Effects of Stimulus Luminance, Stimulus Color and Intra-Stimulus Color Contrast on Visual Field Mapping in Neurologically Impaired Adults Using Flicker Pupil Perimetry

Eye and Brain (2023) doi: 10.2147/EB.S409905

Portengen BL
Porro GL*
Bergsma D
Veldman EJ
Imhof SM
Naber M*

* These authors contributed equally to this work.

6.1 Abstract

PURPOSE: To improve pupillary responses and diagnostic performance of flicker pupil perimetry through alterations in global and local color contrast and luminance contrast in adult patients suffering from visual field defects due to cerebral visual impairment (CVI).

METHODS: Two experiments were conducted on patients with CVI (Experiment 1: 19 subjects, age M and SD 57.9 ± 14.0; Experiment 2: 16 subjects, age M and SD 57.3 ± 14.7) suffering from absolute homonymous visual field (VF) defects. We altered global color contrast (stimuli consisted of white, yellow, cyan and yellow-equiluminant-to-cyan colored wedges) in Experiment 1, and we manipulated luminance and local color contrast with bright and dark yellow and multicolor wedges in a 2-by-2 design in Experiment 2. Stimuli consecutively flickered across 44 stimulus locations within the inner 60 degrees of the VF and were offset to a contrasting (opponency colored) dark background. Pupil perimetry results were compared to standard automated perimetry (SAP) to assess diagnostic accuracy.

RESULTS: A bright stimulus with global color contrast using yellow (p = 0.009) or white (p = 0.006) evoked strongest pupillary responses as opposed to stimuli containing local color contrast and lower brightness. Diagnostic accuracy, however, was similar across global color contrast conditions in Experiment 1 (p = 0.27) and decreased when local color contrast and less luminance contrast was introduced in Experiment 2 (p = .02). The bright yellow condition resulted in highest performance (AUC M = 0.85 ± 0.10, Mdn = 0.85).

CONCLUSIONS: Pupillary responses and pupil perimetry's diagnostic accuracy both benefit from high luminance contrast and global but not local color contrast.

6.2 Introduction

Pupil perimetry utilizes pupillary responses to light stimuli as a measure of visual field sensitivity. The greater the amplitude (or shorter the peak response latency) of a pupil response, the greater the chance that the stimulus was properly seen and processed by the observer (Kardon et al., 1991; Maeda et al., 2017; Portengen et al., 2021; Schmid et al., 2005; Skorkovská et al., 2009). Pupil perimetry produces an objective, continuous and graded response, while standard automated perimetry (SAP) outputs a subjective threshold that measures the light intensity required to trigger sensory perception. As such, pupil perimetry could be useful for patients unable to reliably provide verbal and/or motor feedback during SAP (i.e. young or neurologically impaired individuals; Goodwin, 2014; Portengen et al., 2020).

Traditionally, pupil perimetry uses presentations of white stimuli with high brightness to evoke pupil responses. The reasoning behind goes as follows: the brighter the stimulus, the more robust (i.e., high signal-to-noise ratio) the pupil response, and the better the diagnostic performance. Interestingly, the pupil not only responds to luminance when a luminance contrast is created between a bright stimulus and a dark background. It also responds to other physiological, psychological, neurological factors and sensory modalities (Brown et al., 2012; Donofrio, 2011; Drew et al., 2001; Knapen et al., 2016; Odgaard et al., 2003; Strauch et al., 2022; van Hooijdonk et al., 2019; Wetzel et al., 2016; Zele, Adhikari, et al., 2018). In line with this, the pupil has been shown to respond to a multitude of contrast modalities, such as changes in luminance (Ukai, 1985), spatial frequency (Barbur et al., 1992), and color contrast (Barbur et al., 1992; Gamlin et al., 1998; Kelbsch et al., 2019; Tsujimura et al., 2006; Walkey et al., 2005). Moreover, the speed and amplitude of these so-called pupil orienting responses (Strauch et al., 2022) seem to scale with stimulus saliency (Laeng & Endestad, 2012; Mathôt & Van der Stigchel, 2015; Naber et al., 2011; Sperandio et al., 2018; Suzuki et al., 2019). Hence, increased saliency through combined color and luminance contrast between stimulus and background results in stronger pupil responses because a substantial component of pupillary responses consists of color processing (Portengen et al., 2023). Following this rationale, saliency of a stimulus could increase by introducing an additional stimulus-background and intra-stimulus color contrast component. When salience improves, pupil responses are also expected to improve, and potentially the diagnostic accuracy of pupil perimetry may also be enhanced (Portengen et al., 2023).

Here we focus on assessing color pupil perimetry on patients with homonymous hemianopia caused by cerebral damage to the visual cortex. While hemianopic patients often suffer from large and mostly absolute scotomas, they are known to experience difficulties in reliably performing SAP tests (Goodwin, 2014). Only few studies showed that pupils of patients with homonymous hemianopia are

unresponsive to color stimuli in their damaged hemifield (Barbur, 2003). Most studies, however, showed reduced pupillary responses to white stimuli in the damaged visual field (VF) (Naber et al., 2018). It is also important to stress that it is currently unclear whether better diagnostic performance of pupil perimetry can be achieved by enhancing pupil responses through stimulus enhancements like adding color. Conversely, while pupillary responses generally benefit from strong luminance contrasts by showing highly luminant stimuli superimposed on dark backgrounds (Naber et al., 2018; Portengen et al., 2021), recent developments in pupil perimetry advocate less luminant stimuli with reduced blue content (i.e. yellow) to increase test performance of multifocal pupil perimetry in healthy subjects and patients with glaucoma and age-related macular degeneration (Carle et al., 2022; Ho et al., 2010). Between-subject variance to blue-containing stimuli is hypothesized to stem from lens brunescence and the variable density of the blue-blocking macular pigment (Pokorny et al., 1987; van de Kraats et al., 2006; Weale, 1988). Despite these great efforts to improve multifocal pupil perimetry, it is still unclear how luminance and color independently affect the diagnostic performance of *flicker* pupil perimetry in neurologically impaired individuals.

In this paper we report on a study that tested whether alterations to global and local color contrast and to luminance contrast affect not only pupil responses but also the diagnostic accuracy of pupil perimetry in patients suffering from cerebral visual impairment (CVI), a patient population in which SAP is not always suited. More specifically, the goal of this study is to investigate whether stimulus color, stimulus intra-color and stimulus luminance contrast effects positively impact diagnostic accuracy of pupil perimetry in patients suffering from homonymous visual field defects due to neurological impairment.

6.3 Methods

6.3.1 Participants

All participants (Experiment 1: 19, of which 4 female, age M and SD 57.9 ± 14.0; Experiment 2: 16, of which 3 female, age M and SD 57.3 ± 14.7) suffered from absolute homonymous visual field defects (VFDs) due to neurological impairment. This sample size was determined based on previous studies that showed significant effects of flicker pupil perimetry. See the ***Table S1*** for patient demographics. Two more participants were invited but were excluded because their VFDs were of a relative nature. Some participants did not complete both experiments due to personal reasons.

The experiments were approved by the local ethical committee of Utrecht University (approval number FETC19-006) and conformed to the tenets of the Declaration of Helsinki. Participants gave written informed consent prior to participation. Furthermore, they received financial reimbursement for participation (€12,50 per hour) and travel costs. Patients were requested to refrain from alcohol or caffeine consumption at least two hours before each session.

6.3.2 Apparatus and stimuli

All experiments were conducted in a darkened room without ambient light. Stimuli were generated on a Dell desktop computer (Dell Technologies, Round Rock, TX) with the Windows 7 operating system (Microsoft, Redmond, WA), using MATLAB (MathWorks, Natick, MA) and the Psychtoolbox 3 and Eyelink toolbox extensions (Brainard, 1997; Cornelissen et al., 2002; Kleiner et al., 2007; Pelli, 1997). We used a 143 by 63 cm LG OLED65B8PLA (LG Electronics, Seoul, South Korea) monitor with a resolution of 1920 by 1080 and a refresh rate of 60 Hz to display stimuli. Stimulus luminance was measured with a PR-650 SpectraScan Colorimeter (Photo Research Inc., Chatsworth, CA, USA). Pupil size and gaze angle were tracked with an EyeLink 1000 eye-tracker (SR Research, ON, Canada; 0.5-degree accuracy of gaze angle), which recorded only the right eye from above through a hot (infra-red reflecting) mirror (tower mount). The EyeLink toolbox extension for the Psychtoolbox(Cornelissen et al., 2002) on the presentation computer enabled communication and stimulus presentation synchronization with the pupil size recordings on the eye-tracking computer. Start and stop triggers and stimulus presentation messages were sent from the presentation computer to the eye-tracking computer by means of an Ethernet cable with negligible latency (for more details, see the SR Research manual). A participant's head and viewing distance were fixed using a forehead- and chinrest at a 75-cm distance from the monitor. The eye-tracker calibration procedure consisted of a five-point grid and took ~1 minute. The Eyelink tracker software outputs pupil size in arbitrary units rather than absolute pupil diameter in millimeters, and we refrained from converting the units as the current study only concerns within-subject comparisons.

Figure 1. Four stimulus color conditions (i.e., white, cyan, yellow-equiluminant-to-cyan, and yellow) were tested, each with 44 different stimulus locations distributed across the inner 60-degrees of the visual field (a). On every stimulus location a wedge flickered color-to-black at a 2 Hz frequency for 5 seconds (b). To ensure accurate retinotopic stimulation, a gaze-contingent stimulus presentation was used (c), i.e., online correction of stimulus locations for saccades from fixation target. Participants were instructed to report the appearance of cues around stimuli which appeared in ~40 percent of the trials for 0.25 seconds (d).

Experiment 1 – Stimulus color contrast

The stimuli consisted of white, yellow, cyan and yellow-equiluminant-to-cyan (equi-yellow) colored wedges with 100% brightness (212 cd/m2, x, y: 276, 285; 212 cd/m2, x, y: 406, 554; 134 cd/m2, x, y: 179, 235 respectively, the equi-yellow differed per participant), each presented consecutively at one of the 44 stimulus locations (see ***Figure 1a*** and ***1b***). Subjectively equal brightness (equiluminance) between yellow and cyan was established using a flicker fusion calibration before start of the experiment; a cyan screen was presented continuously while a yellow color flickered on top of the background at a 30 Hz frequency. The luminance of the yellow color was adjusted until the flickering was the least noticeable. Subsequently, this yellow color was used as the yellow-equiluminant-to-cyan color condition. This equiluminance was introduced to control for the effect of the higher luminance of the yellow stimuli on the pupil when compared to the cyan stimuli. During the experiment, the size of a wedge was increased as a function of eccentricity using a cortical magnification factor (radial width = eccentricity1.12 in degrees) to activate approximately equal numbers of neurons by both central and peripheral stimuli (e.g. see Rosenholtz, 2016). Stimuli flickered between colored and black at 2 Hz for five seconds per trial, and a red fixation point was placed at the center of the presentation monitor (see ***Figure 1b***). A flicker paradigm was used as it is known to produce oscillatory pupil orienting responses with amplitudes reflecting the degree a stimulus onset is visually processed (i.e. stimulus salience; Naber et al., 2018; Portengen et al., 2021; Portengen, Porro, et al., 2022). The stimuli were superimposed on an opponency colored (i.e., as modelled by the CIELAB color space, a three-dimensional color space which covers the entire gamut of human color perception, such as a yellow/ocher stimulus on a dark cyan background) background with 28% saturation (Portengen et al., 2023). The pupil response thus consisted of both luminance and color components.

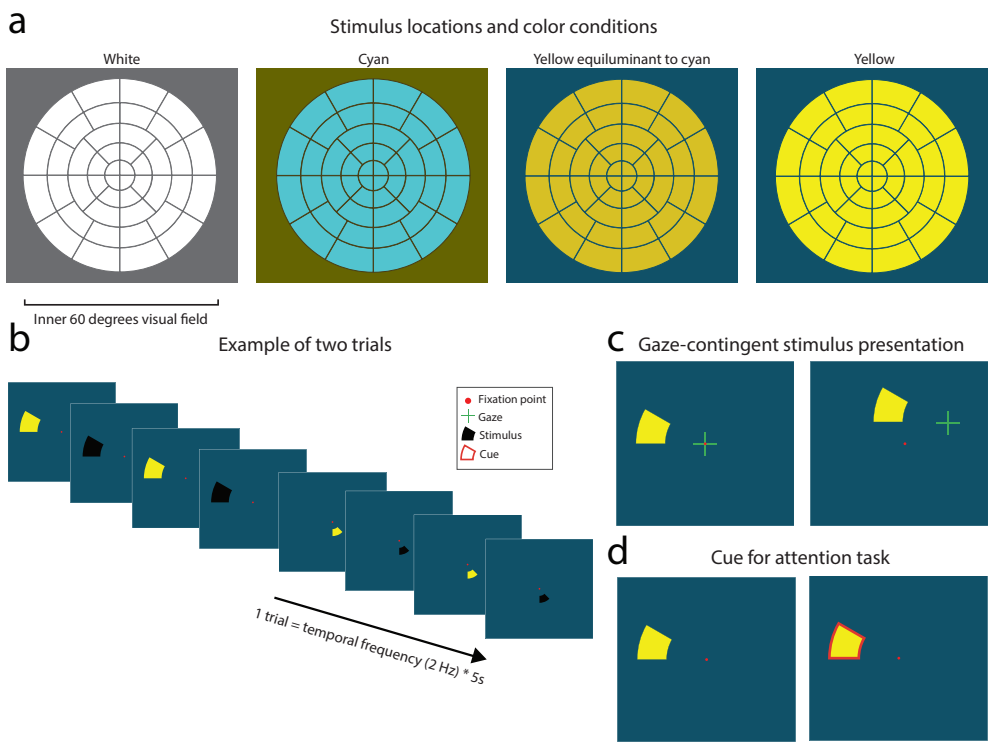

Experiment 2 – Stimulus luminance and intra-stimulus color contrast

The aim of Experiment 2 was to explore the effect of (i) local (intra-stimulus) color contrast (as opposed to global color contrast between stimulus and background) and (ii) stimulus luminance on pupillary responses and diagnostic accuracy. Experiment 2 was similarly set-up to Experiment 1 but the stimulus differed: a 100% (bright) and 75% (dark) brightness yellow and multicolor wedge flickered between

Figure 2. Four color and brightness conditions of Experiment 2: yellow and multicolor stimulus wedges at 100% and 75% brightness (a). Experiment set-up did not differ from Experiment 1; the same stimulus locations, gaze-contingent stimulus presentation and attention task were used. For the multicolor conditions, wedge color composition was comprised of smaller white, yellow, red, and green wedges which semi-randomly varied at every appearance within a trial (b).

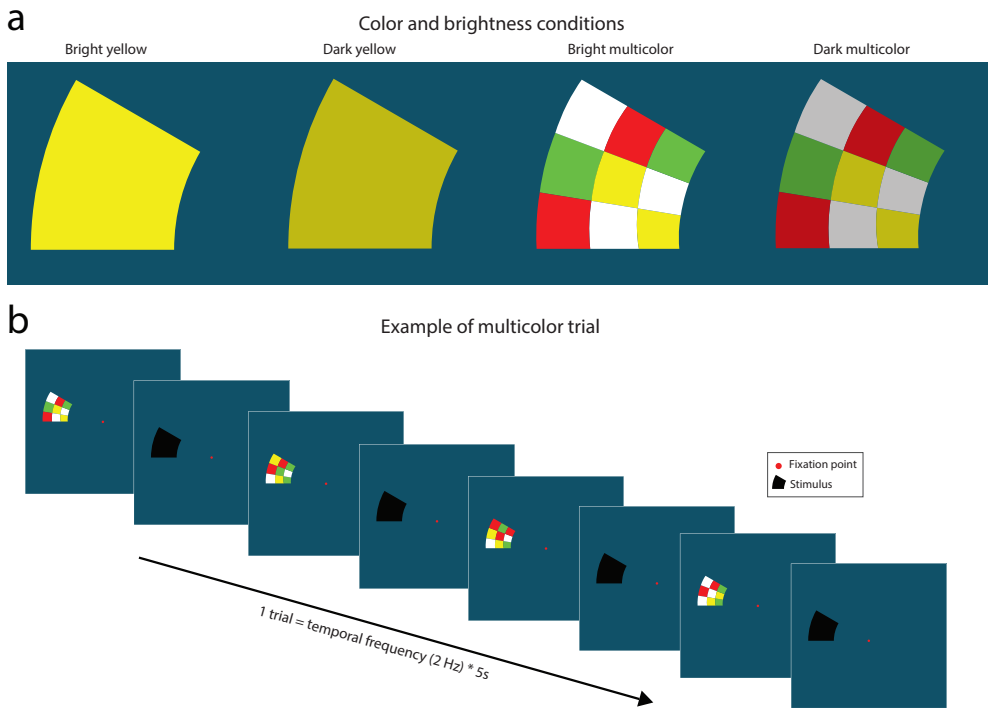

colored and black (***Figure 2a*** and ***2b***). The multicolor wedge consisted of nine smaller wedges colored white, red, green, and yellow in a semirandom pattern which changed for every new appearance. All wedges were superimposed on a 28% brightness blue background.

6.3.3 Procedure

Participants were instructed to continuously gaze at the red fixation point in the middle of the screen. We additionally instructed participants to covertly attend the flickering stimuli, each presented in a gaze-contingent manner (see ***Figure 1c***), and report the appearance of cues because attention to stimuli has been shown to evoke stronger pupil responses (Binda & Murray, 2015; Portengen et al., 2021). These cues consisted of thin red edges around the flickering stimuli that appeared in ~40 percent of the trials for 0.25 seconds (see ***Figure 1d***). If the eye tracker recorded less than 80% of the available data in a 5 second trial (e.g., due to excessive blinking), the trial was recycled at the end of the experiment block. Participants were tested at varying times of the day. Only the right eye was recorded, the left eye was patched with an (adhesive) eye patch. Test duration for each stimulus variant was 220 seconds (5 second stimulus presentation, 44 stimulus regions). Recalibrations were performed after each block. Each experiment lasted 880 seconds (44 stimulus locations * 5 seconds per location * 4 stimulus colors), excluding (re)calibration and breaks.

6.3.4 Analysis

The continuous pupil recordings were analyzed in an event-related manner with the first stimulus onset per new location as start events. Blinks were detected and filtered using a speed threshold of 4 standard deviations (SD) above the mean. The detected blink periods shorter than 600ms were interpolated with a Piecewise Cubic Hermite Interpolating Polynomial (PCHIP) method (interp1 MATLAB function). Trials with less than 80% data were removed from analysis. To filter out low frequency noise and create baseline corrected traces showing pupillary oscillation patterns around zero, we subtracted pupil traces filtered with a 2nd order Butterworth filter with a 1 Hz cut-off frequency (i.e., we applied a high-pass filter). High frequency noise was removed by filtering the high-pass filtered pupil traces with a 5th order Butterworth filter with a 15 Hz cut-off frequency. Pupil traces were filtered per event (i.e., per stimulus location). Pupil traces were then converted to power spectral density estimates in the frequency domain using a fast Fourier transform (FFT) per trial. The power

measurement at 2 Hz reflected the amplitude of the pupil oscillation pattern evoked by a stimulus and served as the main dependent variable. We now refer to this measurement as the pupil response amplitude. To determine statistical significance of differences in pupil response amplitudes across stimulus color conditions and stimulus luminance, we performed one- and two-way repeated-measures analyses of variance (ANOVA). Post-hoc paired double-sided t-tests were performed to test for differences in pupil response amplitudes and discriminative power across conditions.
Performance of each stimulus color and luminance condition was based on how well it distinguished between seen or not seen stimuli. Most recent standard automated perimetry (SAP) results served as ground truth to create subjective perimetry maps per subject; all stimulus locations were scored (0 = invisible, 1 = visible) to create a dichotomous outcome for analysis. Performance was then evaluated through calculation of the area under the curve (AUC) of the receiver operating characteristics (ROC) with visibility as dichotomous dependent variable and pupil oscillation power as independent variable. Using signal detection theory, the degree of overlap between pupil response amplitudes distributions of the intact versus defect visual field locations could be estimated. An AUC of 0.5 means that the compared distributions are not dissociable (i.e. low sensitivity), while an AUC of 1.0 means that the distributions do not overlap (i.e. high sensitivity). Normalized two-dimensional pupil sensitivity maps were created to graphically visualize visual field defects as measured with pupil perimetry. Experiment data, and analysis files are available on https://osf.io/uj4gr

6.4 Results

6.4.1 Experiment 1

For Experiment 1, the aim was to assess the effect of four global color contrast conditions (i.e. white, yellow, cyan and yellow-equiluminant-to-cyan; see ***Figure 1a***) on pupillary responses and discriminative power in CVI patients. First, pupil responses to on- and offsets of the 2 Hz flickering stimuli were inspected. ***Figure 3a*** shows the averaged pupillary response across all 44 stimulus locations for an exemplary subject when stimulated in the intact (black line) and damaged (red line) VF. For this particular subject, the oscillation amplitude appears greater for the intact as compared to the damaged VF. To estimate whether this effect generalized across color conditions, we computed

pupil response amplitudes based on the FFT-estimated oscillation power at 2 Hz as measure of pupil sensitivity per condition (for FFT-based power density estimates of the exemplary subject, see ***Figure 3b***). When plotting the average pupil response amplitudes across trials for this subject, we indeed observed consistently stronger responses to stimuli presented in intact as compared with damaged

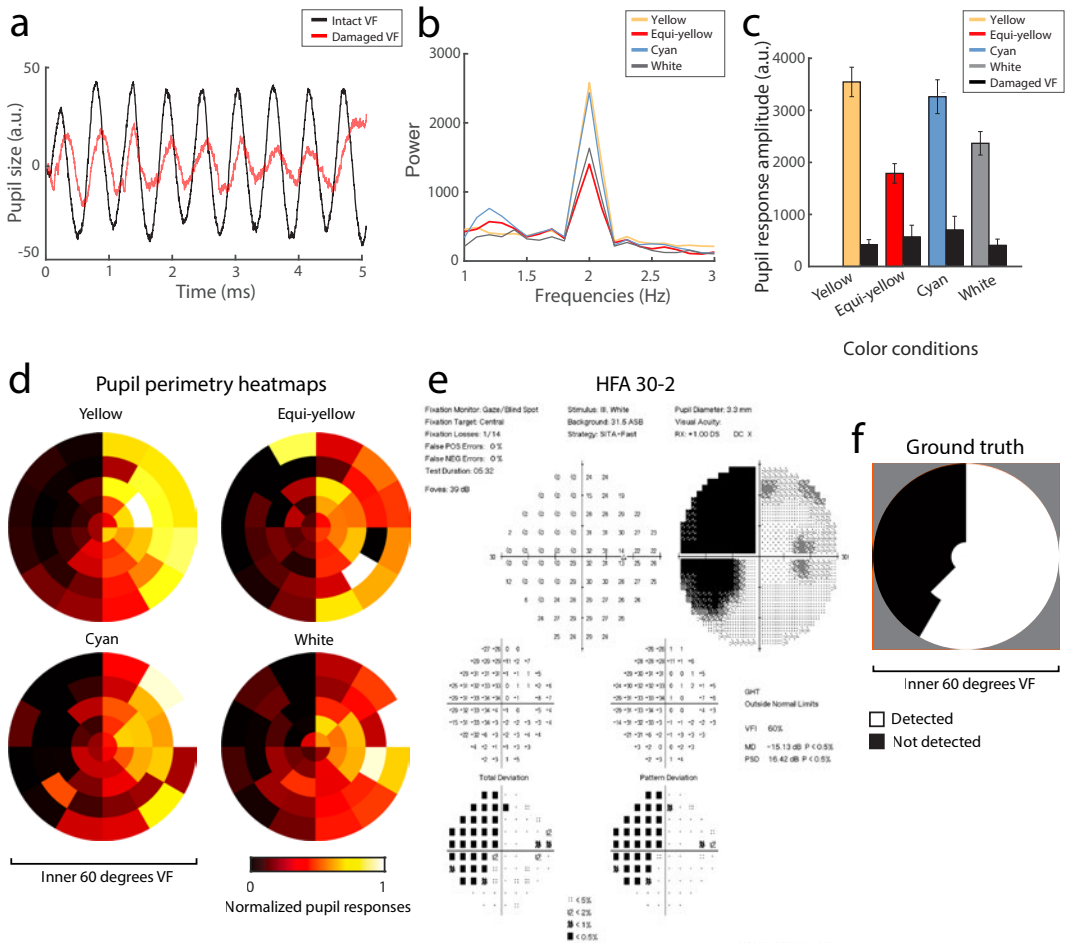

Figure 3. Results of an exemplary subject of Experiment 1. Relative pupil size over time (a) for intact (black line) and damaged (red line) visual field (VF) averaged across all 44 stimulus locations. The FFT computed pupil oscillation power (b) peaks at 2 Hz across all conditions (yellow, yellow-equiluminant-to-cyan, cyan and white). (c) Shows the pupil response amplitude with standard errors, first averaged across stimuli and then divided between the intact and damaged VF (see panel f for an example of VF segmentation) across stimulus color conditions. Note that all pupil sizes are outputted in arbitrary units (a.u.) rather than absolute millimetres due to the Eyelink tracker software. Normalized pupil perimetry heatmaps (d) of the inner 60-degrees of the VF show pupil sensitivities per stimulus location (weak sensitivity: red to black, strong sensitivity: yellow to white). (e) Displays standard perimetry (SAP) Humphrey Field Analyzer (HFA) 30-2 results of the same subject. (f) Shows the converted SAP results (black = damaged VF, white = intact VF) which served as ground truth for the analysis in panel c.

VF regions (***Figure 3c***). This effect was also consistent across all four color conditions. To investigate statistical differences in pupil response amplitudes for intact regions across conditions for all subjects (***Figure 4a***), a one-way repeated measures ANOVA revealed a significant main effect of color on pupil response amplitudes ($F_{3,18}$ = 2.93, p = 0.04). Post-hoc comparisons between conditions revealed that the pupil response amplitudes to yellow and white stimuli (presented on cyan and dark gray backgrounds, respectively) differed significantly from the yellow-equiluminant-to-cyan condition (see ***Table S2*** for post-hoc tests), which evoked the weakest pupillary responses overall. As such, we observed potentially favorable pupil responses to white and fully luminant yellow stimuli.

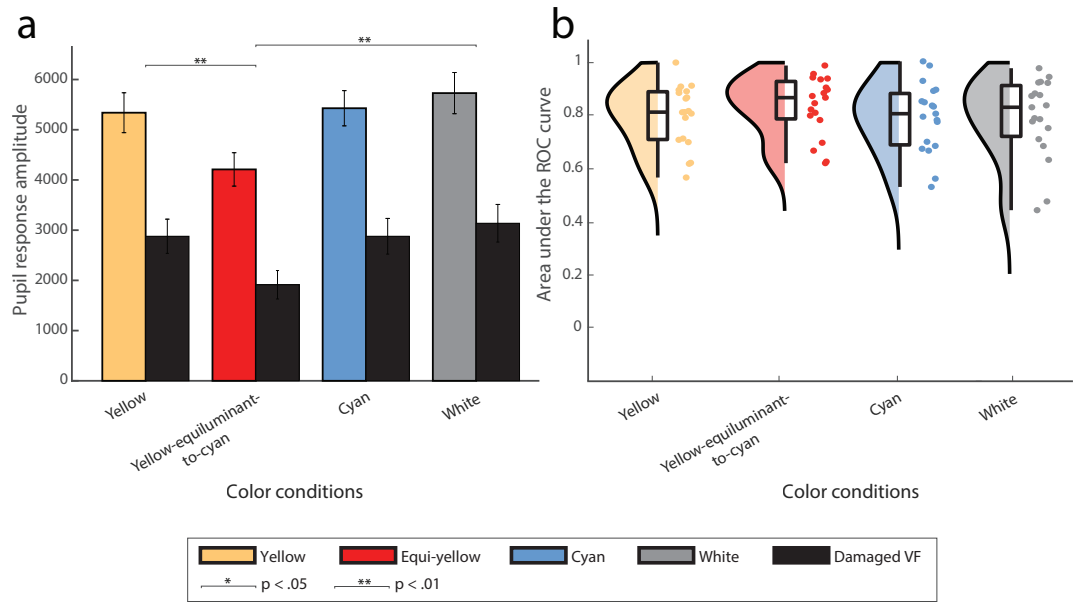

Figure 4. Pupil response amplitudes for intact and damaged VF, averaged across stimuli and subjects for all four stimulus color conditions, are plotted in (a). Asterisks reflect statistical significance between conditions (for p < .05, ** for p < .01). Raincloud plot (a hybrid plot consisting of a halved violin plot, a box-and-whisker plot with median, first and third quartile and standard errors, and scattered individual measurements) comparing discriminative performance (area under the receiver operating characteristics [AUC] curve) across conditions (yellow, yellow-equiluminant-to-cyan, cyan and white) is shown in (b).*

However, not only strong signals, but also discriminative power matters for pupil perimetry. To further explore which color condition resulted in the best detection of damaged VF regions, we plotted the visual field maps. ***Figure 3d*** and ***3e*** show visual field maps of one test subject (see ***Figure S1*** for all subjects) for objective pupil

perimetry and subjective conventional automated perimetry (i.e. SAP), respectively. Both pupil perimetry and Humphrey Field Analyzer (HFA) 30-2 revealed a similar partial left side hemianopia. These similarities between the pupil perimetry conditions and SAP extended to most subjects, but some pupil perimetry maps revealed individual differences between conditions (e.g. for subject s14 the patterns were similar for the yellow and yellow-equiluminant-to-cyan conditions, but not for cyan and white). To examine discriminative power across conditions, AUC values were calculated by comparing pupil response amplitudes across trials for intact versus damaged regions per subject. The segmentation of intact and damaged VF regions was based on SAP results. Original SAP results (***Figure 3e***) were converted to dichotomous (binary) measures to create the two categories of intact versus damaged regions as ground truth (see ***Figure 3f*** for this conversion of the current exemplary subject and Supplementary Figure S1 for all participants). ***Figure 4b*** displays a raincloud plot with AUC values that highlight the discriminative power of pupil perimetry between intact and damaged regions for all participants across conditions. The averaged AUCs did not significantly differ across color conditions (M and SD = 0.80 ± 0.12, 0.83 ± 0.11, 0.79 ± 0.13 and 0.79 ± 0.15; Mdn = 0.81, 0.86, 0.81, 0.83 for yellow, equi-yellow, cyan and white, respectively; $F_{3,16} = 1.36$, $p = 0.27$). This means that overall discriminative power was similar across conditions despite the differences in pupil response amplitudes.

6.4.2 Experiment 2

We were also interested in the effect of increases in local color contrast and decreases in brightness of stimuli on pupillary responses and the discriminative performance of pupil perimetry. As such, in Experiment 2 we compared four conditions in a 2-by-2 design, with 2 bright and 2 dark stimulus conditions, each with or without a local color contrast condition (see Figure 2). Like in Experiment 1, pupil size of a different exemplary subject than that was presented for Experiment 1 showcased a stronger oscillatory pattern over time at 2Hz evoked by the flickering wedges presented at intact as compared with damaged regions (see ***Figure 5a*** and ***5b***). Again, this effect was consistent across all color and luminance conditions (i.e., yellow and multicolor at 75% and 100% luminance). Pupil response amplitudes were also computed per condition for this exemplary subject, showing stronger pupil responses for bright as compared to dark stimuli (***Figure 5c***). To investigate whether a similar pattern was seen across all subjects, we performed a two-way repeated measures ANOVA that

revealed a significant main effect of brightness ($F_1 = 18.06$, $p < .001$), but no significant effects were found for local color contrast. Post-hoc paired student's t-tests indicated that increased stimulus brightness enhances pupil responses (see ***Figure 6a*** and ***Table S3***).

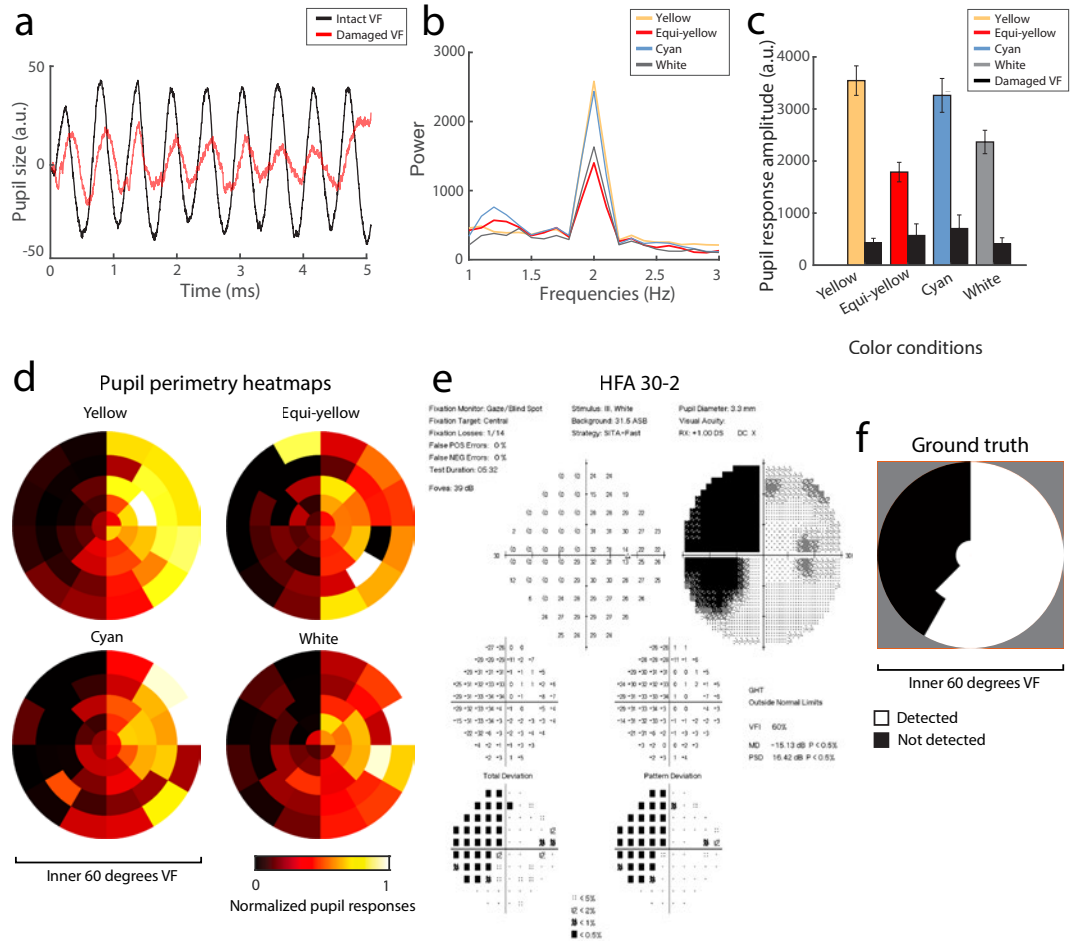

Figure 5. The same as Figure 3 but now for Experiment 2 with a new set of conditions (i.e. a 2-by-2 design with bright and dark yellow and multicolor conditions) and a different exemplary subject. Relative pupil size over time (a) for intact (black line) and damaged (red line) visual field (VF) averaged across all 44 stimulus locations. The FFT computed pupil oscillation power (b) peaks at 2 Hz across all conditions (bright and dark yellow and multicolor). (c) Shows the pupil response amplitude with standard errors, first averaged across stimuli and then divided between the intact and damaged VF (see panel f for an example of VF segmentation) across stimulus color conditions. Note that all pupil sizes are outputted in arbitrary units (a.u.) rather than absolute millimeters due to the Eyelink tracker software. Normalized pupil perimetry heatmaps (d) of the inner 60-degrees of the VF show pupil sensitivities per stimulus location (weak sensitivity: red to black, strong sensitivity: yellow to white). (e) Displays standard perimetry (SAP) Humphrey Field Analyzer (HFA) 30-2 results of the same subject. (f) Shows the converted SAP results (black = damaged VF, white = intact VF) which served as ground truth for the analysis in panel c.

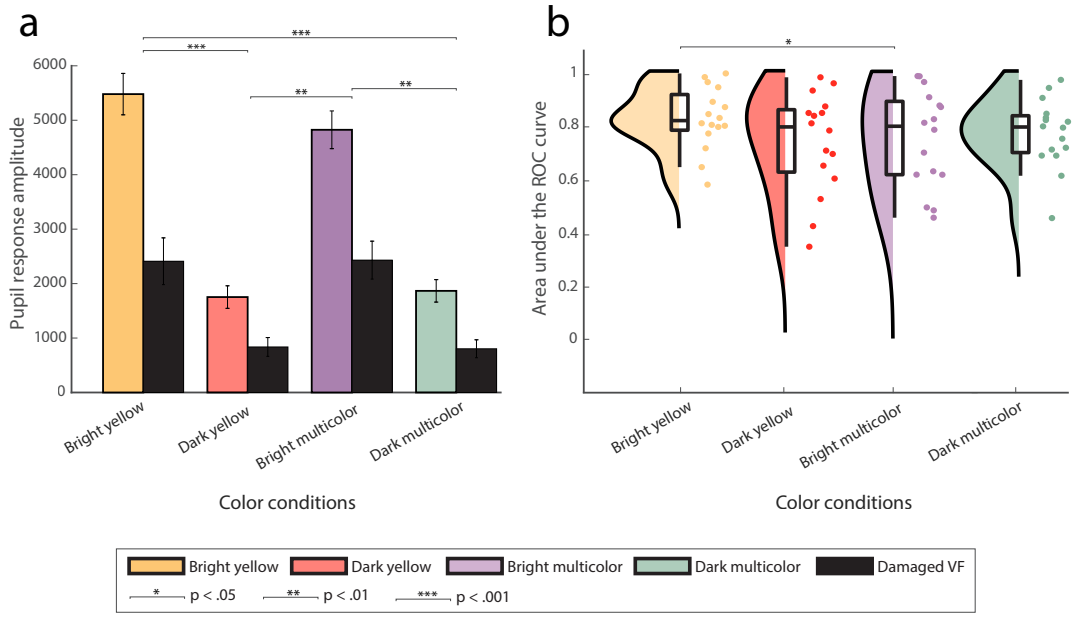

Figure 6. Similar plots to Figure 4 but now for the conditions used in Experiment 2. Pupil response amplitudes for intact and damaged VF, averaged across stimuli and subjects for all four conditions, are plotted in (a). Asterisks reflect statistical significance between conditions (for p < .05, ** for p < .01, *** for p < .001). Raincloud plot comparing discriminative performance (area under the receiver operating characteristics [AUC] curve) across conditions (bright and dark yellow and multicolor) is shown in (b).*

Figure 5d-f show the conventional HFA 30-2 and pupil perimetry results for the aforementioned exemplary subject. These maps also showed an overlapping pattern, as was the case for most subjects (see ***Figure S2***). Interestingly, some patients exhibited individual differences across conditions (e.g. in subjects s7 and s14 the dark yellow condition indeed shows an overlapping pattern while the bright yellow condition did not). The calculated discriminative power across conditions is shown in ***Figure 6b***. Average AUC values across subjects were highest for the bright yellow condition (M = 0.85 ± 0.10, Mdn = 0.85) as opposed to dark yellow (M = 0.78 ± 0.16, Mdn = 0.83), bright multicolor (M = 0.79 ± 0.15, Mdn = 0.83) and dark multicolor (M = 0.81 ± 0.11, Mdn = 0.83) conditions. The two-way repeated measures ANOVA revealed no significant main effects for local color contrast and brightness but did show a significant crossover interaction (F_{15} = 7.39, p = .02). Post-hoc analyses (***Table S4***) indicated that a bright yellow stimulus *without* local intra-color contrast enhanced pupil perimetry performance more than a stimulus *with* local intra-color contrast.

6.5 Discussion

The aim for this study was to test whether alterations to global and local color contrast and to luminance contrast affect not only pupil responses but also diagnostic performance of flicker pupil perimetry performance for detecting visual field defects in patients suffering from visual field defects due to cerebral visual impairment (CVI).
In Experiment 1, four stimulus color conditions (i.e., white, yellow, cyan and yellow-equiluminant-to-cyan) with a complementary colored background were investigated. Although fully luminant yellow and white stimuli affected pupillary responses more strongly, discriminative power was similar across all conditions, including the cyan and yellow-equiluminant stimuli. This result is not fully in line with the hypothesis of Maeda et al.(2017) stating that pupil responses to blue light presented in the damaged visual field may still occur when the subcortical intrinsically photosensitive retinal ganglion cell (ipRGC) pathway remains intact. Hypothetically, if blue-absent colors are used for stimuli and a blue colored background was used to desensitize, it would be possible to more accurately distinguish the damaged from the intact visual field in patients only suffering from cortical damage (excluding ipRGC) but not retinal damage (including ipRGC). Residual blue light- and ipRGC-driven pupil responses then do not contaminate the impaired cortically driven pupil responses depending on feedback from the visual cortex. As such, the use of yellow rather than blue stimuli would be advocated in case of testing CVI patients and several research groups have started using chromatic pupil perimetry to improve diagnostic performance of pupil perimetry (Carle et al., 2013; Chibel et al., 2016; Kelbsch et al., 2019; Maeda et al., 2017). However, ipRGCs not only receive input from melanopsin, but are also affected by rods and cones (Dacey et al., 2005; Gamlin et al., 2007; Young & Kimura, 2008; Zele, Feigl, et al., 2018). Thus, rod- and cone-driven pupil responses can still be observed if blue-absent light is used. This may explain the homogenous results across color conditions found in this study.
Although our results show that chromatic stimuli do not substantially impact diagnostic performance, chromatic pupil perimetry could provide additional information about another aspect of a patient's visual system as opposed to a solely luminance-based pupil perimetry method. The pupil perimetry heatmaps of some patients (see ***Figures S1*** and ***S2***) were very similar across chromatic conditions. Interestingly, for others only a certain color condition resembled the SAP results (e.g. only the bright yellow or multicolor condition

resulted in strong diagnostic performance, while other conditions showed differing patterns from SAP). This within-subject chromatic pupil sensitivity variability could stem from some form of blindsight which causes the pupil to respond to only certain colors along the edge of the visual field defect. Future studies on a larger study population might provide insight regarding these possibly blindsight-like processes to not only motion, but also color. In time, not one but multiple chromatic variants per visual field location in a patient may portray visual field function most accurately with pupil perimetry. Pupil orienting responses (i.e., pupil responses to salient events such as onsets of bright stimuli) scale with stimulus saliency (Strauch et al., 2022). Adding local color contrast and optimal spatial frequency to a stimulus should increase saliency and pupil responses therewith (Barbur & Thomson, 1987; Portengen et al., 2023; Slooter & van Norren, 1980; Young et al., 1995). Interestingly, our results show that an increase in local (intra-stimulus) color contrast (and thus saliency) did not improve the responses. Conversely, our results show that not local intra-stimulus color contrast, but more global contrast with a single-colored stimulus and a contrasting background color achieves greatest pupillary responses. Thus, color contrast of lower spatial frequency presumably contributes less to saliency than expected. Moreover, contrary to results from prior research using multifocal pupil perimetry (Carle et al., 2022; Ho et al., 2010), the flicker pupil perimetry method does not benefit from stimuli with decreased brightness. Specifically, fully luminant and single-color stimuli (regardless of choice of color) with an opponency colored background increases saliency and discriminative performance in the currently studied patient population.

The pupil perimetry method used in the current study was first proposed by Naber et al. (2018) Since then, several improvements were introduced: (i) luminance and color contrast components between stimulus and background (Portengen et al., 2021, 2023), (ii) stimuli adjusted for the cortical magnification factor (Portengen, Porro, et al., 2022), and (iii) optimized analyses (i.e., calculating FFT pupil power as opposed to standard deviation, coherence or signal-to-noise ratio, PCHIP interpolation as opposed to a cubic spline). All this has led to improved diagnostic performance. For example, the normalized pupil perimetry heatmaps of the current method showcased similarity to the standard automated perimetry (SAP) results. Also, a high discriminative power was achieved; a mean AUC of 0.85, the highest test performance when compared to prior research and other pupil perimetry methods assessed in CVI patients (Naber et al., 2018; Schmid et al., 2005; Skorkovská et al., 2009; Yoshitomi et al., 1999). Other methods that utilize pupillary responses to assess visual sensitivity consist of unifocal (Asakawa et al., 2010; Kelbsch et al., 2016; Tatham et al., 2014) and multifocal (Carle et al., 2014, 2015) stimulus presentations or multiple frequency tagging (Ajasse et al., 2022). Their attempts mainly focused on detecting glaucoma, a disease which asks for long-term monitoring to detect small decrements of function in the peripheral visual field. We suggest that pupil perimetry might be more suited to the screening of visual field defects (VFDs) caused by brain disease (e.g. cerebral infarction or tumor) which are more often larger and less prone to subtle changes. A limitation to this study (and other studies involving pupil perimetry) is the small sample size. It is important to assess pupil perimetry's performance in larger study populations to truly objectivate its role in visual field assessment. It is also important to note that the pupil perimetry method is hindered by the larger stimuli needed to evoke robust pupillary responses, resulting in a visual sensitivity map with low spatial resolution. SAP provides a more precise estimation of visual field function due to the smaller stimuli used. Nevertheless, pupil perimetry might be a valuable addition to SAP in the diagnostic workup of suspected VFDs.

As a matter of fact, in certain situations VF assessment with pupil perimetry has merit over SAP. The gaze-contingent presentation of stimuli ensures accurate retinotopic stimulation. Along with its apparent objectivity (thus eliminating the need for subjective motor responses), pupil perimetry might prove useful for patients suspected of malingering or for young and multi-handicapped patients unable to reliably provide verbal and/or motor feedback during SAP. Also, pupil perimetry can be used in a more patient-friendly way by using head-mounted apparatus (Kimura et al., 2019). Future research might focus on the application of virtual reality technology as a cheap alternative to increase applicability in children (Portengen, Naber, et al., 2022), a patient demographic which is well known to have unreliable SAP measurements (Morales & Brown, 2001; Patel et al., 2015; Portengen et al., 2020; Tschopp et al., 1998).

6.6 Conclusion

To conclude, high diagnostic performance was found using varying types of chromatic and non-chromatic flicker pupil perimetry for the assessment of visual field defects in patients with CVI. The addition of local color contrast did not positively impact pupil response sensitivity. As such, we recommend the use of bright stimuli without a local color contrast component offset to a darker and contrasting background to achieve best visual field test results.

6.7 References

Ajasse, S., Vignal-Clermont, C., Mohand-Saïd, S., Coen, C., Romand, C., & Lorenceau, J. (2022). One minute Multiple Pupillary Frequency Tagging test to assess visual field defects. *MedRxiv*, 2022.01.24.22269632. https://doi.org/10.1101/2022.01.24.22269632

Asakawa, K., Shoji, N., Ishikawa, H., & Shimizu, K. (2010). New approach for the glaucoma detection with pupil perimetry. *Clinical Ophthalmology (Auckland, N.Z.), 4*(1), 617–623. https://www.ncbi.nlm.nih.gov/pubmed/20668724

Barbur, Harlow, & Sahraie. (1992). Pupillary responses to stimulus structure, colour and movement. *Ophthalmic and Physiological Optics, 12*(2), 137–141. https://doi.org/10.1111/j.1475-1313.1992.tb00276.x

Barbur, J. L. (2003). Learning from the Pupil: Studies of Basic Mechanisms and Clinical Applications. *The Visual Neurosciences, 2-Vol. Set*, 641–656. https://doi.org/10.7551/MITPRESS/7131.003.0046

Barbur, J. L., & Thomson, W. D. (1987). Pupil response as an objective measure of visual acuity. *Ophthalmic and Physiological Optics, 7*(4), 425–429. https://doi.org/10.1111/j.1475-1313.1987.tb00773.x

Binda, P., & Murray, S. O. (2015). Spatial attention increases the pupillary response to light changes. *Journal of Vision, 15*(2), 1–1. https://doi.org/10.1167/15.2.1

Brainard, D. H. (1997). The Psychophysics Toolbox. *Spatial Vision, 10*(4), 433–436. https://doi.org/10.1163/156856897X00357

Brown, T. M., Tsujimura, S. I., Allen, A. E., Wynne, J., Bedford, R., Vickery, G., Vugler, A., & Lucas, R. J. (2012). Melanopsin-based brightness discrimination in mice and humans. *Current Biology, 22*(12), 1134–1141. https://doi.org/10.1016/j.cub.2012.04.039

Carle, C. F., James, A. C., Kolic, M., Essex, R. W., & Maddess, T. (2014). Luminance and colour variant pupil perimetry in glaucoma. *Clinical & Experimental Ophthalmology, 42*(9), 815–824. https://doi.org/10.1111/ceo.12346

Carle, C. F., James, A. C., Kolic, M., Essex, R. W., & Maddess, T. (2015). Blue multifocal pupillographic objective perimetry in glaucoma. *Investigative Ophthalmology and Visual Science, 56*(11), 6394–6403. https://doi.org/10.1167/iovs.14-16029

Carle, C. F., James, A. C., & Maddess, T. (2013). The pupillary response to color and luminance variant multifocal stimuli. *Investigative Ophthalmology and Visual Science, 54*(1), 467–475. https://doi.org/10.1167/iovs.12-10829

Carle, C. F., James, A. C., Sabeti, F., Kolic, M., Essex, R. W., Shean, C., Jeans, R., Saikal, A., Licinio, A., & Maddess, T. (2022). Clustered Volleys Stimulus Presentation for Multifocal Objective Perimetry. *Translational Vision Science and Technology, 11*(2), 5–5. https://doi.org/10.1167/tvst.11.2.5

Chibel, R., Sher, I., ben Ner, D., Mhajna, M. O., Achiron, A., Hajyahia, S., Skaat, A., Berchenko, Y., Oberman, B., Kalter-Leibovici, O., Freedman, L., & Rotenstreich, Y. (2016). Chromatic Multifocal Pupillometer for Objective Perimetry and Diagnosis of Patients with Retinitis Pigmentosa. *Ophthalmology, 123*(9), 1898–1911. https://doi.org/10.1016/j.ophtha.2016.05.038

Cornelissen, F. W., Peters, E. M., & Palmer, J. (2002). The Eyelink Toolbox: Eye tracking with MATLAB and the Psychophysics Toolbox. *Behavior Research Methods, Instruments, and Computers, 34*(4), 613–617. https://doi.org/10.3758/BF03195489

Dacey, D. M., Liao, H. W., Peterson, B. B., Robinson, F. R., Smith, V. C., Pokomy, J., Yau, K. W., & Gamlin, P. D. (2005). Melanopsin-expressing ganglion cells in primate retina signal colour and irradiance and project to the LGN. *Nature 2005 433:7027, 433*(7027), 749–754. https://doi.org/10.1038/nature03387

Donofrio, R. L. (2011). Review Paper: The Helmholtz-Kohlrausch effect. *Journal of the Society for Information Display, 19*(10), 658. https://doi.org/10.1889/jsid19.10.658

Drew, P., Sayres, R., Watanabe, K., & Shimojo, S. (2001). Pupillary response to chromatic flicker. *Experimental Brain Research, 136*(2), 256–262. https://doi.org/10.1007/s002210000605

Gamlin, P. D. R., McDougal, D. H., Pokorny, J., Smith, V. C., Yau, K. W., & Dacey, D. M. (2007). Human and macaque pupil responses driven by melanopsin-containing retinal ganglion cells. *Vision Research, 47*(7), 946–954. https://doi.org/10.1016/J.VISRES.2006.12.015

Gamlin, P. D. R., Zhang, H., Harlow, A., & Barbur, J. L. (1998). Pupil responses to stimulus color, structure and light flux increments in the rhesus monkey. *Vision Research, 38*(21), 3353–3358. https://doi.org/10.1016/S0042-6989(98)00096-0

Goodwin, D. (2014). Homonymous hemianopia: Challenges and solutions. In *Clinical Ophthalmology* (Vol. 8). https://doi.org/10.2147/OPTH.S59452

Ho, Y.-L., Wong, S. S. Y., Carle, C. F., James, A. C., Kolic, M., Maddess, T., & Goh, X.-L. (2010). Multifocal Pupillographic Perimetry With White and Colored Stimuli. *Journal of Glaucoma, 20*(6), 336–343. https://doi.org/10.1097/ijg.0b013e3181efb097

Kardon, R. H., Kirkali, P. A., & Thompson, H. S. (1991). Automated Pupil Perimetry Pupil Field Mapping in Patients and Normal Subjects. *Ophthalmology, 98*(4), 485–496. https://doi.org/10.1016/S0161-6420(91)32267-X

Kelbsch, C., Maeda, F., Strasser, T., Blumenstock, G., Wilhelm, B., Wilhelm, H., & Peters, T. (2016). Pupillary responses driven by ipRGCs and classical photoreceptors are impaired in glaucoma. *Graefe's Archive for Clinical and Experimental Ophthalmology, 254*(7), 1361–1370. https://doi.org/10.1007/s00417-016-3351-9

Kelbsch, C., Stingl, K., Kempf, M., Strasser, T., Jung, R., Kuehlewein, L., Wilhelm, H., Peters, T., Wilhelm, B., & Stingl, K. (2019). Objective measurement of local rod and cone function using gaze-controlled chromatic pupil campimetry in healthy subjects. *Translational Vision Science and Technology, 8*(6). https://doi.org/10.1167/tvst.8.6.19

Kimura, T., Matsumoto, C., & Nomoto, H. (2019). Comparison of head-mounted perimeter (imo®) and Humphrey Field Analyzer. *Clinical Ophthalmology (Auckland, N.Z.), 13*, 501. https://doi.org/10.2147/OPTH.S190995

Kleiner, M., Brainard, D. H., Pelli, D. G., Broussard, C., Wolf, T., & Niehorster, D. (2007). What's new in Psychtoolbox-3? A free cross-platform toolkit for psychophysiscs with Matlab and GNU/Octave. In *Cognitive and Computational Psychophysics* (Vol. 36). http://www.psychtoolbox.org

Knapen, T., De Gee, J. W., Brascamp, J., Nuiten, S., Hoppenbrouwers, S., & Theeuwes, J. (2016). Cognitive and ocular factors jointly determine pupil responses under equiluminance. *PLoS ONE, 11*(5), e0155574. https://doi.org/10.1371/journal.pone.0155574

Laeng, B., & Endestad, T. (2012). Bright illusions reduce the eye's pupil. *Proceedings of the National Academy of Sciences of the United States of America, 109*(6), 2162–2167. https://doi.org/10.1073/pnas.1118298109

Maeda, F., Kelbsch, C., Straßer, T., Skorkovská, K., Peters, T., Wilhelm, B., & Wilhelm, H. (2017). Chromatic upillography in hemianopia patients with homonymous visual field defects. *Graefe's Archive for Clinical and Experimental Ophthalmology, 255*(9), 1837–842. https://doi.org/10.1007/s00417-017-3721-y

Mathôt, S., & Van der Stigchel, S. (2015). New Light on the Mind's Eye: The Pupillary Light Response as Active Vision. *Current Directions in Psychological Science, 24*(5), 374–378. https://doi.org/10.1177/0963721415593725

Morales, J., & Brown, S. M. (2001). The feasibility of short automated static perimetry in children. *Ophthalmology, 108*(1), 157–162. https://doi.org/10.1016/S0161-6420(00)00415-2

Naber, M., Frässle, S., & Einhäuser, W. (2011). Perceptual rivalry: Reflexes reveal the gradual nature of visual awareness. *PLoS ONE, 6*(6), e20910. https://doi.org/10.1371/journal.pone.0020910

Naber, M., Roelofzen, C., Fracasso, A., Bergsma, D. P., van Genderen, M., Porro, G. L., Dumoulin, S. O., & van der Schouw, Y. T. (2018). Gaze-Contingent Flicker Pupil Perimetry Detects Scotomas in Patients With Cerebral Visual Impairments or Glaucoma. *Frontiers in Neurology, 9*(July), 558. https://doi.org/10.3389/fneur.2018.00558

Odgaard, E. C., Arieh, Y., & Marks, L. E. (2003). Cross-modal enhancement of perceived brightness: Sensory interaction versus response bias. *Perception and Psychophysics, 65*(1), 123–132. https://doi.org/10.3758/BF03194789

Patel, D. E., Cumberland, P. M., Walters, B. C., Russell-Eggitt, I., Rahi, J. S., & OPTIC study group, O. study. (2015). Study of Optimal Perimetric Testing in Children (OPTIC): Feasibility, Reliability and Repeatability of Perimetry in Children. *PloS One, 10*(6), e0130895. https://doi.org/10.1371/journal.pone.0130895

Pelli, D. G. (1997). The VideoToolbox software for visual psychophysics: Transforming numbers into movies. *Spatial Vision, 10*(4), 437–442. https://doi.org/10.1163/156856897X00366

Pokorny, J., Smith, V. C., & Lutze, M. (1987). Aging of the human lens. *Applied Optics, 26*(8). https://doi.org/10.1364/ao.26.001437

Portengen, B. L., Koenraads, Y., Imhof, S. M., & Porro, G. L. (2020). Lessons Learned from 23 Years of Experience in Testing Visual Fields of Neurologically Impaired Children. *Neuro-Ophthalmology, 44*(6), 361–370. https://doi.org/10.1080/01658107.2020.1762097

Portengen, B. L., Naber, M., Jansen, D., Boomen, C. van den, Imhof, S. M., & Porro, G. L. (2022). Maintaining fixation by children in a virtual reality version of pupil perimetry. *Journal of Eye Movement Research, 15*(3). https://doi.org/10.16910/JEMR.15.3.2

Portengen, B. L., Porro, G. L., Imhof, S. M., & Naber, M. (2022). Comparison of unifocal, flicker, and multifocal pupil perimetry methods in healthy adults. *Journal of Vision, 22*(9), 7. https://doi.org/10.1167/jov.22.9.7

Portengen, B. L., Porro, G. L., Imhof, S. M., & Naber, M. (2023). The Trade-Off Between Luminance and Color Contrast Assessed With Pupil Responses. *Translational Vision Science & Technology, 12*(1), 15–15. https://doi.org/10.1167/TVST.12.1.15

Portengen, B. L., Roelofzen, C., Porro, G. L., Imhof, S. M., Fracasso, A., & Naber, M. (2021). Blind spot and visual field anisotropy detection with flicker pupil perimetry across brightness and task variations. *Vision Research, 178*(October 2020), 79–85. https://doi.org/10.1016/j.visres.2020.10.005

Rosenholtz, R. (2016). Capabilities and Limitations of Peripheral Vision. In *Annual review of vision science* (Vol. 2, pp. 437–457). Annual Reviews. https://doi.org/10.1146/annurev-vision-082114-035733

Schmid, R., Luedtke, H., Wilhelm, B. J., & Wilhelm, H. (2005). Pupil campimetry in patients with visual field loss. *European Journal of Neurology, 12*(8), 602–608. https://doi.org/10.1111/j.1468-1331.2005.01048.x

Skorkovská, K., Wilhelm, H., Lüdtke, H., & Wilhelm, B. (2009). How sensitive is pupil campimetry in hemifield loss? *Graefe's Archive for Clinical and Experimental Ophthalmology, 247*(7), 947–953. https://doi.org/10.1007/s00417-009-1040-7

Slooter, J., & van Norren, D. (1980). Visual acuity measured with pupil responses to checkerboard stimuli. *Investigative Ophthalmology & Visual Science, 19*(1), 105–108. https://dx.doi.org/

Sperandio, I., Bond, N., & Binda, P. (2018). Pupil Size as a Gateway Into Conscious Interpretation of Brightness. *Frontiers in Neurology, 9*, 1070. https://doi.org/10.3389/fneur.2018.01070

Strauch, C., Wang, C.-A., Einhäuser, W., Van der Stigchel, S., & Naber, M. (2022). Pupillometry as an integrated readout of distinct attentional networks. *Trends in Neurosciences, 0*(0). https://doi.org/10.1016/j.tins.2022.05.003

Suzuki, Y., Minami, T., Laeng, B., & Nakauchi, S. (2019). Colorful glares: Effects of colors on brightness illusions measured with pupillometry. *Acta Psychologica, 198*, 102882. https://doi.org/10.1016/j.actpsy.2019.102882

Tatham, A. J., Meira-Freitas, D., Weinreb, R. N., Zangwill, L. M., & Medeiros, F. A. (2014). Detecting glaucoma using automated pupillography. *Ophthalmology, 121*(6), 1185–1193. https://doi.org/10.1016/j.ophtha.2013.12.015

Tschopp, C., Safran, A. B., Viviani, P., Bullinger, A., Reicherts, M., & Mermoud, C. (1998). Automated visual field examination in children aged 5–8 years: Part I: Experimental validation of a testing procedure. *Vision Research, 38*(14), 2203–2210. https://doi.org/10.1016/S0042-6989(97)00368-4

Tsujimura, S. I., Wolffsohn, J. S., & Gilmartin, B. (2006). Pupil response to color signals in cone-contrast space. *Current Eye Research, 31*(5), 401–408. https://doi.org/10.1080/02713680600681327

Ukai, K. (1985). Spatial pattern as a stimulus to the pupillary system. *Journal of the Optical Society of America A, 2*(7), 1094–1100. https://doi.org/10.1364/josaa.2.001094

Van de Kraats, J., Berendschot, T. T. J. M., Valen, S., & van Norren, D. (2006). Fast assessment of the central macular pigment density with natural pupil using the macular pigment reflectometer. *Journal of Biomedical Optics, 11*(6). https://doi.org/10.1117/1.2398925

Van Hooijdonk, R., Mathot, S., Schat, E., Spencer, H., van der Stigchel, S., & Dijkerman, H. C. (2019). Touch-induced pupil size reflects stimulus intensity, not subjective pleasantness. *Experimental Brain Research, 237*(1), 201–210. https://doi.org/10.1007/S00221-018-5404-2/FIGURES/6

Walkey, H. C., Hurden, A., Moorhead, I. R., Taylor, J. A. F., Barbur, J. L., & Harlow, J. A. (2005). Effective contrast of colored stimuli in the mesopic range: a metric for perceived contrast based on achromatic luminance contrast. *Journal of the Optical Society of America A, 22*(1), 17–28. https://doi.org/10.1364/josaa.22.000017

Weale, R. A. (1988). Age and the transmittance of the human crystalline lens. *The Journal of Physiology, 395*(1). https://doi.org/10.1113/jphysiol.1988.sp016935

Wetzel, N., Buttelmann, D., Schieler, A., & Widmann, A. (2016). Infant and adult pupil dilation in response to unexpected sounds. *Developmental Psychobiology, 58*(3), 382–392. https://doi.org/10.1002/DEV.21377

Yoshitomi, T., Matsui, T., Tanakadate, A., & Ishikawa, S. (1999). Comparison of Threshold Visual Perimetry and Objective Pupil Perimetry in Clinical Patients. *Journal of Neuro-Ophthalmology, 19*(2), 89–99. https://doi.org/10.1097/00041327-199906000-00003

Young, R. S. L., & Kimura, E. (2008). Pupillary correlates of light-evoked melanopsin activity in humans. *Vision Research, 48*(7), 862–871. https://doi.org/10.1016/J.VISRES.2007.12.016

Young, R. S. L., Kimura, E., & Delucia, P. R. (1995). A pupillometric correlate of scotopic visual acuity. *Vision Research, 35*(15), 2235–2241. https://doi.org/10.1016/0042-6989(94)00303-3

Zele, A. J., Adhikari, P., Feigl, B., & Cao, D. (2018). Cone and melanopsin contributions to human brightness estimation. *Journal of the Optical Society of America A, 35*(4), B19–B25. https://doi.org/10.1364/josaa.35.000b19

Zele, A. J., Feigl, B., Adhikari, P., Maynard, M. L., & Cao, D. (2018). Melanopsin photoreception contributes to human visual detection, temporal and colour processing. *Scientific Reports 2018 8:1, 8*(1), 1–10. https://doi.org/10.1038/s41598-018-22197-w

6.8 Supplementary material

Patient	Age	Gender	VA with correction (logMAR)	Visual field defect	Diagnosis	Medication
s1	65	Male	-0.1	RHH	Stroke left occipital cortex	Clopidogrel, ezetimibe, nifedipine, pantoprazole, simvastatine, tamsulosine
s2	56	Male	0	ILQ	Stroke right occipital cortex	Acenocoumarol, acetylsalicylic acid, amlodipine, citalopram, metoprolol, perindopril, rosuvastatin
s3	28	Male	-0.1	RHH	Stroke left occipital cortex after tumor resection left frontal cortex	Levetiracetam
s4	58	Male	0	RHH	Stroke left occipital cortex	Clopidogrel
s5	71	Male	0	ILQ	Stroke right occipital cortex	Simvastatin, apixaban, levetiracetam, hydrochlorothiazide, digoxin, losartan, tramadol
s6	57	Male	-0.1	LHH	Stroke right occipital cortex	Metoprolol, pantoprazole, rosuvastatin, lisinopril, desloratadine
s7	68	Male	0	RHH	Stroke left occipital cortex	Acetylsalicylic acid, simvastatin
s8	73	Male	0	LHH	Stroke right occipital cortex	Clopidogrel, losartan, simvastatin
s9	74	Male	0	LHH	Stroke right occipital cortex	Perindopril, rosuvastatin, clopidogrel, hydrochlorothiazide, amitriptyline, pantoprazole
s10	51	Female	0	LHH	Stroke right occipital cortex	Amlodipine, lisinopril
s11	64	Male	0	LHH	Stroke right occipital cortex	Bisoprolol, eplerenone, perindopril, atorvastatin, acetylsalicylic acid
s12	79	Male	0	LHH	Stroke right occipital cortex	Atorvastatin, acetylsalicylic acid
s13	49	Female	0	LHH	Stroke right occipital cortex	Amlodipine, candesartan, spironolactone
s14	46	Male	0.05	RHH	Stroke left occipital cortex	Acenocoumarol, formoterol, levocetirizine
s15	49	Female	-0.1	SRQ	Stroke left occipital cortex	Clopidogrel, simvastatin
s16	63	Male	0	LHH	Stroke right occipital cortex	Atorvastatin, clopidogrel, amlodipine, lisinopril
s17	57	Male	0	RHH	Stroke left occipital cortex	Simvastatin, clopidogrel, pantoprazole
s18	67	Male	0	ILQ	Stroke right occipital cortex	Clopidogrel, pantoprazole, pravastatin
s19	55	Female	0	SRQ	Stroke left occipital cortex	Valsartan
s20	28	Male	-0.2	LHH	Stroke right occipital cortex after resection arteriovenous malformation	Mebeverine, fexofenadine

Table S1. Patient demographics. VA = visual acuity (in logMAR); LHH = (partial) left homonymous hemianopia; RHH = (partial) right homonymous hemianopia; ILQ = inferior left homonymous quadrantanopia; SRQ = superior right homonymous quadrantanopia.

Figure S1. Converted standard automated perimetry (SAP) and normalized pupil perimetry visual field heatmaps (across color conditions) per subject for Experiment 1. The blue wedges in the pupil perimetry maps represent missing trials.

Table S2. Paired student's t-test comparing pupil response amplitudes across color conditions of Experiment 1. Significant results highlighted in bold font.

	Equiluminant yellow	*Cyan*	*White*
Yellow	t_{18} = 2.91, **p = 0.009**	t_{18} = 0.54, p = 0.60	t_{18} = -0.51, p = 0.62
Equiluminant yellow	-	t_{18} = -1.62, p = 0.12	t_{18} = -3.11, **p = 0.006**
Cyan	-	-	t_{18} = -0.69, p = 0.50

Table S3. Paired student's t-test comparing pupil response amplitudes across conditions of Experiment 2. Significant results highlighted in bold font.

	Dark yellow	*Bright multicolor*	*Dark multicolor*
Bright yellow	t_{15} = 4.60, **p < 0.001**	t_{15} = 0.78, p = 0.45	t_{15} = 4.56, **p < 0.001**
Dark yellow	-	t_{15} = -3.62, **p = 0.002**	t_{15} = -0.97, p = 0.35
Bright multicolor	-	-	t_{15} = 3.65, **p = 0.002**

Table S4. Paired student's t-test comparing discriminative power (AUC) across conditions of Experiment 2. Significant results highlighted in bold font.

	Dark yellow	*Bright multicolor*	*Dark multicolor*
Bright yellow	t_{15} = 2.07, p = 0.57	t_{15} = 2.80, **p = 0.014**	t_{15} = 2.02, p = 0.61
Dark yellow	-	t_{15} = -0.24, p = 0.82	t_{15} = -1.12, p = 0.28
Bright multicolor	-	-	t_{15} = -0.59, p = 0.57

Figure S2. Converted standard automated perimetry (SAP) and normalized pupil perimetry visual field heatmaps (across color conditions) per subject for Experiment 2. The blue wedges in the pupil perimetry maps represent missing trials.

Diagnostic performance of pupil perimetry in detecting hemianopia under standard and virtual reality viewing conditions

Portengen BL
Imhof SM
Naber M*
Porro GL*

* These authors contributed equally to this work.

7.1 Abstract

PURPOSE: To determine the diagnostic performance and reliability of two pupil perimetry (PP) methods in homonymous hemianopia.

METHODS: This cross-sectional monocenter cohort study performed gaze-contingent flicker PP (gcFPP) and a virtual reality version of gcFPP (VRgcFPP) twice on separate occasions in all patients suffering from homonymous hemianopia due to neurological impairment. The main outcomes were (1) test accuracy and (2) test-retest reliability: (1) was measured through area under the receiver operating characteristics curve (AUC) and percentile rank score calculation of (VR)gcFPP results with comparators being SAP and healthy controls, respectively; (2) was evaluated by comparing tests 1 and 2 of both methods within subjects.

RESULTS: Both gcFPP and VRgcFPP were performed in 15 patients (12 males, M_{Age} = 57, SD_{Age} = 15) and 17 controls (6 males, M_{Age} = 53, SD_{Age} = 12). Mean test accuracy was good when compared to SAP (gcFPP: 0.86 ± 0.09 (mean ± SD); VRgcFPP: 0.71 ± 0.13) and high compared to controls (percentile rank gcFPP: 92 ± 13; percentile rank VRgcFPP: 96 ± 15). A high test-retest reliability was found for the proportion intact versus damaged visual field (gcFPP r = 0.95, P < .001, VRgcFPP r = 1.00, P < .001).

CONCLUSIONS: Overall, these results can be summarized as follows: (1) the comparison of pupil response amplitudes between intact versus damaged regions per patient indicate that gcFPP allows for cleaner imaging of intact versus damaged visual field regions than VRgcFPP, (2) the comparisons of average differences in intact versus damaged amplitudes between patients and controls demonstrate high diagnostic performance of both gcFPP and VRgcFPP, and (3) the test-retest reliabilities confirm that both gcFPP and VRgcFPP reliably and consistently measure defects inhomonymous hemianopia.

7.2 Introduction

Standard automated perimetry (SAP) is the current gold standard for visual field (VF) examination, but not always suited for the evaluation of the VF in neurologically impaired patients (Goodwin 2014). Neurologic VF defects (VFD) (e.g., homonymous hemianopia) result in bilateral vision loss affecting the contralateral VF, typically respecting the vertical midline. Such VF loss is relatively easy to simulate (Ghate et al. 2014). Moreover, SAP methods suffer from high test-retest variability (Artes et al. 2002, Piltz & Starita 1990). The poor reproducibility might be caused by retinotopic displacement of small stimuli due to the fixational jitter or microsaccades, and learning and fatigue effects (Maddess 2014, Numata et al. 2017, Wall et al. 2009), which are especially problematic in patients with neurological impairment. There are few alternative solutions that address the above-described problems.

One alternative is pupil perimetry (PP; see Harms 1949), which consists of the measurement of pupillary responses to light stimuli as a measure of the degree of visual attention and consciousness (Naber, Alvarez & Nakayama 2013, Naber, Frässle & Einhäuser 2011, Strauch et al. 2022), that is visual sensitivity. Simply put, pupil responses are strong when a stimulus is shown in the intact VF and weak when the damaged VF is stimulated. As early as 1975, the PP method has been hypothesized to have merit in the assessment of individuals with neurological impairment due to its simple, noninvasive and objective nature (Cibis, Campos & Aulhorn 1975). Over the years, multiple iterations of PP have tried to improve diagnostic performance in this patient population (Asakawa & Ishikawa 2019, Kardon, Kirkali & Thompson 1991, Maeda et al. 2017, Naber et al. 2018, Rajan, Bremner & Riordan-Eva 2002, Schmid et al. 2005, Skorkovská et al. 2009, Takizawa et al. 2018). To the best of our knowledge, gaze-contingent flicker PP (gcFPP) reports the highest diagnostic performance in neurologically impaired patients (Naber et al. 2018), and since this initial publication, improvements of this method have been tested on healthy controls (Portengen et al. 2022, Portengen et al. 2023, Portengen et al. 2021). These improvements included (1) adding color contrast between stimulus and background to evoke stronger pupil responses, (2) scaling stimuli as a function of eccentricity to take into account the cortical magnification factor, and (3) enhancements to pupil response analyses such as better on-line blink detection and trial repetitions rather than trial rejections. However, whether these improvements have led to improvements in diagnostic performance remains to be validated in patients.

Another development in the gcFPP method is the novel implementation of a head-mounted device with virtual reality (VR) technology, dubbed VRgcFPP (Portengen et al. 2022). VR applications in the ophthalmic practice are relatively new, but promising (Alawa et al. 2021, Deiner, Damato & Ou 2020, Gestefeld et al. 2020, He et

al. 2019, Mees et al. 2020, Razeghinejad et al. 2021, Tsapakis et al. 2017, Tsapakis et al. 2018). Particularly, VR seems to be preferred over screen-based approaches by patients (Soans et al. 2021). VRgcFPP has shown merit in (healthy) young children due to its free range of movement, engaging visual task, and reliable pupil measurements with a built-in eye tracker (Portengen et al. 2022). Its ability to assess the visual field, however, has not yet been evaluated in patients with homonymous hemianopia. Also, the test-retest reliability of (VR)gcFPP has so far not been studied.

The current study aims to explore the diagnostic performance of an improved version of pupil perimetry (i.e., gcFPP) and a novel virtual reality-based pupil perimetry method (i.e., VRgcFPP) in detecting visual field defects of patients suffering from neurological impairment by assessing sensitivity and test-retest reliability.

7.3 Methods

7.3.1 Study design and participants

This cross-sectional cohort study included patients suffering from absolute homonymous visual field defects due to neurological impairment who completed both a gcFPP and a VRgcFPP test on two separate occasions. Information on demographic characteristics included age, sex, visual acuity, diagnosis and medication. The study also included healthy controls who were tested once. The latter group were asked about any ophthalmologic problems prior to participation but did not receive ophthalmologic screening.

The study was approved by the local ethical committee of Utrecht University (protocol number 20-238) and conformed to the ethical considerations of the Declaration of Helsinki. Participants gave written informed consent prior to participation. Furthermore, they received (financial) reimbursement for participation (€12,50 per hour) and travel costs.

7.3.2 Apparatus and stimuli

The apparatus used for the presentation of stimuli and measurement of pupillary responses have been described extensively in previous studies. For a more detailed description of apparatus and stimuli, please refer to (Portengen, Porro et al. 2022, Portengen et al. 2023) for the gcFPP method and (Portengen, Naber et al. 2022) for the VRgcFPP method.

The stimuli consisted of black-yellow flickering wedges presented across 44 stimulus locations in randomized order within the inner 60 degrees field of vision, superimposed on a dark blue background (30% luminance for an optimal trade-off between luminance and color contrast; see (Portengen et al. 2023) and positioned around a red fixation target (see ***Figure 1***). The gaze-contingent stimulus presentation (i.e., the eye tracking software follows the subject's direction of gaze fixation and updates the position of the flickering stimuli real-time to reflect changes in direction of gaze) ensured stable retinotopic stimulation despite the presence of saccades (Naber et al. 2018). A single test consisted of 220 seconds (44 stimulus locations * 5 seconds per location), excluding instruction and calibration, which consisted of a 5-point calibration grid. During the gcFPP method, only the right eye was measured while the left eye was occluded. For the VRgcFPP method, pupils were measured binocularly to estimate convergence and thus focus of depth in the VR environment. However, only data of the right eye were analyzed to allow comparison with the non-VR gcFPP version. The dual OLED screens allowed a sense of depth to prevent VR-induced simulator sickness.

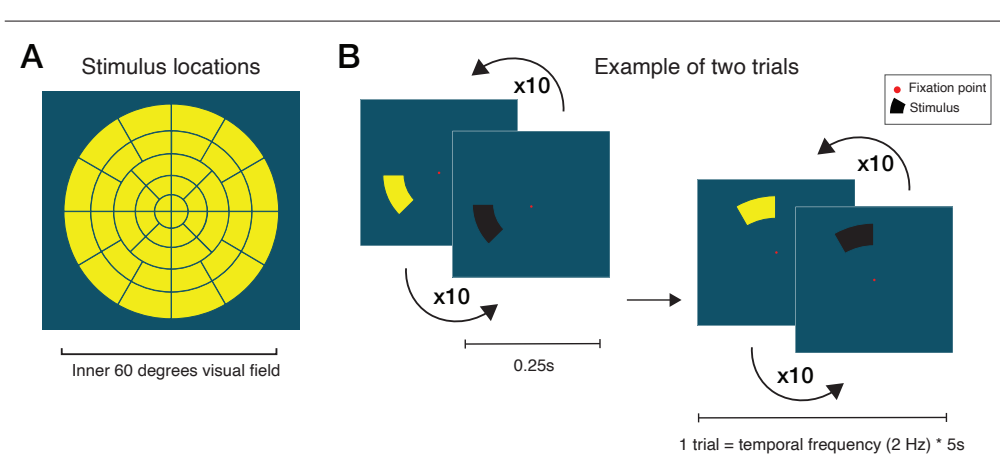

Figure 1. Panel (a) depicts all 44 stimulus locations located within the inner 60 degrees of the visual field used in both experiments. An example of two consecutive trials is shown in (b). A trial consisted of a single stimulus location flickering yellow-and-black at a 2 Hz rate for 5 seconds in a gaze-contingent manner.

7.3.3 Analysis

The pupillometry analysis was identical in both pupil perimetry methods. First stimulus location onsets functioned as start events for the event-related analysis of the continuous pupil output of the integrated eye tracker. From the pupil data, blink episodes were detected and removed using an automated detection blink method by looking for crossings of a speed threshold of 4 standard deviations (SD) above the mean. The removed blink epochs were interpolated with a cubic method. Next, pupil data were baseline-corrected to

enhance inter-subject comparability. A high-pass Butterworth filter (3rd order, 1 Hz cut-off frequency) and a low-pass filter (3rd order, 10 Hz cut-off frequency) followed to remove slow pupil diameter changes and high frequency noise, respectively. Pupil traces per stimulus location were converted to power values in the frequency domain using a fast Fourier transform. The power at 2 Hz reflected the pupil oscillation amplitude and served as the main dependent variable per stimulus location (i.e., 44 amplitudes per participant and per perimetry method). This measurement will henceforth be referred to as the pupil response amplitude. The amplitudes were z-normalized to allow comparison across participants. Z-normalization was accomplished by first calculating the mean and standard deviation of pupil amplitudes across locations per participant and perimetry method. Next, each of the 44 amplitudes per participant were subtracted with the mean and divided by the standard deviation to end up with z-scored amplitudes.

The most recent standard automated perimetry (SAP) results served as ground truth to create subjective perimetry maps per subject; all stimulus locations were scored (0 = damaged, 1 = intact) to create a dichotomous outcome for analysis. The scores were based on significant Total Deviation p-values in the case of HFA 30-2 and the V4 stimulus pattern in the case of Goldmann perimetry and were given while blinded to the pupil perimetry results.

To control for any potential over- or underestimation of VFDs, z-score normalized pupil response amplitudes per stimulus location and per subject were adjusted for supero-inferior and temporo-nasal visual field anisotropies (i.e. physiological increases in pupil responsiveness in the center of the VF as opposed to decreased responses in the periphery, and stronger pupil responses in the upper and temporal than lower and nasal VFs; Hong, Narkiewicz & Kardon 2001, Naber, Alvarez & Nakayama 2013, Naber et al. 2018, Sabeti, James & Maddess 2011, Schmid, Wilhelm & Wilhelm 2000, Skorkovská et al. 2014, Tan et al. 2001). The mean differences in the z-score normalized pupil response amplitudes between the upper-lower and temporal-nasal visual fields of healthy controls were subtracted from the z-score normalized pupil response amplitudes of participants for upper and temporal regions, respectively.

Performance was evaluated using three statistical outcomes. The first method calculated the area under the curve (AUC) of the receiver operating characteristics (ROC) with visibility as dichotomous independent variable that splitted the distribution of 44 pupil response amplitudes, as the dependent variable, in intact (visible) versus damaged (not visible) regions (stimulus) conditions. An AUC score of more than 0.5 indicates that pupil response amplitudes were stronger for intact than damaged regions, whereas an AUC of 1.0 indicates that the amplitudes enabled perfect classification between intact versus damaged regions. To inspect which regions linked to weaker versus strong amplitudes, normalized two-dimensional pupil sensitivity maps were created as graphical visualizations of visual field defects, with black and white regions indicating weakest versus strongest pupil responses (i.e., negative and positive z-scores), respectively. The second method compared pupil perimetry results of patients to healthy controls. The difference between pupil response amplitudes in the intact versus damaged visual field (as indicated by SAP) of patients were plotted against the difference in pupil response amplitude of all healthy controls in corresponding visual field locations. The percentile rank (0 to 100) of the patient's pupil response regarding the distribution within healthy controls could then be extrapolated, with 0 versus 100 percentile scores indicating that differences in amplitudes between intact versus damaged in patients were either smaller or larger when compared to healthy controls. In other words, a percentile score of above 50 means that patients showed much stronger differences in pupil response amplitudes across the visual field than healthy controls, allowing for the statistical detection of visual field defects through the inspection of amplitudes. Thirdly, test-retest reliability between the first and second measurement was estimated using Pearson's correlation coefficients (*r*) of the proportion of z-normalized pupil response amplitudes between intact versus damaged visual fields per stimulus location per subject. The proportion was calculated to mitigate any changes in the variability in pupil response amplitudes across sessions (e.g., a patient may show much weaker responses in a second session due to fatigue). The calculation consisted of first subtracting the amplitude averaged across damaged regions from intact regions, and then dividing this by the amplitude averaged across damaged regions. A proportion value between 0 and 1.0 indicates that z-normalized pupil response amplitudes were stronger for intact than damaged regions in both sessions.

Paired double-sided t-tests (post-hoc tests) determined statistical significance of discriminative performance (intact versus damaged or patient versus control) of pupil perimetry by comparing whether the derived AUC values or percentile rank scores differed significantly from 0.5 or 50 respectively (baseline for no discriminative power) or whether the AUC values differed between pupil perimetry methods.

All analyses were performed using MATLAB software (version R2021b, MathWorks, Natick, MA). Raw data and analyses were made publicly available on open science framework: https://osf.io/6tcva.

7.4 Results

7.4.1 Exemplary subject

The results of an exemplary subject bundled in ***Figure 2*** serve to illustrate how the general diagnostic performance was evaluated. First, pupil responses to on- and offsets of the 2 Hz flickering stimuli were inspected. Pupil size as a function of time per trial, averaged across intact (black line) and damaged (red line) stimulus locations, are plotted in ***Figure 2A***. Then, within-subject diagnostic accuracy was evaluated by comparing z-normalized pupil response amplitudes per stimulus location to the subject's SAP result (see ***Figure 2B***). The AUC of 0.97 indicates that gcFPP could differentiate damaged from intact VFs very well. The discrimination of a patient from a healthy subject through the inspection of the size of the average difference between intact and damaged VFs is another indicator for diagnostic performance. As such, the difference between z-normalized pupil response amplitudes for the intact and damaged VF locations (according to SAP) of a patient was compared to the difference in pupil response amplitudes of the corresponding VF locations of all 17 healthy controls (see ***Figure 2C***). The difference in pupil response amplitudes of the exemplary subject was larger than the difference in all healthy controls (percentile rank score = 100).

Next, test-retest reliability was evaluated by reinviting patients and repeating the tests. The z-normalized pupil response amplitudes across all 44 stimulus locations for the two separate testing occasions were plotted against each other (***Figure 2D***). The correlation of pupil responses to the stimulus locations across test 1 and 2 for the exemplary subject was fairly strong (r = 0.76).
Lastly, two-dimensional VF heatmaps of normalized pupil response amplitudes were plotted for tests 1 and 2 of the gcFPP and the VRgcFPP methods for comparison with SAP results (***Figure 2E***).
Figure 2F portrays the dichotomous (binary) measures which were based on SAP to create the binary categories of intact versus damaged regions. The imaged patterns of SAP and pupil perimetry roughly matched, especially for gcFPP (see ***Supplementary Figure S1*** for the results of gcFPP, VRgcFPP and converted SAP for all patients).

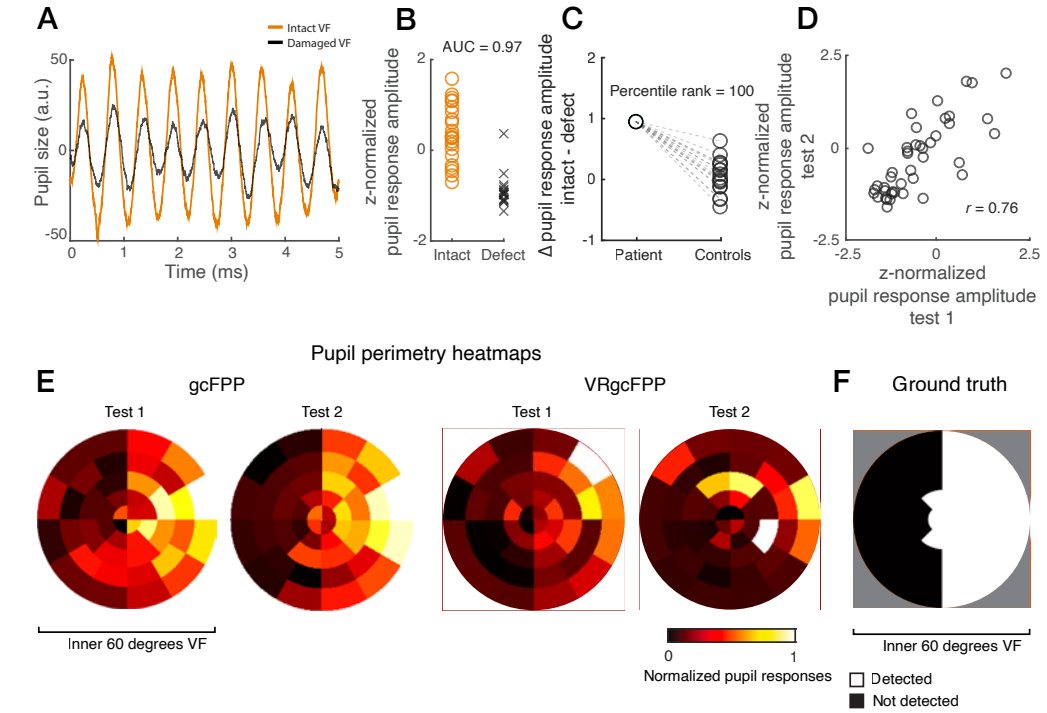

Figure 2. Results of exemplary subject. Panel (A) shows the average pupil size (in arbitrary units) in response to stimuli located in the intact (red/yellow) and damaged (black) visual field (VF) over time. Z-normalized pupil response amplitudes per intact (black circle) and defect (red crosses) VF location are plotted in (B). The graph in (C) plots the difference in pupil response amplitudes between the intact and defect visual field locations and the difference in the corresponding visual fields of all controls. The z-normalized pupil response amplitudes for test 1 and 2 of all 44 stimulus locations are plotted in (D), on which the test-retest reliability (Pearson's correlation coefficient r) was based. Discriminability between patient and controls was calculated using the area under the curve of the receiver operating characteristics (AUC). Panel (E) shows two-dimensional heatmaps of normalized pupil responses of the inner 60 degrees of the VF indicating pupil sensitivities per stimulus location (weak sensitivity: red to black, strong sensitivity: yellow to white) for the gcFPP and VRgcFPP methods. Lastly, (F) shows the converted standard automated perimetry result which served as a binary division (black = damaged VF, white = intact VF) for (A), (B), and (C).

7.4.2 Overall diagnostic performance across patients

This study aimed to assess diagnostic performance of the gcFPP and the novel VRgcFPP methods in CVI patients with hemianopic VFDs. 15 patients (12 males, M_{Age} = 57, SD_{Age} = 15) and 17 controls (6 males, M_{Age} = 53, SD_{Age} = 12) were included. Tests 1 and 2 for the patients were on average 160 days (Mdn_{Days} = 159, SD_{Days} = 158) apart. See the ***Supplementary Table S1*** for all patient characteristics. As mentioned previously, within-subject diagnostic accuracy was evaluated first (***Figure 3A***). When averaging the results across all patients, the gcFPP method (AUC test 1: M = 0.79, SD = 0.11, t_{14} = 4.97, P < .001, AUC

test 2: M = 0.86, SD = 0.09, t_{14} = 6.75, P < .001) performed better than the VRgcFPP method (AUC test 1: M = 0.71, SD = 0.13, t_{14} = 5.80, P < .001, AUC test 2: M = 0.67, SD = 0.15, t_{14} = 4.21, P = .001), and this difference was statistically significant (t_{14} = 2.34, P = .04). More importantly, ***Figure 3B*** shows that gcFPP and VRgcFPP performed comparably in discriminating patients from healthy controls (Percentile rank score gcFPP: M = 92, SD = 13, t_{14} = 12.29, P < .001; Percentile rank score VRgcFPP: M = 96, SD = 15, t_{14} = 11.93, P < .001). Each method's reliability was assessed by comparing pupil response amplitudes across tests 1 and 2 of gcFPP and VRgcFPP, respectively (see ***Figure 3C***). A moderate-to-low within-subject correlation (gcFPP

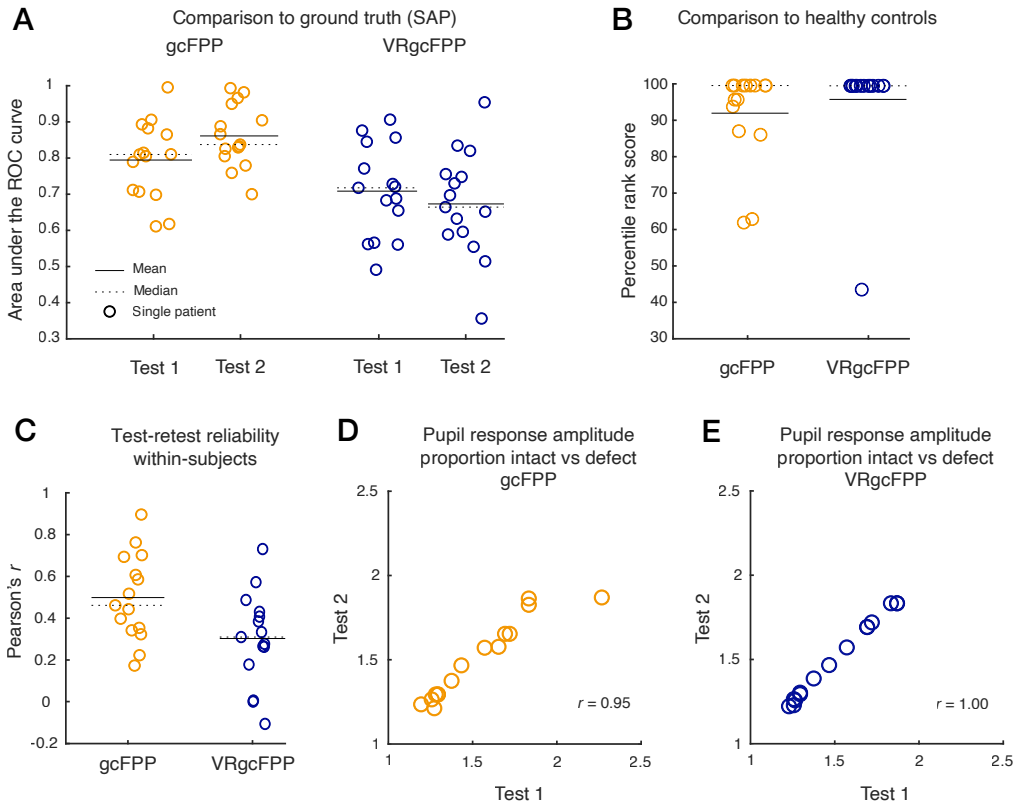

Figure 3. Diagnostic performance of the gcFPP (orange) and VRgcFPP (blue) methods. Panel (A) shows the area under curve (AUC) of the receiver operating characteristics (ROC) per patient, method and testing time when compared to the ground truth (i.e. standard automated perimetry [SAP]). The difference in pupil amplitudes between intact and damaged regions were also compared to healthy controls per method in panel (B) by calculating the percentile rank of pupil responses of patients within a healthy distribution. Test-retest reliability (Pearson's correlation coefficient r) of pupil response amplitudes were evaluated across all visual field regions per subject (C). Similarly, test-retest scores were examined for the proportion pupil response amplitude to stimuli presented in intact versus damaged regions across patients for the gcFPP (D) and the VRgcFPP method (E).

M = 0.50, SD = 0.21; VRgcFPP M = 0.30, SD = 0.22) indicates pupil responses still vary despite very comparable testing conditions. However, when considering the proportion of pupil response amplitudes in intact versus damaged visual fields, which mitigates between-session variabilities in pupil responsiveness, a very high test-retest reliability is found (gcFPP r = 0.95, P < .001, VRgcFPP r = 1.00, P < .001; see ***Figure 3D*** and ***3E***). Overall, these results can be summarized as follows: (1) the comparison of pupil response amplitudes between intact versus damaged regions per patient indicate that gcFPP allows for cleaner imaging of intact versus damaged visual field regions than VRgcFPP, (2) the comparisons of average differences in intact versus damaged amplitudes between patients and controls demonstrate high diagnostic performance of both gcFPP and VRgcFPP, and (3) the test-rest reliabilities confirm that both gcFPP and VRgcFPP reliably and consistently measures defects in neurologically impaired patients.

7.5 Discussion

We assessed the diagnostic performance of gaze-contingent flicker pupil perimetry (gcFPP) in an original campimetry-like setting and a virtual reality setting (VRgcFPP) in a cohort of adult patients suffering from homonymous visual field defects (VFD) due to neurological impairment. Compared to other pupil perimetry methods (Asakawa & Ishikawa 2019, Cibis, Campos & Aulhorn 1975, Kardon, Kirkali & Thompson 1991, Maeda et al. 2017, Rajan, Bremner & Riordan-Eva 2002, Schmid et al. 2005, Skorkovská et al. 2009, Takizawa et al. 2018), this study reports the highest diagnostic accuracy so far. Other methods, such as Matrix frequency doubling technology perimetry or multifocal visual evoked potentials, have been introduced in an effort to accurately and reliably evaluate VFs in neurologically impaired patients (Gedik, Akman & Akova 2007, Goto et al. 2016, Handley, Šuštar & Tekavčič Pompe 2021, Jariyakosol et al. 2021, Sousa et al. 2017, Taravati et al. 2008, Wall, Neahring & Woodward 2002, Yoon et al. 2012), but all exhibited caveats which retained it from adoption in common practice or simply did not reach the diagnostic accuracy of SAP. The current methods' diagnostic performances and ease of use, warrants it as a valuable addition to VF assessment when SAP is unproductive (e.g. the patient is too young, neurologically impaired or suspected of malingering).

Moderate repeatability of pupil response amplitudes between

stimulus locations supports the notion that the pupil expresses baseline variability across time evoked by many factors that modulate cognitive and (para-) sympathetic nervous systems (Binda & Murray 2015, Mathôt et al. 2018, Naber, Alvarez & Nakayama 2013, Naber & Nakayama 2013, Strauch et al. 2022). However, a stronger test-retest reliability (or low test-retest variability) is found for the relative increase in response amplitudes for intact versus damaged (i.e., proportion) visual fields across all patients. This may indicate that the objective pupil perimetry method is more reliable in diagnosing large within-subject deviations in sensitivity across the visual field than SAP, which have been found to have significant intertest threshold variability (Artes et al. 2002, Piltz & Starita 1990). Importantly, half of the patients were tested after a year and the other half after a few days. This dissociation does not impact test-retest reliability. Although only a small cohort was tested, it contributes to the notion that the pupil is a robust measure of visual field sensitivity.
Pupil perimetry shows similar potential in diseases such as age-related macular degeneration (Kelbsch et al. 2020, Rai et al. 2022), diabetic retinopathy (Sabeti et al. 2022) and retinal and optic nerve diseases (Ajasse et al. 2022), but shows varying performance in glaucoma (Naber et al. 2018, Totsuka et al. 2019), even when using a head mounted perimeter (Asakawa & Shoji 2019, Mees et al. 2020). However, it may be argued that pupil perimetry could be epileptogenic in the more at-risk neurologically impaired patient due to the flickering stimuli. Luckily, a recent paper shows that, despite the flickering stimuli used in pupil perimetry, it is even possible to assess patients with epilepsy without inducing seizures although this method discriminated patients from controls with considerably lower performance (Ali et al. 2022).

The importance of assessing the VF in young and neurologically impaired individuals and the poor reliability of SAP in this population (Goodwin 2014, Nuijts et al. 2022, Portengen et al. 2020) stress the need for an objective alternative. The (VR)gcFPP methods show promise by capably distinguishing patients from healthy controls. Interestingly, the VR method was not as accurate as its gcFPP counterpart. The latter used a more sophisticated eye-tracker, possibly explaining the better signal-to-noise ratio as evident in the visual field heatmaps (see Supplementary Figure S1). In other words, VRgcFPP is a capable screening method to investigate whether an individual suspected of a VFD deviates from healthy controls, but it is difficult to pinpoint the exact location of the defect.

The non-VR version will produce more promising results for the latter. This does not mean that VRgcFPP cannot be of use in practice. In fact, by changing the stimulus locations to, for example, only four quadrants, a very rough though fast visual field estimate can be realized for screening purposes. Additionally, the introduction of a small gap between stimulus locations might facilitate a more accurate comparison between results from pupil perimetry and current SAP methods by providing a similar step in sensitivity.

This is not the first time that head-mounted VR technology is harnessed in an attempt to improve feasibility of VF assessment (Alawa et al. 2021, He et al. 2019, Kimura, Matsumoto & Nomoto 2019, Mees et al. 2020, Razeghinejad et al. 2021, Soans et al. 2021, Tsapakis et al. 2017). Despite its many advantages, this relatively young technique remains to be perfected. Future development may lead to the implementation of eye-trackers with better precision to reduce noise and subsequently increase accuracy.

This study is limited by the use of retrospectively gathered (most recent) perimetry results from varying perimeters (i.e. Goldmann and HFA). Prospective SAP testing with one perimetry method would allow for better comparisons. Another limitation consists of the binocular testing during VRgcFPP as it might cause issues in patients unable to accommodate. It is currently not possible to stimulate only one eye in the virtual reality environment, leading to the measurement of combined direct and consensual responses. A future version enabling monocular testing might increase diagnostic accuracy.

7.6 Conclusion

To summarize, gcFPP and VRgcFPP are fast and reliable methods with robust measurements. The VRgcFPP method in particular is cheap and offers a mobile solution, at the sacrifice of some accuracy, for those patients unable to restrict their head movements for prolonged. We recommend the use of these two pupil perimetry methods as complementary tools to the standard visual field work-up of neurologically impaired individuals.

7.7 References

Ajasse, S., Vignal-Clermont, C., Mohand-Saïd, S., Coen, C., Romand, C., & Lorenceau, J. (2022). One minute Multiple Pupillary Frequency Tagging test to assess visual field defects. *MedRxiv*, 2022.01.24.22269632. https://doi.org/10.1101/2022.01.24.22269632

Alawa, K. A., Nolan, R. P., Han, E., Arboleda, A., Durkee, H., Sayed, M. S., Aguilar, M. C., & Lee, R. K. (2021). Low-cost, smartphone-based frequency doubling technology visual field testing using a head-mounted display. *British Journal of Ophthalmology, 105*(3), 440–444. https://doi.org/10.1136/bjophthalmol-2019-314031

Ali, E. N., Lueck, C. J., Carle, C. F., Martin, K. L., Borbelj, A., & Maddess, T. (2022). Response characteristics of objective perimetry in persons living with epilepsy. *Journal of the Neurological Sciences, 436*. https://doi.org/10.1016/j.jns.2022.120237

Artes, P. H., Iwase, A., Ohno, Y., Kitazawa, Y., & Chauhan, B. C. (2002). Properties of perimetric threshold estimates from full threshold, SITA standard, and SITA fast strategies. *Investigative Ophthalmology and Visual Science, 43*(8), 2654–2659. https://iovs.arvojournals.org/article.aspx?articleid=2124008

Asakawa, K., & Ishikawa, H. (2019). Pupil fields in a patient with early-onset postgeniculate lesion. In *Graefe's Archive for Clinical and Experimental Ophthalmology* (Vol. 257, Issue 2). https://doi.org/10.1007/s00417-018-4189-0

Asakawa, K., & Shoji, N. (2019). Challenges to detect glaucomatous visual field loss with pupil perimetry. *Clinical Ophthalmology, 13*. https://doi.org/10.2147/OPTH.S217825

Binda, P., & Murray, S. O. (2015). Spatial attention increases the pupillary response to light changes. *Journal of Vision, 15*(2), 1–1. https://doi.org/10.1167/15.2.1

Cibis, G. W., Campos, E. C., & Aulhorn, E. (1975). Pupillary Hemiakinesia in Suprageniculate Lesions. *Archives of Ophthalmology, 93*(12). https://doi.org/10.1001/archopht.1975.01010020954004

Deiner, M. S., Damato, B. E., & Ou, Y. (2020). Implementing and Monitoring At-Home Virtual Reality Oculokinetic Perimetry During COVID-19. In *Ophthalmology* (Vol. 127, Issue 9, p. 1258). Elsevier. https://doi.org/10.1016/j.ophtha.2020.06.017

Gedik, S., Akman, A., & Akova, Y. A. (2007). Efficiency of Rarebit perimetry in the evaluation of homonymous hemianopia in stroke patients. *British Journal of Ophthalmology, 91*(8). https://doi.org/10.1136/bjo.2006.112607

Gestefeld, B., Koopman, J., Vrijling, A., Cornelissen, F. W., & de Haan, G. (2020). Eye tracking and virtual reality in the rehabilitation of mobility of hemianopia patients: a user experience study. *International Journal of Orientation & Mobility, 11*(1). https://doi.org/10.21307/vri-2020-002

Ghate, D., Bodnarchuk, B., Sanders, S., Deokule, S., & Kedar, S. (2014). The ability of healthy volunteers to simulate a neurologic field defect on automated perimetry. *Ophthalmology, 121*(3). https://doi.org/10.1016/j.ophtha.2013.10.024

Goodwin, D. (2014). Homonymous hemianopia: Challenges and solutions. In *Clinical Ophthalmology* (Vol. 8). https://doi.org/10.2147/OPTH.S59452

Goto, K., Miki, A., Yamashita, T., Araki, S., Takizawa, G., Nakagawa, M., Ieki, Y., & Kiryu, J. (2016). Sectoral analysis of the retinal nerve fiber layer thinning and its association with visual field loss in homonymous hemianopia caused by post-geniculate lesions using spectral-domain optical coherence tomography. *Graefe's Archive for Clinical and Experimental Ophthalmology = Albrecht von Graefes Archiv Fur Klinische Und Experimentelle Ophthalmologie, 254*(4), 745–756. https://doi.org/10.1007/s00417-015-3181-1

Handley, S. E., Šuštar, M., & Tekavčič Pompe, M. (2021). What can visual electrophysiology tell about possible visual-field defects in paediatric patients. In *Eye (Basingstoke)* (Vol. 35, Issue 9). https://doi.org/10.1038/s41433-021-01680-1

Harms, H. (1949). Grundlagen, Methodik und Bedeutung der Pupillenperimetrie für die Physiologie und Pathologie des Sehorgans. *Albrecht von Graefes Archiv Für Ophthalmologie Vereinigt Mit Archiv Für Augenheilkunde, 149*(1–3). https://doi.org/10.1007/BF00684506

He, J., Zhang, S., Wu, P., Zhang, Y., Zheng, X., & Zhou, L. (2019, May 1). A Novel Virtual Reality Design of Portable Automatic Perimetry. *IEEE MTT-S 2019 International Microwave Biomedical Conference, IMBioC 2019 - Proceedings.* https://doi.org/10.1109/IMBIOC.2019.8777783

Hong, S., Narkiewicz, J., & Kardon, R. H. (2001). Comparison of Pupil Perimetry and Visual Perimetry in Normal Eyes: Decibel Sensitivity and Variability. *Investigative Ophthalmology & Visual Science, 42*(5), 957–965. https://dx.doi.org/

Jariyakosol, S., Jaru-Ampornpan, P., Manassakorn, A., Itthipanichpong, R., Hirunwiwatkul, P., Tantisevi, V., Somkijrungroj, T., & Rojanapongpun, P. (2021). Sensitivity and specificity of new visual field screening software for diagnosing hemianopia. *Eye and Brain, 13*. https://doi.org/10.2147/EB.S315403

Kardon, R. H., Kirkali, P. A., & Thompson, H. S. (1991). Automated Pupil Perimetry Pupil Field Mapping in Patients and Normal Subjects. *Ophthalmology, 98*(4), 485–496. https://doi.org/10.1016/S0161-6420(91)32267-X

Kelbsch, C., Lange, J., Wilhelm, H., Wilhelm, B., Peters, T., Kempf, M., Kuehlewein, L., & Stingl, K. (2020). Chromatic pupil campimetry reveals functional defects in exudative age-related macular degeneration with differences related to disease activity. *Translational Vision Science and Technology, 9*(6), 5–5. https://doi.org/10.1167/tvst.9.6.5

Kimura, T., Matsumoto, C., & Nomoto, H. (2019). Comparison of head-mounted perimeter (imo®) and Humphrey Field Analyzer. *Clinical Ophthalmology (Auckland, N.Z.), 13*, 501. https://doi.org/10.2147/OPTH.S190995

Maddess, T. (2014). Modeling the relative influence of fixation and sampling errors on retest variability in perimetry. *Graefe's Archive for Clinical and Experimental Ophthalmology, 252*(10), 1611–1619. https://doi.org/10.1007/s00417-014-2751-y

Maeda, F., Kelbsch, C., Straßer, T., Skorkovská, K., Peters, T., Wilhelm, B., & Wilhelm, H. (2017). Chromatic pupillography in hemianopia patients with homonymous visual field defects. *Graefe's Archive for Clinical and Experimental Ophthalmology, 255*(9), 1837–1842. https://doi.org/10.1007/s00417-017-3721-y

Mathôt, S., Fabius, J., Van Heusden, E., & Van der Stigchel, S. (2018). Safe and sensible preprocessing and baseline correction of pupil-size data. *Behavior Research Methods, 50*(1). https://doi.org/10.3758/s13428-017-1007-2

Mees, L., Upadhyaya, S., Kumar, P., Kotawala, S., Haran, S., Rajasekar, S., Friedman, D. S., & Venkatesh, R. (2020). Validation of a Head-mounted Virtual Reality Visual Field Screening Device. *Journal of Glaucoma, 29*(2), 86–91. https://doi.org/10.1097/IJG.0000000000001415

Naber, M., Alvarez, G. A., & Nakayama, K. (2013). Tracking the allocation of attention using human pupillary oscillations. *Frontiers in Psychology, 4*, 919. https://doi.org/10.3389/fpsyg.2013.00919

Naber, M., Frässle, S., & Einhäuser, W. (2011). Perceptual rivalry: Reflexes reveal the gradual nature of visual awareness. *PLoS ONE, 6*(6), e20910. https://doi.org/10.1371/journal.pone.0020910

Naber, M., & Nakayama, K. (2013). Pupil responses to high-level image content. *Journal of Vision, 13*(6), 7–7. https://doi.org/10.1167/13.6.7

Naber, M., Roelofzen, C., Fracasso, A., Bergsma, D. P., van Genderen, M., Porro, G. L., Dumoulin, S. O., & van der Schouw, Y. T. (2018). Gaze-Contingent Flicker Pupil Perimetry Detects Scotomas in Patients With Cerebral Visual Impairments or Glaucoma. *Frontiers in Neurology, 9*(July), 558. https://doi.org/10.3389/fneur.2018.00558

Nuijts, M. A., Stegeman, I., Van Seeters, T., Borst, M. D., Bennebroek, C. A. M., Buis, D. R., Naus, N. C., Porro, G. L., Van Egmond-Ebbeling, M. B., Voskuil-Kerkhof, E. S. M., Pott, J. R., Franke, N. E., De Vos-Kerkhof, E., Hoving, E. W., Schouten-Van Meeteren, A. Y. N., & Imhof, S. M. (2022). Ophthalmological Findings in Youths With a Newly Diagnosed Brain Tumor. *JAMA Ophthalmology, 140*(10), 982–993. https://doi.org/10.1001/JAMAOPHTHALMOL.2022.3628

Numata, T., Maddess, T., Matsumoto, C., Okuyama, S., Hashimoto, S., Nomoto, H., & Shimomura, Y. (2017). Exploring test-retest variability using high-resolution perimetry. *Translational Vision Science and Technology, 6*(5), 8–8. https://doi.org/10.1167/tvst.6.5.8

Piltz, J. R., & Starita, R. J. (1990). Test-retest variability in glaucomatous visual fields. In *American Journal of Ophthalmology* (Vol. 109, Issue 1, pp. 109–110). https://doi.org/10.1016/s0002-9394(14)75602-8

Portengen, B. L., Koenraads, Y., Imhof, S. M., & Porro, G. L. (2020). Lessons Learned from 23 Years of Experience in Testing Visual Fields of Neurologically Impaired Children. *Neuro-Ophthalmology, 44*(6), 361–370. https://doi.org/10.1080/01658107.2020.1762097

Portengen, B. L., Naber, M., Jansen, D., Boomen, C. van den, Imhof, S. M., & Porro, G. L. (2022). Maintaining fixation by children in a virtual reality version of pupil perimetry. *Journal of Eye Movement Research, 15*(3). https://doi.org/10.16910/JEMR.15.3.2

Portengen, B. L., Porro, G. L., Imhof, S. M., & Naber, M. (2022). Comparison of unifocal, flicker, and multifocal pupil perimetry methods in healthy adults. *Journal of Vision, 22*(9), 7. https://doi.org/10.1167/jov.22.9.7

Portengen, B. L., Porro, G. L., Imhof, S. M., & Naber, M. (2023). The Trade-Off Between Luminance and Color Contrast Assessed With Pupil Responses. *Translational Vision Science & Technology, 12*(1), 15–15. https://doi.org/10.1167/TVST.12.1.15

Portengen, B. L., Roelofzen, C., Porro, G. L., Imhof, S. M., Fracasso, A., & Naber, M. (2021). Blind spot and visual field anisotropy detection with flicker pupil perimetry across brightness and task variations. *Vision Research, 178*(October 2020), 79–85. https://doi.org/10.1016/j.visres.2020.10.005

Rai, B. B., Sabeti, F., Carle, C. F., Rohan, E. M., van Kleef, J. P., Essex, R. W., Barry, R. C., & Maddess, T. (2022). Rapid Objective Testing of Visual Function Matched to the ETDRS Grid and Its Diagnostic Power in Age-Related Macular Degeneration. *Ophthalmology Science, 2*(2). https://doi.org/10.1016/j.xops.2022.100143

Rajan, M. S., Bremner, F. D., & Riordan-Eva, P. (2002). Pupil perimetry in the diagnosis of functional visual field loss. *Journal of the Royal Society of Medicine, 95*(10), 498–500. https://doi.org/10.1258/jrsm.95.10.498

Razeghinejad, R., Gonzalez-Garcia, A., Myers, J. S., & Katz, L. J. (2021). Preliminary Report on a Novel Virtual Reality Perimeter Compared with Standard Automated Perimetry. *Journal of Glaucoma, 30*(1), 17–23. https://doi.org/10.1097/IJG.0000000000001670

Sabeti, F., Carle, C. F., Nolan, C. J., Jenkins, A. J., James, A. C., Baker, L., Coombes, C. E., Cheung, V., Chiou, M., & Maddess, T. (2022). Multifocal pupillographic objective perimetry for assessment of early diabetic retinopathy and generalised diabetes-related tissue injury in persons with type 1 diabetes. *BMC Ophthalmology 2022 22:1, 22*(1), 1–13. https://doi.org/10.1186/S12886-022-02382-2

Sabeti, F., James, A. C., & Maddess, T. (2011). Spatial and temporal stimulus variants for multifocal pupillography of the central visual field. *Vision Research, 51*(2), 303–310. https://doi.org/10.1016/J.VISRES.2010.10.015

Schmid, R., Luedtke, H., Wilhelm, B. J., & Wilhelm, H. (2005). Pupil campimetry in patients with visual field loss. *European Journal of Neurology, 12*(8), 602–608. https://doi.org/10.1111/j.1468-1331.2005.01048.x

Schmid, R., Wilhelm, B., & Wilhelm, H. (2000). Nasotemporal asymmetry and contraction anisocoria in the pupillomotor system. *Graefe's Archive for Clinical and Experimental Ophthalmology, 238*(2). https://doi.org/10.1007/PL00007879

Skorkovská, K., Wilhelm, H., Lüdtke, H., & Wilhelm, B. (2009). How sensitive is pupil campimetry in hemifield loss? *Graefe's Archive for Clinical and Experimental Ophthalmology, 247*(7), 947–953. https://doi.org/10.1007/s00417-009-1040-7

Skorkovská, K., Wilhelm, H., Lüdtke, H., Wilhelm, B., & Kurtenbach, A. (2014). Investigation of summation mechanisms in the pupillomotor system. *Graefe's Archive for Clinical and Experimental Ophthalmology, 252*(7), 1155–1160. https://doi.org/10.1007/s00417-014-2677-4

Soans, R. S., Renken, R. J., John, J., Bhongade, A., Raj, D., Saxena, R., Tandon, R., Gandhi, T. K., & Cornelissen, F. W. (2021). Patients Prefer a Virtual Reality Approach Over a Similarly Performing Screen-Based Approach for Continuous Oculomotor-Based Screening of Glaucomatous and Neuro-Ophthalmological Visual Field Defects. *Frontiers in Neuroscience, 15*. https://doi.org/10.3389/fnins.2021.745355

Sousa, R. M., Oyamada, M. K., Cunha, L. P., & Monteiro, M. L. R. (2017). Multifocal visual evoked potential in eyes with temporal hemianopia from chiasmal compression: Correlation with standard automated perimetry and OCT findings. *Investigative Ophthalmology and Visual Science, 58*(11). https://doi.org/10.1167/iovs.17-21529

Strauch, C., Wang, C.-A., Einhäuser, W., Van der Stigchel, S., & Naber, M. (2022). Pupillometry as an integrated readout of distinct attentional networks. *Trends in Neurosciences, 0*(0). https://doi.org/10.1016/j.tins.2022.05.003

Takizawa, G., Miki, A., Maeda, F., Goto, K., Araki, S., Yamashita, T., Ieki, Y., Kiryu, J., & Yaoeda, K. (2018). Relative Afferent Pupillary Defects in Homonymous Visual Field Defects Caused by Stroke of the Occipital Lobe Using Pupillometer. *Neuro-Ophthalmology, 42*(3). https://doi.org/10.1080/01658107.2017.1367012

Tan, L., Kondo, M., Sato, M., Kondo, N., & Miyake, Y. (2001). Multifocal pupillary light response fields in normal subjects and patients with visual field defects. *Vision Research, 41*(8), 1073–1084. https://doi.org/10.1016/S0042-6989(01)00030-X

Taravati, P., Woodward, K. R., Keltner, J. L., Johnson, C. A., Redline, D., Carolan, J., Huang, C. Q., & Wall, M. (2008). Sensitivity and specificity of the humphrey matrix to detect homonymous hemianopias. *Investigative Ophthalmology and Visual Science, 49*(3). https://doi.org/10.1167/iovs.07-0248

Totsuka, K., Asakawa, K., Ishikawa, H., & Shoji, N. (2019). Evaluation of Pupil Fields Using a Newly Developed Perimeter in Glaucoma Patients. Current *Eye Research*, 44(5). https://doi.org/10.1080/02713683.2018.1562078

Tsapakis, S., Papaconstantinou, D., Diagourtas, A., Droutsas, K., Andreanos, K., Moschos, M. M., & Brouzas, D. (2017). Visual field examination method using virtual reality glasses compared with the humphrey perimeter. *Clinical Ophthalmology, 11*, 1431–1443. https://doi.org/10.2147/OPTH.S131160

Tsapakis, S., Papaconstantinou, D., Diagourtas, A., Kandarakis, S., Droutsas, K., Andreanos, K., & Brouzas, D. (2018). Home-based visual field test for glaucoma screening comparison with Humphrey perimeter. *Clinical Ophthalmology, 12*, 2597–2606. https://doi.org/10.2147/OPTH.S187832

Wall, M., Neahring, R. K., & Woodward, K. R. (2002). Sensitivity and specificity of frequency doubling perimetry in neuro-ophthalmic disorders: A comparison with conventional automated perimetry. *Investigative Ophthalmology and Visual Science, 43*(4).

Wall, M., Woodward, K. R., Doyle, C. K., & Artes, P. H. (2009). Repeatability of automated perimetry: A comparison between standard automated perimetry with stimulus size III and V, matrix, and motion perimetry. *Investigative Ophthalmology and Visual Science, 50*(2), 974–979. https://doi.org/10.1167/iovs.08-1789

Yoon, M. K., Hwang, T. N., Day, S., Hong, J., Porco, T., & McCulley, T. J. (2012). Comparison of Humphrey Matrix frequency doubling technology to standard automated perimetry in neuro-ophthalmic disease. *Middle East African Journal of Ophthalmology, 19*(2), 211–215. https://doi.org/10.4103/0974-9233.95254

7.8 Supplementary material

Patient	Age	Gender	VA with correction (logMAR)	Days between tests	Diagnosis	Medication
s1	65	Male	-0.1	RHH	Stroke left occipital cortex	Clopidogrel, ezetimibe, nifedipine, pantoprazole, simvastatine, tamsulosine
s2	56	Male	0	ILQ	Stroke right occipital cortex	Acenocoumarol, acetylsalicylic acid, amlodipine, citalopram, metoprolol, perindopril, rosuvastatin
s3	28	Male	-0.1	RHH	Stroke left occipital cortex after tumor resection left frontal cortex	Levetiracetam
s4	58	Male	0	RHH	Stroke left occipital cortex	Clopidogrel
s5	71	Male	0	ILQ	Stroke right occipital cortex	Simvastatin, apixaban, levetiracetam, hydrochlorothiazide, digoxin, losartan, tramadol
s6	57	Male	-0.1	LHH	Stroke right occipital cortex	Metoprolol, pantoprazole, rosuvastatin, lisinopril, desloratadine
s7	68	Male	0	RHH	Stroke left occipital cortex	Acetylsalicylic acid, simvastatin
s8	73	Male	0	LHH	Stroke right occipital cortex	Clopidogrel, losartan, simvastatin
s9	74	Male	0	LHH	Stroke right occipital cortex	Perindopril, rosuvastatin, clopidogrel, hydrochlorothiazide, amitriptyline, pantoprazole
s10	51	Female	0	LHH	Stroke right occipital cortex	Amlodipine, lisinopril
s11	64	Male	0	LHH	Stroke right occipital cortex	Bisoprolol, eplerenone, perindopril, atorvastatin, acetylsalicylic acid
s12	79	Male	0	LHH	Stroke right occipital cortex	Atorvastatin, acetylsalicylic acid
s13	49	Female	0	LHH	Stroke right occipital cortex	Amlodipine, candesartan, spironolactone
s14	46	Male	0.05	RHH	Stroke left occipital cortex	Acenocoumarol, formoterol, levocetirizine
s15	49	Female	-0.1	SRQ	Stroke left occipital cortex	Clopidogrel, simvastatin
s16	63	Male	0	LHH	Stroke right occipital cortex	Atorvastatin, clopidogrel, amlodipine, lisinopril
s17	57	Male	0	RHH	Stroke left occipital cortex	Simvastatin, clopidogrel, pantoprazole
s18	67	Male	0	ILQ	Stroke right occipital cortex	Clopidogrel, pantoprazole, pravastatin
s19	55	Female	0	SRQ	Stroke left occipital cortex	Valsartan
s20	28	Male	-0.2	LHH	Stroke right occipital cortex after resection arteriovenous malformation	Mebeverine, fexofenadine

Table S1. Patient demographics. VA = visual acuity (in logMAR); LHH = (partial) left homonymous hemianopia; RHH = (partial) right homonymous hemianopia; ILQ = inferior left homonymous quadrantanopia; SRQ = superior right homonymous quadrantanopia.

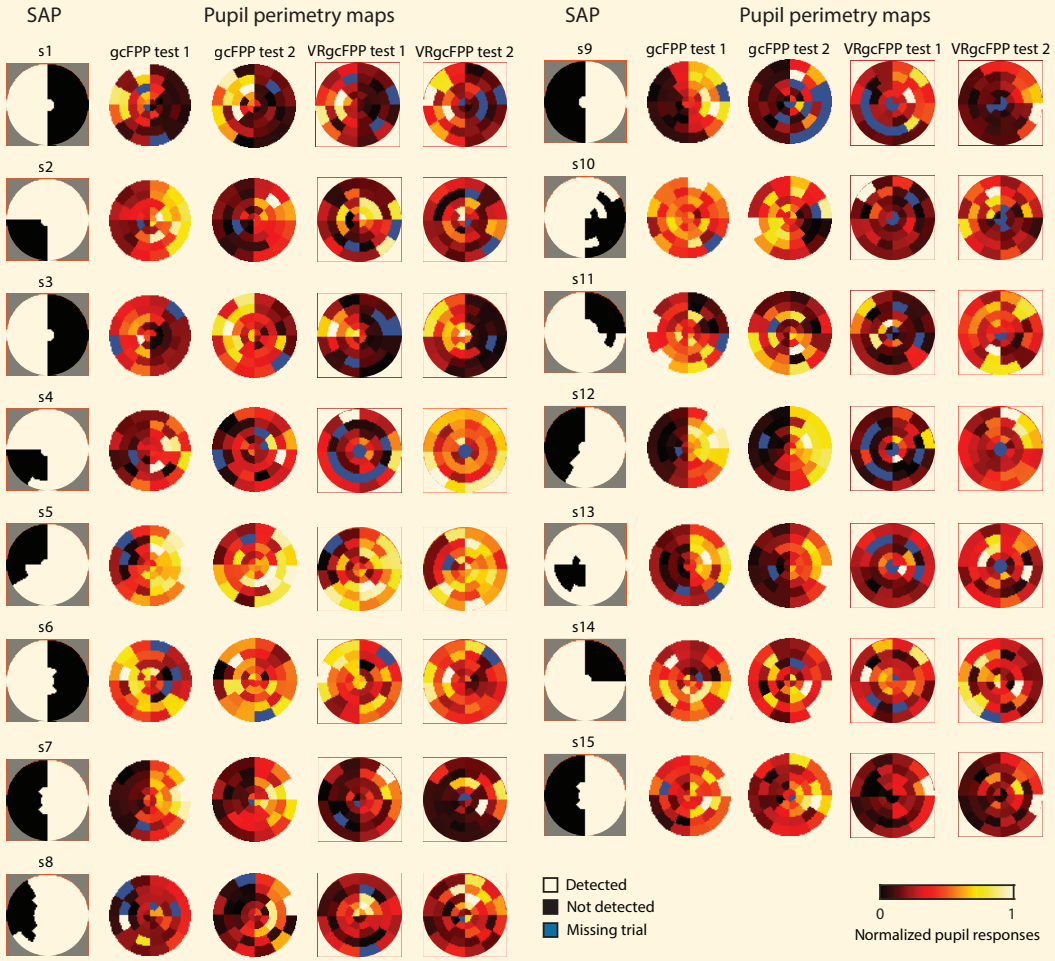

Figure S1. Visual field maps of all patients and tests. The first column shows the ground truth based on standard automated perimetry (SAP; white = detected, black = undetected stimuli during Goldmann kinetic perimetry or Humphrey Field Analyzer testing of the inner 60 degrees of the visual field) per participant (s1-s15). The next four columns show the two-dimensional heatmaps of normalized pupil responses for tests 1 and 2 of the gaze-contingent flicker pupil perimetry (gcFPP) and the virtual reality (VR) gcFPP methods.

Maintaining fixation by children in a virtual reality version of pupil perimetry

Journal of Eye Movement Research (2022) doi: 10.16910/jemr.15.3.2

Portengen BL
Naber M
Jansen D
Van den Boomen C
Imhof SM
Porro GL

8.1 Abstract

The assessment of the visual field in young children continues to be a challenge. Children often do not sit still, fail to fixate stimuli for longer durations, and have limited verbal capacity to report visibility. Therefore, we introduced a head-mounted VR display with gaze-contingent flicker pupil perimetry (VRgcFPP). We presented large flickering patches at different eccentricities and angles in the periphery to evoke pupillary oscillations, and three fixation stimulus conditions to determine best practices for optimal fixation and pupil response quality. A total of twenty children (3-11y) passively fixated a dot, counted the repeated appearance of an animated character (counting task), and watched an animated movie in separate trials of 80s each (20 patch locations, 4s per location). The results showed that gaze precision and accuracy did not differ significantly across the fixation conditions but pupil amplitudes were strongest for the dot and count task. The VR set-up appears to be an ideal apparatus for children to allow free range of movement, an engaging visual task, and reliable eye measurements. We recommend the use of the fixation counting task for pupil perimetry because children enjoyed it the most and it achieved strongest pupil responses.

8.2 Introduction

To this day visual field assessment in children remains challenging due to certain characteristics of standard automated perimetry (SAP; e.g., Humphrey Field Analyzer, Octopus perimeter). These include the task's subjectiveness, the requirement of fixation on a target, uncontrollable learning effects, and the need for prolonged attention. Due to these disadvantages, perimetry tests performed with young children and patients that suffer from cortical damage tend to produce unreliable results (Morales & Brown, 2001; Patel et al., 2015; Tschopp et al., 1998).

Pupil perimetry was developed as an objective alternative to SAP, using the pupillary response to light stimuli across the visual field as a measure of visual sensitivity (Kardon, 1992; Tan et al., 2001; Wilhelm et al., 2000). Conventional pupil perimetry set-ups consist of a monitor and a stand-alone eye tracker. Pupil perimetry has not yet been performed in children even though it circumvents most of the aforementioned challenges in evaluating the visual field with SAP (i.e., subjectiveness and the need for fixation on a target). The reason why pupil perimetry has not yet been applied in children may stem from the remaining requirement to stay seated while fixed in a forehead-chinrest.

Here we propose a novel implementation of gaze-contingent flicker pupil perimetry (Naber et al., 2018) through the use of a head-mounted device (HMD) with virtual reality (VR) technology (VRgcFPP). VR applications in the ophthalmologic practice are relatively new, but promising (Alawa et al., 2021; Deiner et al., 2020; He et al., 2019; Mees et al., 2020; Razeghinejad et al., 2021; Tsapakis et al., 2017, 2018). Particularly, VR allows for freedom of head movement, a child-friendly and engaging environment, and eye measurements using a built-in eye tracker. Eye trackers used for pupil perimetry mostly consist of sophisticated and expensive solutions, such as the Eyelink 1000 Plus (SR Research, Ontario, Canada) or the Tobii Pro Spectrum (Tobii, Danderyd, Sweden), but recent developments now allow high-quality eye-tracking with a HMD.

Also, the immersive environment that VR provides introduces new possibilities to engage children during assessments. Increased attention has been shown to evoke stronger pupillary responses to stimuli (Binda et al., 2013; Mathôt et al., 2013; Naber & Nakayama, 2013) which in turn increases discriminative power (Portengen et al., 2021). Here we questioned how it can be ensured that children show sustained attention for the visual stimuli in a VR environment. An instruction to keep attention will not suffice for young and/or neurologically impaired children. To maintain fixation, a simple fixation point will not be interesting enough to look at, but a fixation object of a type that is too distracting might lead to unwanted pupillary reactions (i.e., noise in the pupil response data). All these aspects could thus hypothetically lead to decreased quality of measurements, denoting its importance to find a balance between increased attention towards fixation and maintaining a good signal-to-noise ratio in the pupillary measurements.

In summary, the aim of this study is to explore whether visual field examination using a virtual reality version of pupil perimetry (VRgcFPP) provides strong pupil responses in children, and what fixation task is best suited for them and what fixation task provides the most reliable results.

8.3 Methods

8.3.1 Participants

The participants consisted of 20 healthy children aged 3 to 11 years old (mean age and SD 7.2 ± 2.4, 14 male). The sample size was similar to prior studies in the field (Alawa et al., 2021; Kelbsch et al., 2020; Neumayr et al., 2020; Portengen et al., 2021). All children had normal or corrected-to-normal visual acuity and no history of visual or neurological disorders. Participants were not tested for visual acuity, but parents were questioned about any signs of visual problems to ensure that vision of the child was good (for details, see procedure). The experiment was approved by the local ethical committee of Utrecht University (approval number FETC19-006) and conformed to the ethical considerations of the Declaration of Helsinki. Participants gave written informed consent together with their caretakers prior to participation. Both participants and caretakers were clearly instructed of their right to withdraw consent and informed that the experiment could be halted prematurely. Researchers observed the child during the experiment for any sign of reluctance or distress, after which the experiment would immediately be ended. Lastly, they received (financial) reimbursement (€8,- per hour) and a phone-based VR headset for participation.

8.3.2 Apparatus

The tests were conducted either in the laboratory or at the residence of the participants. A BTO 17W1090 laptop (BTO, IJsselstein, The Netherlands) with Windows 10 operating system (Microsoft, Redmond, Washington) was used to run the test. The VR environment was built with Unity software (version 2019.4; Unity Technologies, San Francisco, CA, USA). Connected to the laptop was an HTC (HTC Corporation, Taoyuan, Taiwan) Vive Pro Eye VR headset. It consisted of dual 3.5-inch OLED screens with a resolution of 1440x1600 pixels per screen and a refresh rate of 90 Hz to display stimuli. Pupil diameter and gaze were recorded with the built-in Tobii eye tracker (Tobii, Danderyd, Sweden; 90 Hz sampling rate, 0.5-1.1-degree accuracy of gaze angle) and the VIVE SRanipal Runtime and SDK. Adjustment of the HMD and eye tracker calibration (5-point grid) took ~1 min. Two base stations at opposite positions located real-time head position with SteamVR Tracking 2.0. Stimulus properties (i.e., fixation target, frequency, location, size, and order) were inputted with Python software (version 3.7; xml.etree.cElementTree and numpy packages; Python Software Foundation, https://www.python.org/).

8.3.3 Fixation target conditions

The three fixation target conditions used in this study consisted of the presentation of (i) a simple red fixation dot, similar to fixation targets used in standard automated perimetry and conventional pupil perimetry (***Figure 1A***), (ii) an animated child-friendly video of an archeologist in Egypt (chosen for its relatively low luminance, color and spatial contrast; adopted from https://youtu.be/j6PbonHsqW0) with muted sound (***Figure 1B***), and (iii) an engaging counting task in which participants were asked to count the appearances of an animated character at fixation (Pikachu; Pokémon, The Pokémon Company, Minato, Tokyo, Japan, see ***Figure 1C***). This character appeared 14 times within the 80 second trial at varying intervals. All fixation targets were placed on a fixed location within the VR environment independent of head or gaze position. To prevent large saccades in reaction to the fixation target conditions, the three fixation targets were made small by placing them at a simulated distance of 16 m.

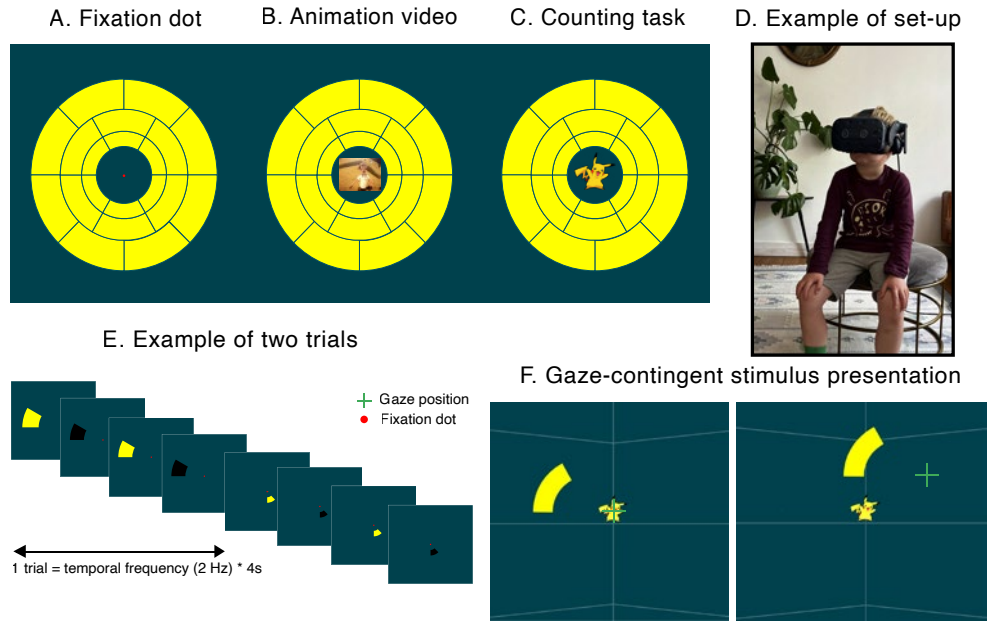

Figure 1. The three fixation target conditions used in this study; a red fixation point (A), an animation video (B), and a counting task (C). Children were seated in a chair where the headset was positioned. A picture of a participant at home (6 years old) is shown in (D). All fixation targets were displayed at a fixed position in the middle of a dark blue virtual reality environment. The 2 Hz flickering yellow-and black stimuli consecutively appeared at the 20 stimulus locations (E). To ensure accurate retinotopic stimulation stimuli were presented in a gaze-contingent manner (F), i.e., online correction of stimulus locations for saccades from fixation target. Note that thin white lines were added to the background to create a sense of depth in the virtual reality environment. Note that the green gaze position cross was not shown during the experiment but is here shown to illustrate the gaze-contingent presentation paradigm.

8.3.4 Environment & stimuli

A dark blue (30% luminance for optimal luminance and color contrast; Portengen et al., submitted) background served as the VR environment. To reduce Simulator Sickness (due to sensory mismatch; Reason, 1978) a sense of depth was simulated through a virtual red platform upon which the participants were placed, and thin dome-like lines. Stimuli were superimposed on the background. The stimuli consisted of black yellow flickering wedges presented across 20 stimulus locations in randomized order within the inner 60 degrees field of vision and positioned around one of three fixation targets with a simulated distance of 10 m, see ***Figure 1***. Note that the inner 16 degrees of the visual field were not stimulated to allow for the fixation conditions to be visible. The black-yellow wedges flickered for 4 seconds (i.e., to collect sufficient pupil data but also keep the experiment relatively short) at a 2 Hz rate and were superimposed on a complementary dark blue background (***Figure 1E***). The 2 Hz flicker frequency is the optimal balance between enough number of evoked pupil responses in a relatively short time window and strong enough pupil responses that can be picked up reliably by the eye tracker (Portengen et al., in prep). The gaze-contingent stimulus presentation (i.e., the eye tracking software follows the subject's direction of gaze fixation and updates the position of the flickering stimuli real-time to reflect changes in direction of gaze; ***Figure 1F***) ensured accurate retinotopic stimulation despite the presence of saccades (Naber et al., 2018).

8.3.5 Procedure

After the informed consent procedure, children and their caretakers completed a demographic questionnaire to ensure no neurologic, ophthalmologic or attentional disorders were present. Upon completion participants were seated on a chair in the center of the room, where the VR HMD was fitted to the child's head (***Figure 1D***). A short adjustment period (~1 min) followed after this. Here the child could look around the VR environment; young children were made aware of the red platform underneath them: "Stay seated, because the floor is lava!". Aside from using this joke as a way to make the children feel more comfortable, the platform also created an extra sense of depth in the otherwise "empty" VR environment. After calibration with a 5-point calibration grid, the experiment started. This consisted of three blocks, each with a fixation target, a 5-second adjustment period and flickering stimuli at 20 locations across the visual field. The children were instructed to fixate their gaze at the fixation target in the middle of the environment. The younger children were encouraged to fixate the center of the screen by verbally expressing the following instructions; (i) during the fixation dot condition, the experimenters reminded a child to keep looking at the dot when its gaze strayed from it, (ii) for the animation video, the experimenters occasionally asked the participating child what was going on in the video, and lastly (iii) children were positively reinforced whenever they counted the appearance of a Pikachu during the counting task condition. The experiment lasted for 240 seconds (3 fixation target blocks * 20 stimulus locations * 4 second stimulus duration). The child could take a break between each block. Total experiment duration, including all trials, breaks, and (re)calibration was on average 15 minutes. Pupils were measured binocularly to estimate convergence and thus focus of depth in the VR environment. The dual OLED screens allowed a sense of depth in the VR environment to prevent VR induced Simulator Sickness.

8.3.6 Analysis

First stimulus location onsets functioned as start events for the event-related analysis of the continuous pupil output of the integrated eye tracker. From the pupil data blink episodes were detected and removed using an automated detection blink method by looking for crossings of a speed threshold of 4 standard deviations (SD) above the mean. The removed blink epochs were interpolated with a cubic method. Next, pupil data were baseline-corrected to enhance inter-subject comparability. A high-pass Butterworth filter (3rd order, 1 Hz cut-off frequency) and a low-pass filter (3rd order, 10 Hz cut-off frequency) followed to remove slow pupil diameter changes and high frequency noise, respectively. Pupil traces per stimulus location were converted to power values in the frequency domain using a fast Fourier transform. The power at 2 Hz reflected the pupil oscillation amplitude and served as the main dependent variable. Furthermore, we were interested in how well each stimulus fixation paradigm retained a child's attention. For this we calculated gaze distance from the fixation target. Distance means and SDs of saccades across fixation conditions were compared. One-way repeated measures ANOVA and paired double-sided t-tests (post-hoc tests) determined statistical significance of pupil amplitudes, fixation accuracy, and fixation precision between fixation conditions. All analyses were performed using Python software (version 3.7; Python Software Foundation, https://www.python.org/). The raincloud plot was created using software developed by (Allen et al., 2021).

8.4 Results

In our study, we set out to investigate whether visual field examination using a virtual reality version of pupil perimetry is feasible and which fixation target condition evoked strongest pupil responses. To do this, pupil data were analyzed to inspect adequate pupil responses to the 2 Hz stimulation. ***Figure 2A*** shows the 2 Hz oscillatory pattern of the pupil traces, averaged across all children, reflecting the stimulus on- and offsets (see Supplementary ***Figure S1*** for separate plots with 95% confidence intervals).

Next, pupil oscillation powers were compared between fixation target conditions (one-way repeated measures ANOVA; $F(2,38) = 3.87$, $p = .030$, partial $\eta^2 = 0.17$). Post-hoc comparisons demonstrated stronger pupil powers of the fixation dot condition ($t(19) = 3.05$, $p = .007$) and the counting task condition ($t(19) = 2.12$, $p = .047$) when compared to the video fixation target. There existed, however, no statistical difference between fixation dot and counting task ($t(19) = 0.73$, $p = .470$). See ***Figure S2-4*** in the Supplementary Materials for the average pupil traces, the average pupil oscillation powers and the pupil oscillation power spectra per stimulus location across fixation target conditions per participant.

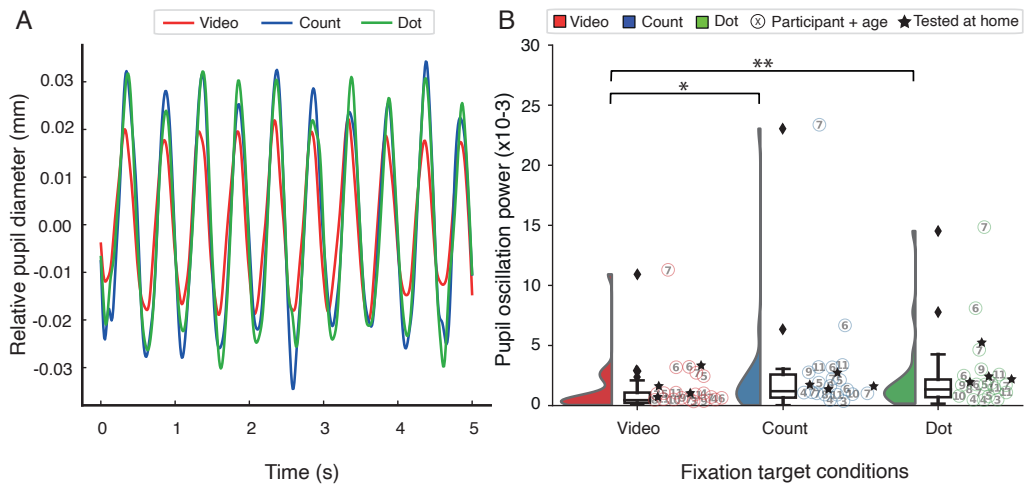

Figure 2. Relative pupil diameter over time for all subjects across fixation target conditions are shown in (A). Pupil traces are averaged across stimulus locations and participants. A raincloud plot depicting the average pupil oscillation powers per fixation target condition are plotted in (B) where the video fixation task (left) is red, the counting task (middle) is blue, and the fixation dot task (right) is green. Individual participants and their age (in years) and test location (i.e., lab or at home (n = 4)) are plotted across fixation conditions. The results show no distinct differences in patterns across age groups or test locations. The fixation dot and counting task conditions provided significantly larger pupil powers than the video fixation target (= p < .05, ** = p < .01).*

Furthermore, we explored which fixation target ensured best fixation behavior. The fixation error from fixation target center (i.e., gaze distance during fixation loss) provided an indication of interest and attention, see ***Figure 3***. A one-way repeated measures ANOVA revealed that gaze accuracy (i.e., mean gaze deviation from fixation center; $F(2,38) = 2.20$, $p = .120$) and gaze precision (i.e., standard deviation of gaze deviation; $F(2,38) = 1.18$, $p = .320$) did not differ significantly across fixation target condition. These results imply that the fixation target conditions did not influence fixation error in the children studied.

After every experiment the investigators queried which fixation target conditions participants enjoyed the most. Almost all (18 out of 20 children) preferred the counting task. The two oldest participants (≥10 years old) favored the fixation dot, likely because the Pokémon character and video targeted matched best with the interest of children younger than 10.

Figure 3. Gaze accuracy and precision of participants; accuracy is defined as the mean gaze deviation from fixation target and precision as the standard deviation of this gaze deviation (A). The gaze accuracy (B) and precision (C) did not significantly differ across fixation target conditions.

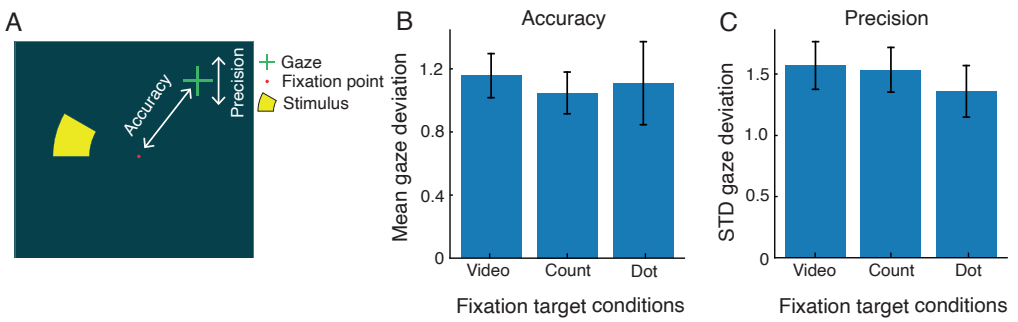

8.5 Discussion

In our study, we set out to investigate whether visual field examination using a virtual reality version of pupil perimetry (VRgcFPP), is feasible in children by testing whether strong pupil responses could be evoked. Moreover, the secondary objectives of this study were to investigate (i) what fixation task is best suited for children, and (ii) which fixation target best captured a child's attention.

The fixation dot and counting task conditions provided strongest pupil responses. One possible explanation for the weaker pupil responses during the animated video fixation target task is the lack

of covert attention for the flickering stimuli (Mathôt et al., 2013; Mathôt & Van der Stigchel, 2015; Naber et al., 2013; Portengen et al., 2021). In addition to attention, the pupil also responds to luminance contrast (Ukai, 1985), color hue (Gamlin et al., 1998; Kelbsch et al., 2019; Tsujimura et al., 2006; Walkey et al., 2005), and spatial frequency (Barbur et al., 1992; Maeda et al., 2017; Ukai, 1985). The video's higher luminance and spatial contrast in comparison to the other two fixation targets could have interfered with the luminance and color contrast between stimulus and background. Interestingly, one participant (S2; see ***Figure S1***) showed higher oscillation power. This participant (aged 7) was hypermetropic and his positive diopter lenses probably enlarged the stimuli resulting in stronger stimulation of the pupil. Elimination of this outlier did not alter the results. Fixation dot and counting task conditions did not differ in pupil response amplitudes. However, all children seemed to enjoy the counting task the most. Although pupil perimetry is an objective testing method, higher intrinsic motivation and attention seem to result in stronger pupil responses (Binda et al., 2013; Binda & Murray, 2015; Mathôt & Van der Stigchel, 2015; Naber et al., 2013; Portengen et al., 2021). Attention was drawn away only a couple times to the appearing Pikachu in the counting task, meaning that attention was still relatively often at the flickering stimuli, leading to strong pupil responses. On the contrary, attention was almost continuously drawn away from the flickering stimuli towards the central stimuli in the video condition, explaining the weaker pupil oscillations. Thus, providing an engaging and more enjoyable task during a diagnostic visual field test (e.g., a counting or object finding task) is a preferred method for young children. For this reason, some alternatives to SAP have already been introduced (Miranda et al., 2016; Murray et al., 2018; Porro, Hofmann, et al., 1998). The Behavioural Visual Field screening (BEFIE) test (Koenraads et al., 2015) and SVOP (Murray et al., 2018) are examples of visual field tests, specifically developed with very young and neurologically impaired children in mind, that are tolerated better than conventional SAP methods. To illustrate, the BEFIE test managed to shorten time-to-diagnosis of visual field defects substantially in children suffering from brain disease (Portengen et al., 2020) whereas SAP methods are generally performed unreliably in young children due to inability to cooperate, lack of comprehension, and psycho-motor impairment (Neumayr et al., 2020; Patel et al., 2015; Porro, Dekker, et al., 1998; Tschopp et al., 1998). Despite these efforts with subjective and/or confrontational and behavioral perimetry tests, pupil perimetry in VR may even enhance the reliability as well. Additionally, this study showed VRgcFPP is applicable in children as young as three years old, filling a clinical gap where reliable visual field testing up until now was extremely difficult.

Our novel virtual reality implementation of pupil perimetry successfully evoked pupil responses comparable to responses found in previous studies with adults (Naber et al., 2018; Portengen et al., 2021). Gaze-contingent flicker pupil perimetry, as well as other variations of pupil perimetry (Kelbsch et al., 2021; Rosli et al., 2018), proved to objectively measure visual field defects. Our results support the application of a virtual reality version of pupil perimetry in children both in a busy clinical setting, and in a telemedicine setting, or even at familiar places for the child, such as home or school. The experimenters experienced no difficulties when conducting the experiment at the participants' residence. Indeed, various VR-based perimetry methods using inexpensive or smartphone-based VR HMDs have recently been studied with telemedicine in mind (Alawa et al., 2021; Deiner et al., 2020; Tsapakis et al., 2017, 2018). Some feature subjective active report tasks comparable to SAP (Mees et al., 2020; Razeghinejad et al., 2021; Tsapakis et al., 2018) and others apply eye tracking to objectively measure looking responses (He et al., 2019; Wroblewski et al., 2014) in order to assess the visual field. None, however, harnessed the objective pupillary responses to light stimuli like in pupil perimetry.

Gaze distance from fixation target was studied to investigate whether any of the fixation targets captured the child's gaze best. Some of the older children (aged approximately 8 years or older) were more capable of inhibiting saccades during fixation. Children under the age of 6 experienced more trouble maintaining fixation; they seemed to lose interest in the fixation dot earlier than the older children. However, this conclusion is merely based on the qualitative inspection of the data and the sample size was too small to statistically differentiate between age groups.

A limitation to the current study comprises of the lack of assessment of diagnostic accuracy of the VRgcFPP method with respect to detecting scotomas as all children tested did not suffer from visual field defects. Next to that, the eye tracker used in the current HMD is of inferior quality when compared to eye trackers used in standard pupil perimetry (e.g., Eyelink 1000 or Tobii Pro Spectrum; Sipatchin

et al., 2021). It is unclear whether the lower quality has impact on the intended use. We did find clear changes in pupil diameter in response to the flickering stimuli (***Figure 2B***), suggesting that, in line with previous work on gaze-contingent flicker pupil perimetry (Naber et al., 2018; Portengen et al., 2021), the apparatus offers the opportunity to measure differences in sensitivities across the visual field in patients and healthy observers; future experiments with pediatric and adult patients suffering from visual field loss and comparative studies between more expensive eye tracking systems and the VR system used in this study might help shed some light on questions about diagnostic accuracy and applicability of eye-tracking in VR. Since the VR apparatus is an off-the-shelf device, it could not be modified to the smaller head sizes of young children. This resulted in suboptimal calibration and relatively smaller pupil powers in our youngest participants (see S1, S15, and S18 in the ***Supplementary Figure S1***).

8.6 Conclusion

To conclude, our results support the application of this virtual reality version of pupil perimetry (VRgcFPP) for binocularly testing the visual field of children in a busy clinical setting. The VR set-up appears to be an ideal apparatus for children to allow free range of movement, an engaging visual task, and reliable eye measurements. A fixation counting task is recommended for use of pupil perimetry in young children as they enjoyed it the most and it achieved pupil responses as strong as the generally used fixation dot.

8.7 References

Alawa, K. A., Nolan, R. P., Han, E., Arboleda, A., Durkee, H., Sayed, M. S., Aguilar, M. C., & Lee, R. K. (2021). Low-cost, smartphone-based frequency doubling technology visual field testing using a head-mounted display. *British Journal of Ophthalmology, 105*(3), 440–444. https://doi.org/10.1136/bjophthalmol-2019-314031

Allen, M., Poggiali, D., Whitaker, K., Marshall, T. R., van Langen, J., & Kievit, R. A. (2021). Raincloud plots: a multi-platform tool for robust data visualization. *Wellcome Open Research, 4*, 63. https://doi.org/10.12688/wellcomeopenres.15191.2

Barbur, Harlow, & Sahraie. (1992). Pupillary responses to stimulus structure, colour and movement. *Ophthalmic and Physiological Optics, 12*(2), 137–141. https://doi.org/10.1111/j.1475-1313.1992.tb00276.x

Binda, P., & Murray, S. O. (2015). Spatial attention increases the pupillary response to light changes. *Journal of Vision, 15*(2), 1–1. https://doi.org/10.1167/15.2.1

Binda, P., Pereverzeva, M., & Murray, S. O. (2013). Attention to bright surfaces enhances the pupillary light reflex. *Journal of Neuroscience, 33*(5), 2199–2204. https://doi.org/10.1523/JNEUROSCI.3440-12.2013

Deiner, M. S., Damato, B. E., & Ou, Y. (2020). Implementing and Monitoring At-Home Virtual Reality Oculokinetic Perimetry During COVID-19. In *Ophthalmology* (Vol. 127, Issue 9, p. 1258). Elsevier. https://doi.org/10.1016/j.ophtha.2020.06.017

Gamlin, P. D. R., Zhang, H., Harlow, A., & Barbur, J. L. (1998). Pupil responses to stimulus color, structure and light flux increments in the rhesus monkey. *Vision Research, 38*(21), 3353–3358. https://doi.org/10.1016/S0042-6989(98)00096-0

He, J., Zhang, S., Wu, P., Zhang, Y., Zheng, X., & Zhou, L. (2019, May 1). A Novel Virtual Reality Design of Portable Automatic Perimetry. *IEEE MTT-S 2019 International Microwave Biomedical Conference, IMBioC 2019* - Proceedings. https://doi.org/10.1109/IMBIOC.2019.8777783

Kardon, R. H. (1992). Pupil perimetry. In *Current Opinion in Ophthalmology* (Vol. 3, Issue 5, pp. 565–570). https://doi.org/10.1097/00055735-199210000-00002

Kelbsch, C., Lange, J., Wilhelm, H., Wilhelm, B., Peters, T., Kempf, M., Kuehlewein, L., & Stingl, K. (2020). Chromatic pupil campimetry reveals functional defects in exudative age-related macular degeneration with differences related to disease activity. *Translational Vision Science and Technology, 9*(6), 5–5. https://doi.org/10.1167/tvst.9.6.5

Kelbsch, C., Stingl, K., Jung, R., Kempf, M., Richter, P., Strasser, T., Peters, T., Wilhelm, B., Wilhelm, H., & Tonagel, F. (2021). How lesions at different locations along the visual pathway influence pupillary reactions to chromatic stimuli. *Graefe's Archive for Clinical and Experimental Ophthalmology, 1*, 1–11. https://doi.org/10.1007/s00417-021-05513-5

Kelbsch, C., Stingl, K., Kempf, M., Strasser, T., Jung, R., Kuehlewein, L., Wilhelm, H., Peters, T., Wilhelm, B., & Stingl, K. (2019). Objective measurement of local rod and cone function using gaze-controlled chromatic pupil campimetry in healthy subjects. *Translational Vision Science and Technology, 8*(6). https://doi.org/10.1167/tvst.8.6.19

Koenraads, Y., Braun, K. P. J., van der Linden, D. C. P., Imhof, S. M., & Porro, G. L. (2015). Perimetry in young and neurologically impaired children: the Behavioral Visual Field (BEFIE) Screening Test revisited. *JAMA Ophthalmology, 133*(3), 319–325. https://doi.org/10.1001/jamaophthalmol.2014.5257

Maeda, F., Kelbsch, C., Straßer, T., Skorkovská, K., Peters, T., Wilhelm, B., & Wilhelm, H. (2017). Chromatic pupillography in hemianopia patients with homonymous visual field defects. *Graefe's Archive for Clinical and Experimental Ophthalmology, 255*(9), 1837–1842. https://doi.org/10.1007/s00417-017-3721-y

Mathôt, S., van der Linden, L., Grainger, J., & Vitu, F. (2013). The pupillary light response reveals the focus of covert visual attention. *PloS One, 8*(10). https://doi.org/10.1371/journal.pone.0078168

Mathôt, S., & Van der Stigchel, S. (2015). New Light on the Mind's Eye: The Pupillary Light Response as Active Vision. *Current Directions in Psychological Science, 24*(5), 374–378. https://doi.org/10.1177/0963721415593725

Mees, L., Upadhyaya, S., Kumar, P., Kotawala, S., Haran, S., Rajasekar, S., Friedman, D. S., & Venkatesh, R. (2020). Validation of a Head-mounted Virtual Reality Visual Field Screening Device. *Journal of Glaucoma, 29*(2), 86–91. https://doi.org/10.1097/IJG.0000000000001415

Miranda, M. A., Henson, D. B., Fenerty, C., Biswas, S., & Aslam, T. (2016). Development of a pediatric visual field test. *Translational Vision Science and Technology, 5*(6), 13–13. https://doi.org/10.1167/tvst.5.6.13

Morales, J., & Brown, S. M. (2001). The feasibility of short automated static perimetry in children. *Ophthalmology, 108*(1), 157–162. https://doi.org/10.1016/S0161-6420(00)00415-2

Murray, I. C., Schmoll, C., Perperidis, A., Brash, H. M., McTrusty, A. D., Cameron, L. A., Wilkinson, A. G., Mulvihill, A. O., Fleck, B. W., & Minns, R. A. (2018). Detection and characterisation of visual field defects using Saccadic Vector Optokinetic Perimetry in children with brain tumours. *Eye, 32*(10), 1. https://doi.org/10.1038/s41433-018-0135-y

Naber, M., Alvarez, G. A., & Nakayama, K. (2013). Tracking the allocation of attention using human pupillary oscillations. *Frontiers in Psychology, 4*, 919. https://doi.org/10.3389/fpsyg.2013.00919

Naber, M., & Nakayama, K. (2013). Pupil responses to high-level image content. *Journal of Vision, 13*(6), 7–7.

https://doi.org/10.1167/13.6.7
Naber, M., Roelofzen, C., Fracasso, A., Bergsma, D. P., van Genderen, M., Porro, G. L., Dumoulin, S. O., & van der Schouw, Y. T. (2018). Gaze-Contingent Flicker Pupil Perimetry Detects Scotomas in Patients With Cerebral Visual Impairments or Glaucoma. *Frontiers in Neurology, 9*(July), 558. https://doi.org/10.3389/fneur.2018.00558
Neumayr, L., Pieper, T., Kudernatsch, M., Trauzettel Klosinski, S., & Staudt, M. (2020). Uncovering homonymous visual field defects in candidates for pediatric epilepsy surgery. *European Journal of Paediatric Neurology, 25*, 165–171. https://doi.org/10.1016/j.ejpn.2019.11.003
Patel, D. E., Cumberland, P. M., Walters, B. C., Russell-Eggitt, I., Rahi, J. S., & OPTIC study group, O. study. (2015). Study of Optimal Perimetric Testing in Children (OPTIC): Feasibility, Reliability and Repeatability of Perimetry in Children. *PloS One, 10*(6), e0130895. https://doi.org/10.1371/journal.pone.0130895
Porro, G., Dekker, E. M., Van Nieuwenhuizen, O., Wittebol-Post, D., Schilder, M. B. H., Schenk-Rootlieb, A. J. F., & Treffers, W. F. (1998). Visual behaviours of neurologically impaired children with cerebral visual impairment: An ethological study. *British Journal of Ophthalmology, 82*(11), 1231–1235. https://doi.org/10.1136/bjo.82.11.1231
Porro, G., Hofmann, J., Wittebol-Post, D., Van Nieuwenhuizen, O., Schouw, Y. T. Van Der, Schilder, M. B. H. H., Dekker, M. E. M. M., & Treffers, W. F. (1998). A new behavioral visual field test for clinical use in pediatric neuro-ophthalmology. *Neuro-Ophthalmology, 19*(4), 205–214. https://doi.org/10.1076/noph.19.4.205.3939
Portengen, B. L., Koenraads, Y., Imhof, S. M., & Porro, G. L. (2020). Lessons Learned from 23 Years of Experience in Testing Visual Fields of Neurologically Impaired Children. *Neuro-Ophthalmology, 44*(6), 361–370. https://doi.org/10.1080/01658107.2020.1762097
Portengen, B. L., Roelofzen, C., Porro, G. L., Imhof, S. M., Fracasso, A., & Naber, M. (2021). Blind spot and visual field anisotropy detection with flicker pupil perimetry wacross brightness and task variations. *Vision Research, 178*(October 2020), 79–85. https://doi.org/10.1016/j.visres.2020.10.005
Razeghinejad, R., Gonzalez-Garcia, A., Myers, J. S., & Katz, L. J. (2021). Preliminary Report on a Novel Virtual Reality Perimeter Compared with Standard Automated Perimetry. *Journal of Glaucoma, 30*(1), 17–23. https://doi.org/10.1097/IJG.0000000000001670
Reason, J. T. (1978). Motion sickness adaptation: A neural mismatch model. *Journal of the Royal Society of Medicine, 71*(11), 819–829. https://doi.org/10.1177/014107687807101109
Rosli, Y., Carle, C. F., Ho, Y., James, A. C., Kolic, M., Rohan, E. M. F., & Maddess, T. (2018). Retinotopic effects of visual attention revealed by dichoptic multifocal pupillography. *Scientific Reports, 8*(1), 1–13. https://doi.org/10.1038/s41598-018-21196-1
Sipatchin, A., Wahl, S., & Rifai, K. (2021). Eye-tracking for clinical ophthalmology with virtual reality (Vr): A case study of the htc vive pro eye's usability. *Healthcare (Switzerland), 9*(2), 180. https://doi.org/10.3390/healthcare9020180
Tan, L., Kondo, M., Sato, M., Kondo, N., & Miyake, Y. (2001). Multifocal pupillary light response fields in normal subjects and patients with visual field defects. *Vision Research, 41*(8), 1073–1084. https://doi.org/10.1016/S0042-6989(01)00030-X
Tsapakis, S., Papaconstantinou, D., Diagourtas, A., Droutsas, K., Andreanos, K., Moschos, M. M., & Brouzas, D. (2017). Visual field examination method using virtual reality glasses compared with the humphrey perimeter. *Clinical Ophthalmology, 11*, 1431–1443. https://doi.org/10.2147/OPTH.S131160
Tsapakis, S., Papaconstantinou, D., Diagourtas, A., Kandarakis, S., Droutsas, K., Andreanos, K., & Brouzas, D. (2018). Home-based visual field test for glaucoma screening comparison with Humphrey perimeter. *Clinical Ophthalmology, 12*, 2597–2606. https://doi.org/10.2147/OPTH.S187832
Tschopp, C., Safran, A. B., Viviani, P., Bullinger, A., Reicherts, M., & Mermoud, C. (1998). Automated visual field examination in children aged 5–8 years: Part I: Experimental validation of a testing procedure. *Vision Research, 38*(14), 2203–2210. https://doi.org/10.1016/S0042-6989(97)00368-4
Tsujimura, S. I., Wolffsohn, J. S., & Gilmartin, B. (2006). Pupil response to color signals in cone-contrast space. *Current Eye Research, 31*(5), 401–408. https://doi.org/10.1080/02713680600681327
Ukai, K. (1985). Spatial pattern as a stimulus to the pupillary system. *Journal of the Optical Society of America A, 2*(7), 1094–1100. https://doi.org/10.1364/josaa.2.001094
Walkey, H. C., Hurden, A., Moorhead, I. R., Taylor, J. A. F., Barbur, J. L., & Harlow, J. A. (2005). Effective contrast of colored stimuli in the mesopic range: a metric for perceived contrast based on achromatic luminance contrast. *Journal of the Optical Society of America A*, 22(1), 17–28. https://doi.org/10.1364/josaa.22.000017
Wilhelm, H., Neitzel, J., Wilhelm, B., Beuel, S., Lüdtke, H., Kretschmann, U., & Zrenner, E. (2000). Pupil Perimetry using M-Sequence Stimulation Technique. *Investigative Ophthalmology & Visual Science, 41*(5), 1229–1238. https://dx.doi.org/
Wroblewski, D., Francis, B. A., Sadun, A., Vakili, G., & Chopra, V. (2014). Testing of visual field with virtual reality goggles in manual and visual grasp modes. *BioMed Research International, 2014.* https://doi.org/10.1155/2014/206082

8.8 Supplementary material

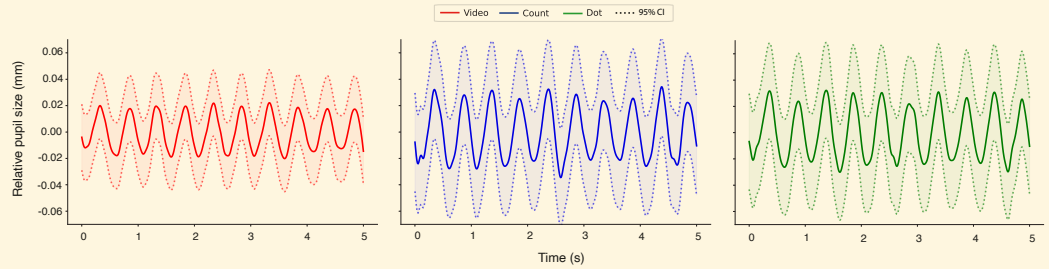

Figure S1. Relative pupil diameter over time with 95% confidence intervals for all subjects across fixation target conditions are shown in red (left panel) for the video fixation target, blue (middle panel) for the counting task fixation target, and green (right panel) for the fixation dot target in green. Pupil traces are averaged across stimulus locations and participants.

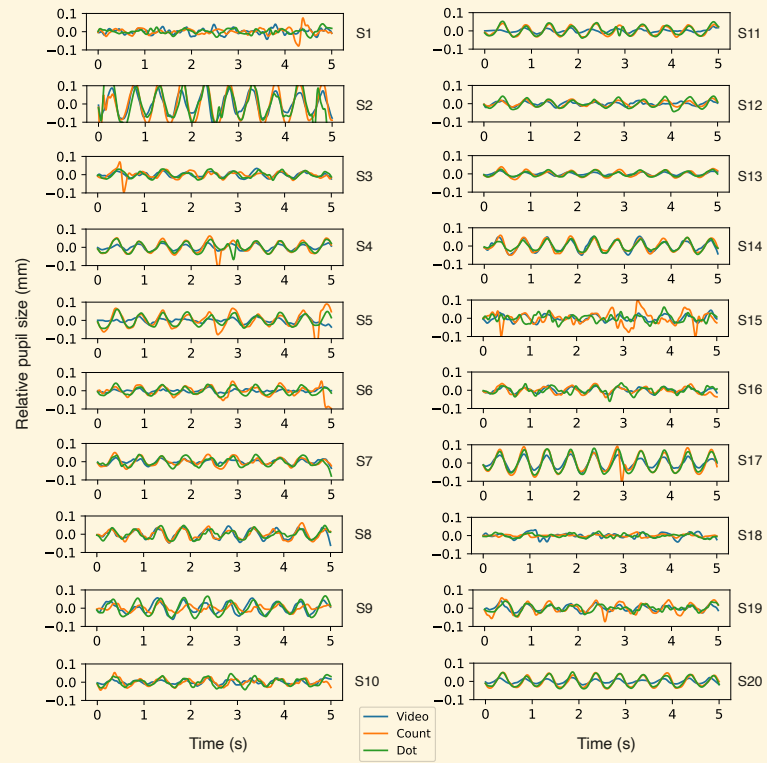

Figure S2. Average pupil traces (i.e., relative change in pupil diameter from baseline) for all subjects (S1-S20) per fixation condition (colors) over time. Pupil traces are averaged across stimulus locations.

Figure S3. Average pupil amplitudes across fixation target conditions per participant (colors)

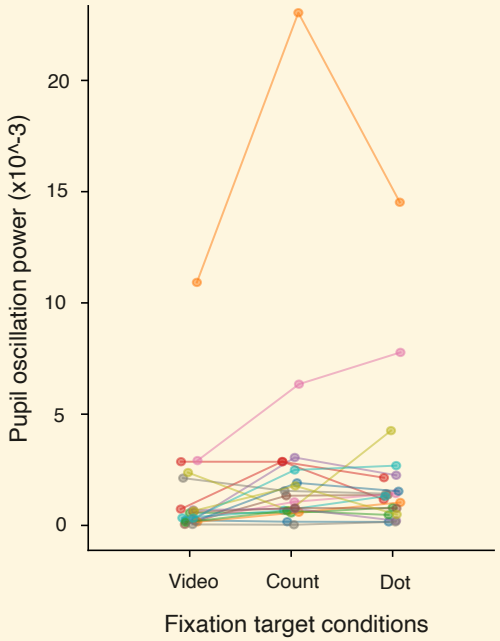

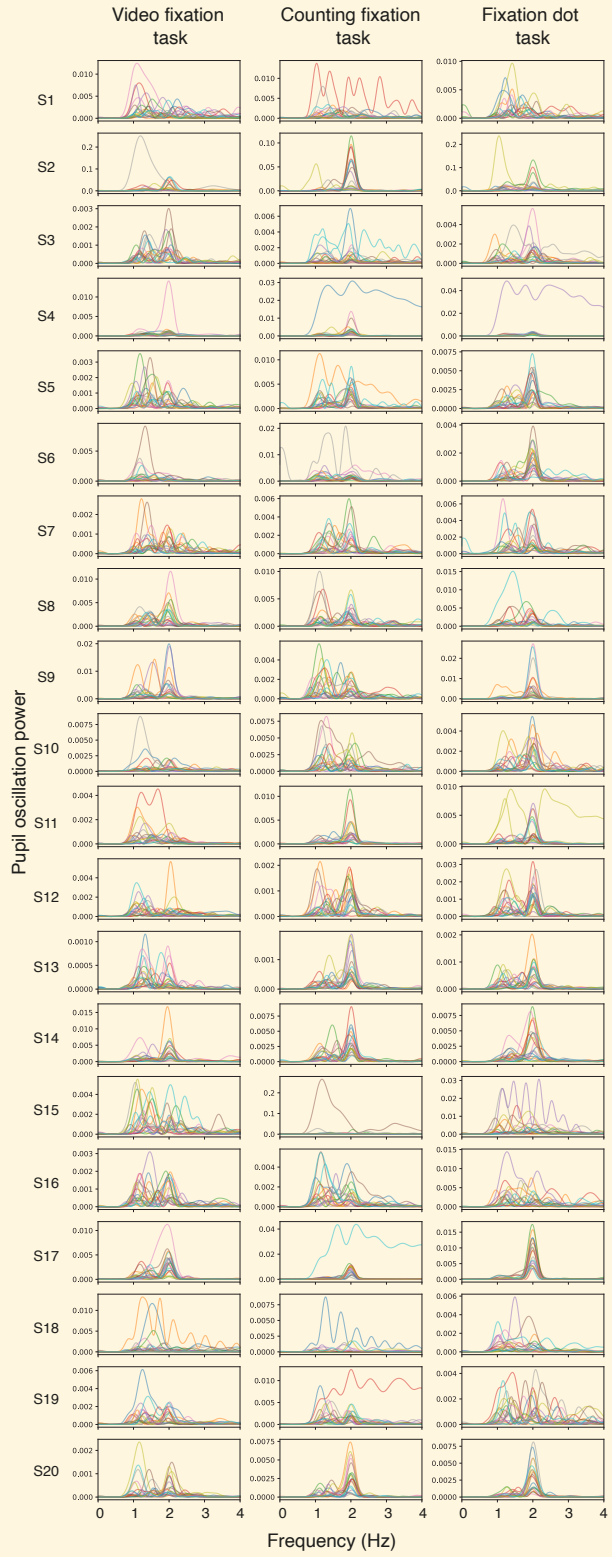

Figure S4. Pupil oscillation power spectra per trial (i.e., stimulus location; different colors) across participants and fixation conditions.

General discussion and future directions

9.1 General discussion

The aim of this thesis was to develop an objective and reliable tool for the early diagnosis of visual field (VF) loss in young and/or neurologically impaired patients. Early VF assessment in children is important as VF loss can be one of the first symptomatic signs of neurological impairment (Van Genderen et al., 2012) and can have large implications for the diagnosis, treatment, follow-up and rehabilitation of neurologically impaired children (Bova et al., 2008; Hart et al., 2013; Jacobson et al., 2010; Molineus et al., 2013; Pike et al., 1994; Reding & Potes, 1988). However, children are often unable to properly recognize and address visual complaints, sometimes even exhibiting unconscious compensatory behaviors (Harbert et al., 2012; Jariyakosol & Peragallo, 2015). Unsurprisingly, it remains challenging to examine their VF in a timely and reliable manner with current technology. ***Chapter 2*** showed that standard automated perimetry (SAP) in neurologically impaired children can only be performed with good reliability in 22-44%. These retrospectively found results seem to concur with a recent nationwide study examining children with brain tumors (Nuijts et al., 2022). It showed that current VF tests could not be performed or were unreliable in 33% of children at the time of brain tumor diagnosis. SAP is thus not well suited for a reliable and timely evaluation of young children. Therefore, an alternative, reliable, and easy to perform VF test is needed to test children properly. The BEFIE test, a behavioral VF test specialized in testing children, was just introduced as such an alternative test. ***Chapter 2*** showed that it could be used to examine the VF of children almost 4 years earlier than SAP. Despite its merit, the BEFIE test still requires time and a trained examiner and observer to gain the cooperation of the child and reliable results. This may be one of the reasons it is not widely used in practice. As such, other methods are needed to avoid underdiagnosing VF impairment in children. Objective VF methods circumvent the need for a psychophysical response of both subject and examiner to gain a measure of VF sensitivity and may subsequently be more suited for young and/or neurologically impaired patients. This thesis focused on the development of pupil perimetry (PP), and the flicker PP method in particular, as an objective VF test method.

9.1.1 Improving the flicker pupil perimetry method

To apply PP as a fast, easy and objective tool in the diagnostic work-up of young and/or neurologically impaired patients, the method had to first be improved. Subsequently, ***chapters 3 to 6*** describe incremental improvements in the development of the flicker PP technique first proposed by Naber et al. (2018). Several PP methods have been described which vary in spatial sparseness and sparseness of events (e.g. Kardon et al., 1991; Maddess et al., 2009; Naber et al., 2018; Schmid et al., 2005; Tan et al., 2001; Wilhelm et al., 2000). ***Chapter 3*** compared the performance of three distinctly different pupil perimetry methods in healthy adults: unifocal, flicker and multifocal pupil perimetry. Although all three performed well, the gaze-contingent flicker pupil perimetry (gcFPP) method could best discern large simulated visual field defects. ***Chapter 4*** then investigated whether gcFPP could detect the physiological presence of the blind spot and upper versus lower visual field differences in healthy adults. In doing so, the method illustrated it could evoke pupil responses that were strong enough to detect local, and global differences in pupil sensitivity. Important findings in improving gcFPP's accuracy were (i) the reduction of retinal light scatter with a gray (instead of black) background and (ii) the use of an attention task to enhance pupillary responses. The latter again stressed that the pupil response not only consists of a reaction to light but also comprises an attentional (cognitive) component (Binda & Gamlin, 2017; Binda & Murray, 2015; Mathôt & Van der Stigchel, 2015; Naber et al., 2013). ***Chapter 5*** investigated the trade-off between luminance and color contrast in normal human vision. A substantial component of pupillary responses incorporated color processing. These findings further signify the pupil orienting response as a complex psychophysical signal consisting of physiological, psychological and neurological factors and sensory modalities (Barbur et al., 1992; Brown et al., 2012; Donofrio, 2011; Drew et al., 2001; Gamlin et al., 1998; Knapen et al., 2016; Odgaard et al., 2003; Strauch et al., 2022; Ukai, 1985; Wetzel et al., 2016; Zele et al., 2018). More robust and sensitive pupil measurements could thus potentially be achieved by introducing color contrast between stimulus and background to the gcFPP method. ***Chapter 6*** investigated this by altering global and local color contrast and luminance contrast in neurologically impaired patients. The findings indeed showed that pupillary responses and therewith diagnostic performance of gcFPP benefit from high luminance and color contrast between stimulus and background. All these improvements led to stronger and more robust pupillary measurements. For instance, luminance and color contrast components between stimulus and background were introduced to increase salience and decrease the occurrence of retinal light scatter,

resulting in more robust pupil measurements. Also, stimulus size was adjusted for the cortical magnification factor to equalize pupil responses across eccentricities as approximately equal numbers of neurons with receptive fields in both central and peripheral visual regions were stimulated (Rosenholtz, 2016). This allowed for more accurate pupil response comparisons between VF locations without the distortion by anisotropies. Other important improvements were the optimized analyses: (i) calculating the fast Fourier transformed pupil power instead of signal-to-noise ratios, standard deviations or coherence, and (ii) PCHIP interpolation instead of cubic splines for missing data.

The above-mentioned advancements eventually culminated in the gcFPP method described in ***chapter 7***. High discriminative power and good reliability was achieved in neurologically impaired adults. We were able to produce visual field heatmaps very similar to the patient's most recent SAP results: the achieved mean AUC of 0.85 and high test-retest reliability (r = 0.95) encompass the highest test performance in neurologically impaired adults when compared to prior research and other PP methods (Naber et al., 2018; Schmid et al., 2005; Skorkovská et al., 2009; Yoshitomi et al., 1999).

9.1.2 Invention of a virtual reality version

Parallel to the development of "conventional" flicker PP or gcFPP, we sought to further tailor the gcFPP method to suit the assessment of young children. A virtual reality (VR) head mounted device with built-in eye tracker allows the child to freely move their head while their eyes are recorded. VR applications in ophthalmologic research (e.g. VR converted SAP methods or eye movement based VF tests) are gaining popularity because of their low cost, portability, versatility, and positive user experience (Alawa et al., 2021; Deiner et al., 2020; Gestefeld et al., 2020; He et al., 2019; Mees et al., 2020; Razeghinejad et al., 2021; Soans, Renken, et al., 2021; Tsapakis et al., 2017, 2018). Our VRgcFPP method is the first attempt to create a VR version of pupil perimetry. This thesis tried to validate this new method in two ways: (i) evaluate its diagnostic performance in neurologically impaired adults (***chapter 7***) and (ii) assess its feasibility in healthy children aged 3 to 11 years old (***chapter 8***). We found that the VRgcFPP method was highly reliable and very capable in dissociating visual field defects (VFD) from healthy VFs patients from healthy controls but performed only moderately when compared to SAP. The difference in performance between VRgcFPP and its conventional gcFPP counterpart can most probably be ascribed to the inferior eye tracker technology implemented in head mounted device. Unfortunately, higher quality (built-in) eye trackers are currently not commercially available. As eye tracker technology improves, VRgcFPP's diagnostic performance may significantly improve with it. As illustrated by the disappointing results in SAP (Neumayr et al., 2020; Patel et al., 2015; Porro, Dekker, et al., 1998; Tschopp et al., 1998), diagnostic tests are not necessarily as feasible in children as they are in adults. Young children or sick patients often lack the ability to cooperate, comprehend the task, or suffer from psycho-motor impairment (Good et al., 1994; Mohn & Van Hof-Van Duin, 1983; Porro, Hofmann, Wittebol-Post, Van Nieuwenhuizen, Van Der Schouw, et al., 1998; Wilson et al., 1991). It was therefore important to also evaluate the method in healthy (i.e. to decrease patient burden) young children. Surprisingly, even the youngest participant (3 years old) was not deterred by having the device mounted to its head (see ***chapter 8*** for an example of the set-up). Aside from its inherent portability and the fast, reliable and objective pupillary measurements, the VRgcFPP exhibited another benefit over VF measurement with SAP: an interactive counting task to gain the child's attention and cooperation. Such a behavioral component has been shown to be particularly well suited to children (chapter 2; Koenraads et al., 2015; Porro, Hofmann, et al., 1998). The VRgcFPP method thus manages to harness the multisensory psychophysical pupillary responses in an engaging way to reliably and objectively measure visual sensitivity. Although the PP methods seem promising state-of-the-art techniques, there are still some considerations before implementing PP in the clinical practice. These will be discussed in the next section.

9.2 Future directions and perspectives

9.2.1 Improvements to the method

As previously described, this thesis made several advancements in the PP technique to reliably evoke and measure pupillary responses. Naturally, there still exist some areas upon which to improve. The VRgcFPP method might benefit most substantially from technical advancement. If eye tracking technology improves, a higher quality camera may be integrated with VR technologies to facilitate more robust and reliable measurements. However, one of the advantages of the PP technique is its versatility. If eye tracker technology fails to improve or if the VR headset is too big and heavy to fit on

young children's heads, there are still other ways to assess their pupil sensitivities. An eye tracker that specializes in the pupillary measurements of children (e.g. Tobii Spectrum Pro) might then be combined with a large monitor to create a child's version of conventional gcFPP. The major advantage of such eye trackers is that head fixation (which might deter young children from cooperation) is not necessary to still reliably record the pupil.
The gcFPP set-up is currently still in the experimental phase. To be of value in the clinical setting, exportable patient test results with progression analyses should be implemented. Another interesting aspect lies not in finetuning the current technique, but in combining compatible techniques. It may then be possible to create a more seamless patient experience. In fact, some promising techniques that also use eye trackers are eye movement-based VF tests (Pel et al., 2013; Soans, Grillini, et al., 2021) and measurement of visual acuity or color perception through objective pupillary responses (Barbur et al., 1992; Barbur & Thomson, 1987; Cocker et al., 1994). Hypothetically, a combination of these techniques could thus make it possible to simultaneously measure visual acuity, color perception and the visual field with an eye tracker while the patient passively watches a movie on a large monitor.

9.2.2 Role of pupil perimetry in clinical practice

It is tempting to already recommend the use of PP in clinical practice. The cheap and portable VRgcFPP may have a role as a screening device for children at consultation or general practitioner offices. Besides, its implementation may positively impact doctor delay such as described in ***chapter 2***. Furthermore, gcFPP may also prove useful for patients suspected of malingering or for young and multi-handicapped neurologically impaired patients unable to reliably provide verbal and/or motor feedback during SAP due to its fast,

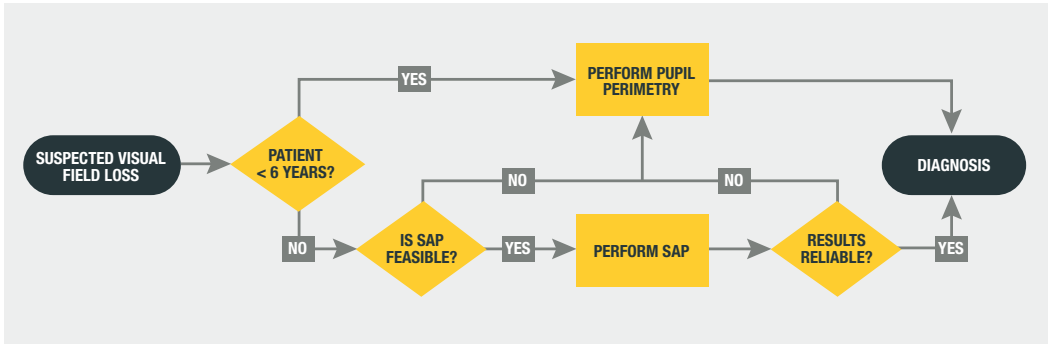

Figure 9.1 Suggestion for the implementation of pupil perimetry as a complementary tool to the diagnostic work-up of young and/or neurologically impaired patients. SAP = standard automated perimetry

reliable and objective measurements. However, the method has some limitations. PP's feasibility, for example, is hampered by the larger stimuli needed to evoke robust pupillary responses. This results in visual sensitivity maps of low spatial resolution, while SAP provides more precise visual field estimates. As such, it is important to stress PP's role of a complementary tool to the current work-up of visual field assessment. ***Figure 9.1*** illustrates a suggestion for a decision scheme in neurologically impaired patients.

Moreover, the studies described in this thesis represent only the first steps in determining the utility of this diagnostic tool. To be incorporated into practice, a test must not only have technical validity (i.e. is the measurement true?), but also clinical validity (i.e. is the result clinically meaningful?) and clinical utility (i.e. is the result clinically meaningful?). As such, the case-control study designs used have a potential risk of selection bias: participants with known VFDs were compared to healthy controls while in clinical practice patients are only suspected of having a disease. This risk is inherent to test research of new diagnostic tools. Now PP's merit in healthy adults, neurologically impaired adults and healthy children has been established, PP should first be piloted in neurologically impaired children. Also, to more accurately establish its role in visual field assessment, future research should focus on establishing age-based normative. Then, clinical utility must be quantified by adopting an add-on strategy (Bossuyt et al., 2012): the existing diagnostic work-up should be offset to the same work-up, but with the addition of PP (see ***Figure 9.1***). Only then can the independent predictive contribution of PP to the existing diagnostic information in a clinical context truly be evaluated.
Lastly, it is generally important to be aware that anything new is often thought of as being inherently better than anything already in use (i.e. pro-innovation bias; Rogers & Havens, 1962). This bias towards new technology has a risk of clinicians favoring a new technology even if it is still unproven. For example, the novel head-mounted perimeters that apply the HFA technology in a VR environment do not differ from conventional apparatus in technical characteristics despite being marketed as novel. The head-mounted perimeters use the same testing algorithms as conventional SAP, still rely on subjective feedback from the patient and will likely suffer from the same test-retest variability. Such a device may thus have merit for clinics that do not already own a conventional HFA device or temporary clinics that provide care in developing countries but should not replace

functioning SAP devices. Special care should be exercised to prove a technology's worth over existing technology to prevent superfluous investments.

9.3 Conclusion

In conclusion, this thesis highlights the need for objective and reliable visual field assessments in young and neurologically impaired patients and subsequently represents a first step in the development of a new objective method: gaze-contingent flicker pupil perimetry (gcFPP). After implementation of several technological and theoretical improvements, high diagnostic performance and reliability was found for conventional gcFPP, while the newly developed virtual reality version of gcFPP displayed moderate diagnostic performance and high reliability. The promising results merit further development of the technology, but future research must further quantify flicker pupil perimetry's role in ophthalmological screening and monitoring of young and neurologically impaired patients.

9.4 References

Alawa, K. A., Nolan, R. P., Han, E., Arboleda, A., Durkee, H., Sayed, M. S., Aguilar, M. C., & Lee, R. K. (2021). Low-cost, smartphone-based frequency doubling technology visual field testing using a head-mounted display. *British Journal of Ophthalmology, 105*(3), 440–444. https://doi.org/10.1136/bjophthalmol-2019-314031

Barbur, Harlow, & Sahraie. (1992). Pupillary responses to stimulus structure, colour and movement. *Ophthalmic and Physiological Optics, 12*(2), 137–141. https://doi.org/10.1111/j.1475-1313.1992.tb00276.x

Barbur, J. L., & Thomson, W. D. (1987). Pupil response as an objective measure of visual acuity. *Ophthalmic and Physiological Optics, 7*(4), 425–429. https://doi.org/10.1111/j.1475-1313.1987.tb00773.x

Binda, P., & Gamlin, P. D. (2017). Renewed Attention on the Pupil Light Reflex. In *Trends in Neurosciences* (Vol. 40, Issue 8, pp. 455–457). NIH Public Access. https://doi.org/10.1016/j.tins.2017.06.007

Binda, P., & Murray, S. O. (2015). Keeping a large-pupilled eye on high-level visual processing. In *Trends in Cognitive Sciences* (Vol. 19, Issue 1, pp. 1–3). Trends Cogn Sci. https://doi.org/10.1016/j.tics.2014.11.002

Bossuyt, P. M. M., Reitsma, J. B., Linnet, K., & Moons, K. G. M. (2012). Beyond diagnostic accuracy: The clinical utility of diagnostic tests. In *Clinical Chemistry* (Vol. 58, Issue 12). https://doi.org/10.1373/clinchem.2012.182576

Bova, S. M., Giovenzana, A., Signorini, S., La Piana, R., Uggetti, C., Bianchi, P. E., & Fazzi, E. (2008). Recovery of visual functions after early acquired occipital damage. *Developmental Medicine & Child Neurology, 50*(4), 311–315. https://doi.org/10.1111/j.1469-8749.2008.02044.x

Brown, T. M., Tsujimura, S. I., Allen, A. E., Wynne, J., Bedford, R., Vickery, G., Vugler, A., & Lucas, R. J. (2012). Melanopsin-based brightness discrimination in mice and humans. *Current Biology, 22*(12), 1134–1141. https://doi.org/10.1016/j.cub.2012.04.039

Cocker, K. D., Moseley, M. J., Bissenden, J. G., & Fielder, A. R. (1994). Visual acuity and pupillary responses to spatial structure in infants. *Investigative Ophthalmology and Visual Science, 35*(5), 2620–2625. https://iovs.arvojournals.org/article.aspx?articleid=2161200

Deiner, M. S., Damato, B. E., & Ou, Y. (2020). Implementing and Monitoring At-Home Virtual Reality Oculo-kinetic Perimetry During COVID-19. In *Ophthalmology* (Vol. 127, Issue 9, p. 1258). Elsevier. https://doi.org/10.1016/j.ophtha.2020.06.017

Donofrio, R. L. (2011). Review Paper: The Helmholtz-Kohlrausch effect. *Journal of the Society for Information Display, 19*(10), 658. https://doi.org/10.1889/jsid19.10.658

Drew, P., Sayres, R., Watanabe, K., & Shimojo, S. (2001). Pupillary response to chromatic flicker. *Experimental Brain Research, 136*(2), 256–262. https://doi.org/10.1007/s002210000605

Gamlin, P. D. R., Zhang, H., Harlow, A., & Barbur, J. L. (1998). Pupil responses to stimulus color, structure and light flux increments in the rhesus monkey. *Vision Research, 38*(21), 3353–3358. https://doi.org/10.1016/S0042-6989(98)00096-0

Gestefeld, B., Koopman, J., Vrijling, A., Cornelissen, F. W., & de Haan, G. (2020). Eye tracking and virtual reality in the rehabilitation of mobility of hemianopia patients: a user experience study. *International Journal of Orientation & Mobility, 11*(1). https://doi.org/10.21307/vri-2020-002

Good, W. V, Jan, J. E., DeSa, L., Barkovich, A. J., Groenveld, M., & Hoyt, C. S. (1994). Cortical visual impairment in children. *Survey of Ophthalmology, 38*(4), 351–364. https://doi.org/10.1016/0039-6257(94)90073-6

Harbert, M. J., Yeh-Nayre, L. A., O'Halloran, H. S., Levy, M. L., & Crawford, J. R. (2012). Unrecognized visual field deficits in children with primary central nervous system brain tumors. *Journal of Neuro-Oncology, 107*(3), 545–549. https://doi.org/10.1007/s11060-011-0774-3

Hart, M. G., Sarkies, N. J., Santarius, T., & Kirollos, R. W. (2013). Ophthalmological outcome after resection of tumors based on the pineal gland. *Journal of Neurosurgery, 119*(2), 420–426. https://doi.org/10.3171/2013.3.JNS122137

He, J., Zhang, S., Wu, P., Zhang, Y., Zheng, X., & Zhou, L. (2019, May 1). A Novel Virtual Reality Design of Portable Automatic Perimetry. *IEEE MTT-S 2019 International Microwave Biomedical Conference, IMBioC 2019* - Proceedings. https://doi.org/10.1109/IMBIOC.2019.8777783

Jacobson, L., Rydberg, A., Eliasson, A.-C., Kits, A., & Flodmark, O. (2010). Visual field function in school-aged children with spastic unilateral cerebral palsy related to different patterns of brain damage. *Developmental Medicine & Child Neurology, 52*(8), e184–e187. https://doi.org/10.1111/j.1469-8749.2010.03650.x

Jariyakosol, S., & Peragallo, J. H. (2015). The Effects of Primary Brain Tumors on Vision and Quality of Life in Pediatric Patients. *Seminars in Neurology, 35*(5). https://doi.org/10.1055/s-0035-1563571

Kardon, R. H., Kirkali, P. A., & Thompson, H. S. (1991). Automated Pupil Perimetry Pupil Field Mapping in Patients and Normal Subjects. *Ophthalmology, 98*(4), 485–496. https://doi.org/10.1016/S0161-6420(91)32267-X

Knapen, T., De Gee, J. W., Brascamp, J., Nuiten, S., Hoppenbrouwers, S., & Theeuwes, J. (2016). Cognitive and ocular factors jointly determine pupil responses under equiluminance. *PLoS ONE, 11*(5), e0155574. https://doi.org/10.1371/journal.pone.0155574

Koenraads, Y., Braun, K. P. J., van der Linden, D. C. P., Imhof, S. M., & Porro, G. L. (2015). Perimetry in young and neurologically impaired children: the Behavioral Visual Field (BEFIE) Screening Test revisited. *JAMA Ophthalmology, 133*(3), 319–325. https://doi.org/10.1001/jamaophthalmol.2014.5257

Maddess, T., Bedford, S. M., Goh, X. L., & James, A. C. (2009). Multifocal pupillographic visual field testing in glaucoma. *Clinical & Experimental Ophthalmology, 37*(7), 678–686. https://doi.org/10.1111/j.1442-9071.2009.02107.x

Mathôt, S., & Van der Stigchel, S. (2015). New Light on the Mind's Eye: The Pupillary Light Response as Active Vision. *Current Directions in Psychological Science, 24*(5), 374–378. https://doi.org/10.1177/0963721415593725

Mees, L., Upadhyaya, S., Kumar, P., Kotawala, S., Haran, S., Rajasekar, S., Friedman, D. S., & Venkatesh, R. (2020). Validation of a Head-mounted Virtual Reality Visual Field Screening Device. *Journal of Glaucoma, 29*(2), 86–91. https://doi.org/10.1097/IJG.0000000000001415

Mohn, G., & Van Hof-Van Duin, J. (1983). Behavioural and electrophysiological measures of visual functions in children with neurological disorders. *Behavioural Brain Research, 10*(1). https://doi.org/10.1016/0166-4328(83)90163-8

Molineus, A., Boxberger, N., Redlich, A., & Vorwerk, P. (2013). Time to diagnosis of brain tumors in children: A single-centre experience. *Pediatrics International, 55*(3), 305–309. https://doi.org/10.1111/ped.12095

Naber, M., Alvarez, G. A., & Nakayama, K. (2013). Tracking the allocation of attention using human pupillary oscillations. *Frontiers in Psychology, 4*, 919. https://doi.org/10.3389/fpsyg.2013.00919

Naber, M., Roelofzen, C., Fracasso, A., Bergsma, D. P., van Genderen, M., Porro, G. L., Dumoulin, S. O., & van der Schouw, Y. T. (2018). Gaze-Contingent Flicker Pupil Perimetry Detects Scotomas in Patients With Cerebral Visual Impairments or Glaucoma. *Frontiers in Neurology, 9*(July), 558. https://doi.org/10.3389/fneur.2018.00558

Neumayr, L., Pieper, T., Kudernatsch, M., Trauzettel-Klosinski, S., & Staudt, M. (2020). Uncovering homonymous visual field defects in candidates for pediatric epilepsy surgery. European Journal of *Paediatric Neurology, 25*, 165–171. https://doi.org/10.1016/j.ejpn.2019.11.003

Nuijts, M. A., Stegeman, I., Van Seeters, T., Borst, M. D., Bennebroek, C. A. M., Buis, D. R., Naus, N. C., Porro, G. L., Van Egmond-Ebbeling, M. B., Voskuil-Kerkhof, E. S. M., Pott, J. R., Franke, N. E., De Vos-Kerkhof, E., Hoving, E. W., Schouten-Van Meeteren, A. Y. N., & Imhof, S. M. (2022). Ophthalmological Findings in Youths With a Newly Diagnosed Brain Tumor. *JAMA Ophthalmology, 140*(10), 982–993. https://doi.org/10.1001/JAMAOPHTHALMOL.2022.3628

Odgaard, E. C., Arieh, Y., & Marks, L. E. (2003). Cross-modal enhancement of perceived brightness: Sensory interaction versus response bias. *Perception and Psychophysics, 65*(1), 123–132. https://doi.org/10.3758/BF03194789

Patel, D. E., Cumberland, P. M., Walters, B. C., Russell-Eggitt, I., Rahi, J. S., & OPTIC study group, O. study. (2015). Study of Optimal Perimetric Testing in Children (OPTIC): Feasibility, Reliability and Repeatability of Perimetry in Children. *PloS One, 10*(6), e0130895. https://doi.org/10.1371/journal.pone.0130895

Pel, J. J. M., van Beijsterveld, M. C. M., Thepass, G., & van der Steen, J. (2013). Validity and Repeatability of Saccadic Response Times Across the Visual Field in Eye Movement Perimetry. *Translational Vision Science & Technology, 2*(7), 3. https://doi.org/10.1167/tvst.2.7.3

Pike, M. G., Holmstrom, G., Vries, L. S., Pennock, J. M., Drew, K. J., Sonksen, P. M., & Dubowitz, L. M. S. (1994). Patterns Of Visual Impairment Associated With Lesions Of The Preterm Infant Brain. *Developmental Medicine & Child Neurology, 36*(10), 849–862. https://doi.org/10.1111/j.1469-8749.1994.tb11776.x

Porro, G., Dekker, E. M., Van Nieuwenhuizen, O., Wittebol-Post, D., Schilder, M. B. H., Schenk-Rootlieb, A. J. F., & Treffers, W. F. (1998). Visual behaviours of neurologically impaired children with cerebral visual impairment: An ethological study. *British Journal of Ophthalmology, 82*(11), 1231–1235. https://doi.org/10.1136/bjo.82.11.1231

Porro, G., Hofmann, J., Wittebol-Post, D., Van Nieuwenhuizen, O., Schouw, Y. T. Van Der, Schilder, M. B. H. H., Dekker, M. E. M. M., & Treffers, W. F. (1998). A new behavioral visual field test for clinical use in pediatric neuro-ophthalmology. *Neuro-Ophthalmology, 19*(4), 205–214. https://doi.org/10.1076/noph.19.4.205.3939

Porro, G., Hofmann, J., Wittebol-Post, D., Van Nieuwenhuizen, O., Van Der Schouw, Y. T., Schilder, M. B. H., Dekker, M. E. M., & Treffers, W. F. (1998). A new behavioral visual field test for clinical use in pediatric neuro- ophthalmology. *Neuro-Ophthalmology, 19*(4). https://doi.org/10.1076/noph.19.4.205.3939

Razeghinejad, R., Gonzalez-Garcia, A., Myers, J. S., & Katz, L. J. (2021). Preliminary Report on a Novel Virtual Reality Perimeter Compared with Standard Automated Perimetry. *Journal of Glaucoma, 30*(1), 17–23. https://doi.org/10.1097/IJG.0000000000001670

Reding, M. J., & Potes, E. (1988). Rehabilitation outcome following initial unilateral hemispheric stroke: Life Table Analysis Approach. *Stroke, 19*(11). https://doi.org/10.1161/01.STR.19.11.1354

Rogers, E. M., & Havens, A. E. (1962). Predicting Innovativeness. *Sociological Inquiry, 32*(1). https://doi.org/10.1111/j.1475-682X.1962.tb00528.x

Rosenholtz, R. (2016). Capabilities and Limitations of Peripheral Vision. In *Annual review of vision science* (Vol. 2, pp. 437–457). Annual Reviews. https://doi.org/10.1146/annurev-vision-082114-035733

Schmid, R., Luedtke, H., Wilhelm, B. J., & Wilhelm, H. (2005). Pupil campimetry in patients with visual field loss. *European Journal of Neurology, 12*(8), 602–608. https://doi.org/10.1111/j.1468-1331.2005.01048.x

Skorkovská, K., Wilhelm, H., Lüdtke, H., & Wilhelm, B. (2009). How sensitive is pupil campimetry in hemifield loss? *Graefe's Archive for Clinical and Experimental Ophthalmology, 247*(7), 947–953. https://doi.org/10.1007/s00417-009-1040-7

Soans, R. S., Grillini, A., Saxena, R., Renken, R. J., Gandhi, T. K., & Cornelissen, F. W. (2021). Eye-movement–based assessment of the perceptual consequences of glaucomatous and neuro-ophthalmological visual field defects. *Translational Vision Science and Technology, 10*(2). https://doi.org/10.1167/tvst.10.2.1

Soans, R. S., Renken, R. J., John, J., Bhongade, A., Raj, D., Saxena, R., Tandon, R., Gandhi, T. K., & Cornelissen, F. W. (2021). Patients Prefer a Virtual Reality Approach Over a Similarly Performing Screen-Based Approach for Continuous Oculomotor-Based Screening of Glaucomatous and Neuro-Ophthalmological Visual Field Defects. *Frontiers in Neuroscience, 15.* https://doi.org/10.3389/fnins.2021.745355

Strauch, C., Wang, C.-A., Einhäuser, W., Van der Stigchel, S., & Naber, M. (2022). Pupillometry as an integrated readout of distinct attentional networks. *Trends in Neurosciences, 0*(0). https://doi.org/10.1016/j.tins.2022.05.003

Tan, L., Kondo, M., Sato, M., Kondo, N., & Miyake, Y. (2001). Multifocal pupillary light response fields in normal subjects and patients with visual field defects. *Vision Research, 41*(8), 1073–1084. https://doi.org/10.1016/S0042-6989(01)00030-X

Tsapakis, S., Papaconstantinou, D., Diagourtas, A., Droutsas, K., Andreanos, K., Moschos, M. M., & Brouzas, D. (2017). Visual field examination method using virtual reality glasses compared with the humphrey perimeter. *Clinical Ophthalmology, 11*, 1431–1443. https://doi.org/10.2147/OPTH.S131160

Tsapakis, S., Papaconstantinou, D., Diagourtas, A., Kandarakis, S., Droutsas, K., Andreanos, K., & Brouzas, D. (2018). Home-based visual field test for glaucoma screening comparison with Humphrey perimeter. *Clinical Ophthalmology, 12*, 2597–2606. https://doi.org/10.2147/OPTH.S187832

Tschopp, C., Safran, A. B., Viviani, P., Bullinger, A., Reicherts, M., & Mermoud, C. (1998). Automated visual field examination in children aged 5–8 years: Part I: Experimental validation of a testing procedure. *Vision Research, 38*(14), 2203–2210. https://doi.org/10.1016/S0042-6989(97)00368-4

Ukai, K. (1985). Spatial pattern as a stimulus to the pupillary system. *Journal of the Optical Society of America A, 2*(7), 1094–1100. https://doi.org/10.1364/josaa.2.001094

Van Genderen, M., Dekker, M., Pilon, F., & Bals, I. (2012). Diagnosing cerebral visual impairment in children with good visual acuity. *Strabismus, 20*(2), 78–83. https://doi.org/10.3109/09273972.2012.680232

Wetzel, N., Buttelmann, D., Schieler, A., & Widmann, A. (2016). Infant and adult pupil dilation in response to unexpected sounds. *Developmental Psychobiology, 58*(3), 382–392. https://doi.org/10.1002/DEV.21377

Wilhelm, H., Neitzel, J., Wilhelm, B., Beuel, S., Lüdtke, H., Kretschmann, U., & Zrenner, E. (2000). Pupil Perimetry using M-Sequence Stimulation Technique. *Investigative Ophthalmology & Visual Science, 41*(5), 1229–1238. https://dx.doi.org/

Wilson, M., Quinn, G., Dobson, V., & Breton, M. (1991). Normative values for visual fields in 4- to 12-year-old children using kinetic perimetry. *Journal of Pediatric Ophthalmology and Strabismus, 28*(3).

Yoshitomi, T., Matsui, T., Tanakadate, A., & Ishikawa, S. (1999). Comparison of Threshold Visual Perimetry and Objective Pupil Perimetry in Clinical Patients. *Journal of Neuro-Ophthalmology, 19*(2), 89–99. https://doi.org/10.1097/00041327-199906000-00003

Zele, A. J., Adhikari, P., Feigl, B., & Cao, D. (2018). Cone and melanopsin contributions to human brightness estimation. *Journal of the Optical Society of America A, 35*(4), B19–B25. https://doi.org/10.1364/josaa.35.000b19

Summary

English
Nederlands

Summary - *English*

The assessment of the visual field (VF) is an instrumental component of ophthalmological and neurological examination in the clinical practice. VF tests generally are relatively cheap and non-invasive. With it, clinicians can pinpoint the suspected location of damage along the visual pathway Early and proper diagnosis of VF loss in young and/or neurologically impaired individuals is crucial since it plays an important role in the diagnosis, follow-up and rehabilitation of these patients. However, current VF tests are subjective and unreliable in this patient population. As such, this thesis strives to develop an objective and reliable tool for the VF assessment of young and/or neurologically impaired patients.

Chapter 1 serves as a general introduction to VF assessment in young and neurologically impaired patients. Discussed are several testing methods, the anatomy of the visual and pupillary pathways within the brain and important milestones and challenges in the development of pupil perimetry. Lastly, the aims and outline of the thesis are formulated.

Chapter 2 shares insights gained from the experience in testing the VFs of children with neurological impairment. Standard automated perimetry (SAP), the current gold standard in visual field assessment, was only reliable in 22-44%, while the use of a behavioral VF test led to a significant gain in time to diagnosis. The importance of accurate, reliable, and timely VF testing in this population is emphasized as it can lead to better care for neurologically impaired children.

Pupil perimetry is a possible objective alternative to the subjective SAP methods. It depends on pupillary responses to light stimuli as a measure of visual field sensitivity. **Chapter 3** compared the performance of three different pupil perimetry techniques (i.e. unifocal, flicker and multifocal pupil perimetry) in healthy adults. Although all three methods performed well, the gaze-contingent flicker pupil perimetry (gcFPP) could best discern large simulated visual field defects (VFD).

Chapter 4 then investigated whether gcFPP could detect the physiological presence of the blind spot and the upper versus lower VF differences in healthy adults. The method showed to be capable of eliciting pupil responses that were strong enough to detect local, and global differences in pupil sensitivity. Additionally, the results encouraged the use of a gray (instead of black) background to reduce retinal light scatter and the use of an attention task to enhance pupillary responses. The latter again stressed that the pupil response not only consists of a reaction to light but also comprises an attentional (cognitive) component.

Chapter 5 investigated the trade-off between luminance and color contrast in normal human vision. Systematically adjusting both luminance and color contrast revealed that a substantial component of pupillary responses incorporated color processing. These findings provide insights into the mechanisms underlying visual perception and emphasize the importance of considering both luminance and color contrast in visual stimuli.

Subsequently, **chapter 6** examined how different visual stimulus characteristics influenced the accuracy of visual field mapping with flicker pupil perimetry in neurologically impaired adults. Altering stimulus luminance, stimulus color, and intra-stimulus color contrast revealed that pupil responses and therewith diagnostic performance of gcFPP benefited from high luminance and color contrast between stimulus and background.

All findings discussed in the previous chapters culminated in the gcFPP method described in **chapter 7**. Diagnostic accuracy and reliability of conventional gcFPP and a novel head-mounted virtual reality version of gcFPP (VRgcFPP) were evaluated in neurologically impaired adults. The conventional gcFPP technique provided visual field heatmaps that resembled SAP results (i.e. high discriminative power) and were repeatable (i.e. good reliability). The VRgcFPP method also showcased high reliability and could capably dissociate VFDs from healthy VFs. However, when compared to SAP, its accuracy was only moderate.

Chapter 8 then investigated the feasibility of the VRgcFPP method in healthy children aged 3-11 years by comparing three fixation tasks. The head-mounted device was well tolerated in all children and evoked strong pupillary responses. An interactive fixation task ensured the child's attention and cooperation. The findings indicated that children were able to maintain fixation effectively during the virtual reality-based test, demonstrating the potential of this technology for objective VF assessments in pediatric populations.

Summary - *Nederlands*

De beoordeling van het gezichtsveld (GV) is een essentieel onderdeel van oogheelkundige en neurologische onderzoeken in de klinische praktijk. GV testen zijn over het algemeen relatief goedkoop en niet-invasief. Hiermee kunnen clinici de vermoedelijke locatie van schade langs het visuele pad nauwkeurig bepalen. Een vroege en juiste diagnose van GV verlies bij jonge en/of neurologisch beperkte personen is van cruciaal belang, aangezien het een belangrijke rol speelt bij de diagnose, opvolging en revalidatie van deze patiënten. Huidige GV testen zijn echter subjectief en onbetrouwbaar bij deze patiëntengroep. Daarom streeft deze scriptie naar de ontwikkeling van een objectief en betrouwbaar instrument voor de beoordeling van het GV bij jonge en/of neurologisch aangedane patiënten.

Hoofdstuk 1 dient als algemene inleiding tot de GV beoordeling bij jonge en neurologisch aangedane patiënten. Besproken worden verschillende test methoden, de anatomie van de visuele- en pupilreactiepaden in de hersenen, en belangrijke mijlpalen en uitdagingen in de ontwikkeling van pupil perimetrie. Tot slot worden de doelstellingen en de opzet van dit proefschrift geformuleerd.

Hoofdstuk 2 deelt inzichten die zijn verkregen uit ervaring met het testen van het GV van kinderen met neurologische beperkingen. Standaard geautomatiseerde perimetrie (SAP), de huidige gouden standaard in GV beoordeling, was slechts betrouwbaar bij 22-44%, terwijl het gebruik van een gedrags-GV test leidde tot aanzienlijke tijdwinst bij de diagnose. Het belang van nauwkeurige, betrouwbare en tijdige GV onderzoeken bij deze populatie wordt benadrukt, omdat dit kan leiden tot een betere zorg voor neurologisch aangedane kinderen.

Pupil perimetrie is een mogelijk objectief alternatief voor de subjectieve SAP-methoden. Het gebruikt de pupilreacties op lichtstimuli als maat voor de gevoeligheid van het gezichtsveld. **Hoofdstuk 3** vergeleek de prestaties van drie verschillende pupilperimetrie technieken (unifocaal, flikker en multifocaal) bij gezonde volwassenen. Hoewel alle drie de methoden goed presteerden, kon de flikker pupil perimetrie (gcFPP) het beste grote gesimuleerde gezichtsvelddefecten (GVD) onderscheiden.

Hoofdstuk 4 onderzocht vervolgens of gcFPP de fysiologische aanwezigheid van de blinde vlek en de verschillen tussen het bovenste en onderste gezichtsveld kon detecteren bij gezonde volwassenen. De methode bleek in staat om pupilreacties op te wekken die sterk genoeg waren om lokale en globale verschillen in pupilgevoeligheid te detecteren. Bovendien moedigden de resultaten het gebruik van een grijze (in plaats van zwarte) achtergrond aan om retinale lichtverstrooiing te verminderen, en het gebruik van een aandachtstaak om pupilreacties te verbeteren. Dit benadrukte opnieuw dat de pupilreactie niet alleen een reactie op licht is, maar ook een aandacht (cognitief) component bevat.

Hoofdstuk 5 onderzocht het compromis tussen luminantie- en kleurcontrast in normaal menselijk zicht. Door zowel luminantie als kleurcontrast systematisch aan te passen, werd aangetoond dat een aanzienlijk deel van de pupilreacties kleurverwerking omvatte. Deze bevindingen bieden inzicht in de mechanismen die ten grondslag liggen aan visuele waarneming en benadrukken het belang van zowel luminantie- als kleurcontrast bij visuele stimuli.

Vervolgens onderzocht **hoofdstuk 6** hoe verschillende kenmerken van visuele stimuli de nauwkeurigheid van de GV beoordeling beïnvloeden met behulp van gcFPP bij neurologisch beperkte volwassenen. Door stimulusluminantie, stimuluskleur en intra-stimulus kleurcontrast te veranderen, werd aangetoond dat pupilreacties en daarmee de diagnostische prestaties van gcFPP baat hadden bij een hoge luminantie en kleurcontrast tussen stimulus en achtergrond.

Alle bevindingen die in de vorige hoofdstukken zijn besproken, culmineren in de gcFPP-methode zoals beschreven in **hoofdstuk 7**. De diagnostische nauwkeurigheid en betrouwbaarheid van conventionele gcFPP en een nieuwe head-mounted virtual reality-versie van gcFPP (VRgcFPP) werden geëvalueerd bij neurologisch aangedane volwassenen. De conventionele gcFPP-techniek leverde gezichtsveldkaarten op die overeenkwamen met SAP-resultaten (d.w.z. een hoge onderscheidingskracht) en herhaalbaar waren (d.w.z. goede betrouwbaarheid). De VRgcFPP-methode toonde ook een hoge betrouwbaarheid en kon GVD'en effectief onderscheiden van gezonde GV'en. De nauwkeurigheid ervan was echter slechts matig in vergelijking met SAP.

Hoofdstuk 8 onderzocht vervolgens de haalbaarheid van de VRgcFPP-methode bij gezonde kinderen in de leeftijd van 3-11 jaar door drie fixatietaken te vergelijken. Het op het hoofd gefixeerde apparaat werd goed verdragen door alle kinderen en riep sterke pupilreacties op. Een interactieve fixatietaak zorgde voor de aandacht en medewerking van het kind. De bevindingen gaven aan dat kinderen effectief fixatie konden behouden tijdens de test in virtual reality, wat het potentieel van deze technologie voor objectieve GV-beoordelingen bij pediatrische populaties aantoont.

Appendices

Appendices - *List of publications*

Related to this thesis

Portengen BL, Koenraads Y, Imhof SM, Porro GL. Lessons learned from 23 years of experience in testing visual fields of neurologically impaired children. *Neuro-Ophthalmology*. 2020;44(6):361–370. doi:10.1080/01658107.2020.1762097

Portengen BL, Roelofzen C, Porro GL, Imhof SM, Fracasso A, Naber M. Blind spot and visual field anisotropy detection with flicker pupil perimetry across brightness and task variations. *Vision Res*. 2021;178(October2020):79–85. doi:10.1016/j.visres.2020.10.005

Portengen BL, Porro GL, Imhof SM, Naber M. Comparison of unifocal, flicker, and multifocal pupil perimetry methods in healthy adults. *J Vis*. 2022;22(9):7. doi:10.1167/jov.22.9.7

Portengen BL, Naber M, Jansen D, et al. Maintaining fixation by children in a virtual reality version of pupil perimetry. *J Eye Mov Res*. 2022;15(3). doi:10.16910/JEMR.15.3.2

Portengen BL, Porro GL, Imhof SM, Naber M. The trade-off between luminance and color contrast assessed with pupil responses. *Transl Vis Sci Technol.* 2023;12(1):15. doi:10.1167/TVST.12.1.15

Portengen BL, Porro GL, Bergsma D, Veldman EJ, Imhof SM, Naber M. Effects of Stimulus Luminance, Stimulus Color and Intra-Stimulus Color Contrast on Visual Field Mapping in Neurologically Impaired Adults Using Flicker Pupil Perimetry. *Eye Brain*. 2023;15:77-89. doi:10.2147/EB.S409905

Portengen BL, Imhof SM, Naber M, Porro GL. Diagnostic performance of pupil perimetry in detecting hemianopia under standard and virtual reality viewing conditions. *Under review at Graefe's Archive for Clinical and Experimental Ophthalmology*

Other

Ten Brink AF, Van Heijst M, ***Portengen BL***, Naber M, Strauch C. Uncovering the (un) attended: Pupil light responses index persistent biases of spatial attention in neglect. *Cortex.* 2023;167:101-114. doi:10.1016/j.cortex.2023.06.008

Appendices - *Acknowledgements (dankwoord)*

Dit proefschrift kon niet tot stand worden gebracht zonder de tijd en steun van vele anderen. Allereerst wil ik alle kinderen, ouders/verzorgers, studenten en patiënten die deelgenomen hebben aan de studies in dit proefschrift hartelijk bedanken.
Ik wil mijn diepste dankbaarheid uitspreken aan mijn promotieteam voor de fijne begeleiding de afgelopen jaren. Giorgio, met jouw inspirerende enthousiasme liep ik altijd weer met goede moed kamertje 27 uit. Jouw werk ethos en levensinstelling zijn een inspiratie. Ik heb dan ook genoten van onze gesprekken op de maandagavond en hoop deze de komende jaren nog vaak te herhalen. Marnix, zonder jouw technische expertise waren wij ver van huis geweest. Ik kijk met veel plezier terug op onze discussies, borrels en hardloopsessies. Saskia, ik ben zeer dankbaar dat jij me alle ruimte gaf om mijn promotietraject naar eigen wens vorm te geven. Dankzij jouw flexibiliteit kon ik niet alleen een extra masteropleiding volgen, maar ook een zeer leerzame cursus aan de Columbia University in New York.

Ik ben ook dankbaar voor de bijdragen van en de fijne samenwerking met mijn co-auteurs, en mijn collega-onderzoekers van de oogheelkunde en de experimentele psychologie van de Universiteit Utrecht en de staf en oogartsen in opleiding van het UMC Utrecht. De prettige werkomgeving en de leerzame discussies waren van onschatbare waarde voor de kwaliteit van de studies. Verder wil ik graag Demi Jansen & Tom van Kempen bedanken dat zij gedurende hun masterthesis geholpen hebben met het verzamelen van data. Speciale dank aan de ODAS stichting, de Rotterdamse Stichting Blindenbelangen, de Janivo stichting, de F.P. Fischer stichting en de Stichting Vrienden UMC Utrecht voor hun financiele steun.
Ook mijn dank aan concullega Laukje, mijn steun en toeverlaat tijdens het thuiswerken. Koen, je hebt het boek geweldig vormgegeven, ontzettend bedankt voor je harde werk.

Tot slot wil ik mijn waardering uitspreken naar mijn familie & vrienden voor hun aanmoediging, begrip en steun tijdens deze mooie periode. Speciale dank aan mijn moeder voor al haar wijsheid en zorg alle jaren en mijn twee paranimfen Jan-Bas & Job voor hun tijd en moeite, fantastisch!

Appendices - *About the author*

Brendan Portengen was born on May 21, 1992, in the picturesque city of Leiden, The Netherlands, to parents Saskia and Koen and grew up alongside his brothers Milan and Ruben. After his graduation from the Stedelijk Gymnasium Leiden, he started his medical training in Utrecht from which he obtained his master's degree in Medicine in 2018.

Under the expert guidance of Dr. G.L. Porro, Prof. Dr. S.M. Imhof, and Dr. M. Naber, Brendan commenced his PhD candidacy at the department of ophthalmology at the University Medical Center Utrecht and the department of experimental psychology at Utrecht University. His research endeavors have taken him to various national and international scientific conferences, where he presented his findings, including the Dutch Ophthalmological Society (NOG) annual meeting, the Dutch Ophthalmology PhD Students Congress (DOPS), the 33rd Pupil Colloquium in Murcia, Spain in 2019 and the Association for Research in Vision and Ophthalmology (ARVO) in Denver, May 2022.

Brendan's commitment to academic education extends beyond his primary field, as he successfully graduated from the post-graduate master's program in Epidemiology, specializing in Clinical Epidemiology and Medical Statistics. Eager to broaden his horizons, he also participated in the 2023 Basic Science Course in Ophthalmology at Columbia University, New York.

Parallel to his academic pursuits, Brendan finds joy and balance in his love for sports. Whether it's swimming, cycling, running or hiking in nature, he embraces physical challenges to spend his free time.

In July 2023, Brendan took the next step in his career by starting his residency in ophthalmology at the University Medical Center Utrecht.

fpp

flicker
pupil
perimetry

< BACK TO CONTENT

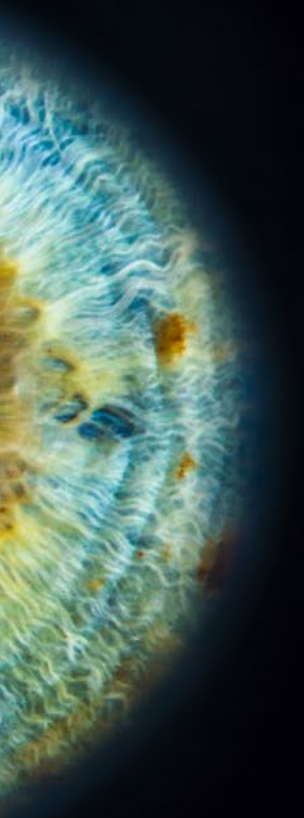

UMC Utrecht

Universiteit Utrecht

ISBN 978-94-6483-730-8